NUREG/CR-6541
INEL-94/0061, Rev. 2

Phenomena Identification and Ranking Tables for Westinghouse AP600 Small Break Loss-of-Coolant Accident, Main Steam Line Break, and Steam Generator Tube Rupture Scenarios

Prepared by
G. E. Wilson, C. D. Fletcher, C. B. Davis,
J. D. Burtt, T. J. Boucher

Idaho National Engineering and Environmental Laboratory
Lockheed Idaho Technologies Company

Prepared for
U.S. Nuclear Regulatory Commission

AVAILABILITY NOTICE

Availability of Reference Materials Cited in NRC Publications

Most documents cited in NRC publications will be available from one of the following sources:

1. The NRC Public Document Room, 2120 L Street, NW., Lower Level, Washington, DC 20555-0001

2. The Superintendent of Documents, U.S. Government Printing Office, P. O. Box 37082, Washington, DC 20402-9328

3. The National Technical Information Service, Springfield, VA 22161-0002

Although the listing that follows represents the majority of documents cited in NRC publications, it is not intended to be exhaustive.

Referenced documents available for inspection and copying for a fee from the NRC Public Document Room include NRC correspondence and internal NRC memoranda; NRC bulletins, circulars, information notices, inspection and investigation notices; licensee event reports; vendor reports and correspondence; Commission papers; and applicant and licensee documents and correspondence.

The following documents in the NUREG series are available for purchase from the Government Printing Office: formal NRC staff and contractor reports, NRC-sponsored conference proceedings, international agreement reports, grantee reports, and NRC booklets and brochures. Also available are regulatory guides, NRC regulations in the *Code of Federal Regulations,* and *Nuclear Regulatory Commission Issuances*.

Documents available from the National Technical Information Service include NUREG-series reports and technical reports prepared by other Federal agencies and reports prepared by the Atomic Energy Commission, forerunner agency to the Nuclear Regulatory Commission.

Documents available from public and special technical libraries include all open literature items, such as books, journal articles, and transactions. *Federal Register* notices, Federal and State legislation, and congressional reports can usually be obtained from these libraries.

Documents such as theses, dissertations, foreign reports and translations, and non-NRC conference proceedings are available for purchase from the organization sponsoring the publication cited.

Single copies of NRC draft reports are available free, to the extent of supply, upon written request to the Office of Administration, Distribution and Mail Services Section, U.S. Nuclear Regulatory Commission, Washington, DC 20555-0001.

Copies of industry codes and standards used in a substantive manner in the NRC regulatory process are maintained at the NRC Library, Two White Flint North, 11545 Rockville Pike, Rockville, MD 20852-2738, for use by the public. Codes and standards are usually copyrighted and may be purchased from the originating organization or, if they are American National Standards, from the American National Standards Institute, 1430 Broadway, New York, NY 10018-3308.

DISCLAIMER NOTICE

NUREG/CR-6541
INEL-94/0061, Rev. 2

Phenomena Identification and Ranking Tables for Westinghouse AP600 Small Break Loss-of-Coolant Accident, Main Steam Line Break, and Steam Generator Tube Rupture Scenarios

Manuscript Completed: June 1997
Date Published: June 1997

Prepared by
G. E. Wilson, C. D. Fletcher, C. B. Davis,
J. D. Burtt, T. J. Boucher

Idaho National Engineering and Environmental Laboratory
Lockheed Idaho Technologies Company
Idaho Falls, ID 83415-3890

T. Lee, NRC Project Manager

Prepared for
Division of Systems Technology
Office of Nuclear Regulatory Research
U.S. Nuclear Regulatory Commission
Washington, DC 20555-0001
NRC Job Code J6008

ABSTRACT

This report revision incorporates new experimental evidence regarding AP600 behavior during small break loss-of-coolant accidents.

This report documents the results of Phenomena Identification and Ranking Table (PIRT) efforts for the Westinghouse AP600 reactor. The purpose of this PIRT is to identify important phenomena so that they may be addressed in both the experimental programs and the RELAP5/MOD3 systems analysis computer code. In Revision 0 of this report, the responses of AP600 during small break loss-of-coolant accident, main steam line break, and steam generator tube rupture accident scenarios were evaluated by a committee of thermal-hydraulic experts. Committee membership included Idaho National Engineering and Environmental Laboratory staff and recognized thermal-hydraulic experts from outside of the laboratory. Each of the accident scenarios was subdivided into separate, sequential periods or phases. Within each phase, the plant behavior is controlled by, at most, a few thermal-hydraulic processes. The committee identified the phenomena influencing those processes, and ranked the influences as being of high, medium, low, or insignificant importance. The primary product of this effort is a series of tables, one for each phase of each accident scenario, describing the thermal-hydraulic phenomena judged by the committee to be important, and the relative ranking of that importance. The rationales for the phenomena selected and their rankings are provided.

This document issue (Revision 2) incorporates an update of the small break loss-of-coolant accident portion of the report. This revision is the result of the release of experimental evidence from AP600-related integral test facilities (ROSA/AP600, OSU, and SPES) and thermal-hydraulic expert review. The activities associated with this update were performed during the period from June 1995 through November 1996.

CONTENTS

FIGURES

TABLES

EXECUTIVE SUMMARY

This report revision incorporates new experimental evidence regarding AP600 behavior during small break loss-of-coolant accidents. The following discussion first describes the baseline report then describes the current revision.

AP600 is a new pressurized water reactor design of the Westinghouse Electric Company that has been submitted to the U. S. Nuclear Regulatory Commission (NRC) for design certification. For its safety, AP600 relies on operation of passive systems. Phenomena Identification and Ranking Table (PIRT) activity has been completed to determine the phenomena that are significant to the response of the AP600 design during certain specific accidents. This report documents the findings of the PIRT activity; these findings may be used as guidance for appropriately focussing analytical and experimental research activities regarding AP600 behavior during accidents.

The accidents addressed in this PIRT were chosen from among Chapter-15 transients that (1) activate or challenge new (passive) safety systems, and (2) produce interactions among those safety systems. This PIRT addresses AP600 behavior expected during small break loss-of-coolant, main steam line break, and steam generator tube rupture accidents. These three categories of accidents are those to be analyzed at the Idaho National Engineering and Environmental Laboratory (INEEL) using the RELAP5/MOD3 computer code. AP600 large break loss-of-coolant accidents are being separately analyzed at Los Alamos National Laboratory (LANL) using the TRAC-PF1 computer code; these accidents are not addressed in this PIRT, but rather will be the subject of future LANL reports. Other accidents, such as station blackout and anticipated transient without scram events, may be addressed in later PIRT efforts at such time as the NRC determines the need.

For this PIRT, the key plant response (also referred to as the Figure of Merit and Primary Safety Criterion) is the minimum reactor vessel inventory.

This PIRT solely addresses the behavior of the full-scale AP600 plant. Although data from experiments benefit this PIRT, no attempt has been made to include in the PIRT effects attributable to the configuration, scaling, or operation of sub-scale experimental facilities designed to provide data for use in assessing AP600 behavior during accidents. These issues will be addressed in a separate post-test analysis report for each transient scenario that is investigated experimentally. These reports will compare: (1) the data obtained in all sub-scale integral experimental facilities, (2) the pertinent scaling issues, and (3) the code capabilities for simulating the behavior observed in the experiments.

The small break loss-of-coolant accident scenario investigated in Revision 2 of this report represents a variety of pipes break in the reactor coolant system. The main steam line break scenario assumed the double-ended rupture of one main steam line inside containment. Two main steam line break scenarios (one leading to ADS activation, and one not) were evaluated in the PIRT. Published analyses indicate that ADS activation is likely to be precluded during a main steam line break accident. The steam generator tube rupture accident scenario assumed the double-ended rupture of one steam generator tube at the tubesheet, in either of the two steam generators. It has been determined these initiating events would not lead to ADS activation, both possibilities were again evaluated in the PIRT, for future reference in multiple failure scenarios.

Originally, the SBLOCA accident scenarios first were subdivided into logical phases (generally involving different controlling thermal-hydraulic processes and behavior). For each accident phase, a key plant response, important parameters for representing that response, and the thermal-hydraulic processes important to the calculation of those parameters were identified. The expected plant behavior during each accident phase was then evaluated and the phenomena believed to be of significance were selected and

ranked. These phases have been combined into a short-term phase and a long-term phase in this revision, as appropriate to evolving evidence that this is a sufficient approach.

The findings of this study, including rationales for the selections and other descriptive and supporting information, are documented in this report. The findings include 15 phenomena that are ranked high, 34 phenomena that are ranked medium and 50 phenomena that are ranked low for the short-term phase. In the long-term phase there were 11 high, 17 medium, and 25 low ranked phenomena. Detailed findings for both phases are presented in Tables 4 through 7 respectively.

This document issue (Revision 2) incorporates an update of the small break loss-of-coolant accident portion of the report. This update is the result of release of the experimental evidence from AP600-related integral test facilities (ROSA/AP600, OSU, and SPES). These tests simulated cold-leg small break loss-of-coolant accidents and the PIRT was updated to reflect the new evidence available from the quick-look test data. The activities associated with this update were performed during the period from June 1995 through November 1996 (activities supporting this revision are discussed in Appendix A).

ACKNOWLEDGMENTS

The authorship list for this report reflects those who directly contributed to the writing of the original document (Revision 0) and the July 1995 version (Revision 1). A team approach to this effort was taken at the INEEL, and the original document was the result of many meetings with many participants. The authors acknowledge the participation of the following INEEL personnel in this effort: R. J. Beelman, R. R. Schultz, M. G. Ortiz, C. H. Heath, J. M. Cozzuol, P. D. Bayless, and S. M. Sloan.

The authors thank the following participants/reviewers from outside INEEL:

General Participants/Reviewers:

G. N. Lauben, T. Lee, and J. Kelly, NRC Office of Nuclear Regulatory Research,

P. Griffith, Massachusetts Institute of Technology,

G. Lellouche, private consultant to INEEL,

G. Slovik and U. S. Rohatgi, Brookhaven National Laboratory, and

B. Boyack, Los Alamos National Laboratory

Others:

The authors thank K. Washington of Sandia National Laboratories and A. Notafrancesco of the NRC Accident Evaluation Branch for their contributions to a better understanding of reactor coolant system/containment interactions.

The authors thank V. K. Dhir of the University of California Los Angeles, who attended the meetings as an observer for the ACRS Thermal Hydraulic Phenomena Subcommittee, for his personal perspectives.

The authors acknowledge the special efforts of R. B. Nielson and K. Argudo for developing the data management tools necessary for efficient handling of the PIRT tabular information and L. Scott for technical editing.

This update is the result of a coordinated effort of the NRC, INEEL, and thermal-hydraulic consultants. Significant support in the analysis of the experimental data was provided by D. Bessette, M. DiMarzo, and J. Kelly of the NRC. A full list of contributors to this update is given in Appendix A, Table A-4.

NOMENCLATURE

ACRS	Advisory Committee on Reactor Safeguards
ADS	Automatic depressurization system
ALWR	Advanced light-water reactor
AP600	Advanced Passive 600 MWe Reactor
CCFL	Countercurrent flow limiting
CHF	Critical heat flux
CMT	Core makeup tank
CSAU	Code scaling, applicability, and uncertainty
DNB	Departure from nucleate boiling
DVI	Direct vessel injection
ECC	Emergency core coolant
ECCS	Emergency core coolant system
INEL	Idaho National Engineering Laboratory
INEEL	Idaho National Engineering and Environmental Laboratory (formerly INEL)
IRWST	In-containment refueling water storage tank
L/D	Ratio of length to diameter
LANL	Los Alamos National Laboratory
LBLOCA	Large break loss-of-coolant accident
LOCA	Loss-of-coolant accident
MSLB	Main steam line break
NPP	Nuclear power plant
NRC	U. S. Nuclear Regulatory Commission
OSU	Oregon State University
PBL	Pressure balance line
PCCS	Passive containment cooling system
PIRT	Phenomena identification and ranking table
PRHR	Passive residual heat removal
PSF	Passive safety feature
RCS	Reactor coolant system
ROSA	Japanese ROSA test facility
S signal	Safeguards initiation signal
SBLOCA	Small break loss-of-coolant accident
SET	Separate effects test
SG	Steam generator
SGTR	Steam generator tube rupture
SNL	Sandia National Laboratories
SPES	Italian SPES test facility
SRV	Safety relief valve

PHENOMENA IDENTIFICATION AND RANKING TABLES FOR WESTINGHOUSE AP600 SMALL BREAK LOSS-OF-COOLANT ACCIDENT, MAIN STEAM LINE BREAK, AND STEAM GENERATOR TUBE RUPTURE SCENARIOS

1. INTRODUCTION

The Advanced Passive 600 MWe (AP600) Reactor is a new reactor design that has been submitted by the Westinghouse Electric Company to the U. S. Nuclear Regulatory Commission (NRC) for design certification. AP600 is a pressurized water reactor that utilizes passive safety features (PSFs). The reactor design includes: (1) a low core volumetric heat generation rate, (2) a low peak-to-average fuel heat flux ratio, (3) a reliance solely upon natural forces, such as gravity and gas pressurization, for safety system operation, and (4) a dependence upon natural phenomena, such as natural convection and condensation, for safety system performance. All PSFs are integrated into the containment, which incorporates heat exchange devices to accommodate removal of core decay heat from the reactor coolant system (RCS) to containment and from the containment to the environment. As a result, during accidents the RCS and containment of this plant interact in a more integral fashion than in current generation light-water reactor designs. AP600 accident safety analysis therefore requires consideration of the interactions among the RCS, containment, and PSFs. This report evaluates the response of AP600 and interactions among its systems during accidents.

The AP600 design is documented in References 8-1 and 8-2; a schematic of the plant is shown in Figure 1. Reference 8-3 provides a detailed discussion of the thermal-hydraulic aspects of the AP600 design on a component-by-component basis. The AP600 is a two-loop pressurized water reactor arranged in a two-hot-leg, four-cold-leg configuration. AP600 is equipped with passive emergency core cooling systems (ECCS). The AP600 design calls for lost coolant to be replenished by RCS-pressure-balanced core makeup tanks (CMTs), gas-pressurized accumulators, and an elevated, gravity-drain, containment-pressure-equalized in-containment refueling water storage tank (IRWST). Once the contents of this tank have been discharged, the resulting containment liquid level exceeds the elevation of the coolant loops, causing liquid to be injected back into the RCS via sump valves. Vaporized coolant that is condensed on the interior of the containment shell is collected and returned to the IRWST. An automatic depressurization system (ADS) is provided to ensure viability of the passive ECCS by limiting the differential pressure between the RCS and containment. A passive decay heat removal system (PRHR) is included to remove decay heat to the IRWST; this is a full-pressure/full-decay-heat system. Passive containment cooling is provided by gravity-driven evaporative cooling external to the containment and is sustainable during dry air natural draft conditions.

Operation of the AP600 PSFs is based upon thermal-hydraulic processes that use low driving forces, such as gravity pressure heads and buoyancy. These processes are significantly different than those found in existing plants, which instead use high driving forces (primarily pump heads) for operation of their safety systems. Therefore, the NRC undertook a research program to improve the reactor thermal-hydraulic simulation computer programs for evaluating the new plant designs. These computer programs generally were developed and verified for evaluating the performance of safety systems in the existing plants.

A methodology termed Code Scaling, Applicability, and Uncertainty (CSAU)[7-1] was developed by the NRC and its contractors as an optional "best-estimate plus uncertainty" approach for determining plant safety margin with respect to the safety criteria required by Federal regulation.[7-2] One of the key features

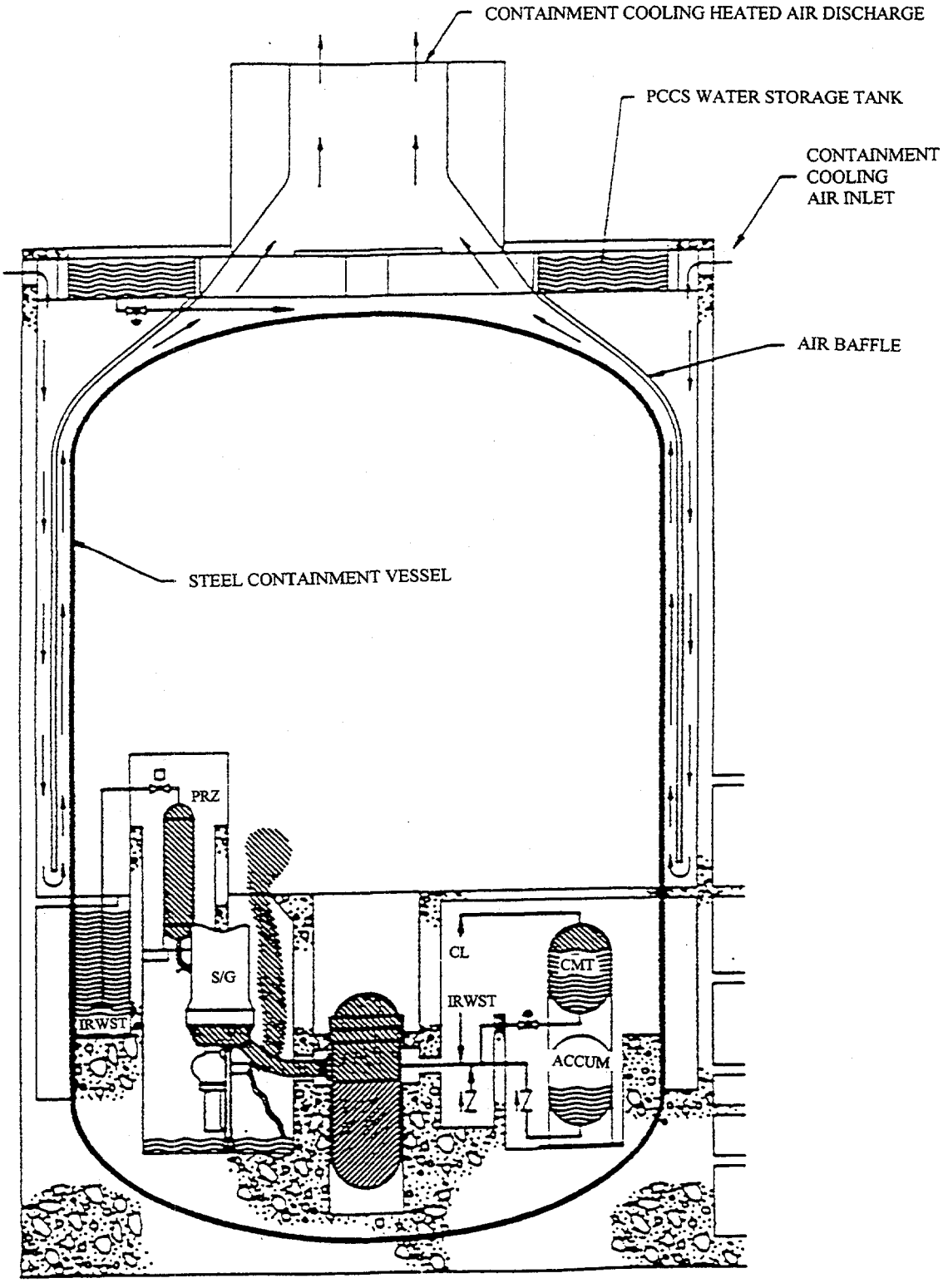

Figure 1. Sketch of AP600 design.

of the CSAU process is the Phenomena Identification and Ranking Table (PIRT) process in which phenomena significant to the plant response are determined, and a relative-importance rank is assigned to each. The PIRT process, by providing researchers with information regarding the significance of the various phenomena for the specific plant design and accident scenarios, provides a method by which research efforts can remain properly focussed. The NRC research staff and its contractors have embarked upon a code development and assessment process which utilizes principles developed for CSAU, including establishment of a PIRT; the process for this advanced light-water reactor thermal-hydraulic research program is shown in Figure 2 (the role of PIRT in this program is described in Section 2). The purpose of PIRT is to assure that the important phenomena are being addressed in both the transient analysis computer codes (Element 3 in the Figure) and the experimental assessment base (Element 2).

The development and use of the AP600 PIRTs are being conducted in three phases. The first PIRT phase (Preliminary) began in 1990 and continued through October 1993. The preliminary PIRTs primarily focussed on phenomena of high and medium importance and on the operation of the new PSFs. The preliminary PIRTs were directed toward experimental facility definition, scaling and test selection, code development of early versions of the RELAP5/MOD3 computer code, and the initial development of a detailed AP600 plant model. The second phase (interim) began in October 1993, concluded in September 1994, and was directed toward a more detailed listing and ranking of phenomena. Revision 0 of this report documented this second phase.

Revision 1 of this report represented the first step of the final PIRT phase. This revision incorporated an update of the SBLOCA portion of the PIRT report based on recently-released experimental evidence from AP600-related integral test facilities (ROSA/AP600, OSU, and SPES). The major impacts of this update on the SBLOCA PIRT were to: (1) change the break definition from 8-inch diameter and smaller breaks at an unspecified location, to 2-inch diameter and smaller breaks in a cold leg, (2) redefine the time phases, and (3) reconsider both the phenomena selected and their rankings. A discussion of the basis for these changes is provided in Section 5.3.

Revision 2 of this report represents the final PIRT phase. This stage focused on consideration of the new evidence provided in the integrated experimental data analysis of the PBLB and DVI line SBLOCA, the integrated experimental data analysis of the IADS, the SBLOCA short-term AHP analysis, SBLOCA PIRT confirmation sensitivity studies, and the short- and long-term scaling analyses. See Appendix G, Table G-4, code E3 for the new experimental evidence used and Appendix A, Table A-4 for a summary of the review activities associated with this revision. A significant impact of this update is the reduction of PIRT SBLOCA phases to a short-term phase and a long-term phase. A discussion of this change is provided in Appendix B.

As a matter of definition, the term "phenomena" as used in this report should be taken to mean "phenomena, processes, component functions, behavior, conditions, and status". As a convenience, and for brevity, we have broadly interpreted the term "phenomena" to include all of these attributes of the thermal-hydraulic systems and their responses. All of the following examples are, therefore, identified as "phenomena" in this report, even though only the first example is truly one: flashing, break mass flow, decay heat, steam generator secondary level, steam generator secondary pressure, nonuniform steam/air distribution, subcooling margin, and primary-to-secondary heat transfer.

Also as a matter of definition, the term "CMT level", as used in this report, refers to the percentage of total core makeup tank volume that is occupied by liquid. This definition is consistent with that used by Westinghouse Electric Company in their AP600-related documents. However, this definition is contrary to that normally associated with indicated levels (such as in steam generators and pressurizers) that instead are based upon differential pressure measurements.

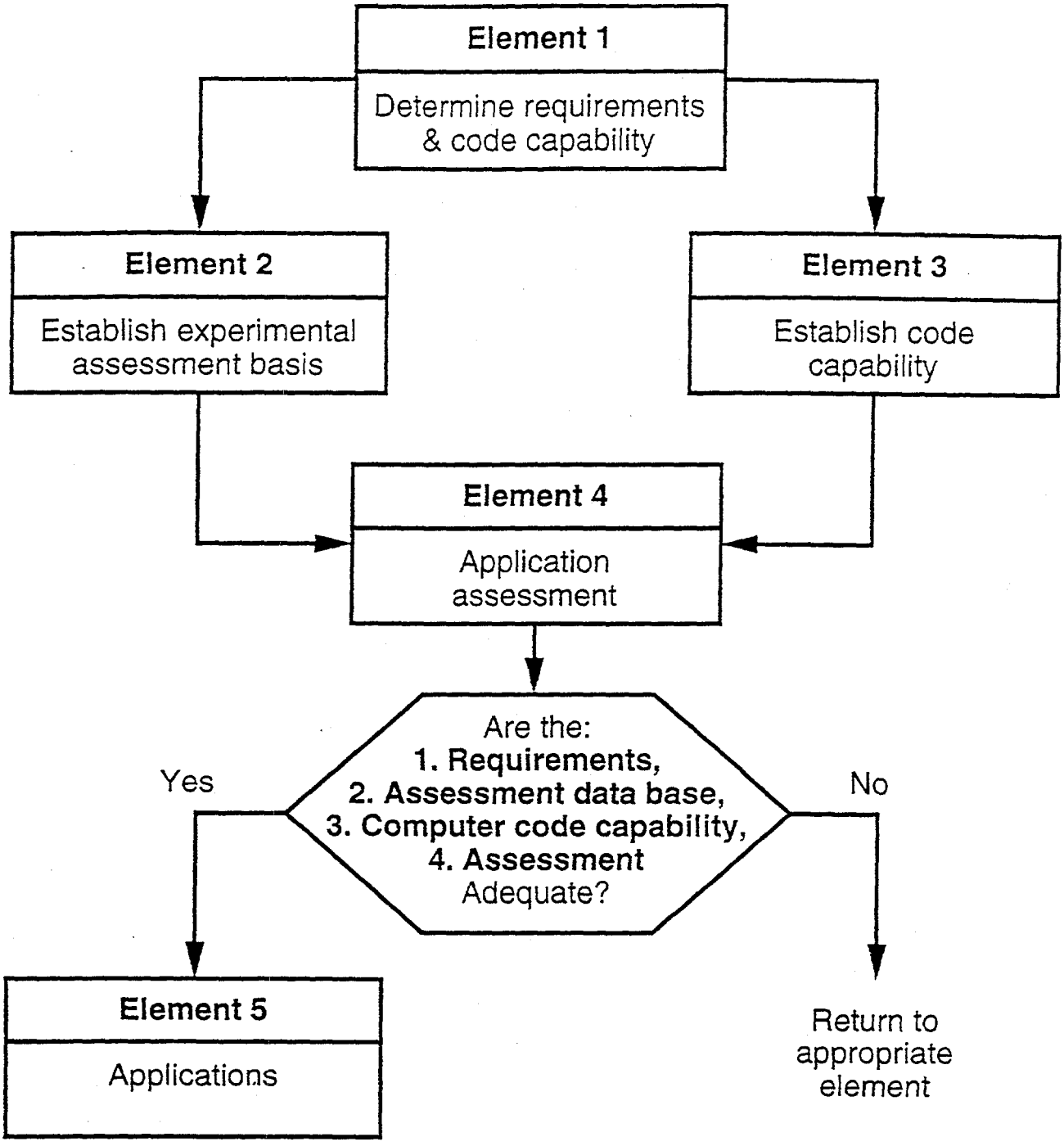

Figure 2. ALWR overall thermal-hydraulic research plan.

The accidents addressed in this PIRT were chosen from among Chapter-15 transients that: (1) activate or challenge new (passive) safety systems and (2) produce interactions among those safety systems. This PIRT addresses AP600 behavior expected during small break loss-of-coolant (SBLOCA), main steam line break (MSLB), and steam generator tube rupture (SGTR) accidents. These three accident categories are those to be analyzed at the INEEL using the RELAP5/MOD3 computer code. AP600 large break loss-of-coolant accidents are being separately analyzed at Los Alamos National Laboratory (LANL) using the TRAC-PF1 computer code; these accidents are not addressed in this PIRT, but rather will be the subject of future LANL reports. Other accidents, such as station blackout and anticipated transient without scram events, may be addressed in later PIRT efforts at such time as the NRC determines the need. This PIRT solely addresses the behavior of the AP600 plant. Although data from experiments benefit this PIRT, no attempt has been made to include in the PIRT effects attributable to the configuration, scaling, or operation of sub-scale experimental facilities designed to provide data for use in assessing AP600 behavior during accidents. These issues will be addressed in a separate post-test analysis report for each transient scenario that is investigated experimentally. These reports will compare: (1) the data obtained in all sub-scale integral experimental facilities, (2) the pertinent scaling issues, and (3) the code capabilities for simulating the behavior observed in the experiments.

A more detailed discussion of the CSAU and PIRT processes is given in Section 2. Section 3 describes the accident scenarios, their subdivision into accident phases, the parameters considered important for characterizing the plant response, and the dominant thermal-hydraulic processes affecting those parameters. Section 4 summarizes the results of the PIRTs. Section 5 discusses analytical and experimental activities related to this PIRT. A summary of the PIRT findings is provided in Section 6 and references are provided in Sections 7 and 8. Appendix A discusses the history of this PIRT effort. Detailed information regarding assumptions, rationales for decisions, and terminology used in the PIRTs is documented in Appendixes B through G, and is referenced from within the main body of the report. Reference 8-4 presents summary descriptions of the AP600 plant systems, automatic plant actions, and interactions among the systems expected during the types of accidents evaluated in this report. Appendices H and I discuss the top-down scaling analyses and the Analytical Hierarchy Process that supported this final PIRT revision.

2. METHODOLOGY

In September 1988, the NRC issued a revised ECCS rule (10 CFR 50.46) for light-water reactors that allows for, as an option to the traditional, conservative "evaluation model" approach, the use of best-estimate computer codes in safety analyses. The key feature of this licensing option is that the licensee must quantify the uncertainty of the calculations and include that uncertainty when comparing calculated results with the acceptance limits. The CSAU methodology is one means by which the uncertainty quantification may be performed. The PIRT activities are a portion of the CSAU process. The CSAU methodology is the culmination of 20 years of ECCS research on current light-water reactors. This research has involved extensive iteration among experiments and analyses, in which the developmental process has matured. As indicated in the introduction, for this application, CSAU and PIRT methods are being employed to properly focus NRC research on the issues relevant to understanding AP600 behavior (for example, through code assessment plans, code development plans, and evaluations of experiment suitability). Section 2.1 summarizes the CSAU methods and Section 2.2 summarizes the PIRT methods.

2.1 CSAU Methodology

The CSAU methodology is shown in Figure 3. The methods are subdivided into three elements:

Under the first element, "Requirements and Code Capabilities," scenario modeling requirements are identified and compared against code capabilities to determine the applicability of the code for the specific plant and accident scenario. Code limitations are also noted during this element. The steps included in this element are identification of the specific plant and accident scenario, identification and ranking of phenomena (the "PIRT", discussed further in Section 2.2), the identification of a "frozen" version of a computer code, obtaining a full set of documentation on that code, and finally a determination of the code's applicability for this situation.

Under the second element, "Assessment and Ranging of Parameters," the capabilities of the code are assessed by comparing calculations against experimental data to determine code accuracy, scale-up capability, and to determine appropriate ranges over which parameter variations must be considered in sensitivity studies. The steps included in this element are: establishing an assessment matrix, defining an appropriate model nodalization, determining the code and experiment accuracies, and determining the effects of scale.

Under the third element, "Sensitivity and Uncertainty Analysis," the individual contributors to uncertainty are calculated, collected, and combined into a total uncertainty. The steps included in this element are: determining the effect of reactor input parameters and state, performing sensitivity calculations, combining biases and uncertainties, and calculation of the total uncertainty.

2.2 PIRT Methodology

The purpose of PIRT is to identify the phenomena that are important to the thermal-hydraulic behavior of a particular plant during a particular accident scenario. In addition, each phenomenon that is deemed of significance is assigned a relative importance ranking, either high, medium, or low in the case of the work documented here. The PIRT activities are conducted by a committee of experts.

The PIRT is developed by first identifying the plant (in this case AP600) and the accident scenarios (in this case, SBLOCA, MSLB and SGTR). In practice, identification of the accident scenario can be problematic. As an example, for the SBLOCA scenario, exactly where is the break? In what pipe, at what orientation, at what distance from the reactor vessel, of what size, and of what opening time? These are all questions that must be answered before the evaluation can proceed.

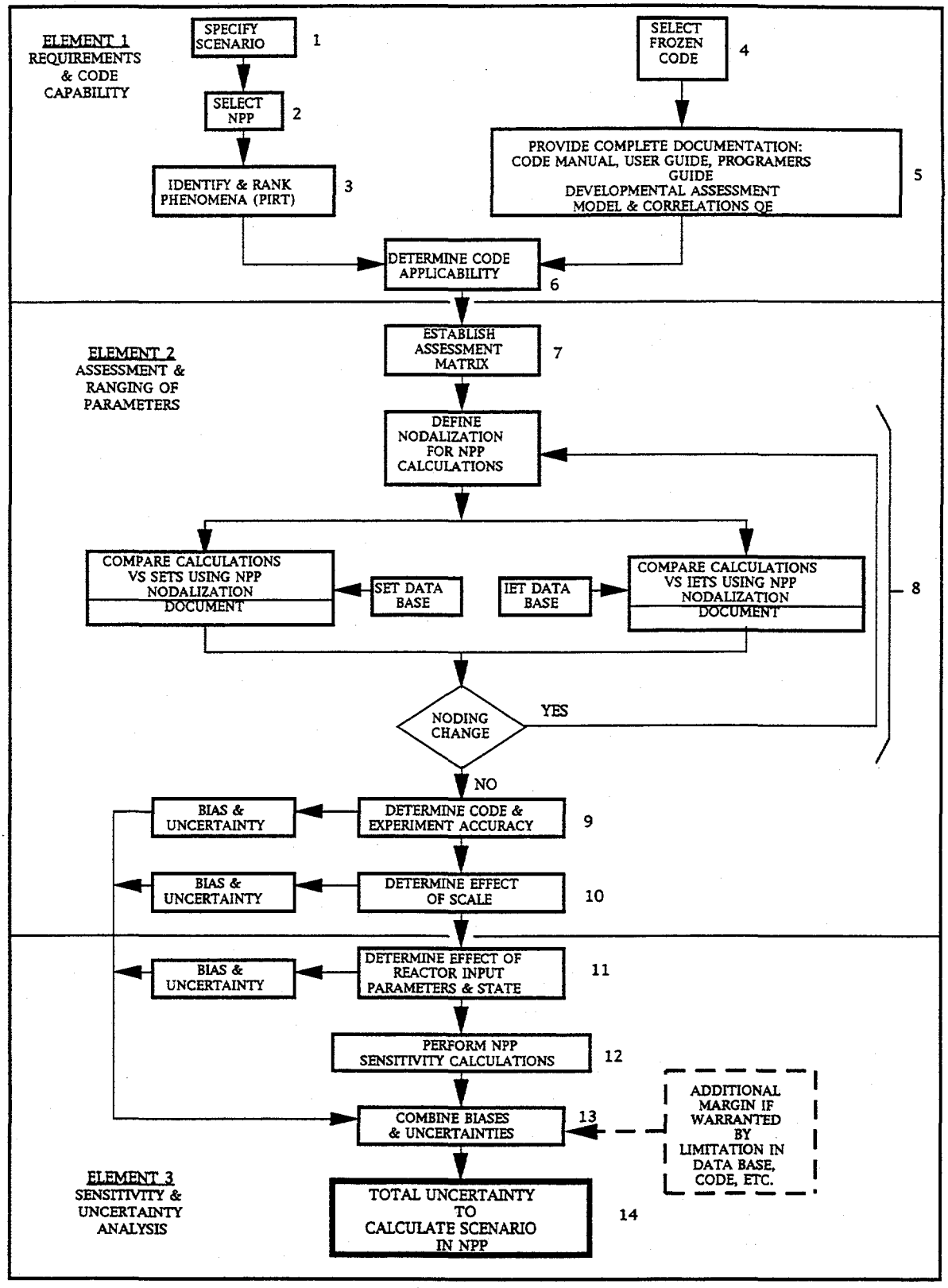

Figure 3. Code scaling, applicability and uncertainty evaluation methodology flow diagram.

The accident scenario is then subdivided into time phases. Typically, this subdivision is based upon a logical progression of key characteristic features of overall plant behavior during the accident sequence. For example, during the AP600 main steam line break, the first part of the sequence is dominated by the blowdown of the secondary coolant system. However, after a time, this behavior ceases (because the secondary system has reached the containment pressure) and a new behavior arises (in this case, reheating of the RCS).

A key step in establishing the context for evaluating candidate phenomena is to determine the evaluation criteria. Figure 4 illustrates the hierarchy of evaluation criteria used in this process. The higher levels are the most general and safety-oriented. In this figure, Levels 1 through 4 are contained in NRC regulations or regulatory guidance. This report deals with Levels 5 through 8 for AP600 SBLOCA, MSLB, and SGTR accidents. Each level must meet the envelope of requirements of criteria for all levels above it. For example, vessel inventory (the Level 5 criterion chosen for SBLOCA assessment) must always be evaluated in a manner that assures acceptable peak fuel rod cladding temperatures. If, for a particular SBLOCA accident sequence, vessel inventory does not provide that assurance, then either the higher-order criteria must be used or a new criterion must be chosen.

For each accident phase, a key response is identified (Level 5 in Figure 4), along with important plant parameters affecting that response (Level 6). The processes that dominate the calculation of the important parameters are then identified (Level 7). Level 8, then, represents the phenomena to be evaluated. The portion of the overall PIRT hierarchy applied and documented in this report is shown in Figure 5. Figures such as this are provided in Section 3 to give the specific evaluation criteria used for each accident time phase.

The PIRT committee then evaluates the phenomena representing or affecting the identified processes and assigns a relative ranking for each phenomenon.

The analytical and experimental supporting evidence used as bases for judging the relative importance of phenomena in this report are identified in Appendix G, Table G-4.

Each phenomenon was assigned a rank using the following simple approach. For each process identified, the PIRT committee decided upon a list of pertinent candidate phenomena and a top-level rank (either high, medium, or low) for the process itself. Then, using their collective expertise, the committee members developed a consensus regarding separation of phenomena on the list into two groups: controlling and contributing. Further, within the contributing group, the members differentiated the phenomena into two subgroups (major contributors and minor contributors) depending upon the expected influence upon the controlling phenomenon. Controlling phenomena were assigned the top-level rank, major contributing phenomena were ranked one level lower, and minor contributing phenomena were ranked two levels lower. Phenomena for which this approach resulted in a ranking of less than "low" were considered insignificant and were discarded. The end product of this effort is a series of tables (one for each phase of each accident) showing the identified phenomena and their relative rankings.

Level	Source	Criteria				Conservatism	Characteristic
1*	10CFR1.11	Protect public healh & safety				Less limiting	Safety
2*	10CFR100	Limit fission product release					
3*	Appendix A	Limit fuel failure		Limit RCS breach	Limit containment breach		
4*	SRP 6.2 Containment		DNBR (PWR), MCPR (BWR),energy deposition, fuel temp.,cladding strain	RCS & steam systems temp & pressure	Limit containment P & T, leakage, hydrogen, etc.		
	SRP 15.1.4 to 15.6.1 Non-LOCA						
	10CFR 50.46 & SRP 15.6.5 LOCA	PCT, oxidation, hydrogen generation, long term cooling, coolable geometry					
5	NUREG/ CR-5818	Vessel inventory**					
6	Interim PIRT	Important parameters					
7	Interim PIRT	Dominant processes					
8	Interim PIRT	Ranked phenomena				More limiting	Behavior

* Levels 1 - 4 are contained in NRC regulations or regulatory guidance
** Level 5 is key plant response criterion used for SBLOCA CSAU assessment

Figure 4. Evaluation criteria hierarchy.

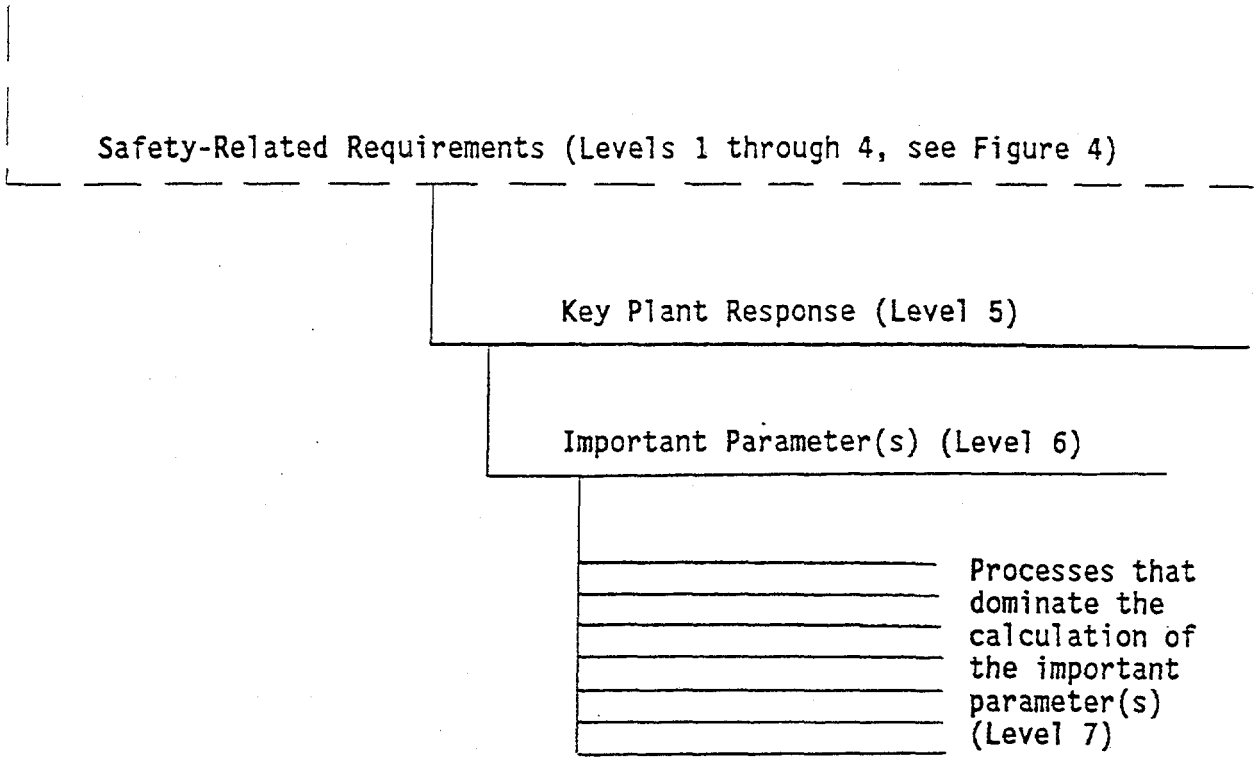

Figure 5. Hierarchy of the AP600 PIRT Process

3. DESCRIPTION OF SEQUENCES, PHASES, IMPORTANT PARAMETERS, AND DOMINANT PROCESSES

This PIRT covers SBLOCA, MSLB, and SGTR AP600 accident scenarios. These scenarios were chosen from among Chapter-15 transients that: (1) activate or challenge the new (passive) safety systems and (2) produce interactions among those safety systems. In all cases, the accident scenarios are assumed to begin at a time when the reactor is operating at full power. The key plant response (also referred to as the Figure of Merit and Primary Safety Criterion) for all three accident scenarios is the minimum reactor vessel inventory.

This section summarizes the accident scenarios investigated, the phases into which the scenarios were subdivided, and the important parameters and dominant processes for each phase. Figure 6 provides overviews of the SBLOCA, MSLB, and SGTR accident sequence progressions, the actions and conditions which define the time phases, and the significant plant behavior and events occurring within each phase. Section 3.1 describes the SBLOCA. For the MSLB and SGTR accidents, ADS actuation, based on CMT level, was uncertain, therefore, both possibilities were considered. Published analyses indicate that ADS activation is likely to be precluded during a MSLB accident. Sections 3.2 and 3.3, respectively, describe the MSLB accident without and with ADS activation. Similarly, Sections 3.4 and 3.5, respectively, describe the SGTR accident without and with ADS activation. The discussions in this section are summaries of the more detailed discussions presented in Appendixes B through F, and the reader is referred there for further information.

3.1 Small Break Loss-of-Coolant Accident

The SBLOCA scenario represents AP600 response to a small pipe break, assuming availability only of safety-grade plant systems. The break orientation is unspecified. Note that this scenario description has been changed significantly in this report revision.

The SBLOCA sequence was originally subdivided into four accident phases. However for this revision, these phases have been combined into two time phases as supported by additional evidence. The short-term phase includes the high pressure phase, the ADS blowdown phase and the initial start of the long-term IRWST phase. The long-term phase includes the rest of the IRWST phase and the long-term sump phase. Figure 6A shows the correlation of the new phase definitions with the Revision 1 phases that are summarized in the following paragraphs. Figures 7 and 8 show the key plant responses, important parameters and processes identified for the two Revision 2 phases.

The short-term phase begins at the time the break opens and proceeds until the IRWST injection flow becomes stable. The reactor and turbine trips occurs when the pressurizer level falls to its scram setpoint value (see Reference 8-4, Table H-2, for a list of plant automatic actions and their corresponding signal set points). Break flow and fluid shrinkage cause the pressurizer level to continue to fall to the S signal set point pressure. S Signal generation causes CMT actuation, main feedwater isolation and reactor coolant pump trip. CMT actuation, in turn, causes the PRHR system actuation. Accumulator injection begins when the RCS pressure falls to the initial accumulator pressure. When the level in either CMT falls to 67.5%, the ADS stage 1 is actuated, followed by stages 2 and 3 at specified time intervals, discharging coolant directing through spargers into the IRWST. ADS stage 4 actuates at a CMT level of 20% with an additional time delay, discharging directly into the containment loop compartments. When the RCS pressure drops sufficiently, the 28 foot driving head of the IRWST begins to inject coolant into the vessel. Onset of stable IRWST injection marks the end of the short-term phase.

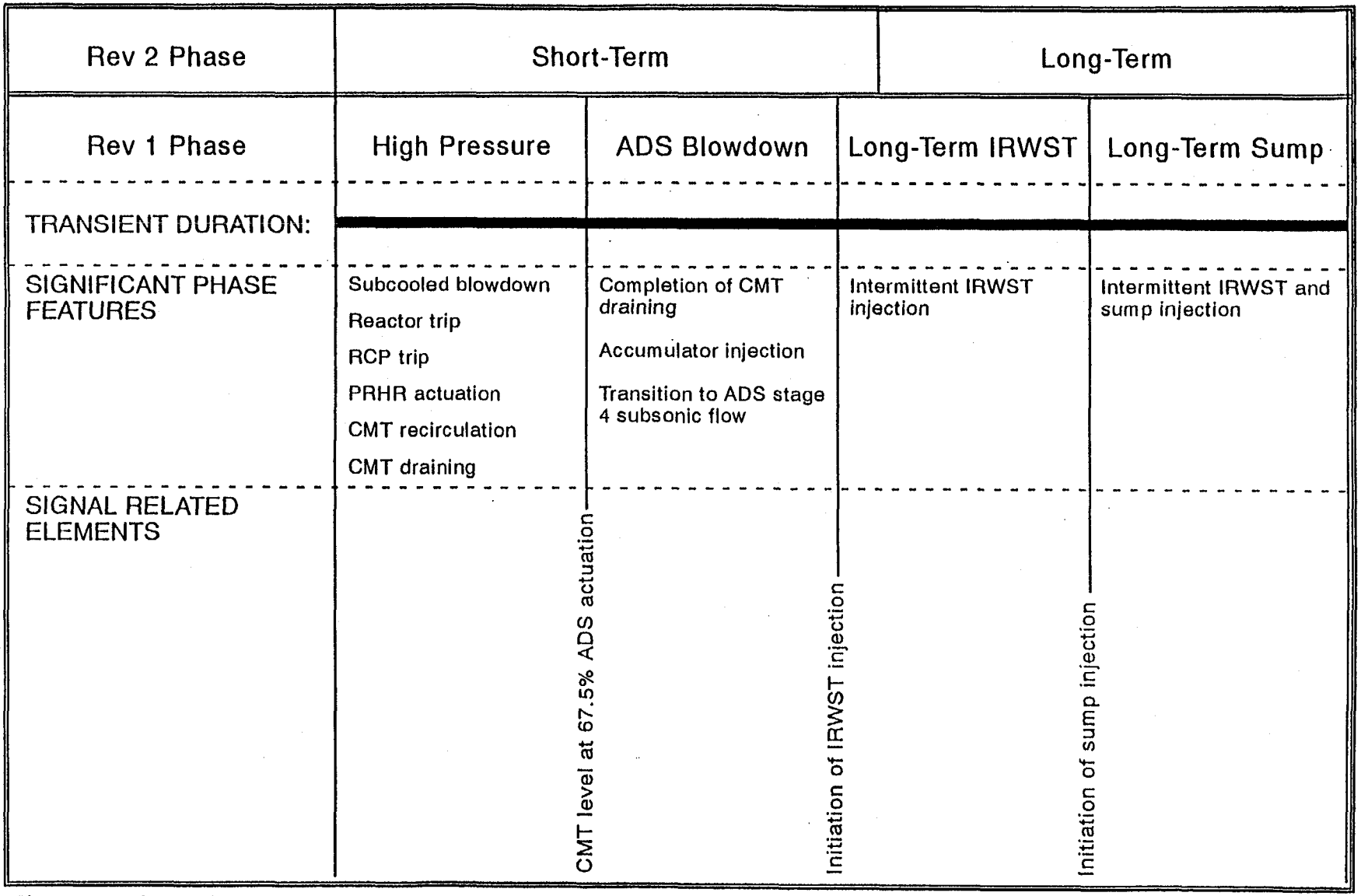

Figure 6A. Phases for AP600 SBLOCA phenomena identification and ranking table.

CCMCDFdD

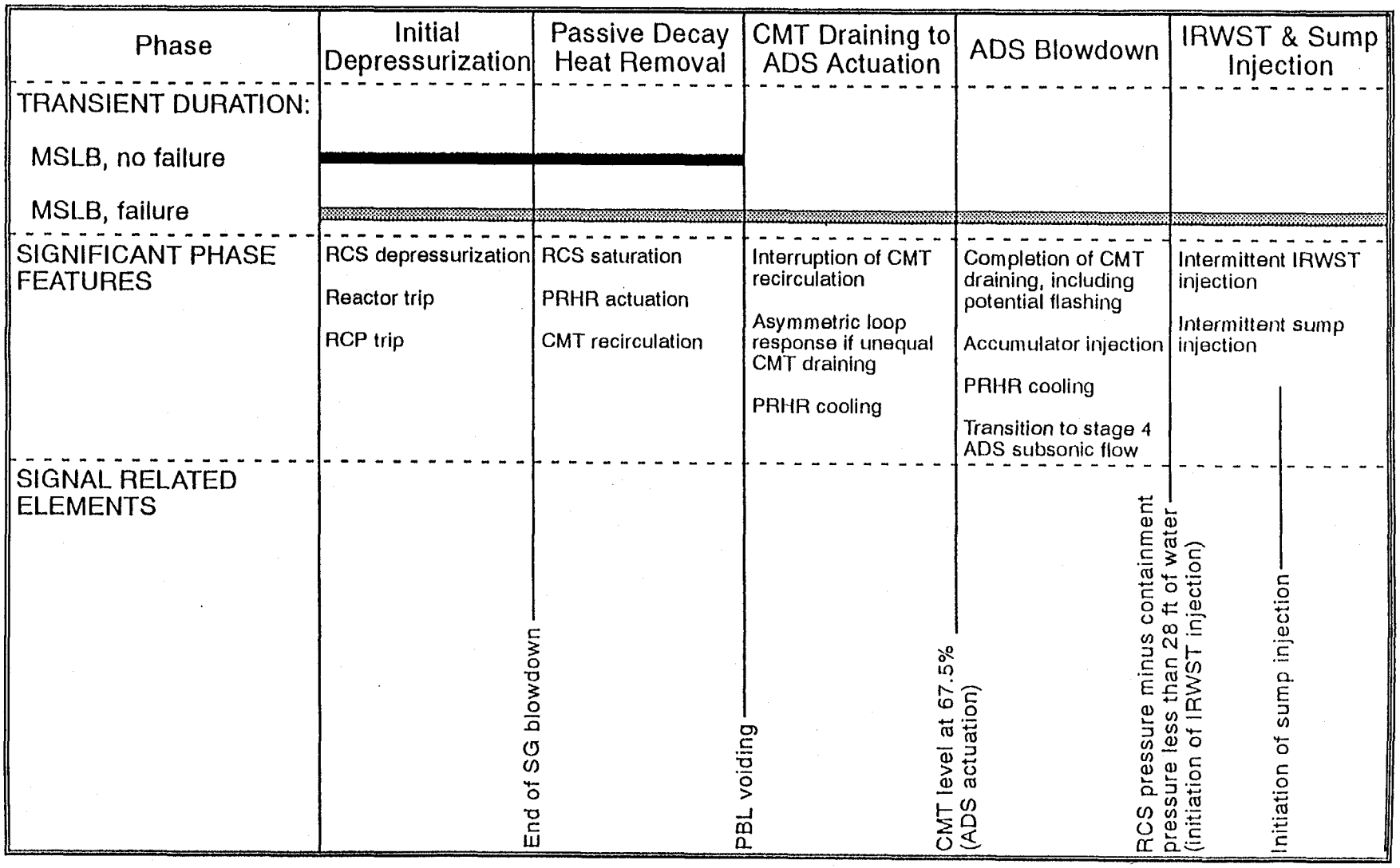

Figure 6B. Phases for AP600 MSLB phenomena identification and ranking tables.

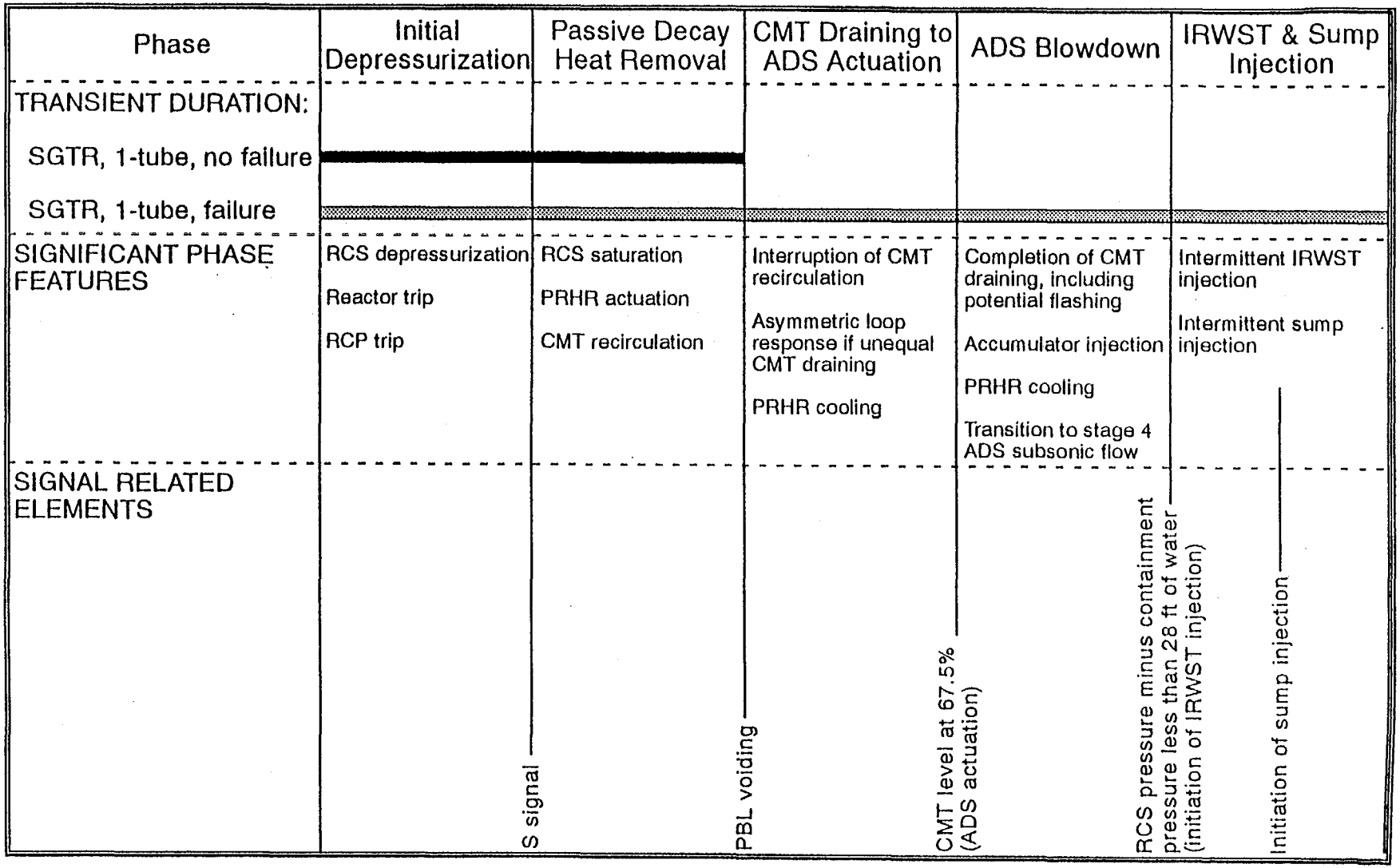

Figure 6C. Phases for AP600 SGTR phenomena identification and ranking tables.

CCMCDF6C

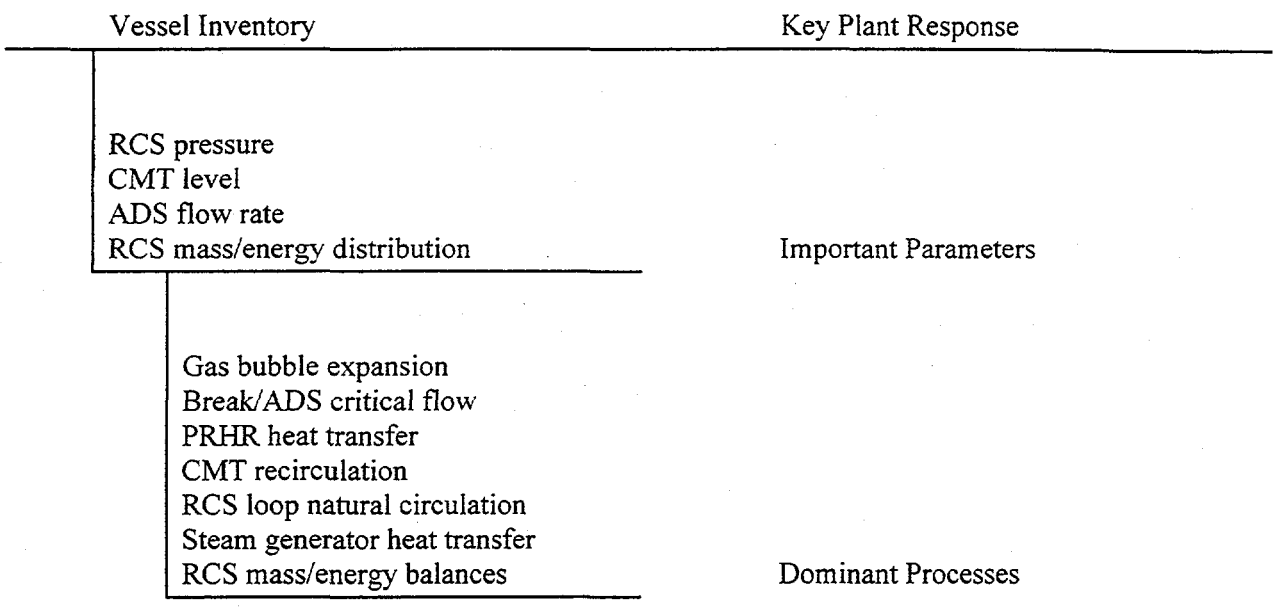

Figure 7. Ranking criteria for the SBLOCA short-term phase.

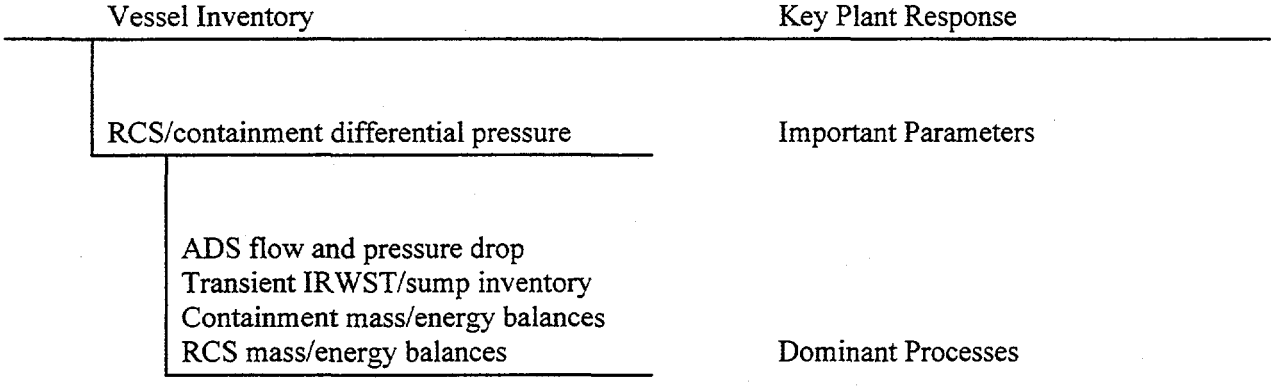

Figure 8. Ranking criteria for the SBLOCA long-term phase.

The parameters of primary importance during the short-term phase are RCS pressure, CMT level, ADS flow rate and the RCS mass and energy distributions. The processes important for accurate simulation of these parameters are: gas bubble expansion, break and ADS critical flow, PRHR heat transfer, CMT recirculation, natural circulation in the RCS loops, steam generator heat transfer, and the RCS mass and energy balances. Later in the short-term phase the CMT level and ADS flow rate are important because they determine the timing of ADS staging and the RCS depressurization rate. The processes important for accurate simulation of these parameters later in the process are the discharge flows (ADS and break, critical and friction-dominated) and the RCS mass and energy.

The long-term phase begins when stable flow is established from the IRWST, through the direct vessel injection lines into the vessel downcomer. Steam and water from the break and ADS stage 4 are passed into the containment where they can collect and flow into the containment sump. The onset of gravity driven sump injection occurs when the sump level has been equalized with the IRWST level. At this point the sump replaces the IRWST as the source of RCS injection. The plant end-state for the SBLOCA includes core-inventory maintenance from sump injection, and decay heat removal across the containment shell to the atmosphere.

The RCS-to-containment differential pressure is judged to be the primary parameter of importance during the long-term phase because it determines the magnitude of the IRWST and sump injection flow rate. The processes important for accurate simulation of this parameter are: ADS flow and pressure drop, the transient IRWST and sump inventories, and the containment and RCS mass and energy balances.

Additional discussions of the SBLOCA sequence are provided in Appendix B and Reference 8-4.

3.2 Main Steam Line Break Without ADS

The MSLB-without-ADS accident scenario represents the AP600 response to the double-ended rupture of one steam line, assuming availability of only safety-grade plant systems. The inner diameter of the ruptured pipe is about 29 inches, but flow limiters, located at the steam line nozzles on the steam generators, have an equivalent diameter of about 16 inches. Therefore, break flow is restricted at the flow limiters rather than at the break location. Other than being inside containment, the break location is unspecified; it may be situated in either steam line. A MSLB results in an overcooling of the RCS system. As the RCS fluid is cooled, it contracts, and the resulting fluid shrinkage has the potential to lower the CMT levels. In this scenario, it is assumed that the CMT level decline (if any) is not sufficient to activate ADS. Published analyses (Reference 7-3) have indicated that it is likely that this assumption is correct. Those analyses evaluated AP600 response to a main steam line break event in which bounding assumptions were applied to maximize the potential for ADS actuation. The analyses show that, even when those assumptions are employed, ADS activation is not indicated.

The MSLB-without-ADS sequence was subdivided into two accident phases (see Figure 6B) that are summarized in the following paragraphs. Figures 9 and 10 show the key plant responses, important parameters and processes identified for the two phases.

The initial depressurization phase begins at the time of the pipe break and proceeds until the time when the affected (i.e., the one connected to the broken steam line) steam generator secondary has depressurized to the containment pressure. The reactor trip occurs during this phase. The steam line piping arrangement is such that both steam generators initially blow down through the double-ended pipe break. However, relatively early in this phase, a steam line isolation signal is generated that results in a blocking of the path for steam from the unaffected steam generator to reach the break location. Behavior during this phase is otherwise dominated by the blowdown of the affected steam generator into the containment and the resulting overcooling of the RCS, due to heat removal across the tubes of the affected steam generator. It is noteworthy that this process is asymmetric, with significant differences in heat loads and fluid temperatures between the affected and unaffected coolant loops. The steam generator primary-to-secondary heat transfer was judged to be the parameter of primary importance during this phase because it dominates the RCS cooldown. The processes important for accurate simulation of this parameter are: break flow, steam generator secondary behavior (level swell and depletion, liquid carry-over, flashing, entrainment), flow through the RCS loops, and asymmetric loop cooldown.

The passive decay heat removal phase begins when the affected steam generator blowdown into the containment has been completed and continues thereafter. This phase is marked by establishment of a final RCS energy balance where heat sources (core decay heat and reverse heat transfer from the unaffected steam generator) are balanced by the heat sink (PRHR heat removal to the IRWST, and from there to the environment via the passive containment cooling system). The effects of CMT cooling during this phase are temporary. Reheating and repressurization of the RCS is expected. The RCS energy distribution was judged to be the parameter of primary importance during this phase. The processes important for accurate simulation of this parameter are: core, steam generator, PRHR, and containment-to-ambient heat transfer, and loop asymmetry effects.

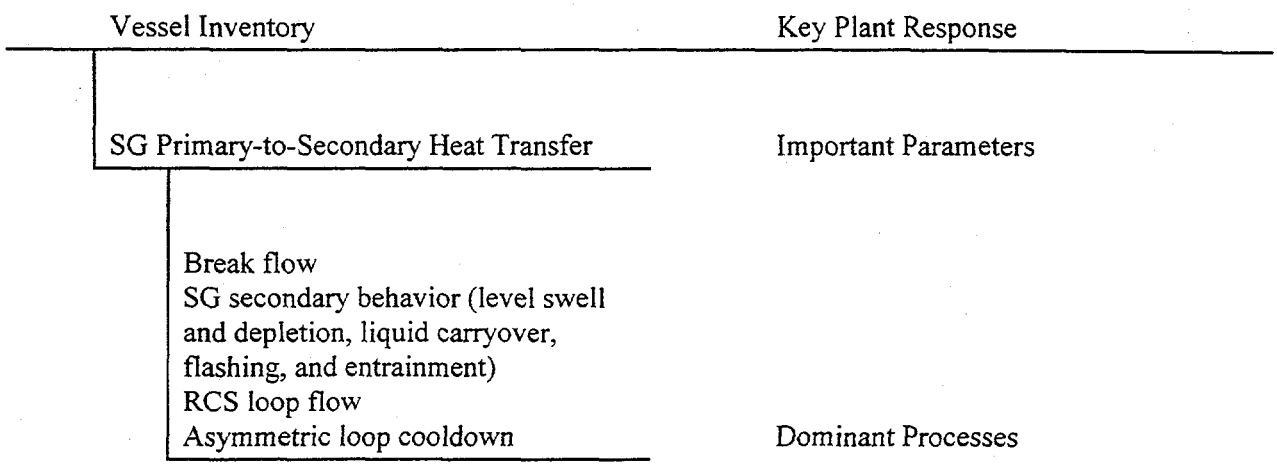

Figure 9. Ranking criteria for the MSLB initial depressurization phase.

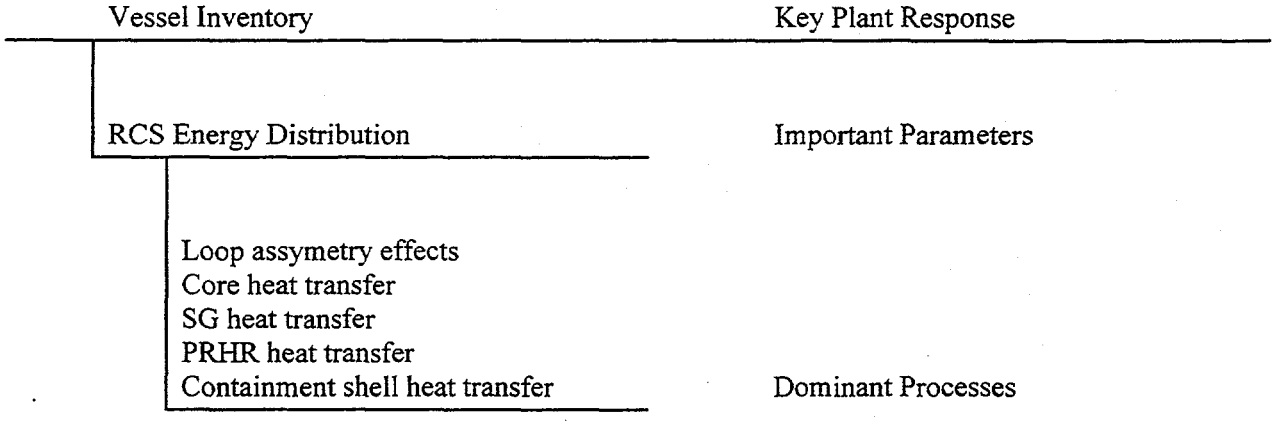

Figure 10. Ranking criteria for the MSLB passive decay heat removal phase.

Additional discussions of the MSLB-without-ADS sequence are provided in Appendix C and Reference 8-4.

3.3 Main Steam Line Break With ADS

The MSLB-with-ADS accident scenario represents the AP600 response to the double-ended rupture of one steam line, with a complicating failure to open the check valve in the discharge line of one of the CMTs. The availability of only safety-grade plant systems is assumed. The inner diameter of the ruptured steam pipe is about 29 inches, but flow limiters, located at the steam line nozzles on the steam generators, have an equivalent diameter of about 16 inches. Therefore, break flow is restricted at the flow limiters rather than at the break location. Other than being located in the containment, the break location is unspecified; it may be situated in either steam line.

A main steam line break results in an overcooling of the RCS. As the primary system fluid is cooled, it contracts, and the resulting fluid shrinkage is assumed to cause the level in the single active CMT to reach the 67.5% setpoint level that results in ADS actuation. In the MSLB-without-ADS accident scenario described in Section 3.2, it was assumed that the CMT level decline would not be sufficient to activate

ADS. This sequence assumes that an additional failure to open the check valve on one of the CMT discharge lines will lead to ADS actuation. The rationale for this assumption was that, with only one CMT active, the total fluid shrinkage of the RCS fluid will lead to a greater decline of the level in the single active CMT, thus increasing the potential for ADS actuation. Published analyses (Reference 7-3) indicate it is likely that the level decline in the active CMT will not be sufficient to initiate ADS. Those analyses evaluated AP600 response to a main steam line break event, in which bounding assumptions were applied to maximize the potential for ADS actuation. One of the bounding assumptions was the CMT discharge line check valve failure. These analyses show that, even when the bounding assumptions are employed, ADS activation is not indicated. The "with ADS" scenario has been left in to accommodate analysis of additional failures that may cause ADS to be activated.

The MSLB-with-ADS sequence was subdivided into five accident phases (see Figure 6B) that are summarized in the following paragraphs. Figures 11 through 15, sequentially, show the key plant responses, important parameters and processes identified for the five phases.

Vessel Inventory	Key Plant Response
SG Primary-to-Secondary Heat Transfer	Important Parameters
Break flow SG secondary behavior (level swell and depletion, liquid carryover, flashing, and entrainment) RCS loop flow Asymmetric loop cooldown	Dominant Processes

Figure 11. Ranking criteria for the MSLB with ADS initial depressurization phase.

Vessel Inventory	Key Plant Response
RCS Energy Distribution	Important Parameters
Loop assymetry effects Core heat transfer SG heat transfer PRHR heat transfer	Dominant Processes

Figure 12. Ranking criteria for the MSLB with ADS passive decay heat removal phase.

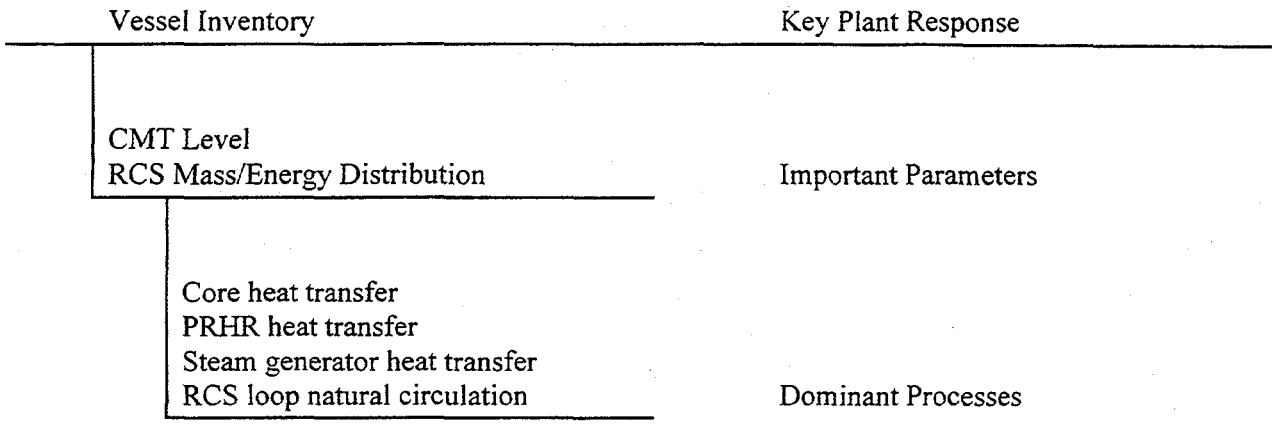

Figure 13. Ranking criteria for the MSLB with ADS CMT draining to ADS actuation phase.

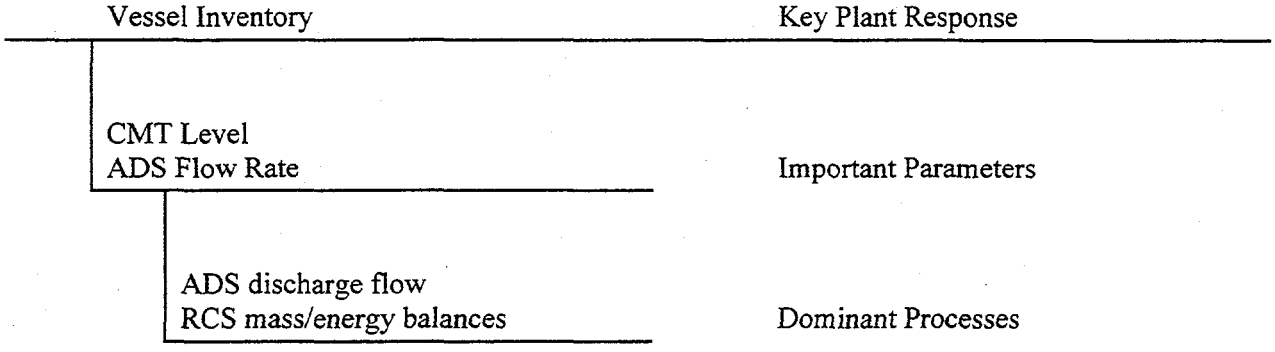

Figure 14. Ranking criteria for the MSLB with ADS blowdown phase.

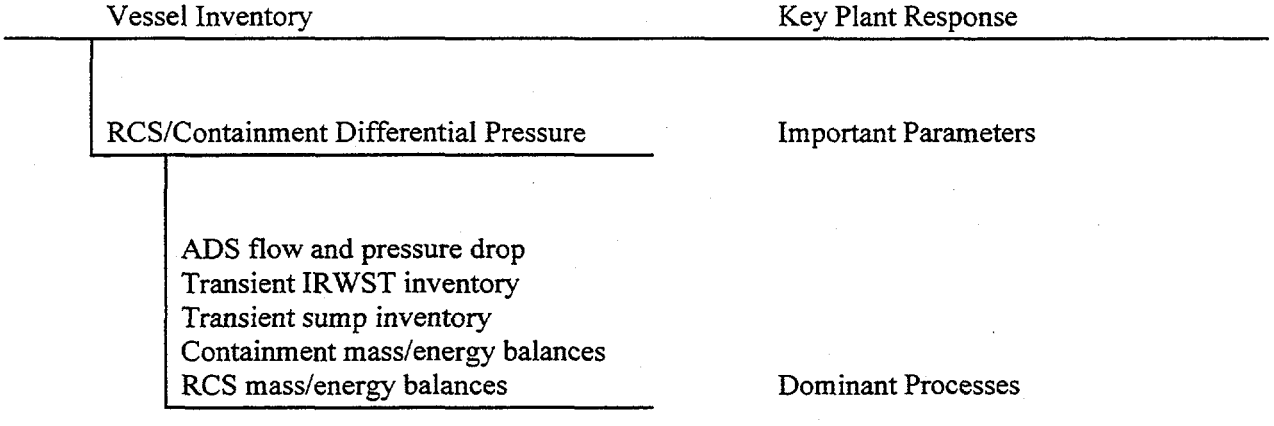

Figure 15. Ranking criteria for the MSLB with ADS IRWST and sump injection phase.

The initial depressurization phase begins at the time of the pipe break and proceeds until the time when the affected (i.e., the one connected to the broken steam line) steam generator secondary side has depressurized to the containment pressure. The reactor trip occurs during this phase. The steam line piping arrangement is such that both steam generators initially blow down through the double-ended pipe

break. However, relatively early in this phase, a steam line isolation signal is generated that blocks the path for steam from the unaffected steam generator to reach the break location. Behavior during this phase is otherwise dominated by the blowdown of the affected steam generator into the containment and the resulting overcooling of the RCS, due to heat removal across the tubes of the affected steam generator. It is noteworthy that this process is asymmetric, with significant differences in heat loads and fluid temperatures between the affected and unaffected coolant loops. The steam generator primary-to-secondary heat transfer was judged to be the parameter of primary importance during this phase because it dominates the RCS cooldown. The processes important for accurate simulation of this parameter are: break flow, steam generator secondary behavior (level swell and depletion, liquid carry-over, flashing, entrainment), flow through the primary coolant loops, and asymmetric loop cooldown.

The passive decay heat removal phase begins when the affected steam generator blowdown into the containment has been completed and proceeds until CMT recirculation ceases (due to voiding in the CMT or its inlet line). This phase is marked by natural circulation-driven coolant loop, CMT, and PRHR flows; asymmetries in RCS temperature distributions are expected. The RCS heat sources are decay heat and reverse heat transfer from the unaffected steam generator. CMT recirculation and the PRHR system are the heat sinks for the RCS. The RCS energy distribution was judged to be the parameter of primary importance because it determines the decay heat removal. The processes important for accurate simulation of this parameter are: core, steam generator, and PRHR heat transfer, and loop asymmetry effects.

The CMT draining-to-ADS actuation phase begins when CMT recirculation ceases and proceeds until the ADS actuation signal is generated (caused by the CMT level falling to 67.5%). The dominant plant behavior during this phase is the draining of the unaffected CMT. The RCS continues depressurizing, and accumulator injection is initiated during this phase. The parameters of primary importance during this phase were judged to be the CMT level, and the RCS mass and energy distributions. The processes important for accurate simulation of these parameters are: core, steam generator, and PRHR heat transfer and natural circulation in the RCS loops.

The ADS blowdown phase begins when the unaffected CMT level has fallen to 67.5% and continues until IRWST injection begins. The dominant plant behavior during this phase is accelerated RCS depressurization as the ADS valve-opening sequence proceeds. IRWST injection begins (and this phase ends) when the RCS-to-containment differential pressure is reduced below the available IRWST static head. The parameters of primary importance during this phase were judged to be the CMT level and ADS flow rate. The processes important for accurate simulation of these parameters are: ADS discharge flow (critical and friction-dominated) and RCS mass and energy balances.

The IRWST and sump injection phase begins when IRWST flow to the RCS is initiated and proceeds thereafter. The dominant plant behavior during this phase consists of gravity flow of water from the IRWST and sump into the RCS, flow from the core into the containment via the ADS fourth stage, and passive cooling of the containment to the environment. The parameter of primary importance during this phase was judged to be the RCS-to-containment differential pressure. The processes important for accurate simulation of this parameter are: transient IRWST inventory, transient sump inventory, containment energy balance, and RCS energy balance.

Additional discussions of the MSLB-with-ADS sequence are provided in Appendix D and Reference 8-4.

3.4 Steam Generator Tube Rupture Without ADS

The SGTR-without-ADS accident sequence is initiated by a double-ended rupture of a single steam generator tube at the tubesheet. The availability of only safety-grade plant systems is assumed. The accident results in the release of RCS coolant into the secondary coolant system and potentially to the atmosphere if the secondary system pressure rises sufficiently to open the steam generator safety relief valves (SRVs). A successful outcome for this accident includes not only assuring that the core is sufficiently cooled, but also assuring that any release through the SRVs is terminated. Although the break size is specified for this accident, its precise location is not. The break may be located in either steam generator, and at either the hot or cold end of the tube. Note that the break configuration results in two flow paths opening between the primary and secondary coolant systems. With the tube broken at the tubesheet, one path is from either the inlet or outlet plenum through the tubesheet into the boiler region. The other path is from the other plenum into the boiler region through the full length of the broken tube. Break flow through the first of these paths is much greater than that through the second path. The net loss of primary coolant and fluid shrinkage due to cooling may allow the level in either CMT to reach the 67.5% setpoint level that results in ADS actuation. In this scenario, it is assumed that the CMT level decline is not sufficient to activate ADS. Published analyses (Reference 7-4) have indicated that it is likely this assumption is correct. Those analyses, which studied the effects of 1, 3, 5, and 25 tubes tupturing, indicated that without additional failures, ADS actuation is not indicated.

The SGTR-without-ADS sequence was subdivided into two accident phases (see Figure 6C) that are summarized in the following paragraphs. Figures 16 and 17 show the key plant responses, important parameters and processes identified for the two phases.

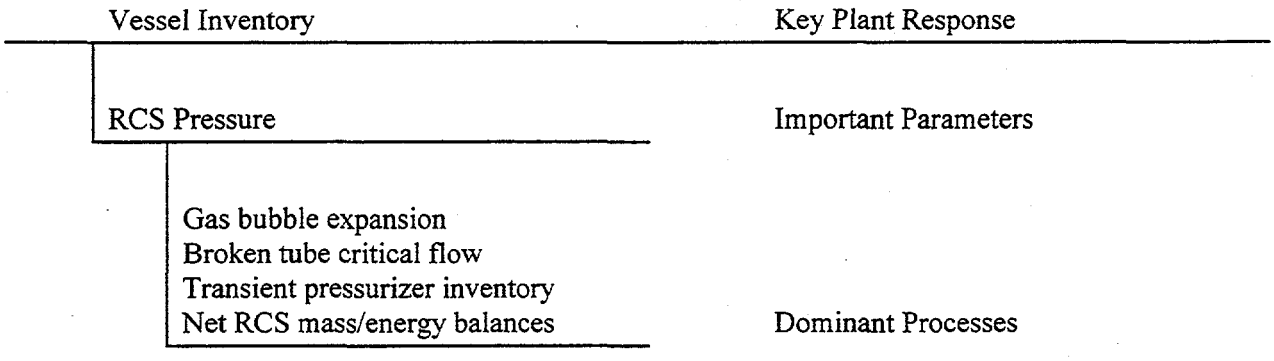

Figure 16. Ranking criteria for the SGTR initial depressurization phase.

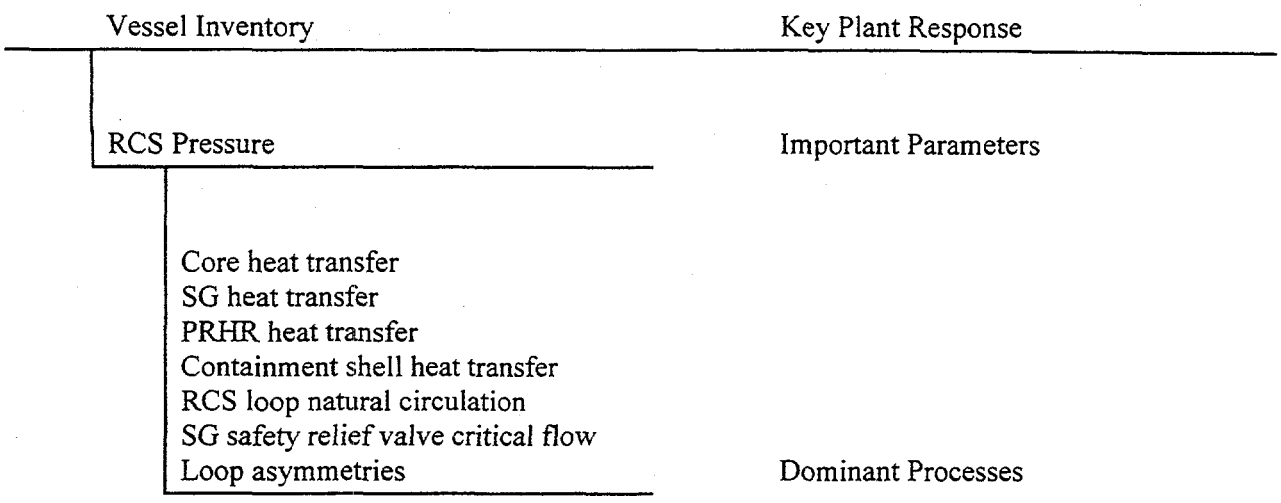

Figure 17. Ranking criteria for the SGTR passive decay heat removal phase.

The initial depressurization phase begins at the time of the tube rupture and proceeds until break flow and fluid shrinkage effects reduce the pressurizer pressure to the setpoint that generates the S signal. The reactor trip occurs during this phase. The steam generator secondary pressure rises, and the SRVs may be lifted, releasing a mixture of primary and secondary fluid to the atmosphere. The RCS pressure was judged to be the parameter of primary importance because it determines the tube rupture flow rate and generation of the S signal. The processes important for accurate simulation of this parameter are gas bubble expansion, the net RCS mass and energy balances, broken steam generator tube critical flow, and transient pressurizer inventory.

The passive decay heat removal phase begins at the time of the S signal and continues thereafter. The S signal actuates the CMT system, trips the reactor coolant pumps, and isolates feedwater. CMT system actuation also results in PRHR system actuation. This phase is marked by establishment of a final RCS/containment energy balance whereby core decay heat is removed through the PRHR and IRWST systems to containment, and from there to the environment via the passive containment cooling system. To terminate the atmospheric release, the PRHR system must be capable of removing the decay heat at a RCS pressure that is below the opening setpoint pressure of the steam generator SRVs. The RCS pressure was judged to be the parameter of primary importance during this phase because it determines the duration of the atmospheric release. The processes important for accurate simulation of this parameter are core, steam generator, PRHR and containment-to-ambient heat transfer, natural circulation in the RCS loops including asymmetries, and steam generator SRV critical flow.

Additional discussions of the SGTR-without-ADS sequence are provided in Appendix E and Reference 8-4.

3.5 Steam Generator Tube Rupture With ADS

The SGTR-with-ADS accident sequence is initiated by a double-ended rupture of a single steam generator tube at the tubesheet, with a complicating additional failure to open the check valve in the discharge line of one CMT. The availability only of safety-grade plant systems is assumed. The accident results in the release of RCS coolant into the secondary coolant system and potentially to the atmosphere if the secondary system pressure rises sufficiently to open the steam generator SRVs. A successful outcome for this accident includes not only assuring that the core is sufficiently cooled, but also assuring that any release through the SRVs is terminated. Although the break size is specified for this accident, its precise location is not. The break may be located in either steam generator, and at either the hot or cold end of the

tube. Note that the break configuration results in two flow paths opening between the primary and secondary coolant systems. With the tube broken at the tubesheet, one path is from either the inlet or outlet plenum through the tubesheet into the boiler region. The other path is from the other plenum into the boiler region through the full length of the broken tube. Break flow through the first of these paths is much greater than that through the second path.

In the SGTR-without-ADS accident scenario described in Section 3.4, it was assumed that the CMT level decline would not be sufficient to activate ADS. The SGTR-with-ADS sequence assumes that an additional failure to open the check valve on one of the CMT discharge lines is sufficient to lead to ADS actuation. The rationale for this assumption is that, with only one CMT active, the mass lost from, and fluid shrinkage of, the RCS fluid would lead to a greater decline of the level in the single active CMT, thus increasing the potential for ADS actuation. Other complicating failures that also might lead to the activation of ADS can be postulated. In particular, simply increasing the number of steam generator tubes that are assumed to rupture can be expected to lead to ADS actuation. The PIRT team dismissed using that approach because assuming rupture of multiple tubes: (1) significantly reduces the probability of sequence occurrence and (2) will result in a RCS break so large that plant response will be similar in many respects to that of the SBLOCA scenario described in Section 3.1. The "with ADS" scenario was left in to accommodate analysis of additional failures.

The SGTR-with-ADS sequence was subdivided into five accident phases (see Figure 6C) that are summarized in the following paragraphs. Figures 18 through 22, sequentially, show the key plant responses, important parameters and processes identified for the five phases.

Vessel Inventory	Key Plant Response
RCS Pressure	Important Parameters
Gas bubble expansion Broken tube critical flow Transient pressurizer inventory Net RCS mass/energy balances	Dominant Processes

Figure 18. Ranking criteria for the SGTR with ADS initial depressurization phase.

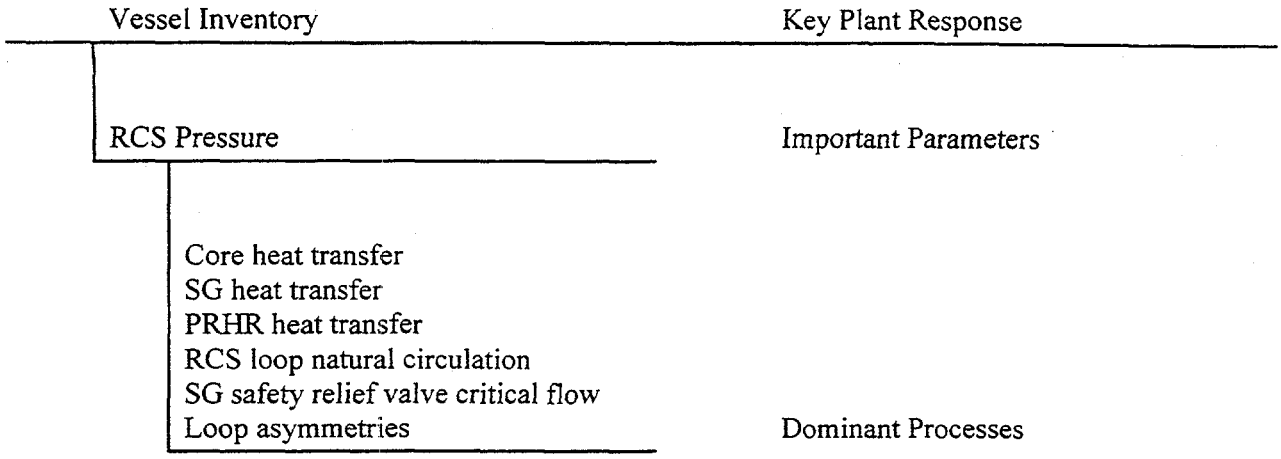

Figure 19. Ranking criteria for the SGTR with ADS passive decay heat removal phase.

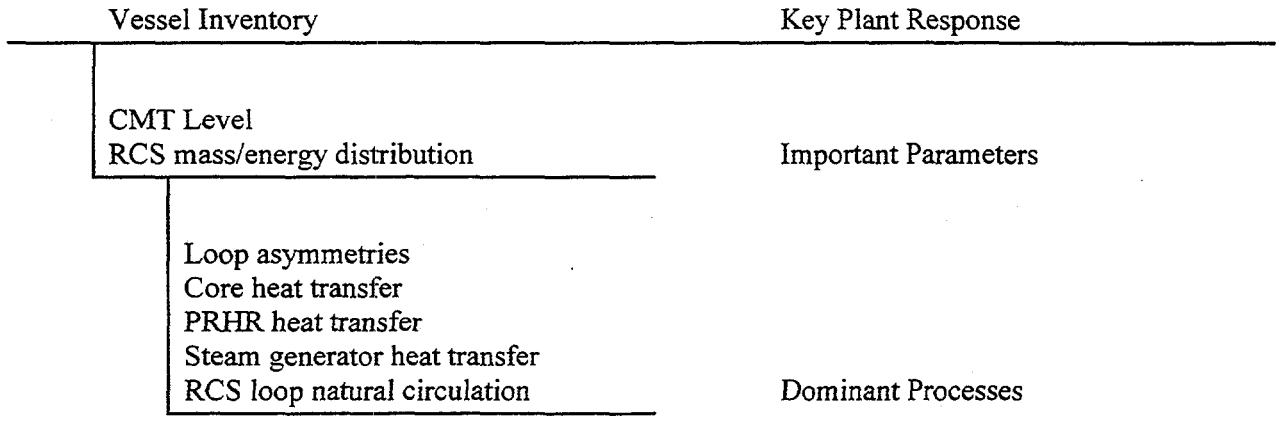

Figure 20. Ranking criteria for the SGTR with ADS CMT draining to ADS actuation phase.

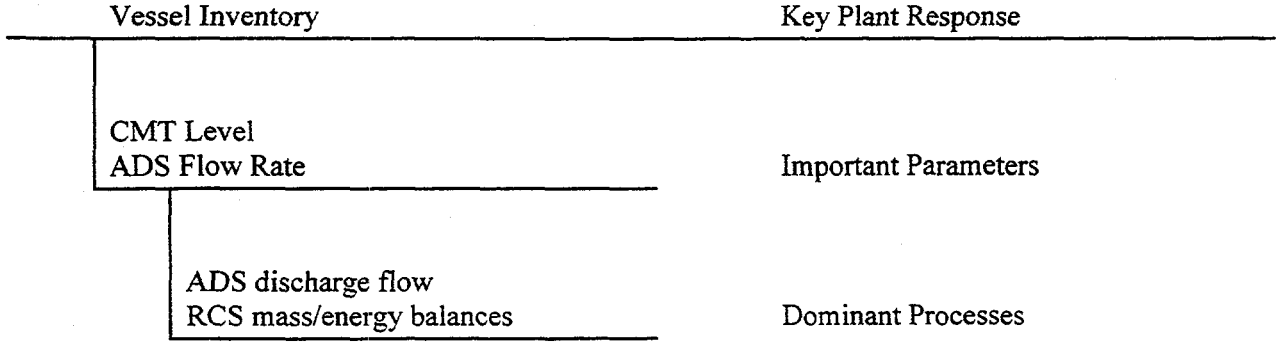

Figure 21. Ranking criteria for the SGTR with ADS blowdown phase.

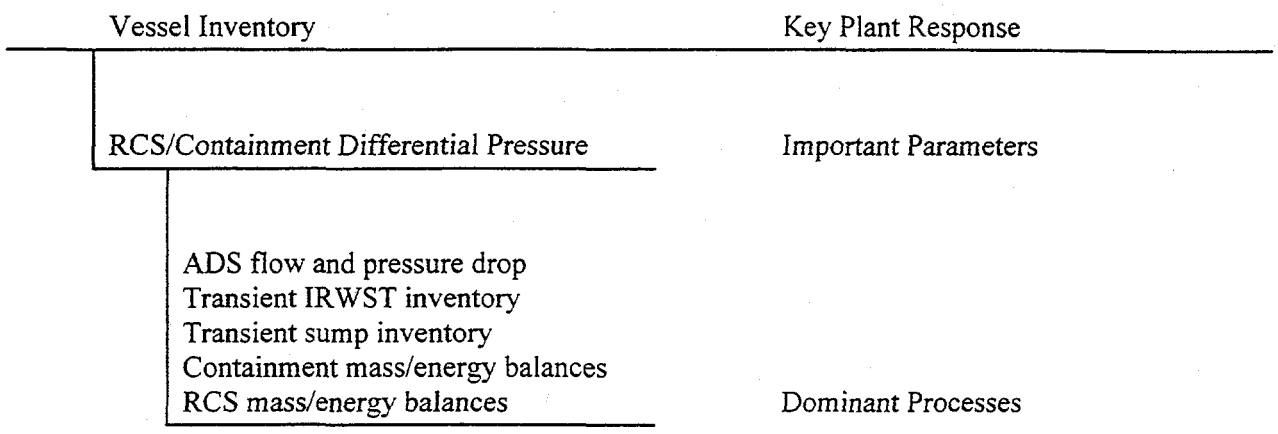

Figure 22. Ranking criteria for the SGTR with ADS IRWST and sump injection phase.

The initial depressurization phase begins at the time of the tube rupture and proceeds until break flow and fluid shrinkage effects reduce the pressurizer pressure to the pressure setpoint that generates the S signal. The reactor trip occurs during this phase. The affected steam generator secondary pressure rises and the SRVs may be lifted, releasing a mixture of primary and secondary fluid to the atmosphere. The RCS pressure was judged to be the parameter of primary importance because it determines the tube rupture flow rate and generation of the S signal. The processes important for accurate simulation of this parameter are: the net RCS mass and energy balances, broken steam generator tube critical flow, transient pressurizer inventory, and gas bubble expansion.

The passive decay heat removal phase begins at the time of the S signal and proceeds until CMT recirculation ceases (due to voiding in the CMT or its inlet line). The S signal actuates the CMT system, trips the reactor coolant pumps, and isolates feedwater. CMT actuation also results in PRHR system actuation. This phase is marked by natural circulation-driven coolant loop, unaffected CMT, and PRHR flows. Due to break and unaffected steam generator effects, asymmetries in RCS mass and energy distributions are expected. Decay heat is removed through break energy release, PRHR heat removal, and CMT recirculation. The unaffected steam generator may act as a heat source to the RCS system during this phase. The RCS pressure was judged to be the parameter of primary importance during this phase because it determines the duration of the atmospheric release through the affected steam generator SRVs. The processes important for accurate simulation of this parameter are: core, steam generator, and PRHR heat transfer, natural circulation in the RCS loops including asymmetries, and steam generator SRV critical flow.

The CMT draining-to-ADS actuation phase begins when unaffected CMT recirculation ceases and proceeds until the ADS actuation signal is generated (caused by the CMT level falling to 67.5%). The dominant plant behavior during this phase is the draining of the unaffected CMT. The parameters of primary importance during this phase were judged to be the CMT level and the RCS mass and energy distributions. The processes important for accurate simulation of these parameters are: core, steam generator, and PRHR heat transfer and natural circulation in the RCS loops including asymmetries.

The ADS blowdown phase begins when the unaffected CMT level has fallen to 67.5% and continues until IRWST injection begins. The dominant plant behavior during this phase is accelerated RCS depressurization as the ADS valve-opening sequence proceeds. IRWST injection begins (and this phase ends) when the RCS-to-containment differential pressure is reduced below the available IRWST static head. It is noteworthy that, during this and the following phase, the break flow (i.e., that through the two flow paths of the broken tube) is expected to reverse. This reverse break flow will result in mass and

energy additions to the RCS. The parameters of primary importance during this phase were judged to be the CMT level and ADS flow rate. The processes important for accurate simulation of these parameters are: ADS discharge flow (critical and friction-dominated) and RCS mass and energy balances.

The IRWST and sump injection phase begins when IRWST flow to the RCS is initiated and proceeds thereafter. The dominant plant behavior during this phase consists of gravity flow of water from the IRWST and sump into the RCS, flow from the core into the containment via the ADS fourth stage, and passive cooling of the containment to the environment. The parameter of primary importance during this phase was judged to be the RCS-to-containment differential pressure. The processes important for accurate simulation of this parameter are: ADS flow and pressure drop, transient IRWST inventory, transient sump inventory, containment mass and energy balances, and RCS mass and energy balances.

Additional discussions of the SGTR-with-ADS sequence are provided in Appendix F and Reference 8-4.

4. RESULTS

Table 1 provides a condensation of the master PIRT tables for all accident scenarios investigated in this report. The accident phases (numbered 1 through 5 near the top of the table) correspond to the chronological order of phases described for the accident scenarios in Appendixes B through F. Note that the actual phase names and definitions vary among the scenarios.

The detailed PIRT results are found in the following appendixes of this report:

Accident	Results presented in
Small break loss-of-coolant accident	Appendix B
Main steam line break	Appendix C
Main steam line break with failure leading to ADS actuation	Appendix D
Steam generator tube rupture	Appendix E
Steam generator tube rupture with failure leading to ADS actuation	Appendix F

For each accident, the key results are displayed in the master tables at the beginning of the corresponding appendix. A separate table is used for each accident phase. The left sides of the master tables show all phenomena that were ranked high, medium, or low. The tables are organized alphabetically by component name (with the exception that containment components are listed last). Within each component listing, the high-ranked phenomena (shown as "H" in the tables) are shown first, the medium-ranked phenomena ("M") second, and the low-ranked phenomena ("L") third.

The right sides of the master tables refer the reader to information supporting the selection and ranking of the phenomena and to background information. The most important of the supporting information is the specific phenomena ranking rationale that is referenced by an "R" code. The table where this information is found is listed at the top of the ranking rationale column; in each appendix, this ranking rationale table immediately follows the master PIRT tables. The remaining codes refer the reader to background information: phenomena definitions, component descriptions, component-specific phenomena considerations, analytical and experimental supporting information, and possible relationships among phenomena. A common set of PIRT background information is used for all accident scenarios; this information is provided in Appendix G and the appropriate reference tables for the background information codes are shown at the tops of the columns in the master PIRT tables.

Table 1. Summary of PIRT results.

Component	Phenomena	SBLOCA		MSLB w/o ADS		MSLB with ADS					SGTR w/o ADS		SGTR with ADS				
		1	2	1	2	1	2	3	4	5	1	2	1	2	3	4	5
Accumulators	Flow	H							H							H	
	Noncondensible effects	M	L						M							M	
ADS	Energy release	H	H						H	H						H	H
	Mass flow	H	H						H	H						H	H
	Choking in complex geometry	M															
	Flow resistance	M							M	M						M	M
	Noncondensible effects	M	L						M	L						M	L
	Condensation in stages 1, 2, and 3 ADS and spargers (in IRWST)	L	L														
Break	Choking in complex geometries										H	H	H	H	M	M	M
	Energy release	M	M	H		H					M	H	M	H	H	M	M
	Flow resistance	M	L	L		L					M	M	M	M	M	L	L
	Mass flow	H	M	H		H					H	H	H	H	H	M	M
	Noncondensible effects	L	L														
Cold legs	Condensation	L	L							L							L
	Flashing	M							L						L	L	
	Loop asymmetry effects	L		M		M		M							M		
	Noncondensible effects	L	L						L	L						L	L
	PBL-to-cold legs tee phase separation	H	L											H	H	L	
	Stored energy release	L	L	L		L			L			L		L		L	
	Thermal Stratification	M															
Core	Boiling	M	M														
	Core channeling			H	L	H	L										
	Flashing	H	L	M	M	M	M		M						L	M	
	Flow resistance	L	L		L		L	L		M		L		L	L		M
	Loop asymmetry effects	L	L											L	L		
	Mass flow, including bypass	M	M												L		
	Noncondensible effects			L		L	L										
	Stored energy release	M	M	L		L			L			L		L		L	
	Subcooling margin	H	M									M		M			
	Two-phase mixture level	H	H						H	H						H	H
	Voiding			M	M	M	M										
CMT	CMT-to-loop differential density	M		L	L	L	M					M		H			
	CMT-to-IRWST differential head	M	M														
	Condensation	M	M					L							L		
	Flashing	M							L						M	L	
	Flow resistance	H	L		L		L	L				L		M	L		
	Level	H			M			H	H			M			H	H	
	Noncondensible effects	L	M	L	L	L	L										
	Thermal stratification and mixing	M		L		L	M	L	L			M		M	L	L	
	Voiding				L		M										
Downcomer/lower plenum	Condensation	M	M							M				L	L	L	M
	Flashing	L							L							L	
	Flow distribution	L			L		L	L									
	Level	M	H						L	H					L	L	H
	Loop asymmetry effects	L	L	M		M								M	M		
	Noncondensible effects	L							L							L	
	Stored energy release	L	L	L		L			L			L		L		L	
Fuel rods	Boron reactivity feedback			L		M											
	CHF/dryout	M	L	M		M											
	Core power/decay heat	H	H	H	H	H	H	H	H	H	H	H	H	H	H	H	H
	Moderator temperature feedback			L		M											

Table 1. (continued).

Component	Phenomena	SBLOCA		MSLB w/o ADS		MSLB with ADS					SGTR w/o ADS			SGTR with ADS			
		1	2	1	2	1	2	3	4	5	1	2	1	2	3	4	5
Fuel rods (cont'd)	Stored energy release	M		L		L			L		L	L	L	L		L	
Hot legs	CCFL	L							M	M						M	M
	Condensation	L	L														
	Countercurrent flow	L	L						M	M						M	M
	Entrainment	L	M						M							M	
	Flashing	M		M		M		L	M			M		M	L	M	
	Horizontal fluid stratification	L	M					M	M	M					M	M	M
	Loop asymmetry effects	L		M		M						M		M			
	Noncondensible effects	L		L	M	L	M		L							L	
	Phase separation in tees	H			M		M	L	H	H					L	H	H
	Stored energy release	L		L		L		L	L			L		L		L	
	Voiding	L		M	M	M	M					M		M			
IRWST	Discharge line flashing									M							M
	Flow and temperature distribution in PRHR bundle region	L			M		M	M				M		M	M		
	Flow resistance	H	H							M							M
	Interphasic condensation	L	L		L		L	L	M			L		L	L	M	
	Pool flow	M			L		L	L	M			L		L	L	M	
	Pool level	L	H		M		M	M	L	M		M				L	M
	Pool to tank structure heat transfer	L	L						L	L						L	L
	Pool thermal stratification	M	H	L	M	L	M	M	L	M		M		M	M	M	M
	Sparger pipe level	M	L														
Pressurizer	Condensation				L												
	CCFL	L							M							M	
	Entrainment/de-entrainment	M							M							M	
	Flashing	M		M		M					H	M	H	M			
	Heater power										H		H				
	Level (inventory)	H	M	M	M	M	M	M			H	M	H	M			
	Level swell	M							M							M	
	Noncondensible effects	L		L	M	L	M		L		L	L	L	L		L	
	Stored energy release	L							L		L		L			L	
	Vapor space behavior			M	M	M	M				H		H				
PRHR	Condensation	L		M	M	M						M		M	M		
	Differential density	L		M	M	M	M	M	L			M		M	M	L	
	Flow resistence	L			M		M	M	L			M		M	M	L	
	Flashing	L							L							L	
	Heat transfer between PRHR and IRWST	M		M	H	M	H	H	M	L		H		H	H	M	L
	Noncondensible effects	L		M	M	M	M	M	L			M		M	M	L	
	Phase separation in tees	L							L							L	
	Voiding	L		M	M	M	M	M				M		M	M		
Pumps	Coastdown performance	L		H		H						L		L			
	Flow resistance	L		L	L	L	L	L				L		L	L		
	Mixing	L															
Steam generators	Asymmetric behavior				M		M	M									
	Condensation in U-tubes											L		L	L		
	Noncondensible effects				M		M	M									
	Primary to secondary heat transfer	M	L		M		M	M	L	L	H	H	H	H	H	L	L
	Secondary level	L			L		L	L				M		M	M	L	L
	Secondary pressure	L			L		L	L			M	M	M	M	M	L	L
	SRV energy release										M	H	M	H	H		
	SRV mass flow										M	H	M	H	H		
	Tube voiding	L			M		M	M				M		M	M		

Table 1. (continued).

Component	Phenomena	SBLOCA		MSLB w/o ADS		MSLB with ADS					SGTR w/o ADS		SGTR with ADS				
		1	2	1	2	1	2	3	4	5	1	2	1	2	3	4	5
Steam generator(primary)	Noncondensible effects			L		L											
	Preferential loop cooldown			H		H											
	Primary to secondary heat transfer			H		H											
	Thermal driving head			M		M											
	Voiding (unaffected loop)			M		M											
Steam generator(secondary)	Entrainment			H		H											
	Flashing (SG and feedwater line)			H		H											
	Level swell and depletion			H		H											
	Tube dryout (affected SG)			M		M											
Steam generator (separator/dryer)	Liquid carry-over			H		H											
Sump	Discharge line flashing									M							M
	Flow resistance		M							M							M
	Fluid temperature		H							M							M
	Level	M	H							M							M
Upper head/upper plenum	Condensation	L	L														
	Entrainment/de-entrainment	M	M						M	H						M	H
	Flashing	L		M		M			M			M		M	L	M	
	Flow split(upper plenum)			M	M	M	M										
	Loop asymmetry effects	L		M		M						M		M			
	Noncondensible effects	L	L														
	Stored energy release	L		L		L			L			L		L		L	
	Two-phase level in upper plenum	L	H														
	Upper head/downcomer bypass flow	L															
	Vapor space compression				M												
	Voiding	M		M	M	M	M	M								L	M
Containment (interior)	Condensate transport			L	M	L	L	L	L	M		M				L	M
	Condensation			L	M	L	L	L	M	M		M				M	M
	Interior to wall heat transfer			M	H	M	L	L	M	H		H				M	H
	Liquid distribution	M	M	L	M	L	L	L	L	M		M				L	M
	Liquid holdup			L	M	L	L	L	L	M		M				L	M
	Liquid subcooling	L	L														
	Natural convection			L	M	L	L	L	L	M		M				L	M
	Noncondensible effects			L	M	L	L	L	L	M		M				L	M
	Nonuniform steam/air distribution			L	M	L	L	L	L	M		M				L	M
	Noncondensible segregation			L	M	L	L	L	L	M		M				L	M
	Passive heat sink			M	M	M	L	L	M	M		M				M	M
	Pressure	M	M														
	Steam-noncondensible mixing			L	M	L	L	L	L	M		M				L	M
Containment (exterior)	Air flow				M				L	M		M				L	M
	Atmospheric temperature				M				L	M		M				L	M
	Chimney effects				M				L	M		M				L	M
	Exterior to ambient heat transfer			L	H	L	L	L	M	H		H				M	H
	Humidity				M				L	M		M				L	M
	PCCS evaporation				M				M	M		M				M	M
	PCCS water flow				M				L	M		M				L	M
	PCCS wetting				M				L	M		M				L	M
	PCCS mixture convective heat transfer				M				L	M		M				L	M
	Radiation heat transfer				M				L	M		M				L	M

5. RELATED ACTIVITIES

Section 5.1 discusses the results of RELAP5 AP600 SBLOCA plant analyses and code capabilities particularly pertinent to this PIRT. Section 5.2 discusses investigations into facility scaling that are related to this PIRT. Section 5.3 evaluates the MSLB and SGTR PIRTS based on SBLOCA experience.

5.1 RELAP5 AP600 SBLOCA Plant Analysis Activities

Analyses using RELAP5/MOD3.2.1.2 and models of the AP600 and experimental facilities at SPES, OSU, and ROSA have been used to assess RELAP5's ability to represent significant AP600 transient phenomena and to confirm PIRT rankings. These analyses have been grouped into three main areas: short-term behavior, long-term behavior, and PIRT specific sensitivity studies.

5.1.1 AP600 SBLOCA Short-term Behavior

Code capabilities for predicting the important AP600 SBLOCA PIRT short-term phase phenomena were assessed using test data from the ROSA, SPES, and OSU integral effects experimental facilities. The short-term phase extends from the time the break opens until steady In-Containment Refueling Water Storage Tank (IRWST) injection flow is established. These capabilities were evaluated for three different AP600 SBLOCA scenarios initiated by: a 1-in. diameter cold leg break, a double-ended Direct Vessel Injection (DVI) line break and a 2-in. diameter Pressure Balance Line (PBL) break. Overall assessment results were compiled by combining the assessment results from among the various accident scenarios, phases, and experimental facilities. The integral effects assessments indicate that the code has the capability to acceptably predict all of the AP600 SBLOCA PIRT high-ranked phenomena as observed in the experiments. Additional information may be found in Reference 8-5.

In review of the PIRT rankings based on these analyses, only one phenomena was recommended for a different ranking. Core flow resistance, previously rated high, is only a small part of the total resistance that flow through the core has to overcome. In fact, it is two orders of magnitude smaller than the resistances of the recirculation loops. Accordingly, phenomena is now rated as low.

5.1.2 AP600 SBLOCA Long-Term Behavior

Analyses were performed to investigate the response of AP600 during the long-term phase of SBLOCA transients. The long-term phase is defined as the remainder of the IRWST injection period and the sump injection period. The analyses used test data from OSU integral effects experiments for the three accident scenarios: a 1-inch diameter cold leg break, a double ended break in a direct vessel injection line, and a 2-inch diameter break in a pressure balance line leading to a CMT. Analyses using a simplified Long Term Cooling Model of both the OSU facility and the AP600. The AP600 containment was modeled simply, using a combination of control volumes and boundary conditions. Bounding sensitivity calculations were performed to investigate the effects of containment pressure, condensate temperature, fraction of condensate from the containment shell to the sump as opposed to the IRWST, and the amount of liquid flowing into dead-end rooms in the containment on long term behavior.

Overall RELAP5/MOD3 version 3.2.1.2 and the LTCMs represented the long term phase of the data reasonably well and was shown to be capable of predicting most of the important phenomena during the long-term phase. There were no recommendations for changes to the PIRT rankings, other than to include IRWST temperature with Sump temperature as a single phenomena in the long term PIRT. Additional information may be found in Reference 7-5.

5.1.3 PIRT Specific Sensitivity Analyses

Six sensitivity analyses were performed as part of a systematic assessment of the PIRT rankings. Each sensitivity was performed using the simplified AP600 RELAP5 model to calculate a 1-inch diameter cold leg SBLOCA. The six sensitivities performed were ADS actuation, flow resistance, ADS4 entrainment, Cold Leg condensation, CMT condensation, and PRHR heat removal. Results of these sensitivity studies were compared to a base case calculation with respect to the figure-of-merit (FOM), minimum vessel inventory. Additional information on these studies can be found in Reference 7-6.

Results of these sensitivity studies showed no core heatup, recovery of core inventory and limited changes in the minimum reactor vessel inventory for realistic variations in the parameters of interest. Only the CMT condensation sensitivity showed a moderate effect on minimum vessel inventory, confirming its ranking in the PIRT.

5.2 AP600 Experimental Facility Scaling

Top-down scaling analyses were performed to evaluate the global system behavior of the experimental data base used for the integral effects code assessments facility. The top-down scaling analyses had three objectives. First, the analyses were performed to determine the sufficiency of the integral test data base for code assessment. The evaluation criterion for sufficiency was whether the expected AP600 behavior is bounded by that observed in the test data. Second, the analyses were performed to determine the relevancy of the data. The evaluation criterion for relevancy was typicality; if the test behavior was typical of AP600, then it was relevant. Third, the analyses were performed to uncover, through comparisons between test data and the corresponding code calculations of the tests, any biases included in the code calculations that pertained to code calculations of AP600 accident behavior. A top-down scaling methodology to attain these objectives was developed and applied. Additional discussion of scaling can be found in Appendix H and in References 7-7 and 7-8.

The results of the top-down scaling analyses indicate that the integral experiment data base is sufficient to justify extending the experimental code assessment results to AP600. The analyses demonstrate that the experimental data base provided by the integral test data encompasses the important phenomena and ranges expected of AP600 during a SBLOCA as defined by the PIRT. While each of the experimental facilities has known sources of distortions, none of these was found to cause the data from any of the facilities to be irrelevant for AP600. The scaling analysis considered these known distortions and included their effects in the data-collapsing process.

Review of the PIRT rankings from a scaling standpoint brought out one significant comment. Break flow, rated high, is less significant to system behavior and minimum vessel inventory than ADS flow and should be rated medium.

5.3 MSLB/SGTR PIRT Evaluation

This section discusses the applicability of the SBLOCA PIRT to MSLB and SGTR transients. The SBLOCA, as documented in this report, was approached systematically, using experimental data and computer code calculations. Additional SBLOCA sensitivities were also performed to confirm the PIRT rankings. This systematic approach was not undertaken for the MSLB and SGTR transients under the assumption that these transients do not lead to activation of the depressurization sequence in AP600 and that key phenomena characteristic for AP600 accident system response was similar for the three transient types.

The current SBLOCA PIRT focuses on a reduced number of phases; only short term and long term phases were considered. The MSLB and SGTR scenarios were divided into more detailed phases for which their PIRTs were developed. This section discusses both scenarios in terms of the original PIRT phases discussed in Sections 3.2 through 3.5 and Appendices C through F. This section evaluates the identified PIRT highly ranked phenomena in light of the more detailed SBLOCA findings. The evaluation is based solely on judgement and was not supported with analyses of any MSLB or SGTR experiments, nor with AP600 sensitivity analyses with the newest code version.

As stated previously, when the MSLB/SGTR PIRTs were developed, it was unclear whether either transient would activate ADS. Studies to date (References 7-3 and 7-4) indicate neither transient will actuate ADS. However, both MSLB and SGTR with ADS transients are incorporated in this report as they are pertinent for cases where multiple additional failures are assumed.

5.3.1 Main Steam Line Break without ADS

This transient, discussed in Section 3.2 and Appendix C, differs significantly from the SBLOCA transients because there is no breach of the primary system. In particular, the initial depressurization phase is governed by different processes than the initial depressurization phase of a SBLOCA. The coolant mass inventory does not change in this scenario, although rapid cooling and shrinkage of the primary coolant will cause the coolant levels in the vessel to decrease.

Initial Depressurization Phase

With respect to the vessel inventory, steam generator primary-to-secondary heat transfer is the most important parameter during this phase. This heat transfer controls the pressure of the primary system and shrinkage of the primary coolant as heat is removed through the affected steam generator. This process differs markedly from a SBLOCA and its phenomenology (particularly break flow and steam generator secondary behavior cannot be confirmed by SBLOCA experiments and analyses.

Passive Decay Heat Removal Phase

The most important parameter during this phase is the RCS energy distribution. The dominant processes that controlled this phase were loop asymmetry effects, core heat transfer, steam generator heat transfer, PRHR heat transfer and containment shell heat transfer. This phase is similar to a SBLOCA later portion of the high pressure phase when the PRHR removes heat from the primary system and a recirculation of the CMT occurs. For this phase, only decay heat and PRHR-to-IRWST heat transfer were ranked high. The SBLOCA PIRT also rates these phenomena high and this experience is directly applicable to the MSLB transient since these phenomena define the essential energy input and output for both transients.

The SBLOCA PIRT also rates CMT related phenomena such as thermal stratification and level high. CMT behavior is very important and determines if and how the automatic depressurization sequence occurs. Therefore, although SBLOCA experience is applicable for the MSLB, CMT phenomena may need to be ranked higher.

5.3.2 Main Steam Line Break with ADS

This transient is similar to the transient discussed in Section 5.3.1; however, it is assumed that the overcooling induced by the steam line rupture is sufficient to shrink the primary coolant to levels allowing activation of the ADS. To maximize coolant shrinkage, only one CMT is assumed to drain. Previous analyses have shown that even with this assumption, it is unlikely that a MSLB will lead to ADS

activation. No new analyses were performed. More information on this transient is included in Section 3.3 and Appendix D.

Initial Depressurization Phase

This phase is defined as in Section 5.3.1 and is dominated by primary-to-secondary heat transfer. This phase is not typical of a SBLOCA and the results of those studies are not directly applicable.

Passive Decay Heat Removal Phase

Energy distribution was judged to be the most important parameter during this phase. Only decay heat and PRHR-to-IRWST heat transfer were ranked high. The MSLB system behavior is similar to the SBLOCA system behavior in the later portion of the high pressure phase before ADS activation. Both phenomena were also ranked high in the SBLOCA PIRT. The MSLB transient may also depend on which steam generator and which CMT is affected, signifying asymmetric effects.

The coolant shrinkage and associated level drop in the reactor vessel and cold legs will be different from those in the SBLOCA, where mass is removed through the break and flashing occurs in the upper plenum. The processes leading to CMT draining will therefore be different in these two transients. Recognition of the higher importance of CMT related phenomena is applicable to the MSLB.

CMT Draining to ADS Actuation Phase

The behavior of the unaffected CMT and the energy distribution (decay heat and PRHR-to-IRWST heat transfer were judged the most important parameters affecting this phase. In SBLOCA these same parameters are similarly important. The SBLOCA analyses have shown that the steam generator in the CMT loop has a determining effect on CMT draining. In a MSLB, this effect may be even more pronounced depending on which steam generator is affected. Based on the SBLOCA analyses, the addition of voiding/draining behavior of SG-C to the high ranked phenomena is recommended.

ADS Blowdown Phase

The MSLB PIRT ranks the accumulator noncondensible effects, ADS energy and mass release, two-phase mixture level in the core, CMT level, decay heat, and phase separation in tees as high. This phase of the MSLB is very similar to the ADS blowdown phase in SBLOCA. The transient is dominated by the processes associated with coolant and energy depletion through the ADS valves. The effects of steam generators, PRHR or breaks is secondary. It is judged that the SBLOCA phenomena during this phase are representative enough for the MSLB transient and thus the SBLOCA PIRT rankings can be directly adopted.

IRWST and Sump Injection Phase

For this phase, the effects of the transient initiator (the MSLB) are overridden by the ADS actuation and blowdown. Thus, the transient has similar characteristics to the SBLOCA transient. The dominant phenomena and their importance are the same. This phase of the MSLB is fully confirmed by SBLOCA experience.

5.3.3 Steam Generator Tube Rupture without ADS

The SGTR transient evaluated in this report (Section 3.4 and Appendix E) assumes a double ended rupture of a single steam generator tube at the tube sheet. The phenomena are ranked with regard to vessel inventory. The scenario assumes that RCS coolant loss through the break and coolant shrinkage are not sufficient to reduce the level in the CMT to initiate the ADS sequence.

Initial Depressurization Phase

The most important parameter in this phase is RCS pressure which controls the break flow. In SBLOCAs, the breaks are located in different places, so the results of the SBLOCA analyses and experiments are not directly applicable and cannot be used to confirm the importance of choking or the effects of the SGTR's complex flow paths. The break mass flow rate controls the events very early in the transient and should be ranked high. The pressurizer will control the RCS more in a SGTR event because the break is smaller and the discharge occurs against higher pressure; thus the pressurizer phenomena is more important in this transient. Primary-to-secondary heat transfer also plays a more important role in a SGTR event because the process is removes more energy that the break. In SBLOCA, the reverse is true. Therefore, the ranking of this heat transfer mechanism for SGTRs cannot be confirmed by the SBLOCA analyses.

Passive Decay Heat Removal Phase

In this phase, flow of primary coolant into the affected steam generator continues. The energy from the RCS is removed by PRHR, CMT, and break flow. The flow distribution and processes within the RCS are sufficiently different from SBLOCA processes that the SGTR cannot be directly confirmed by the SBLOCA PIRT analyses. Phenomena associated with the affected steam generator, such as break flow, Safety Relief Valve mass, and energy release, are exceptionally unique for this transient.

Containment heat transfer, rated high for this phase, should not be too different from the SBLOCA containment heat transfer; therefore it is recommended that this phenomenon's ranking be downgraded in the future. Also, the experience of SBLOCA indicated that entrainment and de-entrainment in the upper plenum is less important than previously judged. This experience is applicable to the SGTR event and these rankings are recommended for downgrading.

5.3.4 Steam Generator Tube Rupture with ADS

The Steam Generator Tube Rupture event discussed in Section 3.5 and Appendix F assumed that one of the CMT check valves failed and the CMT did not drain. The unaffected CMTs draining was enhanced and lead to ADS actuation.

Initial Depressurization Phase

This phase is similar to the first phase of the SGTR without ADS (Section 5.3.3) and all comments are applicable to this event as well.

Passive Decay Heat Removal Phase

This phase is similar to the second phase of the SGTR without ADS (Section 5.3.3) and all comments are applicable to this event as well.

CMT Draining to ADS Actuation Phase

Recirculation through the CMT is interrupted at the beginning of this phase and draining begins. This draining eventually leads to ADS actuation. The draining process in this SGTR event is very similar to the draining in any transient. The experience of SBLOCA is directly applicable.

ADS Blowdown Phase

This phase in the SGTR transient is very similar to the ADS blowdown phase in SBLOCA. The transient is dominated by processes associated with coolant and energy depletion through the ADS valves. Effects of the steam generators, PRHR, or break are secondary. SBLOCA phenomena for this phase are enough representative and the PIRT rankings can be used.

IRWST and Sump Injection Phase

For this phase, the effects of the transient initiator (SGTR) are overridden by ADS blowdown and the transient becomes very similar to the long term phase of SBLOCA, with the same dominant processes and phenomena. This part of the SGTR transient is fully confirmed by the SBLOCA analyses.

6. SUMMARY

PIRT activities have been completed for AP600 response to SBLOCA, MSLB, and SGTR accident scenarios. In particular, the PIRT for the SBLOCA accident scenario has been further developed based on new evidence from AP600-related experimental test facilities, AHP and scaling analyses, and additional thermal-hydraulic expert review. The findings from these PIRTs may be used to provide general guidance for the focussing of research efforts. These findings are summarized in Table 1 (that is presented in Section 4).

Many users of this PIRT may find the summary information in Table 1 more useful if it is rearranged in different ways. The following tables are included for that purpose:

Table 2 summarizes the PIRT findings with the phenomena sorted alphabetically by phenomena name. The number of occurrences of high, medium, and low rank shown in this table are the sum of all such occurrences among the 16 phases comprising the 5 accidents evaluated in this PIRT.

Table 3 summarizes the PIRT findings with the phenomena sorted alphabetically according to component name. The number of occurrences of high, medium, and low rank shown in this table are the sum of all such occurrences among the 16 phases comprising the 5 accidents evaluated in this PIRT.

Finally, the PIRT findings are summarized with the phenomena sorted by the number of occurrences (again, with a maximum of 16) at each particular rank. Tables 4, 5, and 6 show this information for high-, medium-, and low-ranked phenomena, respectively.

The components, phenomena, and rankings shown in Tables 1 through 6 are identical; these tables differ only in the manner in which the information is sorted and presented.

Table 2. AP600 PIRT summary - frequency of occurrence of ranks sorted by phenomena.

Phenomena	Component	Frequency at Indicated Rank		
		High	Medium	Low
Air flow	Containment (exterior)	0	4	2
Asymmetric behavior	Steam generators	0	3	0
Atmospheric temperature	Containment (exterior)	0	4	2
Boiling	Core	0	2	0
Boron reactivity feedback	Fuel rods	0	1	1
CCFL	Hot legs	0	4	1
	Pressurizer	0	2	1
CHF/dryout	Fuel rods	0	3	1
Chimney effects	Containment (exterior)	0	4	2
Choking in complex geometries	Break	4	3	0
Choking in complex geometry	ADS	0	1	0
CMT-to-IRWST differential head	CMT	0	2	0
CMT-to-loop differential density	CMT	1	3	3
Coastdown performance	Pumps	2	0	3
Condensate transport	Containment (interior)	0	4	6
Condensation	CMT	0	2	2
	Cold legs	0	0	4
	Containment (interior)	0	6	4
	Downcomer/lower plenum	0	4	3
	Hot legs	0	0	2
	Pressurizer	0	0	1
	PRHR	0	6	1
	Upper head/upper plenum	0	0	2
Condensation in stages 1, 2, and 3 ADS and spargers (in IRWST)	ADS	0	0	2
Condensation in U-tubes	Steam generators	0	0	3
Core channeling	Core	2	0	2
Core power/decay heat	Fuel rods	16	0	0
Countercurrent flow	Hot legs	0	4	2
Differential density	PRHR	0	8	3
Discharge line flashing	IRWST	0	2	0
Discharge line flashing	Sump	0	2	0
Energy release	ADS	6	0	0
	Break	5	6	0
Entrainment	Hot legs	0	3	1
Entrainment	Steam generator(secondary)	2	0	0
Entrainment/de-entrainment	Pressurizer	0	3	0
	Upper head/upper plenum	2	4	0
Exterior to ambient heat transfer	Containment (exterior)	4	2	4
Flashing	CMT	0	2	2
	Cold legs	0	1	3
	Core	1	6	2
	Downcomer/lower plenum	0	0	3
	Hot legs	0	7	2
	Pressurizer	2	5	0
	PRHR	0	0	3

Table 2. (continued).

Phenomena	Component	Frequency at Indicated Rank		
		High	Medium	Low
Flashing	Upper head/upper plenum	0	6	2
Flashing (SG and feedwater line)	Steam generator(secondary)	2	0	0
Flow	Accumulators	3	0	0
Flow and temperature distribution in PRHR bundle region	IRWST	0	6	1
Flow distribution	Downcomer/lower plenum	0	0	4
Flow resistance	ADS	0	5	0
	Break	0	6	5
	CMT	1	1	6
	Core	0	2	8
	IRWST	2	2	0
	Pumps	0	0	9
	Sump	0	3	0
	PRHR	0	6	3
Flow split(upper plenum)	Upper head/upper plenum	0	4	0
Fluid temperature	Sump	1	2	0
Heat transfer between PRHR and IRWST	PRHR	6	5	2
Heater power	Pressurizer	2	0	0
Horizontal fluid stratification	Hot legs	0	7	1
Humidity	Containment (exterior)	0	4	2
Interior to wall heat transfer	Containment (interior)	4	4	2
Interphasic condensation	IRWST	0	2	8
Level	CMT	5	2	0
	Downcomer/lower plenum	3	1	3
	Sump	1	3	0
Level (inventory)	Pressurizer	3	8	0
Level swell	Pressurizer	0	3	0
Level swell and depletion	Steam generator(secondary)	2	0	0
Liquid carry-over	Steam generator (separator/dryer)	2	0	0
Liquid distribution	Containment (interior)	0	6	6
Liquid holdup	Containment (interior)	0	4	6
Liquid subcooling	Containment (interior)	0	0	2
Loop asymmetry effects	Cold legs	0	4	1
	Core	0	0	4
	Downcomer/lower plenum	0	4	2
	Hot legs	0	4	1
	Upper head/upper plenum	0	4	1
Mass flow	ADS	6	0	0
	Break	8	3	0
Mass flow, including bypass	Core	0	2	1
Mixing	Pumps	0	0	1
Moderator temperature feedback	Fuel rods	0	1	1
Natural convection	Containment (interior)	0	4	6
Noncondensible effects	Accumulators	0	3	1
	ADS	0	3	3
	Break	0	0	2

Table 2. (continued).

Phenomena	Component	Frequency at Indicated Rank		
		High	Medium	Low
Noncondensible effects	CMT	0	1	5
	Cold legs	0	0	6
	Containment (interior)	0	4	6
	Core	0	0	3
	Downcomer/lower plenum	0	0	3
	Hot legs	0	2	5
	Pressurizer	0	2	9
	PRHR	0	8	3
	Steam generator(primary)	0	0	2
	Steam generators	0	3	0
	Upper head/upper plenum	0	0	2
Noncondensible segregation	Containment (interior)	0	4	6
Nonuniform steam/air distribution	Containment (interior)	0	4	6
Passive heat sink	Containment (interior)	0	8	2
PBL-to-cold legs tee phase separation	Cold legs	3	0	2
PCCS evaporation	Containment (exterior)	0	6	0
PCCS mixture convective heat transfer	Containment (exterior)	0	4	2
PCCS water flow	Containment (exterior)	0	4	2
PCCS wetting	Containment (exterior)	0	4	2
Phase separation in tees	Hot legs	5	2	2
	PRHR	0	0	3
Pool flow	IRWST	0	3	6
Pool level	IRWST	1	6	3
Pool thermal stratification	IRWST	1	10	3
Pool to tank structure heat transfer	IRWST	0	0	6
Preferential loop cooldown	Steam generator(primary)	2	0	0
Pressure	Containment (interior)	0	2	0
Primary to secondary heat transfer	Steam generator(primary)	2	0	0
Primary to secondary heat transfer	Steam generators	5	4	5
Radiation heat transfer	Containment (exterior)	0	4	2
Secondary level	Steam generators	0	3	6
Secondary pressure	Steam generators	0	5	6
Sparger pipe level	IRWST	0	1	1
SRV energy release	Steam generators	3	2	0
SRV mass flow	Steam generators	3	2	0
Steam-noncondensible mixing	Containment (interior)	0	4	6
Stored energy release	Cold legs	0	0	8
	Core	0	2	6
	Downcomer/lower plenum	0	0	8
	Fuel rods	0	1	8
	Hot legs	0	0	8
	Pressurizer	0	0	5
	Upper head/upper plenum	0	0	7
Subcooling margin	Core	1	3	0
Thermal driving head	Steam generator(primary)	0	2	0
Thermal Stratification	Cold legs	0	1	0

Table 2. (continued).

Phenomena	Component	Frequency at Indicated Rank		
		High	Medium	Low
Thermal stratification and mixing	CMT	0	4	6
Tube dryout (affected SG)	Steam generator(secondary)	0	2	0
Tube voiding	Steam generators	0	6	1
Two-phase level in upper plenum	Upper head/upper plenum	1	0	1
Two-phase mixture level	Core	6	0	0
Upper head/downcomer bypass flow	Upper head/upper plenum	0	0	1
Vapor space behavior	Pressurizer	2	4	0
Vapor space compression	Upper head/upper plenum	0	1	0
Voiding	CMT	0	1	1
Voiding	Core	0	4	0
Voiding	Hot legs	0	6	1
Voiding	PRHR	0	8	1
Voiding	Upper head/upper plenum	0	7	1
Voiding (unaffected loop)	Steam generator(primary)	0	2	0

Table 3. AP600 PIRT summary - frequency of occurrence of ranks sorted by components.

Component	Phenomena	Frequency at Indicated Rank		
		High	Medium	Low
Accumulators	Flow	3	0	0
	Noncondensible effects	0	3	1
ADS	Energy release	6	0	0
	Mass flow	6	0	0
	Choking in complex geometry	0	1	0
	Flow resistance	0	5	0
	Noncondensible effects	0	3	3
	Condensation in stages 1, 2, and 3 ADS and spargers (in IRWST)	0	0	2
Break	Choking in complex geometries	4	3	0
	Energy release	5	6	0
	Flow resistance	0	6	5
	Mass flow	8	3	0
	Noncondensible effects	0	0	2
Cold legs	Condensation	0	0	4
	Flashing	0	1	3
	Loop asymmetry effects	0	4	1
	Noncondensible effects	0	0	6
	PBL-to-cold legs tee phase separation	3	0	2
	Stored energy release	0	0	8
	Thermal Stratification	0	1	0
Core	Boiling	0	2	0
	Core channeling	2	0	2
	Flashing	1	6	2
	Flow resistance	0	2	8
	Loop asymmetry effects	0	0	4
	Mass flow, including bypass	0	2	1
	Noncondensible effects	0	0	3
	Stored energy release	0	2	6
	Subcooling margin	1	3	0
	Two-phase mixture level	6	0	0
	Voiding	0	4	0
CMT	CMT-to-loop differential density	1	3	3
	CMT-to-IRWST differential head	0	2	0
	Condensation	0	2	2
	Flashing	0	2	2
	Flow resistance	1	1	6
	Level	5	2	0
	Noncondensible effects	0	1	5
	Thermal stratification and mixing	0	4	6
	Voiding	0	1	1
Downcomer/lower plenum	Condensation	0	4	3
	Flashing	0	0	3
	Flow distribution	0	0	4
	Level	3	1	3
	Loop asymmetry effects	0	4	2

Table 3. (continued).

Component	Phenomena	Frequency at Indicated Rank		
		High	Medium	Low
Downcomer/lower plenum	Noncondensible effects	0	0	3
	Stored energy release	0	0	8
Fuel rods	Boron reactivity feedback	0	1	1
	CHF/dryout	0	3	1
	Core power/decay heat	16	0	0
	Moderator temperature feedback	0	1	1
	Stored energy release	0	1	8
Hot legs	CCFL	0	4	1
	Condensation	0	0	2
	Countercurrent flow	0	4	2
	Entrainment	0	3	1
	Flashing	0	7	2
	Horizontal fluid stratification	0	7	1
	Loop asymmetry effects	0	4	1
	Noncondensible effects	0	2	5
	Phase separation in tees	5	2	2
	Stored energy release	0	0	8
	Voiding	0	6	1
IRWST	Discharge line flashing	0	2	0
	Flow and temperature distribution in PRHR bundle region	0	6	1
	Flow resistance	2	2	0
	Interphasic condensation	0	2	8
	Pool flow	0	3	6
	Pool level	1	6	3
	Pool to tank structure heat transfer	0	0	6
	Pool thermal stratification	1	10	3
	Sparger pipe level	0	1	1
Pressurizer	Condensation	0	0	1
	CCFL	0	2	1
	Entrainment/de-entrainment	0	3	0
	Flashing	2	5	0
	Heater power	2	0	0
	Level (inventory)	3	8	0
	Level swell	0	3	0
	Noncondensible effects	0	2	9
	Stored energy release	0	0	5
	Vapor space behavior	2	4	0
PRHR	Condensation	0	6	1
	Differential density	0	8	3
	Flow resistence	0	6	3
	Flashing	0	0	3
	Heat transfer between PRHR and IRWST	6	5	2
	Noncondensible effects	0	8	3
	Phase separation in tees	0	0	3
PRHR	Voiding	0	8	1

Table 3. (continued).

Component	Phenomena	Frequency at Indicated Rank		
		High	Medium	Low
Pumps	Coastdown performance	2	0	3
	Flow resistance	0	0	9
	Mixing	0	0	1
Steam generators	Asymmetric behavior	0	3	0
	Condensation in U-tubes	0	0	3
	Noncondensible effects	0	3	0
	Primary to secondary heat transfer	5	4	5
	Secondary level	0	3	6
	Secondary pressure	0	5	6
	SRV energy release	3	2	0
	SRV mass flow	3	2	0
	Tube voiding	0	6	1
Steam generator(primary)	Noncondensible effects	0	0	2
	Preferential loop cooldown	2	0	0
	Primary to secondary heat transfer	2	0	0
	Thermal driving head	0	2	0
	Voiding (unaffected loop)	0	2	0
Steam generator(secondary)	Entrainment	2	0	0
	Flashing (SG and feedwater line)	2	0	0
	Level swell and depletion	2	0	0
	Tube dryout (affected SG)	0	2	0
Steam generator (separator/dryer)	Liquid carry-over	2	0	0
Sump	Discharge line flashing	0	2	0
	Flow resistance	0	3	0
	Fluid temperature	1	2	0
	Level	1	3	0
Upper head/upper plenum	Condensation	0	0	2
	Entrainment/de-entrainment	2	4	0
	Flashing	0	6	2
	Flow split(upper plenum)	0	4	0
	Loop asymmetry effects	0	4	1
	Noncondensible effects	0	0	2
	Stored energy release	0	0	7
	Two-phase level in upper plenum	1	0	1
	Upper head/downcomer bypass flow	0	0	1
	Vapor space compression	0	1	0
	Voiding	0	7	1
Containment (interior)	Condensate transport	0	4	6
	Condensation	0	6	4
	Interior to wall heat transfer	4	4	2
	Liquid distribution	0	6	6
	Liquid holdup	0	4	6
	Liquid subcooling	0	0	2
	Natural convection	0	4	6
	Noncondensible effects	0	4	6
	Nonuniform steam/air distribution	0	4	6

Table 3. (continued).

Component	Phenomena	Frequency at Indicated Rank		
		High	Medium	Low
Containment (interior)	Noncondensible segregation	0	4	6
	Passive heat sink	0	8	2
	Pressure	0	2	0
	Steam-noncondensible mixing	0	4	6
Containment (exterior)	Air flow	0	4	2
	Atmospheric temperature	0	4	2
	Chimney effects	0	4	2
	Exterior to ambient heat transfer	4	2	4
	Humidity	0	4	2
	PCCS evaporation	0	6	0
	PCCS water flow	0	4	2
	PCCS wetting	0	4	2
	PCCS mixture convective heat transfer	0	4	2
	Radiation heat transfer	0	4	2

Table 4. AP600 PIRT summary - high ranked phenomena sorted by frequency of occurrence.

Phenomena	Component	Frequency of High Rank
Core power/decay heat	Fuel rods	16
Mass flow	Break	8
Energy release	ADS	6
Mass flow	ADS	6
Two-phase mixture level	Core	6
Heat transfer between PRHR and IRWST	PRHR	6
Energy release	Break	5
Level	CMT	5
Phase separation in tees	Hot legs	5
Primary to secondary heat transfer	Steam generators	5
Choking in complex geometries	Break	4
Exterior to ambient heat transfer	Containment (exterior)	4
Interior to wall heat transfer	Containment (interior)	4
Flow	Accumulators	3
PBL-to-cold legs tee phase separation	Cold legs	3
Level	Downcomer/lower plenum	3
Level (inventory)	Pressurizer	3
SRV energy release	Steam generators	3
SRV mass flow	Steam generators	3
Core channeling	Core	2
Flow resistance	IRWST	2
Flashing	Pressurizer	2
Heater power	Pressurizer	2
Vapor space behavior	Pressurizer	2
Coastdown performance	Pumps	2
Liquid carry-over	Steam generator (separator/dryer)	2
Preferential loop cooldown	Steam generator(primary)	2
Primary to secondary heat transfer	Steam generator(primary)	2
Entrainment	Steam generator(secondary)	2
Flashing (SG and feedwater line)	Steam generator(secondary)	2
Level swell and depletion	Steam generator(secondary)	2
Entrainment/de-entrainment	Upper head/upper plenum	2
CMT-to-loop differential density	CMT	1
Flow resistance	CMT	1
Flashing	Core	1
Subcooling margin	Core	1
Pool level	IRWST	1
Pool thermal stratification	IRWST	1
Fluid temperature	Sump	1
Level	Sump	1
Two-phase level in upper plenum	Upper head/upper plenum	1

Table 5. AP600 PIRT summary - medium ranked phenomena sorted by frequency of occurrence.

Phenomena	Component	Frequency of Medium Rank
Pool thermal stratification	IRWST	10
Passive heat sink	Containment (interior)	8
Level (inventory)	Pressurizer	8
Differential density	PRHR	8
Noncondensible effects	PRHR	8
Voiding	PRHR	8
Flashing	Hot legs	7
Horizontal fluid stratification	Hot legs	7
Voiding	Upper head/upper plenum	7
Energy release	Break	6
Flow resistance	Break	6
PCCS evaporation	Containment (exterior)	6
Condensation	Containment (interior)	6
Liquid distribution	Containment (interior)	6
Flashing	Core	6
Voiding	Hot legs	6
PRHR bundle region	IRWST	6
Pool level	IRWST	6
Condensation	PRHR	6
Flow resistence	PRHR	6
Tube voiding	Steam generators	6
Flashing	Upper head/upper plenum	6
Flow resistance	ADS	5
Flashing	Pressurizer	5
Heat transfer between PRHR and IRWST	PRHR	5
Secondary pressure	Steam generators	5
Thermal stratification and mixing	CMT	4
Loop asymmetry effects	Cold legs	4
Air flow	Containment (exterior)	4
Atmospheric temperature	Containment (exterior)	4
Chimney effects	Containment (exterior)	4
Humidity	Containment (exterior)	4
PCCS mixture convective heat transfer	Containment (exterior)	4
PCCS water flow	Containment (exterior)	4
PCCS wetting	Containment (exterior)	4
Radiation heat transfer	Containment (exterior)	4
Condensate transport	Containment (interior)	4
Interior to wall heat transfer	Containment (interior)	4
Liquid holdup	Containment (interior)	4
Natural convection	Containment (interior)	4
Noncondensible effects	Containment (interior)	4
Noncondensible segregation	Containment (interior)	4
Nonuniform steam/air distribution	Containment (interior)	4
Steam-noncondensible mixing	Containment (interior)	4
Voiding	Core	4
Condensation	Downcomer/lower plenum	4

Table 5. (continued).

Phenomena	Component	Frequency of Medium Rank
Loop asymmetry effects	Downcomer/lower plenum	4
CCFL	Hot legs	4
Countercurrent flow	Hot legs	4
Loop asymmetry effects	Hot legs	4
Vapor space behavior	Pressurizer	4
Primary to secondary heat transfer	Steam generators	4
Entrainment/de-entrainment	Upper head/upper plenum	4
Flow split(upper plenum)	Upper head/upper plenum	4
Loop asymmetry effects	Upper head/upper plenum	4
Noncondensible effects	Accumulators	3
Noncondensible effects	ADS	3
Choking in complex geometries	Break	3
Mass flow	Break	3
CMT-to-loop differential density	CMT	3
Subcooling margin	Core	3
CHF/dryout	Fuel rods	3
Entrainment	Hot legs	3
Pool flow	IRWST	3
Entrainment/de-entrainment	Pressurizer	3
Level swell	Pressurizer	3
Asymmetric behavior	Steam generators	3
Noncondensible effects	Steam generators	3
Secondary level	Steam generators	3
Flow resistance	Sump	3
Level	Sump	3
CMT-to-IRWST differential head	CMT	2
Condensation	CMT	2
Flashing	CMT	2
Level	CMT	2
Exterior to ambient heat transfer	Containment (exterior)	2
Pressure	Containment (interior)	2
Boiling	Core	2
Flow resistance	Core	2
Mass flow, including bypass	Core	2
Stored energy release	Core	2
Noncondensible effects	Hot legs	2
Phase separation in tees	Hot legs	2
Discharge line flashing	IRWST	2
Flow resistance	IRWST	2
Interphasic condensation	IRWST	2
CCFL	Pressurizer	2
Noncondensible effects	Pressurizer	2
Thermal driving head	Steam generator(primary)	2
Voiding (unaffected loop)	Steam generator(primary)	2
Tube dryout (affected SG)	Steam generator(secondary)	2
SRV energy release	Steam generators	2

Table 5. (continued).

Phenomena	Component	Frequency of Medium Rank
SRV mass flow	Steam generators	2
Discharge line flashing	Sump	2
Fluid temperature	Sump	2
Choking in complex geometry	ADS	1
Flow resistance	CMT	1
Noncondensible effects	CMT	1
Voiding	CMT	1
Flashing	Cold legs	1
Thermal Stratification	Cold legs	1
Level	Downcomer/lower plenum	1
Boron reactivity feedback	Fuel rods	1
Moderator temperature feedback	Fuel rods	1
Stored energy release	Fuel rods	1
Sparger pipe level	IRWST	1
Vapor space compression	Upper head/upper plenum	1

Table 6. AP600 PIRT summary - low ranked phenomena sorted by frequency of occurrence.

Phenomena	Component	Frequency of Low Rank
Flow resistance	Pumps	9
Noncondensible effects	Pressurizer	9
Flow resistance	Core	8
Interphasic condensation	IRWST	8
Stored energy release	Cold legs	8
Stored energy release	Downcomer/lower plenum	8
Stored energy release	Fuel rods	8
Stored energy release	Hot legs	8
Stored energy release	Upper head/upper plenum	7
Condensate transport	Containment (interior)	6
Flow resistance	CMT	6
Liquid distribution	Containment (interior)	6
Liquid holdup	Containment (interior)	6
Natural convection	Containment (interior)	6
Noncondensible effects	Cold legs	6
Noncondensible effects	Containment (interior)	6
Noncondensible segregation	Containment (interior)	6
Nonuniform steam/air distribution	Containment (interior)	6
Pool flow	IRWST	6
Pool to tank structure heat transfer	IRWST	6
Secondary level	Steam generators	6
Secondary pressure	Steam generators	6
Steam-noncondensible mixing	Containment (interior)	6
Stored energy release	Core	6
Thermal stratification and mixing	CMT	6
Flow resistance	Break	5
Noncondensible effects	CMT	5
Noncondensible effects	Hot legs	5
Primary to secondary heat transfer	Steam generators	5
Stored energy release	Pressurizer	5
Condensation	Cold legs	4
Condensation	Containment (interior)	4
Exterior to ambient heat transfer	Containment (exterior)	4
Flow distribution	Downcomer/lower plenum	4
Loop asymmetry effects	Core	4
CMT-to-loop differential density	CMT	3
Coastdown performance	Pumps	3
Condensation	Downcomer/lower plenum	3
Condensation in U-tubes	Steam generators	3
Differential density	PRHR	3
Flashing	Cold legs	3
Flashing	Downcomer/lower plenum	3
Flashing	PRHR	3
Flow resistence	PRHR	3
Level	Downcomer/lower plenum	3
Noncondensible effects	ADS	3

Table 6. (continued).

Phenomena	Component	Frequency of Low Rank
Noncondensible effects	Core	3
Noncondensible effects	Downcomer/lower plenum	3
Noncondensible effects	PRHR	3
Phase separation in tees	PRHR	3
Pool level	IRWST	3
Pool thermal stratification	IRWST	3
Air flow	Containment (exterior)	2
Atmospheric temperature	Containment (exterior)	2
Chimney effects	Containment (exterior)	2
Condensation	CMT	2
Condensation	Hot legs	2
Condensation	Upper head/upper plenum	2
and spargers (in IRWST)	ADS	2
Core channeling	Core	2
Countercurrent flow	Hot legs	2
Flashing	CMT	2
Flashing	Core	2
Flashing	Hot legs	2
Flashing	Upper head/upper plenum	2
Heat transfer between PRHR and IRWST	PRHR	2
Humidity	Containment (exterior)	2
Interior to wall heat transfer	Containment (interior)	2
Liquid subcooling	Containment (interior)	2
Loop asymmetry effects	Downcomer/lower plenum	2
Noncondensible effects	Break	2
Noncondensible effects	Steam generator(primary)	2
Noncondensible effects	Upper head/upper plenum	2
Passive heat sink	Containment (interior)	2
PBL-to-cold legs tee phase separation	Cold legs	2
PCCS mixture convective heat transfer	Containment (exterior)	2
PCCS water flow	Containment (exterior)	2
PCCS wetting	Containment (exterior)	2
Phase separation in tees	Hot legs	2
Radiation heat transfer	Containment (exterior)	2
Boron reactivity feedback	Fuel rods	1
CCFL	Hot legs	1
CCFL	Pressurizer	1
CHF/dryout	Fuel rods	1
Condensation	Pressurizer	1
Condensation	PRHR	1
Entrainment	Hot legs	1
PRHR bundle region	IRWST	1
Horizontal fluid stratification	Hot legs	1
Loop asymmetry effects	Cold legs	1
Loop asymmetry effects	Hot legs	1
Loop asymmetry effects	Upper head/upper plenum	1

Table 6. (continued).

Phenomena	Component	Frequency of Low Rank
Mass flow, including bypass	Core	1
Mixing	Pumps	1
Moderator temperature feedback	Fuel rods	1
Noncondensible effects	Accumulators	1
Sparger pipe level	IRWST	1
Tube voiding	Steam generators	1
Two-phase level in upper plenum	Upper head/upper plenum	1
Upper head/downcomer bypass flow	Upper head/upper plenum	1
Voiding	CMT	1
Voiding	Hot legs	1
Voiding	PRHR	1
Voiding	Upper head/upper plenum	1

7. REFERENCES

7-1. Technical Program Group, *Quantifying Reactor Safety Margins - Application of CSAU Methodology to a LBLOCA*, Idaho National Engineering Laboratory, NUREG/CR-5249, July 1989.

7-2. 10 CFR 50, Part 46, "Acceptance Criteria for Emergency Core Cooling Systems (ECCS) for Light Water Nuclear Power Reactors," U. S. Federal Register.

7-3. C. B. Davis and M. B. Rubin, *MSLB in AP600 with Maximum Cooldown*, Letter Report PDB-33-94, Idaho National Engineering Laboratory, Lockheed Idaho Technologies Co., November 22, 1994.

7-4. P. D. Bayless to F. Odar, *Transmittal of SGTR Study Report, JCN J6008*, PDB-1-96, January 15, 1996.

7-5. C. B. Davis, et al., "Evaluation and Assessment of RELAP5/MOD3, Version 3.2.1.2 for Simulating the Long Term Phase of Small Break Loss-of-Coolant Accidents in the AP600", INEL-96/0395, October 1996.

7-6. R. L. Moore, et al., "AP600 SBLOCA PIRT Sensitivity Studies: ADS Actuation, Flow Resistance, ADS4 Junction Phase Separation, CMT Condensation, Cold Leg Condensation and PRHR Heat Transfer", Letter Report GEW-06-97, Idaho National Engineering and Environmental Laboratory, Lockheed Martin Idaho Technologies Co, March 24, 1997.

7-7. M. G. Ortiz, et al., "Application of the Global Scaling Analysis Tools to the AP600 Integration Study", INEL-96/0117, November 1996.

7-8. S. Banerjee, et al., "Topdown Scaling Analysis Methodology for the AP600 Integral Tests", INEL-96/400, November 1996.

8.0 PROPRIETARY REFERENCES

8-1. *AP600 Standard Safety Analysis Report*, Simplified Passive Advanced Light Water Reactor Plant Program, Westinghouse Electric Company, June 26, 1992, and revisions. (Proprietary document; not publicly available.)

8-2. "AP600 Design Changes," Westinghouse Electric Company, presentation to U. S. Nuclear Regulatory Commission, February 22, 1994. (Proprietary document; not publicly available.)

8-3. R. J. Beelman, S. M. Sloan, and J. E. Fisher, *AP600 Quality Assured RELAP5 Input Model Description*, Idaho National Engineering Laboratory, EGG-NRE-10824, August 12, 1993. (Proprietary document; not publicly available.)

8-4. C. D. Fletcher, et al., *Interim Phenomena Identification and Ranking Tables for Westinghouse AP600 Small Break Loss-of-Coolant Accident, Main Steam Line Break, and Steam Generator Tube Rupture Scenarios*, Appendix H, INEL-94/0061, Revision 1, July 1995. (Proprietary document; not publicly available.)

8-5. C. D. Fletcher, et al., "Adequacy Evaluation of RELAP5/MOD3 for Simulating AP600 Small Break Loss-of-Coolant Accidents", INEL-96/0380, October 1996. (Proprietary document; not publicly available.)

Appendix A - AP600 PIRT Development Process

The AP600 LWR is a new advanced passive design that has been submitted to the USNRC for design certification. Within the certification process the USNRC is performing selected system thermal hydraulic response audit studies to help confirm parts of the vendor's safety analysis submittal. Because of certain innovative design features of the safety systems it was also necessary for the USNRC to develop new experimental data and related advances in the system thermal hydraulic analysis computer code. The compressed design certification schedule required parallel, rather than series, execution of the design certification related research. Therefore, the PIRT process was used to integrate and focus the experimental and analytical work to obtain a sufficient and cost effective research effort.

The PIRTs were based on information originating in AP600 specific experiments, the integrated analyses of the data from these experiments, scaling analyses related to the experimental facilities and the plant design, and sensitivity calculations related to computer code simulation of the plant. The experimental program included separate effect tests (SET) in the PRHR, CMT and ADS facilities. Integral effect test (IET) data were centered in the SPES, ROSA, and OSU facilities. The integrated experimental data analyses included test series related to cold leg breaks, direct vessel injection (DVI) line breaks, pressure balance line breaks, MSLB and SGTR transients. The scaling analyses were directed toward understanding the degree of prototypicality of the experimental facilities as related to the AP600 plant design, so that the data could be compared as a whole. Sensitivity studies were directed toward determining the effects of one-by-one variations in highly ranked phenomena on the plant response for reasonable ranges of uncertainty in these parameters.

The primary role of the AP600 PIRTs was to provide a technically-based structure for the efficient and phenomenologically correct development of the thermal-hydraulic systems analysis codes that are being used by the NRC in the process of reactor design certification. In the context used here, "code development" includes the development of new experimental data needed to validate a code for its intended use and, thereby, for the code assessment activities. Thus, the PIRTs were used to guide development of:

Experimental facility specifications,
Experimental test specifications,
Code development, and
Code assessment

Ideally, PIRTs are developed to a reasonably mature state, then are followed by the above activities in the sequence shown. This does not preclude the necessary continual feedback between all of these elements as they develop. However, the compressed schedule for the AP600 design certification process required some deviation from this ideal. Although the basic sequence shown above remained, it was necessary to telescope each of the activities, with overlap common among the related research effort. That is, the PIRTs were developed at the same time that other elements of the overall process were being conducted. Accordingly the PIRTs were developed in four stages:

- Preliminary PIRTs
- Original Interim PIRTs (Original issue of this report, commonly referred to as the Rev. 0 PIRTs)
- Updated Interim PIRTs (Revision 1 issue of this report, Rev 1 PIRTs)
- Final PIRTs (Revision 2 issue of this report, Rev 2 PIRTs).

The PIRT development is pictorially highlighted in Figure A-1 and described in the following sections. The use of the PIRTs to help guide other related AP600 research projects is also illustrated in Figure A-1.

The initial PIRT development and use between July 1990 and October 1993 was designated the "preliminary" phase. The PIRTs developed during this phase primarily focussed on the initial designs of the new AP600 passive safety systems and relied on existing information available for the current generation of light-water reactors. The summary information related to this stage of developmental is provided in Table A-1.

The "Rev. 0 interim" phase of PIRT development, reported in original version of this report, was structured specifically to address SBLOCA, MSLB, and SGTR events. Rev. 0 included the work accomplished between October 1993 and September 1994. The focus of this development stage was to expand the preliminary PIRTs to include all subsystems active during the transients of interest. Summary information is provided in Table A-2.

The continuation of interim PIRT development activities, resulted in the "Rev. 1 interim" PIRTs. This stage of development focused on the SBLOCA transient in the context of making the PIRT more realistic as warranted by the evolving new evidence from the experimental research results and its analysis. The 2 inch SBLOCA integrated experimental data analysis was a key data source in this stage of the development. Summary information is shown in Table A-3. These activities were performed between October 1994 and July 1995.

The completion of the PIRT development resulted in the Rev 2 PIRTs that are reported elsewhere in this issue of this report. This stage of development focused on consideration of the new evidence provided in the integrated experimental data analysis of the PBLB and DVI line SBLOCA, the integrated experimental data analysis of the IADS, the SBLOCA short-term AHP analysis, SBLOCA PIRT confirmation sensitivity studies, and the short- and long-term scaling analysis. Summary information is provided in Table A-4. These activities were performed between July 1995 and May 1996.

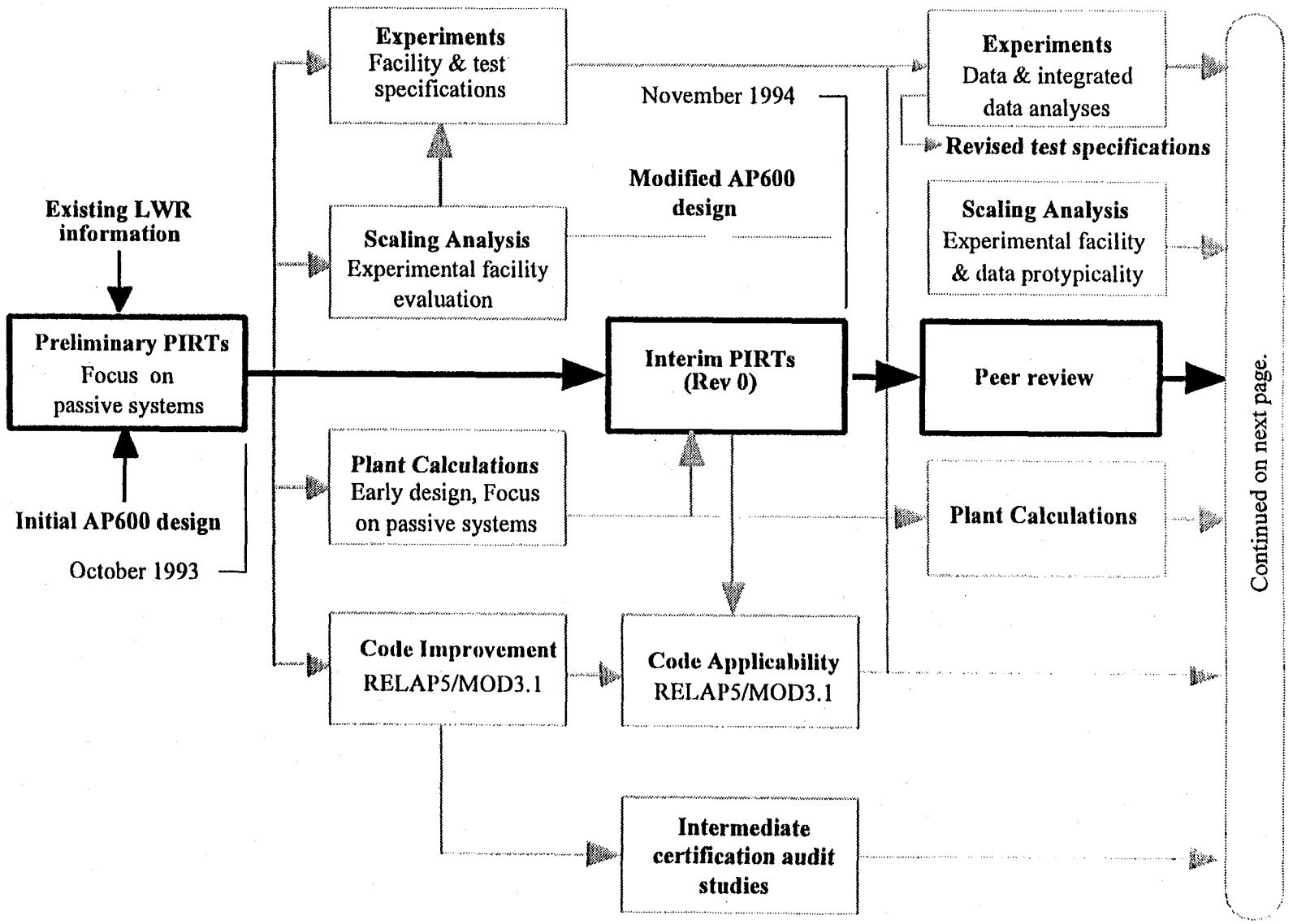

Figure A-1. Development and application of PIRT process to AP600 related research.

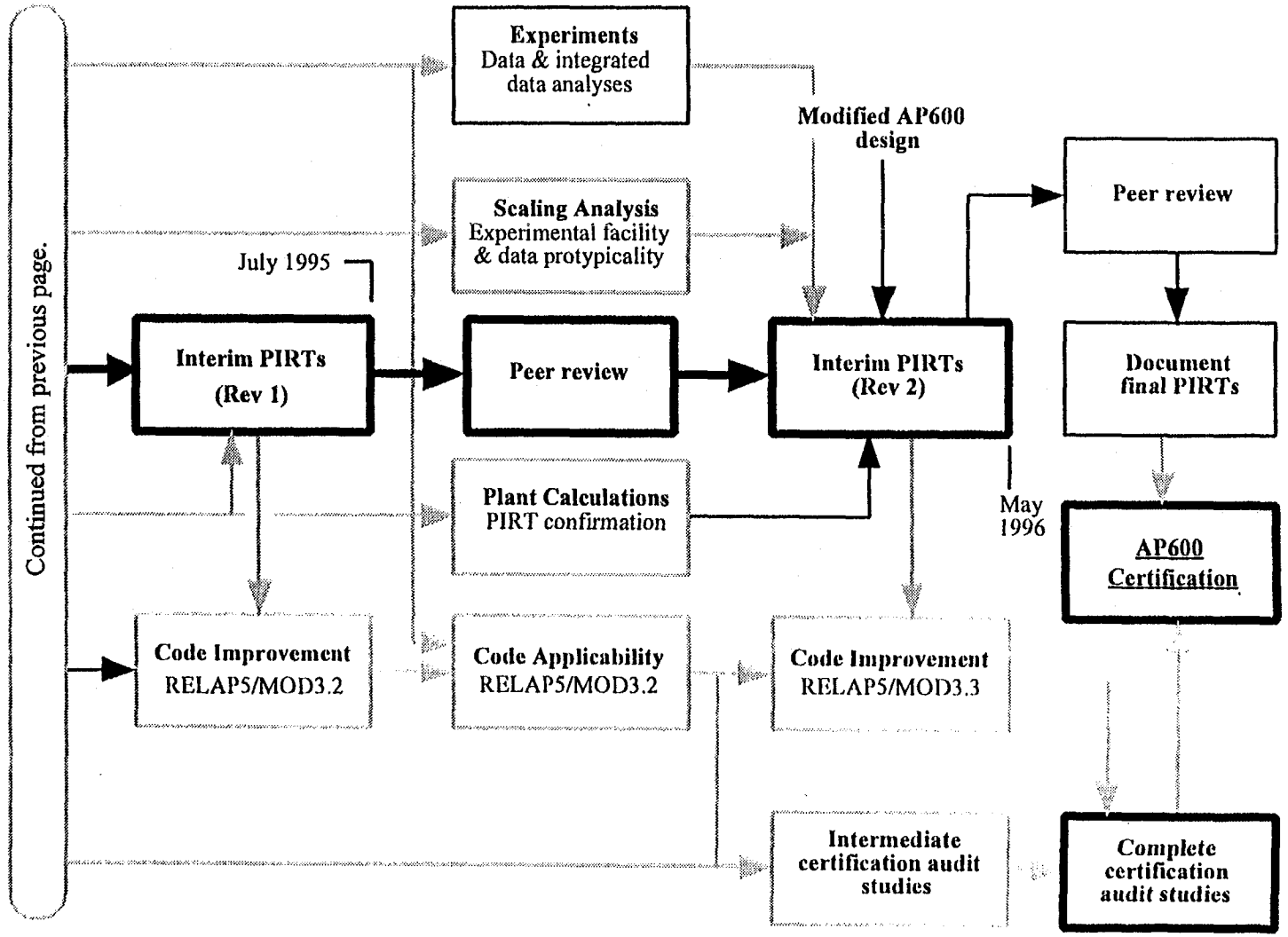

Figure A-1. Development and application of PIRT process to AP600 related research (continued).

Table A-1. Supplemental information for the preliminary phase of AP600 PIRT development.

PIRT Associated Activity	Key Participants	PIRT Releated Information Sources
REVIEW OF METHODOLOGY & PRELIMINARY PIRTS:		
March 3, 1992: ACRS T-H Phenomena Subcommittee Meeting	NRC-RES & INEL staff	S. M. Modro, *Results of RELAP5 Review for Applicability to AP600*, Presentation Handout S. M. Modro, *Key Phenomena, Capability & Limitations of ROSA-IV to Simulate AP600*, Presentation Handout
July 2, 1992: Nuclear Safety Research Review Committee, Advanced Reactors Subcommittee	NRC-RES staff	G. N. Lauben, *CSAU Approach to RELAP5 ALWR Code Development*, Presentation Handout
December 2, 1992: Nuclear Safety Research Review Committee, Advanced Reactors Subcommittee	NRC-RES & INEL staff	S. M. Modro, *Application of the CSAU Methodology to AP600 Analytical Capabilities Development*, Presentation Handout
March 4-5, 1993: ACRS T-H Phenomena Subcommittee Meeting	NRC-RES & INEL staff	G. N. Lauben, *ALWR Code Development & Assessment Process*, Presentation Handout S. M. Modro, *Identification of Key Phenomena & Code Models for Analysis of AP600 Plant Design*, Presentation Handout
EXPERIMENTS:		Scaling and Design of LSTF Modifications for AP600 Testing, NUREG/CR-6066 (Draft, August 1994)
CODE DEVELOPMENT:		*RELAP/MOD3 Code Manual*, NUREG/CR-5535
Code Description		Volumes: 1 (Theory), 2 (Input Description), & 4 (Models and correlations)
Assessment: Developmental		Volume 3 (Developmental Assessment)
Independent, including summary of code version changes		Volume 7 (Independent Assessment)
AP600 NPP MODEL DEVELOPMENT:		R. J. Beelman, et al., *AP600 Quality Assured RELAP5 Input Model Description (Interim)*, EGG-NRE-10824 (Proprietary) (August 1993)

Table A-2. Supplemental information for the Rev. O interim phase of AP600 PIRT development.

PIRT Associated Activity	Key Participants	PIRT Related Information Sources
DEVELOPMENT AND/OR REVIEW OF DETAILED PIRTS:		Focus of meetings
October 1993: Establish common approach to develop detailed AP600 & SBWR PIRTs	NRC-RES & NRR BNL, INEL, LANL	Establish certification related elements, transients to be addressed, code assessment criteria, and phenomena ranking criteria
December 1993: Progress Review, NRC T-H Expert Panel, AP600 & SBWR detailed PIRTs	NRC T-H Consultants (full panel) NRC-RES & NRR BNL, INEL, LANL	T-H Consultants review of and input to initial AP600 & SBWR detailed PIRTs
February 1994: AP600 PIRT Working Meeting	NRC T-H Consultants (full panel) NRC-RES & NRR BNL, INEL, LANL	T-H Consultants, BNL & LANL input to AP600 detailed PIRTs
April 1994: AP600 PIRT Working Meeting	NRC T-H Consultants (full panel) NRC-RES & NRR BNL, INEL, LANL, SNL ACRS Observer	T-H Consultants, BNL, LANL & SNL input to AP600 detailed PIRTs, including special focus on containment
September 1994: AP600 PIRT Working Meeting	NRC T-H Consultants (full panel) NRC-RES & NRR BNL, INEL, LANL ACRS Observers	T-H Consultants, BNL & LANL input to final AP600 interim PIRTs, including documentation
EXPERIMENTS:		Scaling and Design of LSTF Modifications for AP600 Testing, NUREG/CR-6066 (November 1994)
CODE DEVELOPMENT:		*RELAP5/MOD3 Code Manual*, NUREG/CR-5535 (Update to be published 1st quarter CY-1995)
Code Description		Volumes: 1 (Theory), 2 (Input Description), & 4 (Models and correlations)
Assessment: Developmental		Volume 3 (Developmental Assessment)
Independent, including summary of code version changes		Volume 7 (Independent Assessment)

Table A-2. (continued).

PIRT Associated Activity	Key Participants	PIRT Related Information Sources
PIRT CONFIRMATION:		C. B. Davis, *Simplified AP600 Model for PIRT Validations*, Letter Report GEW-29-94 (August 3, 1994) C. B. Davis, *AP600 MSLB with Maximum Cooldown*, Letter Report PDB-33-94 (November 22, 1994)
AP600 NPP MODEL DEVELOPMENT:		R. J. Beelman, et al., *AP600 Quality Assured RELAP5 Input Model Description (Interim)*, EGG-NRE-10824 (Proprietary) (To be updated)

Table A-3. Supplemental information for the Rev. 1 interim phase of AP600 PIRT development.

PIRT Associated Activity	Key Participants	PIRT Related Information Sources
DEVELOPMENT AND/OR REVIEW OF DETAILED PIRTS:		Focus of meetings
November 29 - December 2, 1994 First AP600 Phenomenology Meeting Typical participants are listed in Table A-5	NRC-RES & NRR NRC T-H Consultants (full panel) INEL, LANL	T-H Consultants review of new experimental data and input to potential revisions to the Rev. 0 SBLOCA PIRT
January 12-13, 1995	NRC-RES & INEL	Completion of SBLOCA PIRT revisions began in previous meeting
February 1, 1995 Second AP600 Phenomenology Meeting Typical participants are listed in Table A-5	NRC-RES & NRR NRC T-H Consultants (full panel) INEL, LANL	Review of revised SBLOCA PIRT (Rev. 1)
March 27-28, 1995 ACRS T/H Subcommittee PIRT Review	NRC-RES & NRR NRC T-H Consultants INEL, LANL	Review of revised SBLOCA PIRT (Rev. 1)
June 13-15, 1995 Third AP600 Phenomenology Meeting Typical participants are listed in Table A-5	NRC-RES & NRR NRC T-H Consultants (full panel) INEL, LANL	Continued review of revised SBLOCA PIRT (Rev. 1)
July 1995 Issue of Rev. 1 PIRT Report		

Table A-3. (continued).

PIRT Associated Activity	Key Participants	PIRT Related Information Sources
EXPERIMENTS:		Small Cold-Leg Break LOCA Experiment Results: R. A. Shaw, T. Yonomoto, and Y. Kukita, "Quick Look Report for ROSA/AP600 Experiment AP-CL-03," Japan Atomic Energy Research Institute, Memo 06-249, October 1994. Westinghouse Electric Company, "Quick Look Report for SPES-2 Matrix Test S00401," PXS-T2R-020 (Proprietary), Preliminary, July 1994. Westinghouse Electric Company, "Quick Look Report for OSU Matrix Test SB1," LTCT-T2R-021 (Proprietary), Preliminary, Revision 0, August 1994. Westinghouse Electric Company, "Quick Look Report for OSU Matrix Test SB3," LTCT-T2R-023 (Proprietary), Preliminary, Revision 0, August 1994. Westinghouse Electric Company, "Quick Look Report for OSU Matrix Test SB4," LTCT-T2R-024 (Proprietary), Preliminary, Revision 0, August 1994. Westinghouse Electric Company, "Quick Look Report for OSU Matrix Test SB5," LTCT-T2R-025 (Proprietary), Preliminary, Revision 0, August 1994. Westinghouse Electric Company, "Quick Look Report for OSU Matrix Test SB7," LTCT-T2R-027 (Proprietary), Preliminary, Revision 0, August 1994.

Table A-4. Supplemental information for the Rev. 2 final phase of AP600 PIRT development.

PIRT Associated Activity	Key Participants	PIRT Related Information Sources
DEVELOPMENT AND/OR REVIEW OF DETAILED PIRTS:		Focus of meetings
September 19-21, 1995 Fourth AP600 Phenomenology Meeting Typical participants are listed in Table A-5	NRC-RES & NRR NRC T-H Consultants (full panel) INEL, LANL	T-H Consultants review of new experimental data and input to potential revisions to the Rev. 1 SBLOCA PIRT
January 11-12, 1996	NRC-RES & INEL NRC T-H Consultants (PIRT subgroup) INEL, LANL	Review AHP analysis and suggested Rev. 1 SBLOCA PIRT revisions
January 1996 Fifth AP600 Phenomenology Meeting Typical participants are listed in Table A-5	NRC-RES & NRR NRC T-H Consultants (full panel) INEL, LANL	T-H Consultants review of new experimental data, integrated data analyses, and input to potential revisions to the Rev. 1 SBLOCA PIRT
February 22-23, 1996 ACRS T/H Subcommittee PIRT Review	NRC-RES & NRR NRC T-H Consultants INEL, LANL	Review of proposed Rev. 2 SBLOCA PIRT
March 20-21, 1996 PIRT subgroup meeting	NRC-RES & NRR NRC T-H Consultants (PIRT subgroup) INEL, SNL	Finalize Rev. 2 SBLOCA PIRT
EXPERIMENTS & INTEGRATED DATA ANALYSES		"Adequacy Evaluation of RELAP5/MOD3 for Simulating AP600 Small Break Loss-of-Coolant Accidents", Idaho National Engineering Laboratory, INEL-96/0330 (Proprietary), October 1996.

Table A-5. Typical participants at full panel PIRT review meetings.

Sanjoy Banerjee, University of California, Santa Barbara
Paul Bayless, Idaho National Engineering and Environmental Laboratory
Ron Beelman, Idaho National Engineering and Environmental Laboratory
David Bessette, NRC/RES
Brent Boyack, Los Alamos National Laboratory
Ralph Caruso, NRC/NRR
Marino DiMarzo, NRC
David Ebert, NRC
Farouk Eltawila, NRC
Don Fletcher, Idaho National Engineering and Environmental Laboratory
Peter Griffith, Massachusetts Institute of Technology
Yassin Hassan, Texas A&M University
Mamoru Ishii, Purdue University
Barclay G. Jones, University of Illinois, Champaign-Urbana
Joe M. Kelly, NRC
Tom King, NRC
Gunol Kojasoy, University of Wisconsin, Milwaukee
T. K. Larson, Idaho National Engineering Laboratory
Norm Lauben, NRC/RES
Tim M. Lee, NRC
Gérald S. Lellouche, TDS
Alan Levin, NRC/NRR
Dennis Liles, Los Alamos National Laboratory
John Mahaffy, Pennsylvania State University
S. Michael Modro, Idaho National Engineering and Environmental Laboratory
Frank Odar, NRC/RES
Marcos G. Ortiz, Idaho National Engineering and Environmental Laboratory
Michael Podowski, RPI
Victor Ransom, Purdue University
Walter Rettig, DOE-Idaho
Jose N. Reyes, Oregon State University
Gene Rhee, NRC/RES
Michael Rubin, NRC
Harold Scott, NRC
Louis Shotkin, NRC
Sandra Sloan, Idaho National Engineering and Environmental Laboratory
Donald Solberg, NRC
Neil Todreas, Massachusetts Institute of Technology
Graham Wallis, Dartmouth College
Gary Wilson, Idaho National Engineering and Environmental Laboratory
James T. Han, NRC/RES Paul Boehnert, ACRS Observer
Novak Zuber, ACRS Consultant Observer

Appendix B - Detailed Results, Small Break Loss-of-Coolant Accident PIRT

This appendix presents the detailed results of the small break loss-of-coolant accident (SBLOCA) PIRT. The detailed PIRT results are shown in Tables B-1 and B-2, and the transient description, overall phenomena ranking criteria, and specific ranking rationales are shown in Table B-3. The information in Tables B-1 and B-2 is arranged to correspond with the two phases of the accident scenario. These tables are organized in alphabetical order according to the component name. Within the listings for each component, the pertinent identified phenomena are arranged by order of ranking. The right sides of these tables contain identifier codes that refer the reader elsewhere in this report for further information:

The code labeled "Ranking Rationale" (for example, "R1") leads the reader to a description of the logic leading to the ranking of each specific phenomenon; this information is found in Table B-3 in this appendix.

The code labeled "Phenomena Description" (for example "D1") leads the reader to a general description of each phenomenon; this information is found in Appendix G, Table G-1.

Two codes labeled "Type Geometry" (for example "C1/G1"). The "C" code leads the reader to the physical geometries and general functions of the component under discussion; this information is found in Appendix G, Table G-2. The "G" code leads the reader to more detailed discussion of the specific phenomena associated with each of the components; this information is found in Appendix G, Table G-3.

The "Supporting Evidence" code (for example, "E1") leads the reader to references (geometrical, experimental, and analytical) that provides background and corroborating information. This information is found in Appendix G, Table G-4. It is noted that the supporting evidence is currently being developed in experimental and analytical tasks both inside and outside the PIRT task. Thus, the information in this table can be expected to increase as the supporting tasks are completed.

The "Sublevel Phenomena" code (for example, "S1") leads the reader to a list of contributing phenomena affecting the primary phenomenon. The sublevel phenomena information is found in Appendix G, Table G-5.

Table B-1. PIRT for the short-term phase of a SBLOCA.

			For codes shown in these columns, See Tables:				
			B-3	G-1	G-2/G-3	G-4	G-5
Component	Phenomena	Rank	Ranking Rationale	Phenomena Description	Type Geometry	Supporting Evidence	Sublevel Phenomena
Accumulator	Flow	H	R1	D46	C1/G2	E2	S20
	Noncondensible effects	M	R2	D50	C1/G2	E2	S12
ADS	Energy release	H	R60	D19	C2/G3	E2	S21
	Mass flow	H	R61	D46	C2/G3	E2	S21
	Choking in complex geometry	M	R62	D9	C2/G3	E2	S66
	Flow resistance	M	R63	D27	C2/G3	E2	S11
	Noncondensible effects	M	R64	D50	C2/G3	E2	S12
	Condensation in stages 1, 2, and 3 ADS and spargers (in IRWST)	L	R136	D87	C2	E2	S77
Break	Mass flow	H	R4	D46	C3/G4	E2	S1
	Energy release	M	R3	D19	C3/G4	E2	S1
	Flow resistance	M	R65	D27	C3/G4	E3	S11
	Noncondensible effects	L	R66	D50	C3/G4	E2	S12
Cold legs	PBL-to-cold leg tee phase separation	H	R8	D56	C4/G8	E2	S8
	Thermal stratification	M	R10	D73	C4	E3	S19
	Flashing	M	R6	D21	C4	E3	S5
	Loop asymmetry effects	L	R7	D45	C4/G9	E3	S9
	Noncondensible effects	L	R67	D50	C4	E3	S12
	Condensation	L	R5	D9	C4	E3	S18
	Stored energy release	L	R9	D68	C4/G7	E2	S2
Core	Flashing	H	R11	D21	C5/G12	E2	S5
	Flow resistance	L	R12	D27	C5/G12	E3	S11
	Boiling	M	R101	D94	C5	E2	S78
	Loop asymmetry effects	L	R24	D45	C5/G12	E2	S9

Table B-1. (continued).

			For codes shown in these columns, See Tables:				
			B-3	G-1	G-2/G-3	G-4	G-5
Component	Phenomena	Rank	Ranking Rationale	Phenomena Description	Type Geometry	Supporting Evidence	Sublevel Phenomena
Core, Continued	Subcooling margin	H	R68	D69	C5	E2	S52
	Two-phase mixture level	H	R69	D76	C5	E2	S31
	Mass flow, including bypass	M	R13	D46	C5/G10	E2	S3
	Stored energy release	M	R14	D68	C5/G11	E3	S2
CMT	Flow resistance	H	R18	D27	C6/G13	E3	S11
	Level	H	R19	D39	C6/G14	E2	S13
	CMT-to-loop differential head	M	R15	D17	C6/G13	E3	S10
	CMT-to-loop differential density	M	R15	D17	C6/G13	E3	S10
	Flashing	M	R17	D21	C6/G14	E3	S5
	Thermal stratification and mixing	M	R20	D73	C6/G14	E3	S19
	Condensation	M	R16	D9	C6/G14	E3	S18
	Noncondensible effects	L	R132	D50	C6	E3	S12
Downcomer/ lower plenum	Condensation	M	R21	D9	C7/G18	E2	S18
	Level	M	R23	D39	C7/G17	E2	S13
	Flow distribution	L	R22	D24	C7/G16	E3	S64
	Loop asymmetry effect	L	R24	D45	C7/G16	E3	S9
	Stored energy release	L	R25	D68	C7/G15	E2	S2
	Flashing	L	R70	D21	C7/G18	E2	S5
	Noncondensible effects	L	R71	D68	C7/G9	E2	S12
Fuel rods	Core power/decay heat	H	R26	D12	C8/G20	E2	S4
	CHF/dryout	M	R72	D92	C8/G20	E2	S57
	Stored energy release	M	R27	D68	C8/G21	E3	S2

Table B-1. (continued).

			For codes shown in these columns, See Tables:				
			B-3	G-1	G-2/G-3	G-4	G-5
Component	Phenomena	Rank	Ranking Rationale	Phenomena Description	Type Geometry	Supporting Evidence	Sublevel Phenomena
Hot legs	Phase separation in tees	H	R31	D56	C9/G24	E2	S8
	Flashing	M	R28	D21	C9	E2	S5
	Horizontal fluid stratification	L	R29	D35	C9/G25	E2	S33
	Voiding	L	R33	D78	C9/G25	E2	S54
	CCFL	L	R73	D14	C9/G25	E3	S27
	Condensation	L	R74	D9	C9	E3	S18
	Countercurrent flow	L	R75	D13	C9/G25	E3	S32
	Entrainment	L	R76	D20	C9/G25	E3	S23
	Noncondensible effects	L	R77	D50	C9	E2	S12
	Loop asymmetry effects	L	R30	D45	C9/G23	E2	S9
	Stored energy release	L	R32	D68	C9/G22	E2	S2
IRWST	Flow resistance	H	R135	D27	C10/G27	E2	S11
	Sparger pipe level	M	R79	D89	C10	E3	S75
	Pool thermal stratification	M	R38	D59	C10/G26	E2	S19
	Pool flow	M	R36	D57	C10/G26	E2	S24
	Flow and temperature distribution in PRHR bundle region	L	R34	D23	C10/G26	E3	S24
	Pool level	L	R37	D39	C10/G26	E3	S25
	Interphasic condensation	L	R35	D37	C10/G29	E3	S18
	Pool to tank structure heat transfer	L	R78	D60	C10/G28	E2	S26
Pressurizer	Level (inventory)	H	R41	D39	C14/G33	E2	S13
	Flashing	M	R40	D21	C14/G33	E2	S5
	Entrainment/de-entrainment	M	R81	D20	C14/G36	E2	S23
	Level swell	M	R82	D40	C14/G36	E2	S13
	CCFL	L	R80	D14	C14/G34	E3	S27

Table B-1. (continued).

			For codes shown in these columns, See Tables:				
			B-3	G-1	G-2/G-3	G-4	G-5
Component	Phenomena	Rank	Ranking Rationale	Phenomena Description	Type Geometry	Supporting Evidence	Sublevel Phenomena
Pressurizer, Continued	Noncondensible effects	L	R83	D50	C14	E2	S12
	Stored energy release	L	R84	D68	C14/G35	E2	S2
PRHR	Heat transfer between PRHR and IRWST	M	R45	D32	C12/G30	E3	S28
	Voiding	L	R47	D78	C12/G31	E3	S54
	Condensation	L	R42	D9	C12/G30	E3	S18
	Differential density	L	R43	D17	C12/G30	E3	S10
	Flow resistance	L	R44	D27	C12/G30	E3	S11
	Noncondensible effects	L	R46	D50	C12/G31	E3	S12
	Flashing	L	R85	D21	C12	E2	S5
	Phase separation in tees	L	R86	D56	C12/G31	E2	S8
Pumps	Mixing	L	R50	D90	C15	E3	S73
	Coastdown performance	L	R48	D7	C15/G37	E2	S14
	Flow resistance	L	R49	D27	C15/G38	E2	S15
Steam generators	Primary to secondary heat transfer	M	R53	D33	C16/G39	E2	S53
	Secondary pressure	L	R52	D64	C16/G39	E3	S17
	Tube voiding	L	R54	D75	C16/G39	E3	S16
	Secondary level	L	R51	D63	C16/G39	E2	S7
Upper head / upper plenum	Voiding	M	R59	D78	C18	E2	S54
	Entrainment/de-entrainment	M	R88	D20	C18/G46	E2	S23
	Flashing	L	R55	D21	C18/G45	E3	S5
	Condensation	L	R87	D9	C18	E3	S18
	Stored energy release	L	R57	D68	C18/G47	E2	S2

Table B-1. (continued).

			For codes shown in these columns, See Tables:				
			B-3	G-1	G-2/G-3	G-4	G-5
Component	Phenomena	Rank	Ranking Rationale	Phenomena Description	Type Geometry	Supporting Evidence	Sublevel Phenomena
Upper head / upper plenum, Continued	Upper head/downcomer bypass flow	L	R58	D91	C18	E2	S74
	Loop asymmetry effects	L	R56	D45	C18/G46	E2	S9
	Noncondensible effects	L	R137	D50	C18	E2	S12
	Two-phase level in upper plenum	L	R138	D95	C18	E2	S80
Containment (interior) [1]	Pressure	M	R89	D93	C19	E2	S76
	Liquid distribution	M	R139	D96	C19	E3	S81
	Liquid subcooling	L	R140	D97	C19	E2	S82
Sump	Level	M	R141	D39	C17	E2	S13

[1] It is recognized that the interactions between the containment and RCS are more in AP600 than in current reactor designs. The most important of these are reflected in this PIRT through the indicated parameters. Other parameters, essentially subservient to those indicated here, will be considered in the research associated with containment integrity and adequacy. Thus, the containment parameters identified and ranked here are considered sufficient for the purposes of this PIRT.

Table B-2. PIRT for the long-term phase of a SBLOCA.

			For codes shown in these columns, See Tables:				
			B-3	G-1	G-2/G-3	G-4	G-5
Component	Phenomena	Rank	Ranking Rationale	Phenomena Description	Type Geometry	Supporting Evidence	Sublevel Phenomena
Accumulators	Noncondensible effects	L	R142	D50	C1/G2	E3	S12
ADS	Energy release	H	R90	D19	C2/G3	E2	S21
	Mass flow	H	R91	D46	C2/G3	E2	S21
	Condensation in stage 1, 2 and 3 ADS and sparger (in IRWST)	L	R94	D87	C2	E2	S77
	Noncondensible effects	L	R93	D50	C2/G3	E2	S12
Break	Energy release	M	R95	D19	C3/G4	E2	S1
	Mass flow	M	R96	D46	C3/G4	E2	S1
	Noncondensible effects	L	R97	D50	C3/G4	E2	S12
	Flow resistance	L	R143	D27	C3/G4	E2	S11
Cold legs	Condensation	L	R98	D9	C4	E2	S18
	Noncondensible effects	L	R99	D50	C4	E2	S12
	PBL-to-cold leg tee phase separation	L	R100	D56	C4/G8	E2	S8
	Stored energy release	L	R144	D68	C4/G7	E2	S2
Core	Two-phase mixture level	H	R106	D76	C5	E2	S31
	Boiling	M	R101	D94	C5	E2	S78
	Mass flow, including bypass	M	R104	D46	C5/G10	E2	S3
	Subcooling margin	M	R105	D69	C5	E2	S52
	Stored energy release	M	R145	D68	C5/G11	E3	S2
	Flow resistance	L	R103	D27	C5/G12	E3	S11
	Flashing	L	R102	D21	C5/G12	E3	S5
	Loop asymmetry effects	L	R146	D45	C5/G12	E2	S9
CMT	CMT-to-IRWST differential head	M	R107	D88	C6	E3	S79
	Condensation	M	R108	D9	C6/G14	E3	S18
	Noncondensible effects	M	R110	D50	C6	E3	S12

Table B-2. (continued).

			For codes shown in these columns, See Tables:				
			B-3	G-1	G-2/G-3	G-4	G-5
Component	Phenomena	Rank	Ranking Rationale	Phenomena Description	Type Geometry	Supporting Evidence	Sublevel Phenomena
CMT, Continued	Flow resistance	L	R109	D27	C6/G13	E3	S11
Downcomer/ lower plenum	Level	H	R112	D39	C7/G17	E2	S13
	Condensation	M	R111	D9	C7/G18	E2	S18
	Loop asymmetry effects	L	R146	D45	C7/G16	E3	S9
	Stored energy release	L	R147	D68	C7/G15	E2	S2
Fuel rods	Core power/decay heat	H	R114	D12	C8/G20	E2	S4
	CHF/dryout	L	R113	D92	C8/G20	E3	S57
Hot legs	Entrainment	M	R117	D20	C9/G25	E2	S23
	Horizontal fluid stratification	M	R116	D35	C9/G25	E2	S33
	Countercurrent flow	L	R115	D13	C9/G25	E3	S32
	Condensation	L	R74	D9	C9	E2	S18
IRWST	Flow resistance	H	R118	D27	C10/G27	E2	S11
	Pool level	H	R119	D58	C10/G26	E2	S25
	Pool thermal stratification	H	R121	D59	C10/G26	E2	S19
	Pool to tank structure heat transfer	L	R120	D60	C10/G28	E2	S26
	Sparger pipe level	L	R122	D89	C10	E3	S75
	Interphasic condensation	L	R148	D37	C10/G29	E3	S18
Sump	Fluid Temperature	H	R134	D29	C17	E2	S34
	Level	H	R125	D39	C17	E2	S13
	Flow resistance	M	R133	D27	C17	E3	S11
Pressurizer	Level (inventory)	M	R123	D39	C14/G33	E2	S13
Steam generator	Primary to secondary heat transfer	L	R124	D33	C16/G39	E2	S53

Table B-2. (continued).

			For codes shown in these columns, See Tables:				
			B-3	G-1	G-2/G-3	G-4	G-5
Component	Phenomena	Rank	Ranking Rationale	Phenomena Description	Type Geometry	Supporting Evidence	Sublevel Phenomena
Upper head / upper plenum	Two-phase level in upper plenum	H	R128	D95	C18	E2	S80
	Entrainment/de-entrainment	M	R149	D20	C18/G46	E2	S23
	Condensation	L	R126	D9	C18	E2	S18
	Noncondensible effects	L	R127	D50	C18	E2	S12
Containment (interior) (see footnote 1 of Table B-1)	Pressure	M	R130	D93	C19	E2	S76
	Liquid distribution	M	R129	D96	C19	E3	S81
	Liquid subcooling	L	R131	D97	C19	E2	S82

Table B-3. Transient description and ranking rationale for the SBLOCA PIRT.

Overall Transient Description and Top-level Ranking Rationale

This sequence is initiated by the opening of a small break (2-inch diameter or smaller circular hole) in the reactor coolant system (RCS) cold leg piping without an accompanying single failure in a safety system. Only safety-grade plant systems are assumed to be available. It is assumed that the plant response to this event satisfies the basic plant design objective of core-uncovery avoidance. Therefore, at the top level, phenomena were selected and ranked in this PIRT according to the expected influence upon the reactor vessel inventory response.

The small break loss-of-coolant accident (SBLOCA) was initially subdivided into four time phases. However, beginning with Revision 2, the four phases have been combined into two time phases. The two phases are now referred to as the short-term phase and the long-term phase. The short-term phase is a combination of what was previously referred to as the high pressure phase and the ADS blowdown phase and the initial part of the long-term IRWST phase. The long-term phase is a combination of the long-term IRWST phase and the long-term sump phase. The following sections provide the phase descriptions, the phase-specific PIRT phenomena ranking rationales, and the detailed rationales for the ranked phenomena.

Phase Descriptions and Medium-level Ranking Rationales

Short-Term Phase:

Description - This phase begins when the break opens with the reactor operating at full power (the initial plant thermal-hydraulic conditions are provided in Reference 6, Table H-1). The RCS experiences a blowdown into the containment through the pipe rupture. This process initially is controlled by critical flow at the break and flashing within the pressurizer (where the only initially-saturated fluid in the RCS is located). The mass loss through the break causes the pressurizer level to fall along with the RCS pressure. Reactor and turbine trips are initiated when the pressurizer pressure falls to its scram set point value (Reference 6, Table H-2, provides a list of plant automatic actions and their corresponding signal set points). This occurrence results in the shutdown of the core nuclear reaction and in turbine stop valve closure. Reactor power is quickly reduced to the decay heat rate, and this power reduction causes the average RCS temperature to fall, the RCS fluid to shrink and, therefore, the RCS pressure to fall more rapidly. The steam generator secondary pressures rise rapidly, potentially reaching the safety relief valve opening set point pressure. Break flow and fluid-shrinkage effects cause the pressurizer pressure to continue falling to the S signal set point pressure. S signal generation causes core makeup tank (CMT) actuation, main feedwater isolation, and reactor coolant pump trip. CMT actuation, in turn, causes passive residual heat removal (PRHR) system actuation. The RCS loop flows decline rapidly from a forced-circulation to a natural-circulation condition. Core decay heat is removed from the RCS through a combination of break energy release, CMT recirculation, and PRHR and steam generator heat transfer. The RCS inventory declines further, causing the pressurizer to empty. Continued PRHR cooling causes the RCS to depressurize below the secondary system, and this causes the steam generator heat transfer to reverse. CMT recirculation warms the water in the pressure balance lines (PBLs) and CMTs. The declining RCS pressure and inventory eventually lead to saturation and voiding in the PBLs or CMTs and interruption of CMT recirculation. Accumulator injection begins as the RCS pressure falls to the initial accumulator pressure. When the level in either CMT has declined to 67.5% the Automatic Depressurization System (ADS) stage 1 is actuated (see Reference 6, Table H-2, for details of ADS sequencing). ADS actuation results in a blowdown of the RCS; ADS first, second, and third stages discharge through spargers submerged under water in the IRWST. As the RCS pressure declines, regions with the warmest fluid and those at the lowest pressure preferentially flash first, followed by cooler and higher-pressure regions. Actuations of the ADS second and third stages occur at specified time intervals following ADS first stage actuation. The pressurizer refills as flow exits ADS stages 1, 2, and 3. Actuation of ADS fourth stage occurs upon attaining a level in either CMT of 20%, with an additional

Table B-3. (continued).

time-delay requirement. Unlike the other stages, ADS fourth stage discharges directly into the containment loop compartments. As described for the following phase, the distribution of condensate produced on the containment shell, structures, and equipment can be significant. Plant behavior during this phase is dominated by the RCS blowdown, and this is determined by the RCS mass and energy distributions, especially as they affect the break and ADS flow rates and the CMT level. Flows from the accumulators increase during this phase. Accumulator levels fall, and, eventually, nitrogen is injected from the accumulators into the RCS. Cold water entering the reactor vessel upper plenum/upper head regions may cause condensation-induced rapid refill events in these regions. As the RCS pressure approaches that in the containment, flows through the break and ADS change from choked to friction-dominated. The RCS inventory declines after accumulator injection ends, and it is critical that the core remain covered until IRWST injection begins. This phase ends when the differential pressure between the RCS and containment has been reduced to 12.1 psi. This pressure difference is equivalent to the initial 28-ft static head available for driving fluid from the IRWST into the reactor vessel. The initial IRWST injection rate may be unsteady. Increased injection rates may lead to decreased core steam production, decreased quality and volumetric flow at the fourth stage ADS and, therefore, RCS repressurization which results in a decreased injection rate. Intermittent pressurizer draining may influence this unsteady IRWST injection behavior. Onset and establishment of stable IRWST injection marks the end of the short-term phase.

Important parameters and dominant processes - The parameters of primary importance during this phase are RCS pressure, CMT level, ADS flow rate and the RCS mass and energy distributions. The S signal is generated based on the RCS pressure response. ADS actuation is based on the CMT level response. Both of these parameters are controlled by the RCS mass and energy distributions. The processes important for accurate simulation of these parameters are: gas bubble expansion, break critical flow, PRHR heat transfer, CMT recirculation, natural circulation in the RCS loops, steam generator heat transfer, and the RCS mass and energy balances. Later in the short-term phase the CMT level and ADS flow rate are importance because they determine the timing of ADS staging and the RCS depressurization rate. The processes important for accurate simulation of these parameters later in the process are the discharge flows (ADS and break, critical and friction-dominated) and the RCS mass and energy.

Long-Term Phase:

Description - This phase begins when stable flow is established from the IRWST, through the direct vessel injection lines, into the downcomer of the reactor vessel. This flow replenishes RCS inventory and reverses the downward core level trend. Steam and water flowing from the core are passed out the break and ADS stage 4 into the containment. In the containment, the water from the break and ADS flows into the containment sump. Steam from the break and ADS stage 4 may be condensed on containment structures and internal equipment; this condensate will flow to the containment sump. Steam from the break and ADS stage 4 also may be condensed on the inside of the containment shell, and this condensate is returned via gutters to the IRWST. Core decay heat is removed through the containment shell to its ultimate heat sink (the environment) via evaporative, convective, and radiative heat transfer on the outside of the containment shell. Rapid condensation-induced CMT refills may occur. Most liquid that escapes returning to the IRWST (for example, that flowing from a break or from the ADS fourth stage) is collected in the containment sump, a portion of which is elevated above the core. Gravity-driven injection from the sump, similar to that from the IRWST, returns liquid to the reactor vessel downcomer. The onset of sump injection begins when the sump level has been equalized with the IRWST level. This equalization may occur as a result of flow from the break into the sump, or by opening of valves in the sump discharge lines that allow the IRWST and sump levels to equilibrate. These valves are opened automatically when the IRWST level reaches a minimum set point value. The sump replaces the IRWST as the source of RCS injection. Combined or alternating IRWST/sump injection modes also are possible. Steam and water flowing from the core are passed out the break and ADS stage 4 into the containment. In the containment, the water flowing from the break and ADS stage 4 flows into the containment sump. Steam flowing from

Table B-3. (continued).

the break and ADS stage 4 may be condensed on containment structures and internal equipment; this condensate will flow to the containment sump. Steam flowing from the break and ADS stage 4 also may be condensed on the inside of the containment shell, and this condensate is returned via gutters to the IRWST (from where it, too, may flow into the sump). Core decay heat is removed through the containment shell to its ultimate heat sink (the environment) via evaporative, convective, and radiative heat transfer on the outside of the containment shell. The sump injection rate may be unsteady. Increased injection rates may lead to decreased core steam production, decreased quality and volumetric flow at the fourth stage ADS and, therefore, RCS repressurization which results in a decreased injection rate. Gravity-driven injection from the sump, similar to that from the IRWST, returns liquid to the reactor vessel downcomer. Rapid condensation-induced refills of the hot or cold leg regions may occur. The plant end-state for this accident includes core-inventory maintenance from sump injection, and decay heat removal, across the containment shell, to the atmosphere.

Important parameters and dominant processes - The RCS-to-containment differential pressure is judged to be the primary parameter of importance because it determines the magnitude of the IRWST and sump injection flow rate. The processes important for accurate simulation of this parameter are: ADS flow and pressure drop, the transient IRWST inventory, and the sump inventories and the containment and RCS mass and energy balances.

Detailed Phenomena Ranking Rationales

Ranking rationale for the phenomena in Tables B-1 through B-2

Code	Ranking Rationale
R1	Accumulator flow is ranked high during the short-term phase. Accumulator injection flow is large and a major contributor to the RCS mass and energy balances. When the accumulator is depleted of liquid, noncondensible gas (nitrogen) is expelled into the RCS through the DVI lines. Tests indicate that accumulator flow is essential to inventory replacement through this phase for the DEDVI transient and during the ADS blowdown sub-phase for the remaining SBLOCAs. Tests indicate that accumulator flow provides significant core subcooling and therefore helps set the initial conditions for reactor vessel liquid boiloff to the minimum level prior to IRWST injection.
R2	Accumulator noncondensible effects are ranked medium during the short-term phase. Accumulator flow is a significant contributor to the reactor coolant system energy balance (see R1) and this flow is determined by the differential pressure between the accumulator gas bubble and RCS. Expansion of the nitrogen gas bubble within the accumulator controls the differential pressure between the accumulator and RCS and, therefore, the rate at which liquid flows from the accumulator into the RCS and the time at which the accumulator is depleted of liquid. The effects of nitrogen entering the RCS are discussed separately for each component.
R3	Break energy release is ranked medium during the short-term phase. RCS mass loss at the break was judged more important than the RCS energy loss at the break (which is ranked high, see R4) because RCS depressurization is controlled by the loss of mass and resulting expansion of vapor spaces (for example, in the pressurizer and reactor vessel upper head). However, the break energy release is a major term in the RCS energy balance and directly affects distribution of fluid energy within the RCS.

Table B-3. (continued).

Ranking rationale for the phenomena in Tables B-1 through B-2

Code	Ranking Rationale
R4	Break mass flow is ranked high during the short-term phase. During the early stages of this phase, the dominant processes include critical flow at the break and net RCS mass balance. During this period the break flow dominates the RCS mass balance. However, during ADS blowdown the break mass flow is judged to be less significant than the ADS mass flow. The break is the main source of inventory depletion, which eventually leads to CMT draining, which in turns leads to ADS actuation, and an increased rate of inventory depletion. More important, however, is the fact that the ADS actuation causes the RCS to depressurize to the level at which the AP600 can transition to long-term-cooling. Thus, the break has a dominant impact on all four of the key system-level processes, i.e., depressurization, inventory depletion, inventory replacement, and core cooling.
R5	Cold leg condensation is ranked low during the short-term phase. Cold leg condensation effects may alter the break flow, alter reactor vessel downcomer and core levels, or result in water hammer events. The steam for this condensation may be passed from the reactor vessel upper plenum and head regions, through the vessel internal bypass paths, into the upper downcomer and cold leg regions. However a SBLOCA sensitivity study addressing condensation in the cold leg shows that condensation in the cold legs has little effect on the overall transient results. Thus, the ranking has been reduced to "Low".
R6	Cold leg flashing is ranked medium during the short-term phase. RCS flashing during this phase is preferential (i.e., it is based on localized pressures and temperatures). Flashing affects the RCS mass distribution, one of the important parameters for this phase. In addition, steam produced by flashing in the cold legs (or elsewhere, and convected into the cold legs) may enter the pressure balance line to replace liquid drained from the CMT. The CMT draining process determines the staging of ADS. RCS flashing affects the RCS mass and energy distributions during the ADS blowdown phase.
R7	Cold leg loop asymmetry effects are ranked low during the short-term phase. Asymmetric conditions (pressures, temperatures, flow rates) within and/or between RCS components may be present. The sources of these asymmetries are the break location (i.e., it is situated at a single location in the RCS), and the plant configuration (the pressurizer and PRHR system are connected on one coolant loop while the CMTs are connected on the other). Asymmetric effects in the cold leg were ranked low only because they may influence fluid conditions present at the break and, thereby, alter the distribution of RCS mass and energy.
R8	PBL-to-cold leg tee phase separation is ranked high during the short-term phase. As the CMT drains, void may be convected into the pressure balance line through this tee and this process has a direct effect upon the CMT level that is one of the important parameters for this phase.
R9	Cold leg stored energy release is ranked low during the short-term phase. The rate of stored energy release from piping walls was judged smaller than the other contributors to the RCS energy balance (fuel rod decay heat, and PRHR and steam generator heat transfer).

Table B-3. (continued).

Ranking rationale for the phenomena in Tables B-1 through B-2

Code	Ranking Rationale
R10	Cold leg thermal stratification is ranked medium during the short-term phase. Experimental data from ROSA/AP600 test AP-CL-03 (1-inch cold leg break) indicate extreme thermal stratification of water within the cold legs (with warm water residing over cold). This stratification alters the break flow because, even though the cold leg may be liquid-filled, the temperature of water exiting the break becomes a function of the break location on the circumference of the pipe. However; this stratification is believed to be caused by the configuration of the ROSA facility and is not typical of AP600.
R11	Core flashing is ranked high during the short-term phase. RCS flashing affects the RCS mass and energy distributions during the ADS blowdown phase. Flashing is preferential, with the RCS regions with the warmest water and lowest pressure flashing first. Therefore, the core region will be one of the first to flash. Core flashing also has implications for core cooling (see R68, R69, and R72).
R12	Core flow resistance is ranked low during the short-term phase. The core flow is large and positive, during the ADS blowdown sub-phase as RCS fluid rushes toward the ADS system inlets (all are located on the hot legs). However, core flow resistance produces a pressure drop that is a two orders of magnitude lower than the pressure drop for flow from the RCS, through the ADS, into the containment.
R13	Core mass flow (including bypass) is ranked medium during the short-term phase. Although this phenomenon affects the coolant loop differential pressures, it has a minimal influence on the primary system mass and energy distributions, as compared with the other ranked phenomena in the break, core, PRHR, and steam generator components.
R14	Core stored energy release is ranked medium during the short-term phase. The rate of stored energy release from non-fuel structures in the core region was judged comparable to the other contributors to the RCS energy balance (fuel rod decay heat, and PRHR and steam generator heat transfer). Fuel rod stored energy release is listed separately (see R27) from the core region non-fuel structures.
R15	CMT-to-loop differential density and head is ranked medium during the short-term phase. This phenomenon refers to the difference in fluid densities between the vertical sections of the CMT inlet and outlet regions. The inlet region primarily consists of the pressure balance line (PBL). The outlet region primarily consists of the CMT itself, and its discharge line. The PBL volume is small and so it is readily flushed with warm water entering from the cold legs. The CMT volume is large, its water is initially very cold (at the containment temperature) and, therefore, it is only slowly warmed by flow entering from the PBL. It is this CMT-to-loop differential density from which the driving head for CMT recirculation, a dominant process during this phase, arises. The equilibrium CMT recirculation flow rate is that which balances this driving head with the loop frictional pressure drop.
R16	CMT condensation is ranked medium during the short-term phase. The CMT level response is primarily determined by phenomena external to the CMT (primarily those affecting the RCS mass and energy balances and distributions) or from flashing within the CMT. Condensation-induced CMT refill events can alter the manner in which the CMTs drains.

Table B-3. (continued).

Ranking rationale for the phenomena in Tables B-1 through B-2

Code	Ranking Rationale
R17	CMT flashing is ranked medium during the short-term phase. If water in the CMT flashes, then steam will rise to the top of the tank and enter the high point of the pressure balance line. Sufficient void collected at that location breaks the siphon path through the pressure balance line and results in termination of CMT recirculation. The importance phenomenon is break-size dependent. Onset of CMT draining due to flashing occurs for smaller break sizes, where the period of CMT recirculation is longer. The manner in which the CMT flashes influences the CMT level behavior. Actuation of the ADS fourth stage (a major event during the ADS blowdown phase) is based upon the CMT level attaining a minimum set point level.
R18	CMT flow resistance is ranked high during the short-term phase. The CMT flow resistance (in particular that associated with its discharge line, check valve, and orifice) significantly affects the CMT recirculation and draining rates. Actuation of the ADS fourth stage (a major event during the ADS blowdown phase) is based upon sufficient CMT draining so that the CMT level attains a minimum set point. Tests indicate that after ADS 4 actuation, and just prior to IRWST injection, the remaining source of coolant for the core is from the CMTs, CMT flow, dictated by CMT level and line resistance is essential to inventory replacement
R19	CMT level is ranked high during the short-term phase. ADS actuation is based upon CMT level attaining a minimum set point level. See R18 for additional justification.
R20	CMT thermal stratification and mixing is ranked medium during the short-term phase. Thermal stratification and mixing influences affects the CMT flashing and draining behavior, and, therefore, the CMT level response. Actuation of the ADS fourth stage (a major event during the ADS blowdown phase) is based upon the CMT level attaining a minimum set point. In addition, tank thermal stratification also has a minor effect on the CMT recirculation rate because it alters the CMT recirculation driving head (see R15).
R21	Downcomer condensation is ranked medium during the short-term phase. RELAP5 AP600 plant SBLOCA simulations (see Reference 8) have shown that interphasic condensation of steam flowing from the upper head through the bypass into the upper portion of the reactor vessel downcomer can significantly alter the break flow and progression of a SBLOCA sequence. Steam condensed in the downcomer or cold legs is unavailable to flow out the break. Data from ROSA/AP600 test AP-CL-03 (1-inch diameter cold leg break) indicate that significant redistribution of RCS inventory can result from this phenomenon. Subcooled water is supplied to the downcomer from the CMTs and accumulators via the DVI lines. Steam is supplied to the downcomer from RCS flashing and from upper head-to-downcomer bypass flow.
R22	Downcomer/lower plenum flow distribution is ranked low during the short-term phase. The flow rates and temperatures of fluids in the cold legs are asymmetric. These asymmetries are related to the break location, the CMTs being connected to the cold legs of only one of the two coolant loops, and the PRHR system being connected to the other loop. Downcomer flow distribution represents the fluid mixing processes that determine the RCS energy distribution, one of the important parameters listed for this phase.

Table B-3. (continued).

Ranking rationale for the phenomena in Tables B-1 through B-2

Code	Ranking Rationale
R23	Downcomer level is ranked medium during the short-term phase. A downcomer level forms during this phase because of steam flow (from the upper head into the upper downcomer through the bypass nozzles), flashing, and asymmetries in the cold leg fluid conditions between the CMT and pressurizer loops (see R7). However, during this phase, the downcomer level has only a minimal effect on the CMT level and RCS mass and energy distributions, the important parameters for this phase.
R24	Core and downcomer/lower plenum loop asymmetry effects are ranked low during the short-term phase. Asymmetric conditions (pressures, temperatures, flow rates) within and/or between RCS components may be present. The sources of these asymmetries are the break location (i.e., it is situated at a single location in the RCS), and the plant configuration (the pressurizer and PRHR system are connected on one coolant loop while the CMTs are connected on the other). Downcomer fluid temperature asymmetries may affect fluid conditions present at the break, and, thereby, significantly alter the distribution of RCS mass and energy (also see R22, and R23).
R25	Downcomer/lower plenum stored energy release is ranked low during the short-term phase. The rate of stored energy release from vessel walls and system internals was judged smaller than the other contributors to the RCS energy balance (fuel rod decay heat, and PRHR and steam generator heat transfer).
R26	Fuel rod core power/decay heat is ranked high during the short-term phase. This phenomenon is the primary energy source in the RCS energy balance. Removal of this heat is the basic safety issue for a SBLOCA. Subsequent to ADS 4 operation, liquid boiloff due to core decay heat is the primary mechanism for reactor vessel inventory depletion.
R27	Fuel rod stored energy release is ranked medium during the short-term phase. With the reactor in operation, the fuel stored energy is considerable. However, release of this energy into the reactor coolant occurs only over a short period following reactor trip. This phenomenon therefore affects the RCS energy balance, but is temporary, so its influence is small as compared with that of the core power/decay heat (that is ranked high, see R26).
R28	Hot leg flashing is ranked medium during the short-term phase. RCS flashing affects the RCS mass and energy distributions during the high pressure and ADS blowdown phases. Flashing is preferential, with the RCS regions with the warmest water and lowest pressure flashing first. In the hot leg, the flashing rate affects the hot leg flow regime. High flashing rates result in homogeneous conditions while low flashing rates result in stratified conditions (steam over water) in the hot legs. This distinction significantly affects the state of fluid exiting all ADS stages.
R29	Hot leg horizontal fluid stratification is ranked low during the short-term phase. The PRHR system inlet and the ADS stage 4 lines connect to the tops of the hot leg pipes. If steam resides in the upper portion of the hot leg, then it may freely enter the PRHR and ADS-4 systems; this steam flow may entrain liquid. The hot leg likely will be stratified during this phase. This phenomena affects the state of the fluid entering the PRHR and ADS-4 systems and, thereby, PRHR system heat removal and ADS-4 energy and mass flow.

Table B-3. (continued).

Ranking rationale for the phenomena in Tables B-1 through B-2

Code	Ranking Rationale
R30	Hot leg loop asymmetry effects are ranked low during the short-term phase. Asymmetric conditions (pressures, temperatures, flow rates) within and/or between RCS components may be present. The sources of these asymmetries are the break location (i.e., it is situated at a single location in the RCS), and the plant configuration (the pressurizer and PRHR system are connected on one coolant loop while the CMTs are connected on the other). During this phase, asymmetry between the two hot legs may result because the PRHR inlet is connected to only one hot leg and this effect may alter the overall plant response (for example, through its affect on flashing behavior).
R31	Hot leg phase separation in tees is ranked high during the short-term phase. This phenomenon influences ADS energy release and mass flow because it controls the quality of the fluid entering ADS stages 1, 2, and 3 (via the pressurizer surge line tee) and ADS stage 4 (through the ADS-4 tees). A recent ADS-4 phase separation sensitivity study shows that phase separation in the ADS-4 tees has little effect on the overall transient results.
R32	Hot leg stored energy release is ranked low during the short-term phase. The rate of stored energy release from piping walls was judged smaller than the other contributors to the RCS energy balance (fuel rod decay heat, and PRHR and steam generator heat transfer). During the ADS blowdown phase the flow of heat is expected to be a minor contributor to the overall RCS energy balance; energy loss through the ADS is expected to dominate that balance.
R33	Hot leg voiding is ranked low during the short-term phase. Hot leg voiding affects both the state of the fluid entering the PRHR system and the natural circulation flow rate through the RCS coolant loops.
R34	IRWST flow and temperature distribution in the PRHR bundle region is ranked low during the short-term phase. Heat transfer between the PRHR and IRWST is listed as a dominant process for this phase (see R45). The flow rate and temperature of the IRWST fluid flowing through the PRHR bundle significantly influence PRHR heat transfer because they affect the tube outer-wall heat transfer coefficient and heat sink temperature.
R35	IRWST interphasic condensation is ranked low during the short-term phase. ADS stages 1, 2, and 3 discharge RCS fluid into the IRWST through two spargers. The fluid flowing through the spargers has a high steam content, perhaps superheated, at the near-atmospheric pressure inside the tank. However, the IRWST fluid is initially subcooled, so high interphase condensation rates are anticipated. This phenomenon affects: (1) the manner in which the IRWST performs the quenching process, (2) the state of the IRWST fluid (that later is injected into the RCS), and (3) the containment pressure.
R36	IRWST pool flow is ranked medium during the short-term phase. This phenomenon affects: (1) the manner in which the IRWST performs the quenching process, (2) the state of the IRWST fluid (that later is injected into the RCS), and (3) the containment pressure.
R37	IRWST pool level is ranked low during the short-term phase. The initial IRWST pool level is only slightly above the elevation span of the upper horizontal PRHR tube bundle region. Boil-off from the IRWST pool lowers the usable PRHR bundle heat transfer area. During this phase, pool inventory can only be replenished by condensate returning from the interior of the containment shell (steam may be supplied to the shell from break effluent or IRWST boil-off). After ADS stages 1, 2, and 3 unchoke, the pool level has a minor effect upon the pressure at the ADS sparger and, therefore, upon the ADS flow rate.

Table B-3. (continued).

Ranking rationale for the phenomena in Tables B-1 through B-2

Code	Ranking Rationale
R38	IRWST pool thermal stratification is ranked medium during the short-term phase. Pool thermal stratification affects the heat sink temperature on the outside of the PRHR tubes. The heat sink temperature is that of the fluid flowing through the PRHR tube bundle and not that of the fluid residing in the pool away from the bundle. However, pool thermal stratification affects the temperature of the fluid that is convected from the open pool into the PRHR tube bundle region. During the ADS blowdown phase this phenomenon affects: (1) the manner in which the IRWST performs the quenching process, (2) the state of the IRWST fluid (that later is injected into the RCS), and (3) the containment pressure.
R39	Not used.
R40	Pressurizer flashing is ranked medium during the short-term phase. RCS depressurization is first controlled by flashing within the pressurizer because during normal reactor operation it contains the only initially-saturated water in the RCS. After the pressurizer empties, RCS depressurization is controlled by flashing elsewhere (core, hot leg, reactor vessel upper head).
R41	Pressurizer level (inventory) is ranked high during the short-term phase. The first part of the ADS blowdown occurs through stages 1 through 3, the inlets for which are connected to the top of the pressurizer. The pressurizer fluid mass is large during this phase. The fluid residing at the top of the pressurizer flows through the ADS system, affecting its energy release and mass flow (these phenomena are also ranked high, see R60 and R61). After ADS 4 actuation, and just prior to IRWST injection, one of the remaining sources of coolant for the core is from the pressurizer. Draining of the pressurizer acts as an inventory replacement mechanism.
R42	PRHR condensation is ranked low during the short-term phase. This phenomenon is a contributor to PRHR-to-IRWST heat transfer (that is ranked medium, see R45). The convective thermal resistance inside the PRHR tubes is sensitive to (among other things) the presence or absence of the condensation process.
R43	PRHR differential density is ranked low during the short-term phase. This phenomenon is a contributor to the PRHR-to-IRWST heat transfer (that is ranked medium, see R45). The differential density (i.e., the difference in density between the fluids in the inflow and outflow sides of the PRHR system piping) is the driving force for flow through the primary side of the PRHR system. The flow through the PRHR tubes affects the convective thermal resistance on the inside surfaces of the PRHR tubes (also see R42).
R44	PRHR flow resistance is ranked low during the short-term phase. The total resistance of the PRHR system (including the entire flow loop through the core) balances the driving force created by the differential density (see R43). The PRHR system flow rate is determined by this balance, and the total loop resistance is dominated by the PRHR system components (the heat exchanger and the inlet and outlet piping) and not by the non-PRHR components (such as the core and RCS loop piping). The flow through the PRHR tubes affects the convective thermal resistance on the inside surfaces of the PRHR tubes.

Table B-3. (continued).

Ranking rationale for the phenomena in Tables B-1 through B-2

Code	Ranking Rationale
R45	Heat transfer between the PRHR and IRWST is ranked medium during the short-term phase. During the early portion of this phase, the PRHR system represents the main mechanism by which the core decay power is removed from the RCS to the containment. During the latter part of short-term phase the RCS energy balance is dominated by the ADS energy release and not by PRHR-to-IRWST heat transfer. The data from ROSA/AP600 test AP-CL-03 (1-inch diameter cold leg break) indicate that PRHR effects are diminished following ADS actuation.
R46	PRHR noncondensible effects are ranked low during the short-term phase. Noncondensible gas (hydrogen) evolves from solution during the RCS depressurization. Noncondensible effects can alter the heat transfer processes on the inside of the PRHR tubes. In addition, a large volume of noncondensible gas accumulated at the high point of the PRHR inlet line (it is an inverted trap configuration) may block the path for flow through the PRHR heat exchanger.
R47	PRHR voiding is ranked low during the short-term phase. This phenomenon has many influences on the PRHR-to-IRWST heat transfer (that is ranked medium, see R45). As steam void increases, the PRHR system differential density, flow rate, and heat transfer rate increase. However, voiding due to noncondensible gas entering the PRHR system may have the opposite result if a gas bubble blocks the line (see R46).
R48	Pump coastdown performance is ranked low during the short-term phase. The reactor coolant pump coastdown behavior influences steam generator and PRHR system heat transfer because it determines the flow rates inside the steam generator and PRHR system tubes. However, this influence is limited by the short duration of the coastdown (it lasts only about 2 minutes) and because the pump head declines exponentially following pump trip.
R49	Pump flow resistance is ranked low for the short-term phase. Here, the pump flow resistance is the locked-rotor resistance that is present following the pump coastdown period. This resistance affects natural circulation flows through the RCS loops (i.e., through the core, hot legs, steam generators, pumps, and cold legs). However, this loop natural circulation pattern is short-lived, ending when the RCS temperatures fall below those of the steam generator secondary systems. This resistance also affects the flow rate through the PRHR system natural circulation loop (i.e., through the core, hot leg, PRHR inlet, PRHR heat exchanger, PRHR outlet, pump, and cold leg). Flows through this loop are expected to continue throughout this phase. However, for this natural circulation loop, the total flow resistance is dominated by the PRHR system components (the heat exchanger and the inlet and outlet lines) and not by the pump locked-rotor resistance.

Table B-3. (continued).

Ranking rationale for the phenomena in Tables B-1 through B-2

Code	Ranking Rationale
R50	Pump mixing is ranked low during the short-term phase. This mixing refers to turbulence induced by water flow through the reactor coolant pump impellers following pump coastdown. This phenomenon influences thermal stratification of water within the cold legs (that was observed in ROSA/AP600 test AP-CL-03 and is ranked medium, see R10). The PRHR system outlet is connected to the outlet plenum of the steam generator on one RCS coolant loop. Water flowing out of the PRHR system is cold (approaching the temperature of the water in the IRWST). Cold water entering the plenum preferentially flows downward, through the reactor coolant pump impellers, into the two cold legs on that RCS coolant loop. The test data indicate the cold water stratifies on the bottom of the cold leg piping, thus potentially affecting break flow. The influence of this phenomena has on the cold leg thermal stratification may be determined by the status of the impeller (i.e., whether it is locked, or free-wheeling in this situation).
R51	Steam generator secondary level is ranked low during the short-term phase. A low level can reduce the available tube heat-transfer area. A reduction of the secondary level swell (due to the declining steam generator heat load) will tend to reduce the mixture level on the outside of the steam generator tubes. However, the secondary level likely will remain sufficiently high to cover the U-tubes.
R52	Steam generator secondary pressure is ranked low during the short-term phase. The secondary system generally is saturated (subcooling existing at full power operation is removed shortly following reactor trip). The secondary pressure is, therefore, an indication of the secondary-side temperature available to exchange heat with the RCS through the steam generator tubes.
R53	Steam generator tube heat transfer is ranked medium during the short-term phase. The steam generator secondary system is a heat sink for the RCS during the early part of this phase, but it becomes a heat source to the RCS later during the phase because the RCS temperatures fall below those of the secondary (due to CMT and PRHR cooling effects). This phenomenon is ranked medium because it is a major term in the RCS energy balance equation during the time when heat flow is from the primary to secondary systems. Reverse heat flow (i.e. secondary-to-primary) is a temporary phenomenon because heat addition to the RCS fluid inside the tubes causes boiling and voiding within the tubes. This voiding blocks the path for further RCS loop natural circulation flow through the steam generators, and interruption of this flow loop thermally decouples the primary and secondary systems. During the ADS blowdown phase the RCS energy balance is dominated by decay heat addition and ADS energy removal and not by steam generator heat transfer during this phase. The steam generators are essentially thermally-decoupled from the RCS from a lack of liquid inside the steam generator tubes.
R54	Steam generator tube voiding is ranked low during the short-term phase. This phenomenon is the mechanism for interruption of RCS loop natural circulation flow (see R53).
R55	Upper plenum/upper head flashing is ranked low during the short-term phase. RCS flashing affects the RCS mass and energy distributions during the ADS blowdown phase. Flashing is preferential, with the RCS regions with the warmest water and lowest pressure flashing first. Data from ROSA/AP600 test AP-CL-03 (1-inch diameter cold leg break) indicated that hot fluid was convected upward from the core into these regions during the previous phase. The fluid temperatures were altered by this flow, thereby affecting the pressures at which these regions flash.

Table B-3. (continued).

Ranking rationale for the phenomena in Tables B-1 through B-2

Code	Ranking Rationale
R56	Upper plenum loop asymmetry effects are ranked low during the short-term phase. Asymmetric conditions (pressures, temperatures, flow rates) within and/or between RCS components may be present. The sources of these asymmetries are the break location (i.e., it is situated at a single location in the RCS), and the plant configuration (the pressurizer and PRHR system are connected on one coolant loop while the CMTs are connected on the other). Asymmetric effects in the upper plenum are potentially of importance because the flow split at this location affects the conditions of the fluid entering the PRHR system inlet that is located on only one hot leg.
R57	Upper plenum/upper head stored energy release is ranked low during the short-term phase. The RCS pressure and saturation temperature fall rapidly during this phase. As a result, remaining stored heat in metal structures of this component is available to flow into the RCS coolant. However, this flow of heat is expected to be a minor contributor to the overall RCS energy balance; energy loss through the ADS is expected to dominate that balance.
R58	Upper head-to-downcomer bypass flow is ranked low during the short-term phase. Steam flowing through this path may be condensed in the downcomer or cold legs or may reach the break. The cold legs are thermally stratified during this phase. This behavior is of importance as it affects the temperature of fluid presented at the break and, therefore the break flow rate. Although small, this flow path is the most direct communication path between the hot and cold leg regions and may be active during the chaotic RCS fluid conditions expected during this phase. See R5, R10 and R21 for more discussion.
R59	Upper head/upper plenum voiding is ranked medium during the short-term phase. Data from ROSA/AP600 test AP-CL-03 (1-inch diameter cold leg break) indicated that hot fluid was convected upward from the core into the upper plenum/upper head regions during the previous phase. The fluid temperatures were altered by this flow, affecting the pressures at which the these regions flashed. In that test, these regions first voided, then were refilled due to condensation. This behavior resulted in a significant redistribution of RCS inventory.
R60	ADS energy release is ranked high during the short-term phase. This release is the dominant outflow term in the RCS energy balance.
R61	ADS mass flow is ranked high during the short-term phase. This flow is the dominant outflow term in the RCS mass balance.
R62	ADS choking in complex geometry is ranked medium during the short-term phase. Choking in the ADS lines, valves, and fittings controls the ADS flow (ranked high, see R61) through all stages until the differential pressure between the RCS and containment has been sufficiently reduced. The piping configurations of the ADS stages are different and all are complex, resulting in uncertainty regarding the choking locations, fluid states, and discharge coefficients. This uncertainty affects the choked flow rate. A portion of this uncertainty regards phase separation at tees located within the ADS piping networks.
R63	ADS flow resistance is ranked medium during the short-term phase. The ADS flow resistance controls the ADS flow (ranked high, see R61) through all stages after unchoking occurs (when the differential pressure between the RCS and containment has been sufficiently reduced).

Table B-3. (continued).

Ranking rationale for the phenomena in Tables B-1 through B-2

Code	Ranking Rationale
R64	ADS noncondensible effects are ranked medium during the short-term phase. Noncondensible gases (nitrogen, expelled into the RCS from the accumulators and hydrogen emerging from solution due to RCS depressurization) will find their way to all ADS stages. Noncondensible gas in the RCS fluid affects the ADS flow (ranked high, see R61) and energy release (ranked high, see R60) in both the choked and unchoked situations.
R65	Break flow resistance is ranked medium during the short-term phase. The break flow resistance controls the break flow (ranked high, see R4) after unchoking occurs, mainly during the ADS blowdown sub-phase (when the differential pressure between the RCS and containment has been sufficiently reduced).
R66	Break noncondensible effects are ranked low during the short-term phase. Noncondensible gases (nitrogen, expelled into the RCS from the accumulators and hydrogen emerging from solution due to RCS depressurization) will find their way to the break. Noncondensible gas in the RCS fluid affects the break flow (ranked high, see R4) and energy release (ranked medium, see R3) in both the choked and unchoked situations.
R67	Cold leg noncondensible effects are ranked low during the short-term phase. Nitrogen expelled from the accumulators accumulates in this region of the RCS and disposition of nitrogen affects the ADS and break mass flow and energy release rates (see R60, R61, R3 and R4).
R68	Core subcooling margin is ranked high during the short-term phase. In this PIRT, the core is assumed to remain covered (the core two-phase mixture level is ranked high, see R69) and, in that case, the fuel rods will not heat up. The subcooling margin affects core flashing and boiling behavior.
R69	Core two-phase mixture level is ranked high during the short-term phase. This phenomenon affects core cooling; the core two-phase mixture level must be above the top of the core to prevent fuel rod heat-up.
R70	Downcomer/lower plenum flashing is ranked low during the short-term phase. RCS flashing affects the RCS mass and energy distributions during the ADS blowdown phase.
R71	Downcomer/lower plenum noncondensible effects are ranked low during the short-term phase. Nitrogen expelled from the accumulators accumulates in this region of the RCS and disposition of nitrogen affects the ADS and break mass flow and energy release rates (see R60, R61, R3 and R4) and may affect the CMT level response.
R72	Fuel rod critical heat flux/dryout is ranked medium during the short-term phase. This phenomenon affects core cooling. During this phase, RCS pressure falls, RCS mass is lost, RCS voids increase, and this provides a possibility for core uncovery and fuel rod heat-up.
R73	Hot leg CCFL is ranked low during the short-term phase. This phenomenon contributes to the hot leg phase separation process (see R31) because it affects the fluid state and flow regime in the hot leg.
R74	Hot leg condensation is ranked low during the short-term and long-term phases. Data from ROSA/AP600 test AP-CL-03 (1-inch diameter cold leg break) indicate that, in general, significant redistribution of RCS inventory can result from condensation phenomenon. Steam may be supplied to the hot legs through the steam generators while subcooled liquid may be supplied to the hot legs through the core.

Table B-3. (continued).

Ranking rationale for the phenomena in Tables B-1 through B-2

Code	Ranking Rationale
R75	Hot leg countercurrent flow is ranked low during the short-term phase. This phenomenon contributes to the hot leg phase separation process (see R31) because it affects the fluid state and flow regime in the hot leg.
R76	Hot leg entrainment is ranked low during the short-term phase. This phenomenon contributes to the hot leg phase separation process (see R31) because it affects the fluid state and flow regime in the hot leg.
R77	Hot leg noncondensible effects are ranked low during the short-term phase. Noncondensible gases (nitrogen expelled from the accumulators and hydrogen emerging from solution during RCS depressurization) compete with steam for flow through all stages of the ADS. These gases affect the ADS energy release (ranked high, see R60). However, the effects of noncondensible gases are both temporary and diminishing. The total noncondensible mass is limited to that available from the accumulators plus that available in solution; this mass is small when compared with the RCS water mass. Once expelled to the containment through the ADS or break, noncondensible gases can no longer affect RCS behavior.
R78	IRWST pool-to-tank heat transfer is ranked low during the ADS short-term phase. Over the long term, the energy removed from the pool to its surroundings may be important, but during this phase this term in the IRWST energy balance was judged to be significantly smaller the ADS energy addition term.
R79	IRWST sparger pipe level is ranked medium during the short-term phase. Wall condensation inside the ADS stage 1, 2, and 3 discharge lines (in the regions of these pipes submerged under water in the IRWST) may affect the ADS flow rates through these pipes. This phenomenon also may be associated with water hammer events in these pipes.
R80	Pressurizer CCFL is ranked low during the short-term phase. ADS activation causes significant refill of the pressurizer (that had drained during the short-term phase). As ADS stage 1, 2, and 3 flow declines, the pressurizer liquid inventory drains back into the RCS, and this draining is affected by CCFL at the pressurizer tank/surge line connection.
R81	Pressurizer entrainment/de-entrainment is ranked medium during the short-term phase. This phenomenon affects both the level swell within the pressurizer tank and the carryover of liquid droplets into ADS stages 1, 2, and 3. The ADS energy release and mass flow are ranked high, see R60 and R61.
R82	Pressurizer level swell is ranked medium during the short-term phase. If the pressurizer level resides below the top of the tank then steam exits ADS stages 1 through 3, the inlets for which are connected to the top of the pressurizer. However, if the level swells to the top of the tank, then two-phase mixture (or single-phase liquid) enters ADS stages 1 through 3. This phenomenon therefore affects the ADS mass flow and energy release rates that are ranked high (see R60 and 61).

Table B-3. (continued).

Ranking rationale for the phenomena in Tables B-1 through B-2

Code	Ranking Rationale
R83	Pressurizer noncondensible effects are ranked low during the short-term phase. Noncondensible gases (nitrogen from the accumulators and hydrogen emerging from solution during RCS depressurization) will flow out the ADS stages 1, 2 and 3, the inlets for which are connected to the top of the pressurizer. These noncondensible gases will affect the ADS energy release (rated high, see R60). However, the effects of noncondensible gases are both temporary and diminishing. The total noncondensible mass is limited to that available from the accumulators plus that available in solution; this mass is small when compared with the RCS water mass. Once expelled to the containment through the ADS or break, noncondensible gases can no longer affect RCS behavior.
R84	Pressurizer stored energy release is ranked low during the short-term phase. The RCS pressure and saturation temperature fall rapidly during this phase. As a result, remaining stored heat in metal structures of this component is available to flow into the RCS coolant. However, this flow of heat is expected to be a minor contributor to the overall RCS energy balance; energy loss through the ADS is expected to dominate that balance.
R85	PRHR flashing is ranked low during the short-term phase. RCS flashing affects the RCS mass and energy distributions during the ADS blowdown phase.
R86	PRHR phase separation in tees is ranked low during the short-term phase. This is the only instance where phase separation in tees has been ranked for the PRHR component. For normal PRHR flow situations, tee phase separation is primarily of interest at the PRHR inlet line connection on the hot leg and, for these normal situations, this phenomenon was included in the listings for the hot leg component. However, for the ADS blowdown situation, RCS conditions are chaotic, and the question is the manner in which the PRHR system outlet tee (on the steam generator outlet plenum) might perform under potential reverse-flow conditions. Because the PRHR inlet line is connected directly to one of the ADS fourth-stage inlet lines, reverse flow through the PRHR system is likely to develop as RCS fluid rushes out the ADS fourth stage.
R87	Upper plenum/upper head condensation is ranked low during the short-term phase. Data from ROSA/AP600 test AP-CL-03 (1-inch diameter cold leg break) indicate that hot fluid was convected upward from the core into these regions during the low pressure phase. The fluid temperatures were altered by this flow, affecting the pressure at which these regions flashed during ADS blowdown. Additionally, in that test, these regions first voided, then refilled due to condensation events. This behavior resulted in a significant redistribution of RCS inventory.
R88	Upper plenum entrainment/de-entrainment is ranked medium during the short-term phase. The entrainment, de-entrainment, and storage of liquid in the upper plenum region affects the pressure drop and convection of fluid through the hot legs to all ADS stages.
R89	Containment interior pressure is ranked medium during the short-term phase. The containment interior receives flow directly from ADS stage 4. In addition, the IRWST (that receives the flow from ADS stages 1, 2, and 3) resides in the containment interior. The containment interior pressure determines the RCS pressures and the times at which the various ADS stage flows unchoke. Thereafter, the ADS mass flow and energy release (ranked high, see R60 and 61) are determined by the differential pressure between the RCS and the containment interior.

Table B-3. (continued).

Ranking rationale for the phenomena in Tables B-1 through B-2

Code	Ranking Rationale
R90	ADS energy release is ranked high during the long-term phase. The release through ADS stage 4 is the dominant outflow term in the RCS energy balance. ADS stages 1, 2, and 3 are inactive during this phase unless the IRWST level is below the spargers or, if the spargers are covered, the head created by their submergence is less than the differential pressure between the RCS and containment. The energy release and mass flow rate through ADS 4 dictate the back pressure to IRWST injection. Tests indicate that multiple failures of ADS 4 valves would hamper IRWST injection causing the reactor vessel level to drop significantly. ADS 4 flow affects both inventory depletion and replacement.
R91	ADS mass flow is ranked high during the long-term phase. The flow through ADS stage 4 is the dominant outflow term in the RCS mass balance. ADS stages 1, 2, and 3 are inactive during this phase unless the head of the submergence of the ADS spargers under water in the IRWST becomes less than the differential pressure between the RCS and containment. See R90 for additional justification.
R92	Not used.
R93	ADS noncondensible effects are ranked low during the long-term phase. Noncondensible gases (nitrogen expelled into the RCS from the accumulators and hydrogen emerging from solution due to RCS depressurization) will find their way to all ADS stages. Noncondensible gas in the RCS fluid affects the ADS mass flow and energy release (that are ranked high, see R90 and R91). However, these effects will be to a lesser extent than during the short-term phase (where they were ranked medium, see R64). Peak flow of nitrogen from the accumulators into the RCS and peak dissolution of hydrogen occur during ADS blowdown.
R94	ADS condensation (in stages 1, 2, and 3 piping and spargers in IRWST) is ranked low during the long-term phase. ADS stages 1, 2, and 3 are active during this phase when the head of the submergence of the ADS spargers under water in the IRWST becomes less than the differential pressure between the RCS and containment. Wall condensation inside the ADS stage 1, 2, and 3 discharge lines (especially in the regions of these pipes submerged under water in the IRWST) may affect ADS flow through these pipes. This phenomenon also may be associated with water hammer events in these pipes.
R95	Break energy release is ranked medium during the long-term phase. This release is a contributing outflow term in the RCS energy balance. However, because the break size is assumed to be small, the break energy release was judged to be less significant than the ADS energy release (that is ranked high, see R90).
R96	Break mass flow is ranked medium during the long-term phase. The break flow contributes to the RCS mass balance. However, because the break size is assumed to be small, the break mass flow was judged to be less significant than the ADS mass flow (that is ranked high, see R91).
R97	Break noncondensible effects are ranked low during the long-term phase. Noncondensible gases (nitrogen expelled into the RCS from the accumulators and hydrogen emerging from solution due to RCS depressurization) will find their way to the break. The presence of noncondensible gas in the RCS fluid affects the break energy release and mass flow (that are ranked medium, see R95 and 96).

Table B-3. (continued).

Ranking rationale for the phenomena in Tables B-1 through B-2

Code	Ranking Rationale
R98	Cold leg condensation is ranked low during the long-term phase. Experimental data from Oregon State University cold leg SBLOCA tests indicate CMT refill behavior due to condensation during this phase. Refill is caused by cold water entering the CMTs through the pressure balance lines. Condensation in the cold leg may be a precursor or contribute to this behavior. The potential for a similar cold-leg refill behavior is present in the long-term sump phase. Subcooled water is supplied from the reactor vessel downcomer and steam is available from the upper head-to-downcomer bypass path. As with the CMT refill behavior, cold leg refill events would alter the distribution of the RCS inventory.
R99	Cold leg noncondensible effects are ranked low during the long-term phase. Noncondensible gases (nitrogen expelled into the RCS from the accumulators and hydrogen emerging from solution due to RCS depressurization) will find their way to the break that is assumed to be located in the cold leg. The presence of noncondensible gas in the RCS fluid affects the break energy release and mass flow (that are ranked medium, see R95 and 96). In addition, noncondensible gases in the cold legs may influence the CMT refill behavior during this phase (see R98 and R100).
R100	Cold leg-to-PBL phase separation is ranked low during the long-term phase. Experimental data from Oregon State University cold-leg SBLOCA tests indicate CMT refill behavior due to condensation during this phase. The refill was caused by cold water entering the CMTs through the pressure balance lines. Phase separation at the cold leg-to-PBL tee may affect fluid conditions in the pressure balance line, influencing this behavior.
R101	Core boiling is ranked medium during the short-term and long-term phase. Fuel rod decay heat (ranked high, see R26 and R114) is removed to the RCS coolant by convection or boiling heat transfer. Increased core steam production due to boiling results in increasing fluid velocities and pressure drops in the flow through the ADS.
R102	Core flashing is ranked low during the long-term phase. Core flashing will occur during periods when the RCS is depressurizing. The steam produced by flashing adds to that produced by boiling (see R101), thus increasing the velocity and pressure drop of fluid exiting the RCS via the ADS.
R103	Core flow resistance is ranked low during the long-term phase. The core flow resistance is a portion of the total loop flow resistance (this loop is from the IRWST, through the reactor vessel downcomer, core, hot legs, and out ADS stage 4 to the containment). Therefore the core flow resistance can affect the ADS mass flow and energy release that are ranked high (see R90 and R91).
R104	Core mass flow (including bypass) is ranked medium during the long-term phase. This flow supplies coolant to the core so that fuel rod decay heat (ranked high, see R114) may be removed.
R105	Core subcooling margin is ranked medium during the long-term phase. This phenomenon affects core cooling. In this PIRT, the core is assumed to remain covered (the core two-phase mixture level is ranked high, see R106) and, in that case, the fuel rods will not heat up. The subcooling margin affects core flashing and boiling behavior that influences the ADS mass flow and energy release.
R106	Core two-phase level is ranked high during the long-term phase. This phenomenon affects core cooling. The core two-phase mixture level must be above the top of the core to prevent fuel rod heat-up. Steam produced by boiling and flashing in the core swells the core level upward, influencing the upper plenum mixture level (see R128).

Table B-3. (continued).

Ranking rationale for the phenomena in Tables B-1 through B-2

Code	Ranking Rationale
R107	CMT-to-IRWST differential head is ranked medium during the long-term phase. The CMTs may refill during this phase (see R108). The subsequent processes by which the IRWST and CMTs drain will be affected by the relative levels and temperatures of water in the CMT and IRWST.
R108	CMT condensation is ranked medium during the long-term phase. Some tests at the APEX facility at Oregon State University experienced CMT refills due to condensation. However, additional analysis determined that these refills were a scaling artifact of the facility and condensation is not expected to cause the same reaction in AP600.
R109	CMT flow resistance is ranked low during the long-term phase. The CMTs may refill during this phase (see R108). The CMT flow resistance (in particular that associated with its discharge line, check valve, and orifice) determines the subsequent CMT draining rate.
R110	CMT noncondensible effects are ranked medium during the long-term phase. Noncondensible gases (nitrogen expelled into the RCS from the accumulators and hydrogen emerging from solution due to RCS depressurization) may find their way to the pressure balance lines and CMTs. The presence of noncondensible gas in the RCS fluid may influence the CMT refill behavior (see R108).
R111	Downcomer condensation is ranked medium for the long-term phase. Subcooled water is supplied to the downcomer through the DVI lines. Steam may flow through the upper head/downcomer bypass path. If condensation occurs in the downcomer, it can alter the high-ranked downcomer level (see R112).
R112	Downcomer level is ranked high during the long-term phase. This level creates a major portion of the driving force for flow through the core. The static head created by this level is a significant term affecting the RCS/containment pressure balance. The inventory in the Downcomer represents the coolant immediately available to the core during long term cooling. It is an important part of the reactor vessel inventory replacement.
R113	Fuel rod critical heat flux/dryout is ranked low during the long-term phase. This phenomenon affects core cooling, but core decay heat is lower during this phase than it was in the previous phase, where this phenomenon is ranked medium (see R72).
R114	Fuel rod core power/decay heat is ranked high during the long-term phase. This phenomenon is the primary energy source in the RCS energy balance. Removal of this heat is the basic safety issue for a SBLOCA. Subsequent to ADS 4 operation, liquid boiloff due to core decay heat is the primary mechanism for reactor vessel inventory depletion.
R115	Hot leg countercurrent flow is ranked low during the long-term phase. This phenomenon contributes to the highly-ranked hot leg phase separation process (see R117) because it affects the fluid state and flow regime in the hot leg and affects the condition of the fluid exiting ADS.
R116	Hot leg horizontal fluid stratification is ranked medium during the long-term phase. The hot leg flow regime affects the condition of the fluid exiting ADS (see R117).

Table B-3. (continued).

Ranking rationale for the phenomena in Tables B-1 through B-2

Code	Ranking Rationale
R117	Phase separation in hot leg tees is ranked medium during the long-term phase. This phenomenon (at the ADS stage 4 hot leg tee) controls the quality of the fluid entering ADS stage 4 and, thereby, controls the ADS energy release and flow rates. ADS stages 1, 2, and 3 are inactive during this phase unless the head of the submergence of the ADS spargers under water in the IRWST becomes less than the differential pressure between the RCS and containment. If ADS stages 1, 2, and 3 are active, phase separation at the hot leg-to-pressurizer surge line tee controls the quality of fluid passed to the pressurizer (and from there out ADS stages 1, 2, and 3).
R118	IRWST flow resistance is ranked high during the long-term phase. The IRWST flow resistance (in particular, that associated with its discharge line, orifice, valves, and fittings) is one portion of the total resistance of the flow loop (from the IRWST, through the reactor vessel downcomer, core, hot legs, and out ADS to the containment). Therefore this phenomenon affects the core coolant flow rate. IRWST flow rate is governed by IRWST line resistance, IRWST liquid level and primary system pressure. Excessive flow resistance in the IRWST injection lines affects the IRWST injection flow rate. If the vessel liquid boiloff rate exceeds the IRWST injection rate, the reactor vessel liquid level will drop.
R119	IRWST pool level is ranked high during the long-term phase. The IRWST level provides the driving force to push flow through the total resistance of the flow loop (from the IRWST, through the reactor vessel downcomer, core, hot legs, and the ADS to containment). Therefore, the IRWST pool level controls the core cooling flow rate. See R118 for additional justification.
R120	IRWST pool-to-tank heat transfer is ranked low during the long-term phase. Because this phase extends over a long period, the energy removed from the pool to its surrounding walls may have some effect on the IRWST water temperature.
R121	IRWST pool thermal stratification is ranked high during the long-term phase. This phenomenon affects the temperature of the water that is injected into the RCS. During prior phases the IRWST has been warmed from PRHR heat transfer and from ADS stage 1, 2, and 3 discharge. The warming of IRWST water from these processes will be nonuniform to some extent. During this phase, however, these processes have ceased and the IRWST water will tend to thermally stratify, due to buoyancy effects, into a condition where the warmer water resides over colder water. This effect is significant because water injected into the RCS is drawn from the bottom of the IRWST. Because the tank is thermally-stratified, the temperature of the injection water is expected to increase with time. IRWST liquid temperature governs the inlet subcooling to the core and therefore affects the vapor generation rate in the core.
R122	IRWST sparger pipe level is ranked low during the long-term phase. ADS stages 1, 2, and 3 are active during this phase when the head of the submergence of the ADS spargers under water in the IRWST is less than the differential pressure between the RCS and containment. Wall condensation inside the ADS stage 1, 2, and 3 discharge lines (especially in the regions of these pipes submerged under water in the IRWST) may affect the ADS flow rates through these pipes. This phenomenon also may be associated with water hammer events in these pipes.

Table B-3. (continued).

Ranking rationale for the phenomena in Tables B-1 through B-2

Code	Ranking Rationale
R123	Pressurizer level (inventory) is ranked medium during the long-term phase. During the short-term phase, the pressurizer empties (see R40), partially refills and then partially drains (see R80). Cold-leg SBLOCA experiments in the Oregon State University facility indicate that draining of the remaining pressurizer inventory affects the behavior of IRWST injection and ADS flow during this phase. Oscillatory behavior is observed, and pressurizer draining influences these oscillations.
R124	Steam generator tube heat transfer is ranked low during the long-term phase. The RCS energy balance is dominated by decay heat addition and ADS energy removal and not by steam generator heat transfer during this phase. The steam generators are thermally-decoupled from the RCS because the fluid in the secondary system is significantly hotter than the RCS fluid and the tubes have voided. This phenomenon can be important if water can be reintroduced into the steam generator tubes, for example, due to oscillatory behavior in the RCS primary system.
R125	Sump level is ranked high during the long-term phase. Sump injection begins when the sump level has been equalized with the IRWST level. This equalization may occur as a result of flow from the break into the sump, or by opening of valves in the sump discharge lines that allow the IRWST and sump levels to equilibrate. These valves are opened automatically when the IRWST level reaches a minimum setpoint value. As with the IRWST level, the sump level provides a driving force to push flow through the total resistance of the flow loop (from the sump, through the reactor vessel downcomer, core, hot legs, and the ADS to containment). Therefore, this phenomenon affects the core cooling flow rate. During long term cooling, the sump liquid level will dictate the recirculation rates through the core and the "flood-up" level for the entire system. Sump level directly affects core cooling and inventory replacement.
R126	Upper plenum/upper head condensation is ranked low during the long-term phase. Refilling of the upper head/upper plenum regions due to rapid condensation events may alter the state of fluid passed to the hot legs, affecting the ADS energy release and mass flow.
R127	Upper plenum/upper head noncondensible effects are ranked low during the long-term phase. Noncondensible gases (nitrogen expelled into the RCS from the accumulators and hydrogen emerging from solution due to RCS depressurization) may affect the state of the fluid passed into the hot legs and out the ADS (see R93 and R128). In addition noncondensible gases may affect the potential for upper head condensation-induced refill events (see R126).
R128	Upper plenum two-phase level is ranked high during the long-term phase. This level directly affects the ADS energy release and mass flow (ranked high, see R90 and R91) because it determines the condition of the fluid passed into the hot legs and affects differential pressures in this region. See R115 through R117 for related discussions of the hot-leg phenomena.
R129	Containment interior liquid distribution is ranked medium during the long-term phase. This phenomenon affects the IRWST and sump levels during this phase.

Table B-3. (continued).

Ranking rationale for the phenomena in Tables B-1 through B-2

Code	Ranking Rationale
R130	Containment interior pressure is ranked medium during the long-term phase. The containment interior receives flow directly from ADS stage 4. In addition, the IRWST (that may receive flow from ADS stages 1, 2, and 3 during this phase) resides in the containment interior. The ADS mass flow and energy release (ranked high, see R90 and R91) are determined by the differential pressure between the RCS and the containment interior.
R131	Containment interior liquid subcooling is ranked low during the long-term phase. This phenomenon affects the temperature of the IRWST and sump fluids that are the source of RCS injection during this phase.
R132	CMT noncondensible effects are ranked low during the short-term phase. Noncondensible gases (nitrogen expelled into the RCS from the accumulators and hydrogen emerging from solution due to RCS depressurization) may find their way to the pressure balance lines and CMTs. The presence of noncondensible gas in the RCS fluid may influence the CMT refill behavior later, in the long-term phase (see R108).
R133	Sump flow resistance is ranked medium during the long-term phase. The sump flow resistance (in particular, that associated with its discharge line, valves, and fittings) is a portion of the total resistance of the flow loop (from the sump, through the reactor vessel downcomer, core, hot legs, and out ADS to the containment). Therefore, this phenomenon affects the core coolant flow rate.
R134	Sump fluid temperature is ranked high during the long-term phase. This phenomenon represents the temperature of a portion of the water that is injected into the RCS and, therefore, it affects the RCS energy balance. During the short-term phase, the sump has been filled with water expelled from the break and ADS; to some extent, this water has been cooled via heat transfer to containment structures. Fluid in the sump may thermally stratify, in a manner similar to the behavior described for the IRWST (see R121). The temperature of the water injected from the sump into the RCS is that of the fluid residing at the sump-to-DVI line intake. Unlike the corresponding IRWST configuration, this intake is located at an elevation far above the bottom of the sump. Therefore, the temperature of the water injected from the sump may be at the high end of the sump water-temperature range. During long term cooling, the fluid temperature in the sump governs the inlet subcooling to the core and therefore affects the vapor generation rate in the core which is the primary mechanism for reducing reactor vessel liquid inventory.
R135	IRWST flow resistance is ranked high during the short-term phase. The IRWST flow resistance (in particular, that associated with its discharge line, orifice, valves, and fittings) is a large portion of the total resistance of the flow loop (from the IRWST, through the reactor vessel downcomer, core, hot legs, and out ADS to the containment). Therefore this phenomenon affects the core coolant flow rate. The flow resistance in the IRWST injection lines affects behavior of the start of IRWST injection and subsequent reactor vessel refill rates. The IRWST injection rate significantly affects the vessel liquid inventory.
R136	ADS condensation (in stages 1, 2, and 3 piping and spargers in IRWST) is ranked low during the short-term phase. ADS stages 1, 2, and 3 are active during this phase when the head of the submergence of the ADS spargers under water in the IRWST becomes less than the differential pressure between the RCS and containment. Wall condensation inside the ADS stage 1, 2, and 3 discharge lines (especially in the regions of these pipes submerged under water in the IRWST) may affect ADS flow through these pipes. This phenomenon also may be associated with water hammer events in these pipes.

Table B-3. (continued).

Ranking rationale for the phenomena in Tables B-1 through B-2

Code	Ranking Rationale
R137	Upper plenum/upper head noncondensible effects are ranked low during the short-term phase. Noncondensible gases (nitrogen expelled into the RCS from the accumulators and hydrogen emerging from solution due to RCS depressurization) may affect the state of the fluid passed into the hot legs and out the ADS (see R64 and R138).
R138	Upper plenum two-phase level is ranked low during the short-term phase. This level affects the ADS energy release and mass flow because it determines the condition of the fluid passed into the hot legs and affects differential pressures in this region.
R139	Containment interior liquid distribution is ranked medium during the short-term phase. This distribution of water determines the IRWST and sump levels during this phase.
R140	Containment interior liquid subcooling is ranked low during the short-term phase. This phenomenon affects the temperature of the IRWST fluid that is used as the source of RCS injection during this phase. In addition, this phenomenon affects the temperature of the sump fluid that is used as the source of RCS injection during the next phase.
R141	Sump level is ranked medium during the short-term phase in anticipation of its greater influence during the long-term phase.
R142	Accumulator noncondensible effects are ranked low during the long-term phase. Expansion of the nitrogen gas bubble within the accumulator controls the differential pressure between the accumulator and RCS. and, therefore, the rate at which the remaining nitrogen flows from the accumulator into the RCS. The effects of nitrogen entering the RCS are discussed separately for each component.
R143	Break flow resistance is ranked low during the long-term phase. The break flow resistance controls the break flow but this flow is small as compared with ads-4 flow.
R144	Cold leg stored energy release is ranked low during the long-term phase. The rate of stored energy release from piping walls was judged smaller than the other contributors to the RCS energy balance.
R145	Core stored energy release is ranked medium during the long-term phase. The rate of stored energy release from non-fuel structures in the core region was judged smaller than the other contributors to the RCS energy balance.
R146	Core and downcomer/lower plenum loop asymmetry effects are ranked low during the long-term phase. Asymmetric conditions (pressures, temperatures, flow rates) within and/or between RCS components may be present. The sources of these asymmetries are the break location (i.e., it is situated at a single location in the RCS), and the plant configuration (the pressurizer and PRHR system are connected on one coolant loop while the CMTs are connected on the other). Downcomer fluid temperature asymmetries may affect fluid conditions present at the break, and, thereby, significantly alter the distribution of RCS mass and energy.
R147	Downcomer/lower plenum stored energy release is ranked low during the long-term phase. The rate of stored energy release from vessel walls and system internals was judged smaller than the other contributors to the RCS energy balance.

Table B-3. (continued).

Ranking rationale for the phenomena in Tables B-1 through B-2

Code	Ranking Rationale
R148	IRWST interphasic condensation is ranked low during the long-term phase. ADS stages 1, 2, and 3 discharge RCS fluid into the IRWST through two spargers. The fluid flowing through the spargers has a high steam content, perhaps superheated, at the near-atmospheric pressure inside the tank. However, the IRWST fluid is initially subcooled, so high interphase condensation rates are anticipated. This phenomenon affects: (1) the manner in which the IRWST performs the quenching process, (2) the state of the IRWST fluid (that later is injected into the RCS), and (3) the containment pressure.
R149	Upper plenum entrainment/de-entrainment is ranked medium during the long-term phase. The entrainment, de-entrainment, and storage of liquid in the upper plenum region affects the pressure drop and convection of fluid through the hot legs to all ADS stages.

Appendix C - Detailed Results, Main Steam Line Break Without ADS PIRT

This appendix presents the detailed results of the main steam line break (MSLB) sequence without Automatic Depressurization System (ADS) activation PIRT. The detailed PIRT results are shown in Tables C-1 and C-2, and the transient description, overall phenomena ranking criteria, and specific ranking rationales are shown in Table C-3. The information in Tables C-1 and C-2 is arranged to correspond with the two phases of the accident scenario. These tables are organized in alphabetical order according to the component name. Within the listings for each component, the pertinent identified phenomena are arranged by order of ranking. The right sides of these tables contain identifier codes that refer the reader elsewhere in this report for further information:

The code labeled "Ranking Rationale" (for example, "R1") leads the reader to a description of the logic leading to the ranking of each specific phenomenon; this information is found in Table C-3 in this appendix.

The code labeled "Phenomena Description" (for example, "D1") leads the reader to a general description of each phenomenon; this information is found in Appendix G, Table G-1.

Two codes are labeled "Type Geometry" (for example "C1/G1"). The "C" code leads the reader to the physical geometries and general functions of the component under discussion; this information is found in Appendix G, Table G-2. The "G" code leads the reader to more detailed discussion of the specific phenomena associated with each of the components; this information is found in Appendix G, Table G-3.

The "Supporting Evidence" code (for example, "E1") leads the reader to references (geometrical, experimental, and analytical) that provide background and corroborating information. This information is found in Appendix G, Table G-4. It is noted that the supporting evidence is currently being developed in experimental and analytical tasks both inside and outside the PIRT task. Thus, the information in this table can be expected to increase as the supporting tasks are completed.

The "Sublevel Phenomena" code (for example, "S1") leads the reader to a list of contributing phenomena affecting the primary phenomenon. The sublevel phenomena information is found in Appendix G, Table G-5.

Table C-1. PIRT for the initial depressurization phase of a MSLB with no single failure.

			For codes shown in these columns, See Tables:				
			C-3	G-1	G-2/G-3	G-4	G-5
Component	Phenomena	Rank	Ranking Rationale	Phenomena Description	Type Geometry	Supporting Evidence	Sublevel Phenomena
Break	Mass flow	H	R1	D25	C3/G5	E1	S1
	Energy release	H	R1	D26	C3/G5	E1	S1
	Flow resistance	L	R1	D27	C3/G5	E1	S11
Cold legs	Loop asymmetry effects	M	R52	D45	C4/G9	E1	S9
	Stored energy release	L	R51	D68	C4/G7	E1	S2
Core	Core channeling	H	R2	D11	C5	E1	S55
	Flashing	M	R3	D21	C5/G12	E1	S5
	Voiding	M	R3	D78	C5/G12	E1	S54
	Noncondensible effects	L	R4	D50	C5	E1	S12
	Stored energy release	L	R51	D68	C5/G11	E1	S2
CMT	CMT-to-loop differential density	L	R5	D17	C6/G13	E1	S10
	Noncondensible effects	L	R4	D50	C6/G14	E1	S12
	Thermal stratification	L	R5	D73	C6/G14	E1	S19
Downcomer/ lower plenum	Loop asymmetry effects	M	R52	D45	C7/G16	E1	S9
	Stored energy release	L	R51	D68	C7/G15	E1	S2
Fuel rods	Core power/decay heat	H	R8	D12	C8/G20	E1	S4
	CHF	M	R7	D15	C8	E1	S57
	Boron reactivity feedback	L	R6	D3	C8	E1	S56
	Moderator temperature feedback	L	R6	D47	C8	E1	S58
	Stored energy release	L	R51	D68	C8/G21	E1	S2
Hot legs	Flashing	M	R9	D21	C9	E1	S5
	Loop asymmetry effects	M	R52	D45	C9/G23	E1	S9
	Voiding	M	R9	D78	C9/G25	E1	S54
	Noncondensible effects	L	R4	D50	C9	E1	S12
	Stored energy release	L	R51	D68	C9/G22	E1	S2

Table C-1. (continued).

			For codes shown in these columns, See Tables:				
			C-3	G-1	G-2/G-3	G-4	G-5
Component	Phenomena	Rank	Ranking Rationale	Phenomena Description	Type Geometry	Supporting Evidence	Sublevel Phenomena
IRWST	Pool thermal stratification	L	R10	D59	C10/G26	E1	S19
PRHR	Condensation	M	R11	D9	C12/G31	E1	S18
	Differential density	M	R11	D17	C12/G30	E1	S10
	Heat transfer between PRHR and IRWST	M	R12	D32	C12/G30	E1	S28
	Noncondensible effects	M	R11	D50	C12/G31	E1	S12
	Voiding	M	R11	D78	C12/G31	E1	S54
Pressurizer	Flashing	M	R13	D21	C14/G33	E1	S5
	Level (inventory)	M	R14	D39	C14/G33	E1	S13
	Vapor space behavior	M	R14	D77	C14/G33	E1	S60
	Noncondensible effects	L	R15	D50	C14	E1	S12
Pumps	Coastdown performance	H	R16	D7	C15/G37	E1	S14
	Flow resistance	L	R53	D27	C15/G38	E1	S15
Steam generator (primary)	Preferential loop cooldown	H	R18	D61	C16/G40	E1	S61
	Primary to secondary heat transfer	H	R20	D31	C16/G39	E1	S53
	Thermal driving head	M	R19	D72	C16/G41	E1	S59
	Voiding (unaffected loop)	M	R17	D78	C16/G39	E1	S54
	Noncondensible effects	L	R21	D50	C16/G39	E1	S12
Steam generator (secondary)	Entrainment	H	R22	D20	C16/G42	E1	S23
	Flashing (steam generator & feedwater line)	H	R22	D21	C16/G42	E1	S5
	Level swell & depletion	H	R22	D41	C16/G42	E1	S7
	Tube dryout (affected SG)	M	R23	D74	C16/G42	E1	S62
Steam generator (separator/ dryer)	Liquid carry-over	H	R24	D42	C16/G43	E1	S63

Table C-1. (continued).

			For codes shown in these columns, See Tables:				
			C-3	G-1	G-2/G-3	G-4	G-5
Component	Phenomena	Rank	Ranking Rationale	Phenomena Description	Type Geometry	Supporting Evidence	Sublevel Phenomena
Upper head / upper plenum	Flashing	M	R25	D21	C18/G45	E1	S5
	Flow split (upper plenum)	M	R47	D28	C18/G46	E1	S65
	Loop asymmetry effects	M	R52	D45	C18/G46	E1	S9
	Voiding	M	R25	D78	C18/G45	E1	S54
	Stored energy release	L	R51	D68	C18/G47	E1	S2
Containment (interior)	Interior to wall heat transfer	M	R26	D86	C19/G48	E1	S72
	Passive heat sink	M	R26	D81	C19/G48	E1	S67
	Condensate transport	L	R26	D8	C19/G48	E1	S37
	Condensation	L	R26	D9	C19/G48	E1	S18
	Liquid distribution	L	R26	D43	C19/G48	E1	S38
	Liquid holdup	L	R26	D44	C19/G48	E1	S38
	Natural convection	L	R26	D48	C19/G48	E1	S36
	Noncondensible effects	L	R26	D50	C19/G49	E1	S12
	Noncondensible segregation	L	R26	D84	C19/G49	E1	S71
	Nonuniform steam/air distribution	L	R26	D51	C19/G49	E1	S35
	Steam-noncondensible mixing	L	R26	D67	C19/G49	E1	S35
Containment (exterior)	Exterior to ambient heat transfer	L	R26	D83	C20/G50	E1	S70

Table C-2. PIRT for the passive decay heat removal phase of a MSLB with no single failure.

			For codes shown in these columns, See Tables:				
			C-3	G-1	G-2/G-3	G-4	G-5
Component	Phenomena	Rank	Ranking Rationale	Phenomena Description	Type Geometry	Supporting Evidence	Sublevel Phenomena
Core	Flashing	M	R30	D21	C5/G12	E1	S5
	Voiding	M	R30	D78	C5/G12	E1	S54
	Channeling	L	R31	D4	C5	E1	S55
	Flow resistance	L	R59	D27	C5/G12	E1	S11
CMT	Level	M	R33	D39	C6/G14	E1	S13
	CMT-to-loop differential density	L	R32	D17	C6/G13	E1	S10
	Flow resistance	L	R55	D27	C6/G13	E1	S11
	Noncondensible effects	L	R56	D50	C6/G14	E1	S12
	Voiding	L	R28	D78	C6/G13	E1	S54
Downcomer/ lower plenum	Flow distribution	L	R35	D24	C7/G16	E1	S64
Fuel rods	Decay heat	H	R8	D12	C8/G20	E1	S4
Hot legs	Noncondensible effects	M	R36	D50	C9	E1	S12
	Phase separation in tees	M	R36	D56	C9/G24	E1	S8
	Voiding	M	R36	D78	C9/G25	E1	S54
IRWST	Flow & temperature distribution in bundle region	M	R38	D23	C10/G26	E1	S24
	Pool level	M	R38	D39	C10/G26	E1	S25
	Pool thermal stratification	M	R38	D59	C10/G26	E1	S19
	Interphasic condensation	L	R57	D37	C10/G29	E1	S18
	Pool flow	L	R57	D57	C10/G26	E1	S24
PRHR	Heat transfer between PRHR and IRWST	H	R39	D32	C12/G30	E1	S28
	Condensation	M	R40	D9	C12/G31	E1	S18
	Differential density	M	R40	D17	C12/G30	E1	S10
	Flow resistance	M	R58	D27	C12/G30	E1	S11

Table C-2. (continued).

			For codes shown in these columns, See Tables:				
			C-3	G-1	G-2/G-3	G-4	G-5
Component	Phenomena	Rank	Ranking Rationale	Phenomena Description	Type Geometry	Supporting Evidence	Sublevel Phenomena
PRHR, Continued	Noncondensible effects	M	R40	D50	C12/G31	E1	S12
	Voiding	M	R40	D78	C12/G31	E1	S54
Pressurizer	Level (inventory)	M	R41	D39	C14/G33	E1	S13
	Noncondensible effects	M	R42	D50	C14	E1	S12
	Vapor space behavior	M	R41	D77	C14/G33	E1	S60
	Condensation	L	R43	D9	C14	E1	S18
Pumps	Flow resistance	L	R53	D27	C15/G38	E1	S15
Steam generators	Asymmetric behavior	M	R45	D85	C16/G40	E1	S61
	Noncondensible effects	M	R46	D50	C16/G39	E1	S12
	Primary to secondary heat transfer	M	R44	D33	C16/G39	E1	S53
	Tube voiding	M	R46	D78	C16/G39	E1	S54
	Secondary level	L	R61	D63	C16/G39	E1	S7
	Secondary pressure	L	R61	D64	C16/G39	E1	S17
Upper head / upper plenum	Flow split (upper plenum)	M	R47	D28	C18/G46	E1	S65
	Vapor space compression	M	R60	D77	C18/G45	E1	S60
	Voiding	M	R60	D78	C18/G45	E1	S54
Containment (interior)	Interior to wall heat transfer	H	R50	D86	C19/G48	E1	S72
	Condensate transport	M	R48	D8	C19/G48	E1	S37
	Condensation	M	R48	D9	C19/G48	E1	S18
	Liquid distribution	M	R48	D43	C19/G48	E1	S38
	Liquid holdup	M	R48	D44	C19/G48	E1	S38
	Natural convection	M	R49	D48	C19/G48	E1	S36
	Noncondensible segregation	M	R49	D84	C19/G49	E1	S71
	Noncondensible effects	M	R49	D50	C19/G49	E1	S12
	Nonuniform steam/air distribution	M	R49	D51	C19/G49	E1	S35

Table C-2. (continued).

			For codes shown in these columns, See Tables:				
			C-3	G-1	G-2/G-3	G-4	G-5
Component	Phenomena	Rank	Ranking Rationale	Phenomena Description	Type Geometry	Supporting Evidence	Sublevel Phenomena
Containment (interior), continued	Steam-noncondensible mixing	M	R49	D67	C19/G49	E1	S35
	Passive heat sink	M	R49	D81	C19/G48	E1	S67
Containment (exterior)	Exterior to ambient heat transfer	H	R50	D83	C20/G50	E1	S70
	Air flow	M	R50	D2	C20/G50	E1	S69
	Atmospheric temperature	M	R50	D2	C20/G50	E1	S43
	Chimney effects	M	R50	D5	C20/G50	E1	S41
	PCCS evaporation	M	R50	D52	C20/G50	E1	S39
	PCCS mixture convective heat transfer	M	R50	D54	C20/G50	E1	S39
	PCCS water flow	M	R50	D53	C20/G50	E1	S40
	PCCS wetting	M	R50	D55	C20/G50	E1	S42
	Humidity	M	R50	D36	C20/G50	E1	S46
	Radiation heat transfer	M	R50	D62	C20/G50	E1	S45

Table C-3. Transient description and ranking rationale for the MSLB without ADS PIRT

Overall Transient Description and Top-level Ranking Rationale

This sequence is initiated by the double-ended rupture of a main steam line inside containment. The availability only of safety-grade plant systems is assumed. The subsequent plant response is assumed to be within the design goal of recovery to a long term quasi-steady condition that does not require ADS actuation.

Phase Descriptions and Medium-level Ranking Rationales

Initial Depressurization Phase:

Description - This phase begins at the time of the pipe break. Both steam generators begin blowing down into the containment. The flow rates through the two sides of the break are restricted by the steam line flow limiters and are significantly less than those allowed by critical flow through the full open pipe areas. A steam line isolation signal is generated (due either to low steam line pressure, high containment pressure, or low cold leg temperature). This signal results in closure of the main steam isolation valves. Main steam isolation valve closure isolates the unaffected steam generator; its blowdown is arrested, and afterward it acts as a heat source to the reactor coolant system (RCS). Flow from the affected steam generator into containment can not be isolated. During blowdown, steam generator secondary fluid flashes and boils, and the steam produced swells the boiler mixture level, entrains liquid, and sweeps it through and around the separators and dryers and out the break. Performances of the separators and dryers degrade as they are flooded with liquid. Primary-to-affected secondary heat transfer is at a high rate and the RCS fluid is cooled, causing it to shrink. RCS cooling is preferential to the loop containing the affected steam generator; cold leg temperatures differ markedly between the affected and unaffected loops. Because the reactor vessel lower plenum is not necessarily well-mixed, this thermal asymmetry may persist into the core, upper plenum, and hot leg regions. The RCS pressure and pressurizer level fall; the reactor vessel upper head flashes. If not already generated, a reactor trip signal is generated due to low pressurizer pressure. Reactor trip causes the core power to be quickly reduced to the decay heat rate, and this power reduction causes the average RCS temperature to fall faster, the RCS fluid shrinkage rate to increase, and, therefore, the RCS pressure to fall even more rapidly. Declining core pressures and potentially (due to the positive reactor kinetic feedback effects of declining RCS fluid temperatures) increasing core power may cause a departure from nucleate boiling in the core. An S signal is generated due to low pressurizer pressure, low cold leg temperature, low steam generator pressure, or high containment pressure. The S signal causes core makeup tank (CMT) system actuation, reactor coolant pump trip, and feedwater isolation. CMT actuation also results in passive residual heat removal (PRHR) system activation. Note that PRHR may be actuated also by low steam generator level signals, and this may occur prior to CMT actuation (see Reference 6, Table H-2, for details of the PRHR system actuation logic). The RCS loop flows decline rapidly from a forced-circulation to natural-circulation condition and this reduces the RCS heat removal rate. Flow through the unaffected loop ceases, since its steam generator now acts as an RCS heat source. The containment behavior is important because the affected steam generator blowdown proceeds against the containment pressure. In the containment, the break effluent is mixed with nitrogen, and steam is condensed from the mixture on the inside of the containment shell. The heat released to the shell is removed to the atmosphere by evaporation, convection, and radiation to air on the outside of the shell. These processes continue, with the affected secondary inventory and pressure continuously decreasing, until the blowdown of the affected steam generator has been completed. When the affected steam generator secondary has completely dried out, its pressure equilibrates with the containment pressure, an event marking the end of this phase.

Important parameters and dominant processes - The steam generator primary-to-secondary heat transfer rate is judged to be the parameter of primary importance because it dominates the RCS cooldown during

Table C-3. (continued).

this phase. Processes important for accurate simulation of this parameter are: break flow, steam generator secondary behavior (level swell and depletion, liquid carry-over, flashing, entrainment), flow through the RCS loops, and asymmetric loop cooldown.

Passive Decay Heat Removal Phase:

Description - This phase begins when the affected steam generator blowdown is complete. RCS heat sources are decay heat and reverse heat transfer from the unaffected steam generator. CMT recirculation acts as a temporary RCS heat removal mechanism, and the PRHR system acts as the long-term heat removal mechanism. Because the PRHR system is connected to only one of the loops, behavior during this phase is dependent upon which loop is assumed to contain the affected steam generator. Natural circulation-driven RCS loop, CMT, and PRHR flows and asymmetries in RCS temperature distributions are expected. PRHR heat removal may lead to thermal stratification in the in-containment refueling water storage tank (IRWST) that would degrade PRHR performance. Repressurization and heating of the RCS coolant may occur during this phase. RCS temperatures must rise until they are high enough to allow the core decay heat to be removed through the PRHR heat exchanger to the IRWST tank. Because the RCS is a closed system, RCS fluid heating is accompanied by repressurization.

Important parameters and dominant processes - The RCS energy distribution is judged to be the parameter of primary importance because it determines the removal of core decay heat to its ultimate heat sink. The processes important for accurate simulation of this parameter are: core, steam generator, PRHR, and containment shell heat transfer, and loop asymmetry effects.

Detailed Phenomena Ranking Rationales

Ranking rationale for the phenomena in Tables C-1 through C-2

Code	Ranking Rationale
R1	Break mass flow and break energy release are ranked high, and break flow resistance is ranked low during the initial depressurization phase. For the main steam line break (MSLB) accident, the break processes are controlled at the flow limiter that effectively limits the size of the break (the flow area of the flow limiter is significantly less than that of the ruptured steam pipe). The mass flow and energy release control the blowdown of the affected steam generator secondary system that determines the primary-to-secondary heat transfer, the parameter of primary importance during this phase. The flow resistance is ranked low because the break is controlled by critical flow, not frictional flow, processes during most of this phase. The break will unchoke (and, therefore, its flow resistance will be of significance) only near the end of this phase when the affected secondary pressure nears that in the containment.
R2	Core channeling is ranked high during the initial depressurization phase. Fluid mixing/channeling processes within the core directly affect the hot leg fluid temperatures. A large temperature asymmetry exists between the cold legs on the two RCS loops, and it may survive to the core exit. This asymmetry causes the hot leg fluid temperatures to be different. These temperatures are the sources for steam generator primary-to-secondary heat transfer, the parameter of primary importance during this phase.
R3	Flashing and voiding in the core are ranked medium during the initial depressurization phase. These phenomena affect the RCS pressure response (which has some influence on the steam generator primary-to-secondary heat transfer). They also affect the distribution of fluid in the RCS (also see R9).

Table C-3. (continued).

Ranking rationale for the phenomena in Tables C-1 through C-2

Code	Ranking Rationale
R4	Noncondensible effects (due to hydrogen evolving from solution during RCS depressurization) in the core, CMT, and hot legs are ranked low during the initial depressurization phase. Voiding from, and transport of, this hydrogen may influence steam generator primary-to-secondary heat transfer, PRHR system heat transfer, and CMT recirculation. In all three cases, noncondensible gasses collected at the tops of piping networks may interrupt flow through the networks (also see R21).
R5	CMT-to-loop differential density and CMT thermal stratification are ranked low during the initial depressurization phase. CMT cooling of the RCS is small compared with the affected steam generator primary-to-secondary heat transfer. These phenomena are introduced here because they influence the fluid conditions within the CMTs and the CMT recirculation rate. CMT thermal stratification established during this phase is important during the next phase when flashing in the PBL or CMT can interrupt CMT recirculation.
R6	Boron and moderator-temperature reactivity feedback are ranked low in the fuel rod component during the initial depressurization phase. A return to a critical reactor condition is a general concern during the severe RCS fluid overcooling encountered in MSLB accidents. Negative reactivity is introduced by scram rod insertion (at the time of reactor trip) and boron addition to the RCS from the CMTs (after they are activated at the time of the S signal). Positive reactivity is introduced by moderator temperature feedback due to the declining RCS fluid temperatures. Assuming all scram rods are inserted, a return to a critical core condition is not expected; these phenomena were included only to highlight their importance should this assumption later be changed.
R7	Fuel rod critical heat flux is ranked medium during the initial depressurization phase. The potential for a return to a critical core condition is described in R6. This potential, coupled with declining RCS pressure (caused by RCS fluid shrinkage effects), provides the possibility for a fuel rod heat-up due to departure from nucleate boiling. The medium ranking was assigned due to the safety-significance of any such fuel rod heat-up.
R8	Fuel rod core power/decay heat is ranked high during the initial depressurization and passive decay heat removal phases. This phenomenon is ranked high because: (1) it is a major heat source in the RCS energy balance and (2) there is a potential for a return to a critical core condition (see R6 and R7).
R9	Flashing and voiding in the hot legs are ranked medium during the initial depressurization phase. These phenomena affect the natural circulation driving heads of the RCS and PRHR system loops, and, thereby, the steam generator and PRHR heat transfer rates. The natural circulation loop driving heads are enhanced when void is passed from the from hot legs into the steam generators and PRHR system (also see R3).
R10	IRWST pool thermal stratification is ranked low during the initial depressurization phase. This phenomenon affects PRHR-to-IRWST heat transfer (that is ranked medium, see R12).

Table C-3. (continued).

Ranking rationale for the phenomena in Tables C-1 through C-2

Code	Ranking Rationale
R11	Condensation, differential density, noncondensible effects, and voiding in the PRHR are ranked medium during the initial depressurization phase. The convective thermal resistance on the inside surface of the PRHR tubes is sensitive to (among other things) the presence or absence of the condensation process. This sensitivity affects the PRHR heat transfer. The other three phenomena affect the flow through the primary side of the PRHR heat exchanger flow as follows: the differential density (i.e., the difference in density between the fluid in the inflow and outflow sides of the PRHR system piping) is the driving force for flow through the primary side of the PRHR system. Noncondensible effects (hydrogen, see R4) can alter the heat transfer processes on the inside of the tubes. In addition, if large volumes of noncondensible gas accumulate at the high point of the PRHR inlet line (its configuration includes an inverted trap), the path for flow through the PRHR heat exchanger may be blocked by localized voiding in the inlet line.
R12	Heat transfer between the PRHR and IRWST is ranked medium during the initial depressurization phase. This phenomenon affects the RCS cooldown in a manner similar to primary-to-affected steam generator heat transfer (that is ranked high, see R20), but during this phase, the magnitude of the heat removal to the PRHR was judged to be smaller than that to the affected steam generator.
R13	Flashing in the pressurizer is ranked medium during the initial depressurization phase. During RCS depressurization, this flashing adds steam volume to the RCS that slows its depressurization. The RCS pressure response affects the fuel rod critical heat flux during this phase (see R6 and R7). In addition, this phenomenon affects the distribution of the RCS mass (the distribution is altered as fluids in various locations flash at different times).
R14	Pressurizer level and vapor space (expansion) behavior are ranked medium during the initial depressurization phase. For a given RCS cooldown rate, these two phenomena, along with flashing, determine the RCS pressure response (see R13 for the significance of this effect). Similar behavior exists in the reactor vessel upper head (see R25).
R15	Noncondensible effects in the pressurizer are ranked low during the initial depressurization phase. Hydrogen gas will evolve from solution during the depressurization of the RCS. Accumulations of hydrogen in the pressurizer affect the species of the gas in the pressurizer bubble. However, this effect was judged to have less impact on the RCS pressure response than do the effects described in R13 and R14.
R16	Reactor coolant pump coastdown performance is ranked high during the initial depressurization phase. This phenomenon affects both steam generator primary-to-secondary and PRHR heat transfer through its influence on tube inner-surface convective heat transfer coefficients.
R17	Voiding in the primary side of the steam generator u-tubes is ranked medium during the initial depressurization phase. This ranking refers to the tubes of the unaffected steam generator. During this phase, heat removal to the affected steam generator cools the RCS fluid below the temperature of the unaffected steam generator secondary system. Following reactor coolant pump coastdown, the flow through both RCS loops is due to natural circulation. Heat flowing from the unaffected steam generator secondary into the RCS fluid inside the u-tubes can boil this fluid and void the insides of the tubes. This voiding is significant because it blocks the path for further natural circulation flow through the unaffected steam generator u-tubes. Sufficient tube voiding, therefore, thermally decouples the unaffected steam generator from the RCS.

Table C-3. (continued).

Ranking rationale for the phenomena in Tables C-1 through C-2

Code	Ranking Rationale
R18	Preferential RCS loop cooldown (listed in the steam generator primary component) is ranked high during the initial depressurization phase. The asymmetries in cold leg temperatures caused by cooling to the affected steam generator and heating from the unaffected steam generator influence the entire RCS cooldown process. If the asymmetries survive to the core inlet (i.e., fluid mixing in the reactor vessel downcomer is not complete), they may impact core criticality (see R6 and R7). If the asymmetries further survive to the core outlet, they cause the hot leg temperatures will be different, and this affects the heat transfer behavior of both steam generators.
R19	Steam generator primary-side thermal driving head is ranked medium during the initial depressurization phase. This phenomenon refers to the potential to drive natural circulation flow through the RCS loops that is created by the density difference between the fluids in the vertical sections of the steam generator u-tubes, steam generator plena, hot legs, reactor vessel downcomer, core, and upper plenum regions. Natural circulation loop flow is responsible for core and steam generator heat transfer following coastdown of the primary coolant pumps.
R20	Steam generator primary-to-secondary heat transfer is ranked high during the initial depressurization phase. This phenomenon is the parameter of primary importance during this phase.
R21	Noncondensible effects in the steam generator primary system are ranked low during the initial depressurization phase (see R4). It is believed that the affected RCS loop natural circulation flow will be sufficiently high to preclude significant hydrogen accumulation in the U-tubes during this phase.
R22	Entrainment, flashing, and level swell and depletion in the steam generator secondary are all ranked high during the initial depressurization phase. These phenomena determine the convective thermal resistance and sink temperature on the outer surfaces of the affected steam generator u-tubes and, therefore, directly affect primary-to-secondary heat transfer.
R23	Tube dryout (on the outer u-tube surfaces) in the affected steam generator secondary is ranked medium during the initial depressurization phase. This phenomenon influences primary-to-secondary heat transfer because it can reduce the affected steam generator tube area that can effectively remove heat (to be effective, the outer surface must be wetted).
R24	Liquid carry-over in the steam generator separators and dryers is ranked high during the initial depressurization phase. Secondary-side liquid mass that is entrained through or around the separators and dryers by steam flow is lost out the break into the containment. Liquid lost in this manner is not available to remove heat from the RCS. Therefore, this phenomenon has significant influence on the affected steam generator primary-to-secondary heat transfer.
R25	Flashing and voiding in the upper head/upper plenum are ranked medium during the initial depressurization phase. The rationale for the upper plenum region ranking is similar to that given for the core and hot legs in R3 and R9. The rationale for the upper head region ranking is similar to that given for the pressurizer in R13 and R14.

Table C-3. (continued).

Ranking rationale for the phenomena in Tables C-1 through C-2

Code	Ranking Rationale
R26	Two phenomena are ranked medium and nine phenomena are ranked low in the containment interior during the initial depressurization phase. For this MSLB accident, ADS is not activated and the containment interior is important to the plant response only because the break discharges into the containment and this affects PRHR heat removal to the IRWST. The low-ranked phenomena were judged to have minimal influence on RCS behavior, especially prior to flow limiter (break) unchoking that occurs very late during this phase. Interior-to-wall heat transfer and passive heat sink are ranked medium to indicate the significance of storing energy in the containment shell and internal structures during this phase (when the temperature differences between the containment atmosphere and these structures are the greatest).
R27	The containment exterior-to-ambient heat transfer is ranked low during the initial depressurization phase. This phenomenon has only a small influence on RCS behavior (through its effect on PRHR system heat removal, see R26) prior to flow limiter (break) unchoking and only a moderate influence afterward.
R28	Voiding in the CMT is ranked low during the passive residual heat removal phase. Sufficient voiding in the CMT or its inlet line (the PBL) leads to disruption of CMT recirculation. For sequences leading to ADS actuation, this disruption is an important event. However, one of the assumptions of this MSLB accident scenario is that the subsequent CMT draining is inadequate to initiate ADS. Therefore, disruption of CMT recirculation is only significant in this scenario for its minor effect on the RCS energy balance.
R29	Not used.
R30	Flashing and voiding in the core are ranked medium during the passive residual heat removal phase. These phenomena affect the condition of the fluid passed to the hot legs and PRHR system. Therefore, they affect PRHR system natural circulation and heat transfer and the RCS energy balance.
R31	Core flow channeling is ranked low during the passive heat removal phase. This phenomenon is of reduced significance in this phase as compared with the previous phase. Here, the blowdown of the affected steam generator (that was a major cause of asymmetric loop conditions) has been completed. A return to a critical core is of less concern during this phase than during the first phase due to RCS boration from CMT recirculation and increasing RCS temperatures. However, the PRHR system that removes core decay heat to the IRWST is connected to only one loop. Because the temperature of fluid leaving the PRHR system will be very cold, extreme asymmetries in the cold leg temperatures may exist. If there is limited mixing in the downcomer and lower plenum (see R35), and if the core flow is channeled rather than well-mixed, then these asymmetries can survive into the hot legs. Temperature asymmetry in the hot leg affects the fluid entering the PRHR system, and, thereby, its heat removal.
R32	CMT-to-loop differential density is ranked low during the passive decay heat removal phase. During the portion of this phase when the CMTs are recirculating, this phenomenon determines the recirculation rate. If recirculation is lost (see R28), then this phenomenon affects the balance between levels in the CMT and PBL, and this is of significance because ADS actuation (that is assumed not to occur here) is based upon attaining a CMT low-level setpoint.

Table C-3. (continued).

Ranking rationale for the phenomena in Tables C-1 through C-2

Code	Ranking Rationale
R33	The CMT level is ranked medium during the passive decay heat removal phase. This MSLB accident scenario assumes the CMT level will not fall to the low-level setpoint that initiates ADS. This phenomenon is included here only to assure that the appropriateness of that assumption is considered.
R34	Not used.
R35	Flow distribution in the downcomer/lower plenum is ranked low during the passive decay heat removal phase. The rationale for this ranking is the same as described for core channeling during this phase (see R31).
R36	Voiding, phase separation in tees, and noncondensible effects in the hot legs are ranked medium during the passive decay heat removal phase. These phenomena all affect the PRHR-to-IRWST heat transfer because they influence the condition of fluid entering the PRHR system. The PRHR system inlet is connected to the ADS stage 4 line that leaves the top of one hot leg. If that hot leg voids, then steam may be passed into to the PRHR system. If noncondensible gas (hydrogen, see R4) is present in the hot leg and is passed into the PRHR system, then the PRHR system performance may be degraded or terminated (see R11).
R37	Not used.
R38	In the IRWST, flow and temperature distributions in the PRHR bundle region, pool thermal stratification, and pool level are ranked medium during the passive decay heat removal phase. These phenomena affect the PRHR-to-IRWST heat transfer that is ranked high (see R39). Flow and temperature distribution in the PRHR bundle region and pool thermal stratification affect the heat sink temperature and convective thermal resistance on the outer surfaces of the PRHR tubes. The IRWST pool level determines the PRHR tube effective heat transfer area; only tube regions below the pool level will efficiently transfer heat. The pool level response during this accident has not yet been established: The IRWST pool inventory is depleted by boil-off to the containment and is replenished by condensate from the containment shell. A significant fraction of the total PRHR heat transfer area resides in the upper horizontal region of the tube bundle, and this region is only slightly submerged below the pool level present at the time the MSLB occurs. However, the MSLB discharged virtually all of the contents of one steam generator secondary into the containment during the previous phase. A substantial return of condensate from the containment shell to the IRWST is therefore expected, and, therefore, during this phase, the IRWST may be filled to the point of overflowing.
R39	Heat transfer between the PRHR and the IRWST is ranked high during the passive heat removal phase. PRHR heat transfer represents the only continuous means by which the core decay power is removed from the RCS during this phase.

Table C-3. (continued).

Ranking rationale for the phenomena in Tables C-1 through C-2

Code	Ranking Rationale
R40	In the PRHR component, condensation, differential density, voiding, and noncondensible effects are ranked medium during the passive decay heat removal phase. The convective thermal resistance on the inside surface of the PRHR tubes is sensitive to (among other things) the presence or absence of the condensation process. This sensitivity affects the PRHR heat transfer. The other three phenomena affect the flow through the primary side of the PRHR heat exchanger as follows: the differential density (i.e., the difference in density between the fluid in the inflow and outflow sides of the PRHR system piping) is the driving force for flow through the primary side of the PRHR system. Noncondensible effects (hydrogen, see R4) can alter the heat transfer processes on the inside of the tubes. In addition, if large volumes of noncondensible gas accumulate at the high point of the PRHR inlet line (its configuration includes an inverted trap), the path for flow through the PRHR heat exchanger may be blocked by localized voiding in the inlet line.
R41	Pressurizer level and vapor space (compression) behavior are ranked medium during the passive decay heat removal phase. During this phase, the RCS cooldown is reversed and the RCS is heated to the extent necessary so that the PRHR system may remove the core decay power. The pressurizer level increases, and the vapor bubble within the pressurizer is compressed. During this phase, the RCS pressure is determined by the behavior of the pressurizer bubble, along with any bubble present in the reactor vessel upper head (see R60).
R42	Noncondensible effects in the pressurizer are ranked medium during the passive decay heat removal phase. The composition of the gas in the pressurizer bubble that controls RCS pressure during this phase (see R41) is steam and hydrogen (see R4). The gas bubble expansion and contraction characteristics are affected by the gas composition.
R43	Condensation in the pressurizer is ranked low during the passive decay heat removal phase. This condensation influences the RCS pressure through its effect on the mass and composition of the pressurizer gas bubble (see R42). Both wall and interphase condensation remove steam from the bubble.
R44	Steam generator primary-to-secondary heat transfer is ranked medium during the passive decay heat removal phase. The affected steam generator secondary system blew down and dried out during the prior phase. However, heat exchange between the RCS and unaffected steam generator remains a contributor to the RCS energy balance. The unaffected steam generator may act as an RCS heat source or sink, depending upon the relationship between the RCS and unaffected steam generator temperatures. During the prior phase, the unaffected steam generator experienced a partial blowdown; however, the full blowdown of the affected steam generator cooled the RCS below the temperature of the unaffected steam generator secondary. During this phase, the RCS is heated to the temperature needed to remove the core decay power through the PRHR system to the IRWST. If this temperature is below that of the fluid in the unaffected steam generator, then that generator acts as a heat source to the RCS. In this case, the PRHR system must therefore remove both the core decay heat and any heat added to the RCS from the unaffected steam generator. Whenever this equilibrium temperature is above the temperature of the water in the unaffected steam generator secondary, that generator acts as an RCS heat sink.

Table C-3. (continued).

Ranking rationale for the phenomena in Tables C-1 through C-2

Code	Ranking Rationale
R45	Steam generator asymmetric behavior is ranked medium during the passive decay heat removal phase. This asymmetry arises because the affected generator blowdown has been completed, its secondary system has dried out, and there is only limited potential for heat transfer between the RCS and this generator. On the other hand, the unaffected steam generator may continue to exchange heat with the RCS (see R44) during this phase. This thermal asymmetry, coupled with the asymmetry of the PRHR system configuration (it is connected to only one of the two coolant loops), provides the potential for fluids of different temperature to enter the PRHR system. This behavior depends upon (among other things) which steam generator is assumed to have been connected to the broken steam line. The PRHR-to-IRWST heat transfer is directly affected by the temperature of the fluid entering the PRHR system.
R46	Voiding and noncondensible effects inside the unaffected steam generator u-tubes are ranked medium during the passive decay heat removal phase. These phenomena provide a potential to interrupt unaffected RCS loop natural circulation flow and heat exchange with the unaffected steam generator. Here, noncondensible effects refer to hydrogen (see R4), while voiding refers to the possible accumulation of hydrogen at the tops of the u-tube bends in a volume sufficient to block the flow path through the tubes. Voiding also can be caused by boiling of water inside the u-tubes due to heat addition through the tubes (similar to the rationale provided for the previous phase in R17).
R47	Flow split in the upper plenum is ranked medium during the initial depressurization and passive decay heat removal phases. In the first phase, this flow split affects heat removal to the affected steam generator because it determines the flow through the primary side of that steam generator. In the second phase, this flow split affects heat removal/addition to/from the unaffected steam generator (see R44 and R45) for the same reason.
R48	Condensate transport, condensation, liquid distribution, and liquid holdup in the containment interior are ranked medium during the passive decay heat removal phase. These phenomena affect PRHR-to-IRWST heat transfer (ranked high, see R39) through their influence on the IRWST pool level (see R38).
R49	Natural convection, noncondensible segregation, noncondensible effects, nonuniform steam/air distribution, steam-noncondensible mixing, and passive heat sink in the containment interior are ranked medium during the passive decay heat removal phase. These phenomena affect heat transfer processes on the inside surface of the containment shell (interior-to-wall heat transfer is ranked high, see R50).
R50	The containment interior-to-wall and exterior-to ambient heat transfer are ranked high during the passive decay heat removal phase. When combined, these phenomena represent the removal of the reactor decay power across the containment shell to its ultimate heat sink. Nine other containment-exterior phenomena are ranked medium during the passive decay heat removal phase. These phenomena control the heat transfer processes on the containment shell exterior.

Table C-3. (continued).

Ranking rationale for the phenomena in Tables C-1 through C-2

Code	Ranking Rationale
R51	Stored energy release in the cold legs, core (non-fuel structures), downcomer/lower plenum, fuel rods, hot legs, and upper head/upper plenum is ranked low during the initial depressurization phase. This phenomenon represents the removal, to the RCS fluid, of heat stored in the piping walls and other structures during normal reactor operation. The low ranking indicates this phenomenon has a smaller influence on the RCS energy balance than do the other contributors to that balance: core decay power (as distinguished from release of the initial fuel stored energy), steam generator heat transfer, and the PRHR-to-IRWST heat transfer.
R52	Loop asymmetry effects in the cold legs, downcomer/lower plenum, hot legs, and upper plenum are ranked medium during the passive decay heat removal phase. The rationales for these rankings are the same as described in R45 and R47.
R53	Flow resistance in the reactor coolant pumps is ranked low during both the initial depressurization and passive decay heat removal phases. Following the pump coastdown, the locked-rotor resistance of the pump is a significant portion of the total flow resistance through the RCS loops. Therefore, this resistance affects the RCS coolant loop natural circulation flow rates and, thereby, heat exchange between the RCS and the affected and unaffected steam generators. This flow resistance is also present in the PRHR system flow loop; however, total resistance through this flow loop is instead dominated in the PRHR piping and heat exchanger.
R54	Not used.
R55	In the CMT component, flow resistance is ranked low during the passive decay heat removal phase. This flow resistance is dominated in the CMT discharge lines, that include both orifices and check valves. This phenomenon influences the RCS energy balance through its effect on the CMT recirculation rate. If CMT recirculation is interrupted (see R28), this phenomenon also limits the rate at which the CMT may drain.
R56	In the CMT component, noncondensible effects are ranked low during the passive decay heat removal phase. Accumulation of noncondensible gas (hydrogen, see R4) at the top of a PBL (the CMT inlet line) is one mechanism by which voiding may interrupt CMT recirculation (see R28).
R57	Interphase condensation and pool flow in the IRWST are ranked low during the passive decay heat removal phase. These phenomena affect PRHR-to-IRWST heat transfer through their influences on the flow and temperature distributions in the PRHR bundle region (this phenomenon is ranked medium, see R38).
R58	The PRHR flow resistance is ranked medium during the passive decay heat removal phase. The flow resistance through the entire PRHR primary system cooling loop is dominated by components within the PRHR system itself (piping, fittings, and heat exchanger), and not in the associated RCS components (see R53). The PRHR flow resistance determines the PRHR system natural circulation flow rate and, thereby, affects PRHR-to-IRWST heat transfer (by influencing the tube inner surface convective thermal resistance).
R59	The core flow resistance is ranked low during the passive residual heat removal phase. This phenomenon affects PRHR-to-IRWST heat transfer through its influence on the PRHR system natural circulation flow rate. However this influence is less than that of the PRHR system flow resistance (see R53 and R58).

Table C-3. (continued).

Ranking rationale for the phenomena in Tables C-1 through C-2

Code	Ranking Rationale
R60	Voiding and vapor space compression in the upper head/upper plenum component are ranked medium during the passive decay heat removal phase. Both of these phenomena affect the RCS pressure response. The upper head region flashed and voided during the previous phase. During this phase, the vapor bubble is compressed, as the RCS is heated and pressurized in a manner similar to the bubble in the pressurizer (see R41). In addition, if the upper plenum region is voided, then void will enter the hot legs from where it can affect both steam generator and PRHR system heat transfer (see R36, R44, R46, and R47).
R61	Steam generator secondary level and pressure are ranked low during the passive decay heat removal phase. During the prior phase, a portion of the unaffected steam generator inventory was lost out the break. This loss was terminated when the main steam isolation valves closed. A low level in the unaffected steam generator can influence the heat transfer between it and the RCS (see R44) because it may reduce the effective tube heat transfer area. The unaffected steam generator secondary pressure also affects this heat transfer through its influence on the secondary system saturation temperature.

Appendix D - Detailed Results, Main Steam Line Break With ADS PIRT

This appendix presents the detailed results of the main steam line break (MSLB) with Automatic Depressurization System (ADS) activation PIRT. The detailed PIRT results are shown in Tables D-1 through D-5, and the transient description, overall phenomena ranking criteria, and specific ranking rationales are shown in Table D-6. The information in Tables D-1 through D-5 is arranged to correspond with the five phases of the accident scenario. These tables are organized in alphabetical order according to the component name. Within the listings for each component, the pertinent identified phenomena are arranged by order of ranking. The right sides of these tables contain identifier codes that refer the reader elsewhere in this report for further information:

The code labeled "Ranking Rationale" (for example, "R1") leads the reader to a description of the logic leading to the ranking of each specific phenomenon; this information is found in Table D-6 in this appendix.

The code labeled "Phenomena Description" (for example, "D1") leads the reader to a general description of each phenomenon; this information is found in Appendix G, Table G-1.

Two codes are labeled "Type Geometry" (for example "C1/G1"). The "C" code leads the reader to the physical geometries and general functions of the component under discussion; this information is found in Appendix G, Table G-2. The "G" code leads the reader to more detailed discussion of the specific phenomena associated with each of the components; this information is found in Appendix G, Table G-3.

The "Supporting Evidence" code (for example, "E1") leads the reader to references (geometrical, experimental, and analytical) that provide background and corroborating information. This information is found in Appendix G, Table G-4. It is noted that the supporting evidence is currently being developed in experimental and analytical tasks both inside and outside the PIRT task. Thus, the information in this table can be expected to increase as the supporting tasks are completed.

The "Sublevel Phenomena" code (for example, "S1") leads the reader to a list of contributing phenomena affecting the primary phenomenon. The sublevel phenomena information is found in Appendix G, Table G-5.

Table D-1. PIRT for the initial depressurization phase of a MSLB with single failure leading to ADS.

			For codes shown in these columns, See Tables:				
			D-6	G-1	G-2/G-3	G-4	G-5
Component	Phenomena	Rank	Ranking Rationale	Phenomena Description	Type Geometry	Supporting Evidence	Sublevel Phenomena
Break	Mass flow	H	R1	D25	C3/G5	E1	S1
	Energy release	H	R1	D26	C3/G5	E1	S1
	Flow resistance	L	R1	D27	C3/G5	E1	S11
Cold legs	Loop asymmetry effects	M	R104	D45	C4/G9	E1	S9
	Stored energy release	L	R103	D68	C4/G7	E1	S2
Core	Core channeling	H	R2	D11	C5	E1	S55
	Flashing	M	R3	D21	C5/G12	E1	S5
	Voiding	M	R3	D78	C5/G12	E1	S54
	Noncondensible effects	L	R4	D50	C5	E1	S12
	Stored energy release	L	R103	D68	C5/G11	E1	S2
CMT	CMT-to-loop differential density	L	R5	D17	C6/G13	E1	S10
	Noncondensible effects	L	R4	D50	C6/G14	E1	S12
	Thermal stratification	L	R5	D73	C6/G14	E1	S19
Downcomer/ lower plenum	Loop asymmetry effects	M	R104	D45	C7/G16	E1	S9
	Stored energy release	L	R103	D68	C7/G15	E1	S2
Fuel rods	Core power/decay heat	H	R8	D12	C8/G20	E1	S4
	CHF	M	R6	D3	C8	E1	S56
	Boron reactivity feedback	M	R7	D15	C8	E1	S57
	Moderator temperature feedback	M	R6	D47	C8	E1	S58
	Stored energy release	L	R103	D68	C8/G21	E1	S2
Hot legs	Flashing	M	R9	D21	C9	E1	S5
	Loop asymmetry effects	M	R104	D45	C9/G23	E1	S9
	Voiding	M	R9	D78	C9/G25	E1	S54
	Noncondensible effects	L	R4	D50	C9	E1	S12
	Stored energy release	L	R103	D68	C9/G22	E1	S2

Table D-1. (continued).

			For codes shown in these columns, See Tables:				
			D-6	G-1	G-2/G-3	G-4	G-5
Component	Phenomena	Rank	Ranking Rationale	Phenomena Description	Type Geometry	Supporting Evidence	Sublevel Phenomena
IRWST	Pool thermal stratification	L	R10	D59	C10/G26	E1	S19
PRHR	Condensation	M	R11	D9	C12/G31	E1	S18
	Differential density	M	R11	D17	C12/G30	E1	S10
	Heat transfer between PRHR and IRWST	M	R12	D32	C12/G30	E1	S28
	Noncondensible effects	M	R11	D50	C12/G31	E1	S12
	Voiding	M	R11	D78	C12/G31	E1	S54
Pressurizer	Flashing	M	R13	D21	C14/G33	E1	S5
	Level (inventory)	M	R14	D39	C14/G33	E1	S13
	Vapor space behavior	M	R14	D77	C14/G33	E1	S60
	Noncondensible effects	L	R15	D50	C14	E1	S12
Pumps	Coastdown performance	H	R16	D7	C15/G37	E1	S14
	Flow resistance	L	R105	D27	C15/G38	E1	S15
Steam generator (primary)	Preferential loop cooldown	H	R18	D61	C16/G40	E1	S61
	Primary to secondary heat transfer	H	R20	D31	C16/G39	E1	S53
	Thermal driving head	M	R19	D72	C16/G41	E1	S59
	Voiding (unaffected loop)	M	R17	D78	C16/G39	E1	S54
	Noncondensible effects	L	R21	D50	C16/G39	E1	S12
Steam generator (secondary)	Entrainment	H	R22	D20	C16/G42	E1	S23
	Flashing (steam generator & feedwater line)	H	R22	D21	C16/G42	E1	S5
	Level swell & depletion	H	R22	D41	C16/G42	E1	S7
	Tube dryout (affected SG)	M	R23	D74	C16/G42	E1	S62
Steam generator (separator/ dryer)	Liquid carry-over	H	R24	D42	C16/G43	E1	S63

Table D-1. (continued).

			For codes shown in these columns, See Tables:				
			D-6	G-1	G-2/G-3	G-4	G-5
Component	Phenomena	Rank	Ranking Rationale	Phenomena Description	Type Geometry	Supporting Evidence	Sublevel Phenomena
Upper head / upper plenum	Flashing	M	R25	D21	C18/G45	E1	S5
	Flow split (upper plenum)	M	R47	D28	C18/G46	E1	S65
	Loop asymmetry effects	M	R104	D45	C18/G46	E1	S9
	Voiding	M	R25	D78	C18/G45	E1	S54
	Stored energy release	L	R103	D68	C18/G47	E1	S2
Containment (interior)	Interior to wall heat transfer	M	R26	D86	C19/G48	E1	S72
	Passive heat sink	M	R26	D81	C19/G48	E1	S67
	Condensate transport	L	R26	D8	C19/G48	E1	S37
	Condensation	L	R26	D9	C19/G48	E1	S18
	Liquid distribution	L	R26	D43	C19/G48	E1	S38
	Liquid holdup	L	R26	D44	C19/G48	E1	S38
	Natural convection	L	R26	D48	C19/G48	E1	S36
	Noncondensible effects	L	R26	D50	C19/G49	E1	S12
	Noncondensible segregation	L	R26	D84	C19/G49	E1	S71
	Nonuniform steam/air distribution	L	R26	D51	C19/G49	E1	S35
	Steam-noncondensible mixing	L	R26	D67	C19/G49	E1	S35
Containment (exterior)	Exterior to ambient heat transfer	L	R27	D83	C20/G50	E1	S70

Table D-2. PIRT for the passive decay heat removal phase of a MSLB with single failure leading to ADS.

			For codes shown in these columns, See Tables:				
			D-6	G-1	G-2/G-3	G-4	G-5
Component	Phenomena	Rank	Ranking Rationale	Phenomena Description	Type Geometry	Supporting Evidence	Sublevel Phenomena
Core	Flashing	M	R30	D21	C5/G12	E1	S5
	Voiding	M	R30	D78	C5/G12	E1	S54
	Channeling	L	R31	D4	C5	E1	S55
	Flow resistance	L	R107	D27	C5/G12	E1	S11
	Noncondensible effects	L	R32	D50	C5	E1	S12
CMT	CMT-to-loop differential density	M	R33	D17	C6/G13	E1	S10
	Thermal stratification	M	R33	D73	C6/G14	E1	S19
	Voiding	M	R28	D78	C6/G13	E1	S54
	Flow resistance	L	R108	D27	C6/G13	E1	S11
	Noncondensible effects	L	R32	D50	C6/G14	E1	S12
Downcomer/ lower plenum	Flow distribution	L	R35	D24	C7/G16	E1	S64
Fuel rods	Decay heat	H	R8	D12	C8/G20	E1	S4
Hot legs	Voiding	M	R36	D78	C9/G25	E1	S54
	Noncondensible effects	M	R36	D50	C9	E1	S12
	Phase separation in tees	M	R36	D56	C9/G24	E1	S8
IRWST	Flow & temperature distribution in bundle region	M	R38	D23	C10/G26	E1	S24
	Pool level	M	R38	D39	C10/G26	E1	S25
	Pool thermal stratification	M	R38	D59	C10/G26	E1	S19
	Interphasic condensation	L	R109	D37	C10/G29	E1	S18
	Pool flow	L	R109	D57	C10/G26	E1	S24
Pressurizer	Level (inventory)	M	R41	D39	C14/G33	E1	S13
	Noncondensible effects	M	R42	D50	C14	E1	S12
	Vapor space behavior	M	R41	D77	C14/G33	E1	S60

Table D-2. (continued).

			For codes shown in these columns, See Tables:				
			D-6	G-1	G-2/G-3	G-4	G-5
Component	Phenomena	Rank	Ranking Rationale	Phenomena Description	Type Geometry	Supporting Evidence	Sublevel Phenomena
PRHR	Heat transfer between PRHR and IRWST	H	R39	D32	C12/G30	E1	S28
	Differential density	M	R40	D17	C12/G30	E1	S10
	Flow resistance	M	R110	D27	C12/G30	E1	S11
	Noncondensible effects	M	R40	D50	C12/G31	E1	S12
	Voiding	M	R40	D78	C12/G31	E1	S54
Pumps	Flow resistance	L	R105	D27	C15/G38	E1	S15
Steam generators	Asymmetric behavior	M	R45	D85	C16/G40	E1	S61
	Noncondensible effects	M	R59	D50	C16/G39	E1	S12
	Primary to secondary heat transfer	M	R43	D33	C16/G39	E1	S53
	Tube voiding	M	R58	D78	C16/G39	E1	S54
	Secondary level	L	R44	D63	C16/G39	E1	S7
	Secondary pressure	L	R44	D64	C16/G39	E1	S17
Upper head / upper plenum	Flow split (upper plenum)	M	R47	D28	C18/G46	E1	S65
	Voiding	M	R46	D78	C18/G45	E1	S54
Containment (interior)	Condensate transport	L	R48	D8	C19/G48	E1	S37
	Condensation	L	R48	D9	C19/G48	E1	S18
	Interior to wall heat transfer	L	R48	D86	C19/G48	E1	S72
	Liquid distribution	L	R48	D43	C19/G48	E1	S38
	Liquid holdup	L	R48	D44	C19/G48	E1	S38
	Natural convection	L	R48	D48	C19/G48	E1	S36
	Noncondensible effects	L	R48	D50	C19/G49	E1	S12
	Noncondensible segregation	L	R48	D84	C19/G49	E1	S71
	Nonuniform steam/air distribution	L	R48	D51	C19/G49	E1	S35

Table D-2. (continued).

			For codes shown in these columns, See Tables:				
			D-6	G-1	G-2/G-3	G-4	G-5
Component	Phenomena	Rank	Ranking Rationale	Phenomena Description	Type Geometry	Supporting Evidence	Sublevel Phenomena
Containment (interior), continued	Passive heat sink	L	R48	D81	C19/G48	E1	S67
	Steam-noncondensible mixing	L	R48	D67	C19/G49	E1	S35
Containment (exterior)	Exterior to ambient heat transfer	L	R27	D83	C20/G50	E1	S70

Table D-3. PIRT for the CMT draining-to-ADS actuation phase of a MSLB with single failure leading to ADS.

			For codes shown in these columns, See Tables:				
			D-6	G-1	G-2/G-3	G-4	G-5
Component	Phenomena	Rank	Ranking Rationale	Phenomena Description	Type Geometry	Supporting Evidence	Sublevel Phenomena
Cold legs	Loop asymmetry effects	M	R50	D45	C4/G9	E1	S9
Core	Flow resistance	L	R107	D27	C5/G12	E1	S11
CMT	Level	H	R52	D39	C6/G14	E1	S13
	Condensation	L	R53	D9	C6/G14	E1	S18
	Flow resistance	L	R53	D27	C6/G13	E1	S11
	Thermal stratification	L	R53	D73	C6/G14	E1	S19
Downcomer/ lower plenum	Flow distribution	L	R54	D24	C7/G16	E1	S64
Fuel rods	Decay heat	H	R8	D12	C8/G20	E1	S4
Hot legs	Horizontal fluid stratification	M	R55	D35	C9/G25	E1	S33
	Flashing	L	R55	D21	C9	E1	S5
	Phase separation in tees	L	R55	D56	C9/G24	E1	S8
	Stored energy release	L	R51	D68	C9/G22	E1	S2
IRWST	Flow & temperature distribution in PRHR bundle region	M	R38	D23	C10/G26	E1	S24
	Pool level	M	R38	D39	C10/G26	E1	S25
	Pool thermal stratification	M	R38	D59	C10/G26	E1	S19
	Interphasic condensation	L	R109	D37	C10/G29	E1	S18
	Pool flow	L	R109	D57	C10/G26	E1	S24
PRHR	Heat transfer between PRHR and IRWST	H	R39	D32	C12/G30	E1	S28
	Differential density	M	R40	D17	C12/G30	E1	S10
	Flow resistance	M	R110	D27	C12/G30	E1	S11
	Noncondensible effects	M	R40	D50	C12/G31	E1	S12
	Voiding	M	R40	D78	C12/G31	E1	S54
Pressurizer	Level (inventory)	M	R56	D39	C14/G33	E1	S13

Table D-3. (continued).

			For codes shown in these columns, See Tables:				
			D-6	G-1	G-2/G-3	G-4	G-5
Component	Phenomena	Rank	Ranking Rationale	Phenomena Description	Type Geometry	Supporting Evidence	Sublevel Phenomena
Pumps	Coastdown performance	L	R57	D27	C15/G38	E1	S15
Steam generators	Asymmetric behavior	M	R45	D85	C16/G40	E1	S61
	Noncondensible effects	M	R59	D50	C16/G39	E1	S12
	Primary to secondary heat transfer	M	R43	D33	C16/G39	E1	S53
	Tube voiding	M	R58	D78	C16/G39	E1	S54
	Secondary level	L	R44	D63	C16/G39	E1	S7
	Secondary pressure	L	R44	D64	C16/G39	E1	S17
Upper head / upper plenum	Voiding	M	R46	D78	C18/G45	E1	S54
Containment (interior)	Condensate transport	L	R60	D8	C19/G48	E1	S37
	Condensation	L	R48	D9	C19/G48	E1	S18
	Interior to wall heat transfer	L	R48	D86	C19/G48	E1	S72
	Liquid distribution	L	R48	D43	C19/G48	E1	S38
	Liquid holdup	L	R48	D44	C19/G48	E1	S38
	Natural convection	L	R60	D48	C19/G48	E1	S36
	Noncondensible effects	L	R48	D50	C19/G49	E1	S12
	Noncondensible segregation	L	R48	D84	C19/G49	E1	S71
	Nonuniform steam/air distribution	L	R60	D51	C19/G49	E1	S35
	Passive heat sink	L	R48	D81	C19/G48	E1	S67
	Steam-noncondensible mixing	L	R48	D67	C19/G49	E1	S35
Containment (exterior)	Exterior to ambient heat transfer	L	R27	D83	C20/G50	E1	S70

Table D-4. PIRT for the ADS blowdown phase of a MSLB with single failure leading to ADS.

			For codes shown in these columns, See Tables:				
			D-6	G-1	G-2/G-3	G-4	G-5
Component	Phenomena	Rank	Ranking Rationale	Phenomena Description	Type Geometry	Supporting Evidence	Sublevel Phenomena
Accumulators	Mass flow	H	R62	D46	C1/G2	E1	S20
	Noncondensible effects	M	R61	D50	C1/G1	E1	S12
ADS	Energy release	H	R63	D19	C2/G3	E1	S21
	Mass flow	H	R63	D46	C2/G3	E1	S21
	Flow resistance	M	R63	D27	C2/G3	E1	S11
	Noncondensible effects	M	R63	D50	C2/G3	E1	S12
Cold legs	Noncondensible effects	L	R64	D50	C4	E1	S12
	Flashing	L	R66	D21	C4	E1	S5
	Stored energy release	L	R65	D68	C4/G7	E1	S2
Core	Two-phase mixture level	H	R67	D76	C5	E1	S31
	Flashing	M	R80	D21	C5/G12	E1	S5
	Stored energy release	L	R65	D68	C5/G11	E1	S2
CMT	Level	H	R68	D39	C6/G14	E1	S13
	Flashing	L	R53	D21	C6/G14	E1	S5
	Thermal stratification	L	R53	D73	C6/G14	E1	S19
Downcomer/ lower plenum	Flashing	L	R69	D21	C7	E1	S5
	Level	L	R69	D39	C7/G17	E1	S13
	Noncondensible effects	L	R69	D50	C7/G19	E1	S12
	Stored energy release	L	R65	D68	C7/G15	E1	S2
Fuel rods	Decay heat	H	R8	D12	C8/G20	E1	S4
	Stored energy release	L	R65	D68	C8/G21	E1	S2
Hot legs	Phase separation in tees	H	R70	D56	C9/G24	E1	S8
	CCFL	M	R71	D14	C9/G25	E1	S27
	Countercurrent flow	M	R71	D13	C9/G25	E1	S32
	Entrainment	M	R71	D20	C9/G25	E1	S23

Table D-4. (continued).

			For codes shown in these columns, See Tables:				
			D-6	G-1	G-2/G-3	G-4	G-5
Component	Phenomena	Rank	Ranking Rationale	Phenomena Description	Type Geometry	Supporting Evidence	Sublevel Phenomena
Hot legs, Continued	Flashing	M	R71	D21	C9	E1	S5
	Horizontal fluid stratification	M	R71	D35	C9/G25	E1	S33
	Noncondensible effects	L	R69	D50	C9	E1	S12
	Stored energy release	L	R48	D68	C9/G22	E1	S2
IRWST	Interphasic condensation	M	R72	D37	C10/G29	E1	S18
	Pool flow	M	R72	D57	C10/G26	E1	S24
	Pool thermal stratification	L	R72	D59	C10/G26	E1	S19
	Pool level	L	R73	D58	C10/G26	E1	S25
	Pool to tank structure heat transfer	L	R74	D60	C10/G28	E1	S26
PRHR	Heat transfer between PRHR and IRWST	M	R75	D32	C12/G30	E1	S28
	Differential density	L	R76	D17	C12/G30	E1	S10
	Flashing	L	R76	D21	C12	E1	S5
	Flow resistance	L	R76	D27	C12/G30	E1	S11
	Noncondensible effects	L	R76	D50	C12/G31	E1	S12
	Phase separation in tees	L	R76	D56	C12/G31	E1	S8
Pressurizer	CCFL	M	R77	D14	C14/G34	E1	S27
	Entrainment-De-entrainment	M	R77	D20	C14/G36	E1	S23
	Level swell	M	R77	D40	C14/G36	E1	S13
	Noncondensible effects	L	R69	D50	C14	E1	S12
	Stored energy release	L	R65	D68	C14/G35	E1	S2
Steam generators	Primary to secondary heat transfer	L	R78	D33	C16/G39	E1	S53
Upper head / upper plenum	Entrainment/De-entrainment	M	R79	D20	C18/G46	E1	S23
	Flashing	M	R80	D21	C18/G45	E1	S5
	Stored energy release	L	R65	D68	C18/G47	E1	S2

Table D-4. (continued).

			For codes shown in these columns, See Tables:				
			D-6	G-1	G-2/G-3	G-4	G-5
Component	Phenomena	Rank	Ranking Rationale	Phenomena Description	Type Geometry	Supporting Evidence	Sublevel Phenomena
Containment (interior)	Condensation	M	R115	D9	C19/G48	E1	S18
	Interior to wall heat transfer	M	R115	D86	C19/G48	E1	S72
	Passive heat sink	M	R115	D81	C19/G48	E1	S67
	Condensate transport	L	R115	D8	C19/G48	E1	S37
	Liquid distribution	L	R115	D43	C19/G48	E1	S38
	Liquid holdup	L	R115	D44	C19/G48	E1	S38
	Natural convection	L	R115	D48	C19/G48	E1	S36
	Noncondensible effects	L	R115	D50	C19/G49	E1	S12
	Noncondensible segregation	L	R115	D84	C19/G49	E1	S71
	Nonuniform steam/air distribution	L	R115	D51	C19/G49	E1	S35
	Steam-noncondensible mixing	L	R115	D67	C19/G49	E1	S68
Containment (exterior)	Exterior to ambient heat transfer	M	R115	D83	C20/G50	E1	S70
	PCCS evaporation	M	R115	D52	C20/G50	E1	S39
	Air flow	L	R115	D82	C20/G50	E1	S69
	Atmospheric temperature	L	R115	D2	C20/G50	E1	S43
	Chimney effects	L	R115	D5	C20/G50	E1	S41
	Humidity	L	R115	D36	C20/G50	E1	S46
	PCCS mixture convective heat transfer	L	R115	D54	C20/G50	E1	S30
	PCCS water flow	L	R115	D53	C20/G50	E1	S40
	PCCS wetting	L	R115	D55	C20/G50	E1	S42
	Radiation heat transfer	L	R115	D62	C20/G50	E1	S45

Table D-5. PIRT for the IRWST and sump injection phase of a MSLB with single failure leading to ADS.

			For codes shown in these columns, See Tables:				
			D-6	G-1	G-2/G-3	G-4	G-5
Component	Phenomena	Rank	Ranking Rationale	Phenomena Description	Type Geometry	Supporting Evidence	Sublevel Phenomena
ADS	Energy release	H	R81	D19	C2/G3	E1	S21
	Mass flow	H	R81	D46	C2/G3	E1	S21
	Flow resistance	M	R81	D27	C2/G3	E1	S11
	Noncondensible effects	L	R81	D50	C2/G3	E1	S12
Cold legs	Condensation	L	R82	D9	C4	E1	S18
	Noncondensible effects	L	R82	D50	C4	E1	S12
Core	Two-phase mixture level	H	R83	D76	C5	E1	S31
	Flow resistance	M	R83	D27	C5/G12	E1	S11
Downcomer/ lower plenum	Level	H	R84	D39	C7/G17	E1	S13
	Condensation	M	R85	D9	C7/G18	E1	S18
Fuel rods	Decay heat	H	R8	D12	C8/G20	E1	S4
Hot legs	Phase separation in tees	H	R86	D56	C9/G24	E1	S8
	CCFL	M	R87	D14	C9/G25	E1	S27
	Countercurrent flow	M	R87	D13	C9/G25	E1	S32
	Horizontal fluid stratification	M	R88	D35	C9/G25	E1	S33
IRWST	Discharge line flashing	M	R112	D21	C10/G27	E1	S5
	Flow resistance	M	R90	D27	C10/G27	E1	S11
	Pool level	M	R90	D58	C10/G26	E1	S25
	Pool thermal stratification	M	R90	D59	C10/G26	E1	S19
	Pool to tank structure heat transfer	L	R113	D60	C10/G28	E1	S26
PRHR	Heat transfer between PRHR and IRWST	L	R92	D32	C12/G30	E1	S28
Steam generators	Primary to secondary heat transfer	L	R93	D33	C16/G39	E1	S53

Table D-5. (continued).

			For codes shown in these columns, See Tables:				
			D-6	G-1	G-2/G-3	G-4	G-5
Component	Phenomena	Rank	Ranking Rationale	Phenomena Description	Type Geometry	Supporting Evidence	Sublevel Phenomena
Sump	Discharge line flashing	M	R112	D21	C17	E1	S5
	Flow resistance	M	R94	D27	C17	E1	S11
	Fluid temperature	M	R94	D29	C17	E1	S34
	Level	M	R94	D39	C17	E1	S13
Upper head / upper plenum	Entrainment/De-entrainment	H	R95	D20	C18/G46	E1	S23
Containment (interior)	Interior to wall heat transfer	H	R114	D86	C19/G48	E1	S72
	Condensate transport	M	R98	D8	C19/G48	E1	S37
	Condensation	M	R97	D9	C19/G48	E1	S18
	Liquid distribution	M	R98	D43	C19/G48	E1	S38
	Liquid holdup	M	R98	D44	C19/G48	E1	S38
	Natural convection	M	R97	D48	C19/G48	E1	S36
	Noncondensible effects	M	R97	D50	C19/G49	E1	S12
	Noncondensible segregation	M	R97	D84	C19/G49	E1	S71
	Nonuniform steam/air distribution	M	R97	D51	C19/G49	E1	S35
	Passive heat sink	M	R99	D81	C19/G48	E1	S67
	Steam-noncondensible mixing	M	R97	D67	C19/G49	E1	S68

Table D-5. (continued).

			For codes shown in these columns, See Tables:				
			D-6	G-1	G-2/G-3	G-4	G-5
Component	Phenomena	Rank	Ranking Rationale	Phenomena Description	Type Geometry	Supporting Evidence	Sublevel Phenomena
Containment (exterior)	Exterior to ambient heat transfer	H	R114	D83	C20/G50	E1	S70
	Air flow	M	R100	D82	C20/G50	E1	S69
	Atmospheric temperature	M	R101	D2	C20/G50	E1	S43
	Chimney effects	M	R100	D5	C20/G50	E1	S41
	Humidity	M	R101	D36	C20/G50	E1	S46
	PCCS evaporation	M	R100	D52	C20/G50	E1	S39
	PCCS mixture convective heat transfer	M	R100	D54	C20/G50	E1	S40
	PCCS water flow	M	R100	D53	C20/G50	E1	S40
	PCCS wetting	M	R101	D55	C20/G50	E1	S42
	Radiation heat transfer	M	R101	D62	C20/G50	E1	S45

Table D-6. Transient description and ranking rationale for the MSLB with single failure leading to ADS PIRT.

Overall Transient Description and Top-level Ranking Rationale

This sequence is initiated by a double-ended rupture of a main steam line inside containment, with an assumed additional single failure that promotes automatic depressurization system (ADS) actuation. A number of additional failures could potentially lead to ADS actuation: A steam generator tube rupture (SGTR) combined with the MSLB would lead to reactor coolant system (RCS) mass loss, resulting in ADS actuation. However, this accident would represent a multiple-failure event. The ADS could be inadvertently actuated by an operator. However, this event requires operator action considerations, which were not desired to be introduced into the PIRT (these actions will be addressed separately later). The RCS cooldown and shrinkage would be increased if the RCS pumps failed to trip automatically, potentially leading to ADS actuation. However, this event also requires operator action considerations. Failure of one core makeup tank (CMT) discharge line check valve (stuck closed) would result in a greater level reduction in the unaffected CMT, potentially leading to ADS actuation. Since the operators could not correct this failure, a stuck-closed CMT check valve was chosen as the single complicating failure for this PIRT.

For this accident sequence, it is also assumed that only safety-grade plant systems are available and that no uncovery of the core occurs. One of the primary purposes of the PIRT is to ensure that the analysis code(s) have adequate modeling capability for simulating reactor vessel inventory. The important hierarchical elements in the code assessment structure are those affecting reactor vessel inventory as described below.

Phase Descriptions and Medium-level Ranking Rationales

Initial Depressurization Phase:

Description - This phase begins at the time of the pipe break. Both steam generators begin blowing down into the containment. The flow rates through the two sides of the break are restricted by the steam line flow limiters and are significantly less than those allowed by critical flow through the full pipe areas. A steam line isolation signal is generated (due to low steam line pressure, high containment pressure, or low cold leg temperature). This signal results in closure of the main steam isolation valves and isolation of the unaffected steam generator from the broken steam line. Unaffected steam generator blowdown is arrested, and afterward, it acts as a heat source to the RCS. Flow from the affected steam generator into containment can not be isolated. Performances of the separators and dryers degrade as they are flooded with liquid. During blowdown, steam generator secondary fluid flashes and boils, and the steam produced swells the boiler mixture level, entrains liquid, and sweeps it through and around the separators and dryers and out the break. Primary-to-affected secondary heat transfer is at a high rate, and the RCS fluid is cooled, causing it to shrink. RCS cooling is preferential to the loop containing the affected steam generator; cold leg temperatures differ markedly between the affected and unaffected loops. Because the reactor vessel lower plenum is not necessarily well-mixed, this thermal asymmetry may persist into the core, upper plenum, and hot leg regions. The RCS pressure and pressurizer level fall; the reactor vessel upper head flashes. If not already generated, a reactor trip signal is generated due to low pressurizer pressure. Reactor trip causes the core power to be quickly reduced to the decay heat rate, and this power reduction causes the average RCS temperature to fall faster, the RCS fluid shrinkage rate to increase and, therefore, the RCS pressure to fall even more rapidly. Declining core pressures and potentially (due to the positive reactor kinetic feedback effects of declining RCS fluid temperatures) increasing core power may cause a departure from nucleate boiling in the core. An S signal is generated due to low pressurizer pressure, low steam generator pressure, low cold leg temperature, or high containment pressure. The S signal causes: CMT system actuation, reactor coolant pump trip, and feedwater isolation. If the passive residual heat removal (PRHR) system has not already been actuated by low steam generator levels, then

Table D-6. (continued).

CMT actuation results in PRHR actuation as well (see Reference 6, Table H-2, for details of the PRHR system actuation logic). The RCS loop flows decline rapidly from a forced-circulation to natural-circulation condition and this reduces the RCS heat removal rate. Flow through the unaffected loop ceases, since its steam generator now acts as a RCS heat source. The containment behavior is important because the affected steam generator blowdown proceeds against the containment pressure. In the containment, the break effluent is mixed with nitrogen, and steam is condensed from the mixture on the inside of the containment shell. The heat released to the shell is removed to the atmosphere by evaporation, convection, and radiation to air on the outside of the shell. These processes continue, with the affected secondary inventory and pressure continuously decreasing, until the blowdown of the affected steam generator has been completed. When the affected steam generator secondary has completely dried out, its pressure equilibrates with the containment pressure, an event marking the end of this phase.

Important parameters and dominant processes - The primary-to-secondary heat transfer rate is judged to be the parameter of primary importance because it dominates the RCS cooldown. Processes important for accurate simulation of this parameter are: break flow, steam generator secondary behavior (level swell and depletion, liquid carry-over, flashing, entrainment), flow through the RCS loops, and asymmetric loop cooldown.

Passive Decay Heat Removal Phase:

Description - This phase begins when the affected steam generator blowdown is complete. RCS heat sources during this phase are fuel rod decay heat and reverse heat transfer from the unaffected steam generator. RCS heat removal is accomplished by CMT recirculation and PRHR system operation. Because the CMT and PRHR systems each are connected to only one of the RCS loops, behavior during this phase is dependent upon which loops are assumed to contain the affected steam generator and affected CMT. Natural circulation-driven RCS loop, CMT, and PRHR flows and asymmetries in RCS temperature distributions are expected. PRHR heat removal may lead to thermal stratification in the in-containment refueling water storage tank (IRWST) that would degrade PRHR performance. This accident sequence assumes RCS cooling leads to fluid shrinkage and depressurization sufficient to cause ADS actuation. To be consistent with this assumption, recirculation through the unaffected CMT must first be interrupted. This interruption initiates draining in the unaffected CMT, which marks the end of this phase.

Important parameters and dominant processes - The RCS energy distribution is judged to be the parameter of primary importance during this phase because it determines the RCS heat removal. The processes important for accurate simulation of this parameter are: core, steam generator, and PRHR heat transfer and loop asymmetry effects.

CMT Draining to ADS Actuation Phase:

Description - This phase begins at the time that recirculation through the unaffected CMT is interrupted. Plant behavior during this phase is characterized by the CMT draining and the phenomena influencing it. This phase ends when the level in the unaffected CMT has declined to 67.5% and ADS stage 1 is actuated.

Important parameters and dominant processes - The unaffected CMT level and RCS mass and energy distributions are judged to be the parameters of primary importance because they determine the timing of ADS actuation. The processes important for accurate simulation of these parameters are: core, steam generator, and PRHR heat transfer and natural circulation in RCS loops.

Table D-6. (continued).

ADS Blowdown Phase:

Description - This phase begins when the level in either CMT declines to 67.5%. This occurrence produces an ADS actuation signal and, after a time delay, the ADS first stage is actuated (see Reference 6, Table H-2, for details of ADS sequencing). ADS actuation results in a blowdown of the RCS; ADS first, second, and third stages discharge through spargers submerged under water in the IRWST. As the RCS pressure declines, regions with the warmest fluid and those at the lowest pressure preferentially flash first, followed by cooler and higher-pressure regions. Initiations of ADS second and third stages occur at specified time intervals following ADS first stage actuation. Actuation of ADS fourth stage occurs upon attaining a level of 20% in the unaffected CMT, with an additional time-delay requirement. Unlike the other stages, ADS fourth stage discharges directly into the containment loop compartments. Plant behavior during this phase is dominated by the RCS blowdown, and this is determined by the RCS mass and energy distributions, especially as they affect the ADS flow rate and the CMT level. Accumulator injection begins when the RCS pressure falls to the initial accumulator pressure. Accumulator levels fall, and, eventually, nitrogen is injected from the accumulators into the RCS. As the RCS pressure approaches that in the containment, flows through the ADS change from choked to friction-dominated. The RCS inventory declines after the injection of accumulator water ends, and it is critical that the core remain covered until IRWST injection begins. This phase ends when the differential pressure between the RCS and the containment has been reduced to 12.1 psi. This pressure difference is equivalent to the 28-ft static head available for driving fluid from the IRWST into the reactor vessel. Onset of IRWST injection marks the end of the ADS blowdown phase.

Important parameters and dominant processes - The unaffected CMT level and ADS flow rate are judged to be the parameters of primary importance because they determine ADS staging and RCS depressurization rate. The processes important for accurate simulation of these parameters are: ADS discharge flow (critical and friction-dominated) and the RCS mass and energy balances.

IRWST and Sump Injection Phase:

Description - This phase begins when flow commences from the IRWST, through the direct vessel injection lines, into the downcomer of the reactor vessel. This flow replenishes RCS inventory and reverses the downward core level trend. Steam produced in the core is passed out the ADS valves into the containment. Steam reaching the containment is condensed on the inside of the containment shell, and the condensate is returned via gutters to the IRWST, where it is available as a core injection source. Core decay heat is removed through the containment shell to its ultimate heat sink (the environment) via evaporative, convective, and radiative heat transfer on the outside of the containment shell. The IRWST injection rate may be unsteady. Increased injection rates may lead to decreased core steam production, decreased quality and volumetric flow at the fourth stage ADS and, therefore, RCS repressurization which results in a decreased injection rate. Most liquid that escapes returning to the IRWST (for example, that flowing from the ADS fourth stage) is collected in the containment sump which, like the IRWST, is elevated above the elevation span of the core. Some liquid may be trapped in locations where it cannot return to the IRWST or sump. Gravity-driven injection from the sump, similar to that from the IRWST, returns liquid to the reactor vessel downcomer. The plant end-state for this accident includes core inventory maintenance from IRWST and/or sump injections and decay heat removal, across the containment shell, to the atmosphere.

Important parameters and dominant processes - The RCS-to-containment differential pressure is judged to be the parameter of primary importance because it determines the magnitude of the IRWST and sump injection flow rates. The processes important for accurate simulation of this parameter are: ADS flow and pressure drop, transient IRWST inventory, transient sump inventory, and the containment and RCS mass and energy balances.

Table D-6. (continued).

Detailed Phenomena Ranking Rationales

Ranking rationale for the phenomena in Tables D-1 through D-5

Code	Ranking Rationale
R1	Break mass flow and break energy release are ranked high, and break flow resistance is ranked low during the initial depressurization phase. For the main steam line break (MSLB) accident, the break processes are controlled at the flow limiter that effectively limits the size of the break (the flow area of the flow limiter is significantly less than that of the ruptured steam pipe). The mass flow and energy release control the blowdown of the affected steam generator secondary system that determines the primary-to-secondary heat transfer, the parameter of primary importance during this phase. The flow resistance is ranked low because the break is controlled by critical-flow, not frictional-flow, processes during most of this phase. The break will unchoke (and, therefore, its flow resistance will be of significance) only near the end of this phase when the affected secondary pressure nears that in the containment.
R2	Core channeling is ranked high during the initial depressurization phase. Fluid mixing/channeling processes within the core directly affect the hot leg fluid temperatures. A large fluid temperature asymmetry exists between the cold legs on the two loops, and this asymmetry may survive to the core exit, causing the hot leg temperatures to be asymmetric. The hot leg fluid temperatures are the sources for steam generator primary-to-secondary heat transfer, the parameter of primary importance during this phase.
R3	Flashing and voiding in the core are ranked medium during the initial depressurization phase. These phenomena affect the RCS pressure response (which has some influence on the steam generator primary-to-secondary heat transfer). They also affect the distribution of fluid in the RCS (also see R9).
R4	Noncondensible effects (due to hydrogen evolving from solution during RCS depressurization) in the core, CMT, and hot legs are ranked low during the initial depressurization phase. Voiding from, and transport of, this hydrogen may influence steam generator primary-to-secondary heat transfer, PRHR system heat transfer, and CMT recirculation. In all three cases, noncondensible gasses collected at the tops of piping networks may interrupt flow through the networks (also see R21).
R5	CMT-to-loop differential density and CMT thermal stratification are ranked low during the initial depressurization phase. CMT cooling of the RCS is small compared with the affected steam generator primary-to-secondary heat transfer. These phenomena are introduced here because they influence the fluid conditions within the CMTs and the CMT recirculation rate that are important during the phases that follow. CMT thermal stratification established during this phase determines when flashing in the PBL or CMT can interrupt CMT recirculation.

Table D-6. (continued).

Ranking rationale for the phenomena in Tables D-1 through D-5

Code	Ranking Rationale
R6	Boron and moderator-temperature reactivity feedback are ranked medium in the fuel rod component during the initial depressurization phase. A return to a critical reactor condition is a general concern during the severe RCS fluid overcooling encountered in MSLB accidents. Negative reactivity is introduced by scram rod insertion (at the time of reactor trip) and boron addition to the RCS from the CMTs (after they are activated at the time of the S signal). Positive reactivity is introduced by moderator temperature feedback due to the declining RCS fluid temperatures. Assuming all scram rods are inserted, a return to a critical core condition is not expected; these phenomena were included only to highlight their importance should this assumption later be changed. Note these phenomena are ranked medium for this accident (while they were ranked low for the MSLB accident not involving a CMT check valve failure) because less negative boron reactivity is available if only one CMT is operable.
R7	Fuel rod critical heat flux is ranked medium during the initial depressurization phase. The potential for a return to a critical core condition is described in R6. This potential, coupled with declining RCS pressure (caused by RCS fluid shrinkage effects), provides the possibility for a fuel rod heat-up due to departure from nucleate boiling. The medium ranking was assigned due to the safety-significance of any such fuel rod heat-up.
R8	Fuel rod core power/decay heat is ranked high during all five phases. This phenomenon is ranked high because: (1) it is a major heat source in the RCS energy balance and (2) there is a potential for a return to a critical core condition (see R6 and R7).
R9	Flashing and voiding in the hot legs are ranked medium during the initial depressurization phase. These phenomena affect the natural circulation driving heads of the RCS and PRHR system loops and, thereby, the steam generator and PRHR heat transfer rates. The natural circulation loop driving heads are enhanced when void is passed from the from hot legs into the steam generators and PRHR system (also see R3).
R10	IRWST pool thermal stratification is ranked low during the initial depressurization phase. This phenomenon affects PRHR-to-IRWST heat transfer (that is ranked medium, see R12).
R11	Condensation, differential density, noncondensible effects, and voiding in the PRHR are ranked medium during the initial depressurization phase. The convective thermal resistance on the inside surface of the PRHR tubes is sensitive to (among other things) the presence or absence of the condensation process. This sensitivity affects the PRHR heat transfer. The other three phenomena affect the flow through the primary side of the PRHR heat exchanger flow as follows: the differential density (i.e., the difference in density between the fluid in the inflow and outflow sides of the PRHR system piping) is the driving force for flow through the primary side of the PRHR system. Noncondensible effects (hydrogen, see R4) can alter the heat transfer processes on the inside of the tubes. In addition, if large volumes of noncondensible gas accumulate at the high point of the PRHR inlet line (its configuration includes an inverted trap), the path for flow through the PRHR heat exchanger may be blocked by localized voiding in the inlet line.
R12	Heat transfer between the PRHR and IRWST is ranked medium during the initial depressurization phase. This phenomenon affects the RCS cooldown in a manner similar to primary-to-affected steam generator heat transfer (that is ranked high, see R20), but during this phase, the magnitude of the heat removal to the PRHR was judged to be smaller than that to the affected steam generator.

Table D-6. (continued).

Ranking rationale for the phenomena in Tables D-1 through D-5

Code	Ranking Rationale
R13	Flashing in the pressurizer is ranked medium during the initial depressurization phase. During RCS depressurization, this flashing adds steam volume to the RCS that slows its depressurization. The RCS pressure response affects the fuel rod critical heat flux during this phase (see R6 and R7). In addition, this phenomenon affects the distribution of the RCS mass (the distribution is altered as fluids in various locations flash at different times).
R14	Pressurizer level and vapor space (expansion) behavior are ranked medium during the initial depressurization phase. For a given RCS cooldown rate, these two phenomena, along with flashing, determine the RCS pressure response (see R13 for the significance of this effect). Similar behavior exists in the reactor vessel upper head (see R25).
R15	Noncondensible effects in the pressurizer are ranked low during the initial depressurization phase. Hydrogen gas will evolve from solution during the depressurization of the RCS. Accumulations of hydrogen in the pressurizer affect the species of the gas in the pressurizer bubble. However, this effect was judged to have less impact on the RCS pressure response than do the effects described in R13 and R14.
R16	Reactor coolant pump coastdown performance is ranked high during the initial depressurization phase. This phenomenon affects both steam generator primary-to-secondary and PRHR heat transfer through its influence on tube inner-surface convective heat transfer coefficients.
R17	Voiding in the primary side of the steam generator u-tubes is ranked medium during the initial depressurization phase. This ranking refers to the tubes of the unaffected steam generator. During this phase, heat removal to the affected steam generator cools the RCS fluid below the temperature of the unaffected steam generator secondary system. Following reactor coolant pump coastdown, the flow through both RCS loops is due to natural circulation. Heat flowing from the unaffected steam generator secondary into the RCS fluid inside the u-tubes can boil this fluid and void the insides of the tubes. This voiding is significant because it blocks the path for further natural circulation flow through the unaffected steam generator u-tubes. Sufficient tube voiding, therefore, thermally decouples the unaffected steam generator from the RCS.
R18	Preferential RCS loop cooldown (listed in the steam generator primary component) is ranked high during the initial depressurization phase. The asymmetries in cold leg temperatures caused by cooling to the affected steam generator and heating from the unaffected steam generator influence the entire RCS cooldown process. If the asymmetries survive to the core inlet (i.e., fluid mixing in the reactor vessel downcomer is not complete), they may impact core criticality (see R6 and R7). If the asymmetries further survive to the core outlet, the hot leg temperatures will be different, and this affects the heat transfer behavior of both steam generators.
R19	Steam generator primary-side thermal driving head is ranked medium during the initial depressurization phase. This phenomenon refers to the potential to drive natural circulation flow through the RCS loops that is created by the density difference between the fluids in the vertical sections of the steam generator u-tubes, steam generator plena, hot legs, reactor vessel downcomer, core, and upper plenum regions. Natural circulation loop flow is responsible for core and steam generator heat transfer following coastdown of the primary coolant pumps.

Table D-6. (continued).

Ranking rationale for the phenomena in Tables D-1 through D-5

Code	Ranking Rationale
R20	Steam generator primary-to-secondary heat transfer is ranked high during the initial depressurization phase. This phenomenon is the parameter of primary importance during this phase.
R21	Noncondensible effects in the steam generator primary system are ranked low during the initial depressurization phase. It is believed that the affected RCS loop natural circulation flow will be sufficiently high to preclude significant hydrogen accumulation (see R4) in the U-tubes during this phase.
R22	Entrainment, flashing, and level swell and depletion in the steam generator secondary are all ranked high during the initial depressurization phase. These phenomena determine the convective thermal resistance and sink temperature on the outer surfaces of the affected steam generator u-tubes and, therefore, directly affect primary-to-secondary heat transfer.
R23	Tube dryout (on the outer u-tube surfaces) in the affected steam generator secondary is ranked medium during the initial depressurization phase. This phenomenon influences primary-to-secondary heat transfer because it can reduce the affected steam generator tube area that can effectively remove heat (to be effective, the outer surface must be wetted).
R24	Liquid carry-over in the steam generator separators and dryers is ranked high during the initial depressurization phase. Secondary-side liquid mass that is entrained through or around the separators and dryers by steam flow is lost out the break into the containment. Liquid lost in this manner is not available to remove heat from the RCS. Therefore, this phenomenon significantly influences the affected steam generator primary-to-secondary heat transfer.
R25	Flashing and voiding in the upper head/upper plenum are ranked medium during the initial depressurization phase. The rationale for the upper plenum region ranking is similar to that given for the core and hot legs in R3 and R9. The rationale for the upper head region ranking is similar to that given for the pressurizer in R13 and R14.
R26	Two phenomena are ranked medium and nine phenomena are ranked low in the containment interior during the initial depressurization phase. The ADS has not yet been activated and the containment interior is important to the overall plant response only because the break discharges into the containment and this discharge affects PRHR heat removal to the IRWST. The low-ranked phenomena were judged to have minimal influence on RCS behavior, especially prior to flow limiter (break) unchoking that occurs very late during this phase. Interior-to-wall heat transfer and passive heat sink are ranked medium to indicate the significance of storing energy in the containment shell and internal structures during this phase (when the temperature differences between the containment atmosphere and these structures are the greatest).
R27	The containment exterior-to-ambient heat transfer is ranked low during the initial depressurization, passive decay heat removal, and CMT draining-to-ADS actuation phases. This phenomenon has only a small influence on RCS behavior (through its effect on PRHR system heat removal, see R26) prior to flow limiter (break) unchoking and only a moderate influence afterward.
R28	Voiding in the CMT is ranked medium during the passive residual heat removal phase. Sufficient voiding in the CMT or its inlet line (the PBL) leads to disruption of CMT recirculation and this event marks the end of this phase. Disruption of CMT recirculation also has a minor effect on the RCS energy balance.
R29	Not used.

Table D-6. (continued).

Ranking rationale for the phenomena in Tables D-1 through D-5

Code	Ranking Rationale
R30	Flashing and voiding in the core are ranked medium during the passive residual heat removal phase. These phenomena affect the condition of the fluid passed to the hot legs and PRHR system. Therefore, they affect PRHR system natural circulation and heat transfer and the RCS energy balance.
R31	Core flow channeling is ranked low during the passive heat removal phase. This phenomenon is of reduced significance in this phase as compared with the previous phase. Here, the blowdown of the affected steam generator (that was a major cause of asymmetric loop conditions) has been completed. A return to a critical core is of less concern than in the prior phase because the RCS temperatures are increasing and CMT recirculation is borating the RCS. However, the PRHR system that removes core decay heat to the IRWST is connected to only one loop. Because the temperature of fluid leaving the PRHR system will be very cold, extreme asymmetries may exist in the cold leg temperatures. If there is limited mixing in the downcomer and lower plenum (see R35), and if the core flow is channeled rather than well-mixed, then these asymmetries can survive into the hot legs. Temperature asymmetry in the hot leg affects the fluid entering the PRHR system and, thereby, its heat removal.
R32	Noncondensible effects in the core and CMT are ranked low during the passive decay heat removal phase. Hydrogen (see R4) may affect core heat transfer and influence CMT recirculation.
R33	CMT-to-loop differential density and thermal stratification are ranked medium during the passive decay heat removal phase. These phenomena are contributors to the driving force for CMT recirculation.
R34	Not used.
R35	Flow distribution in the downcomer/lower plenum is ranked low during the passive decay heat removal phase. The rationale for this ranking is the same as described for core channeling during this phase (see R31).
R36	Voiding, phase separation in tees, and noncondensible effects in the hot legs are ranked medium during the passive decay heat removal phase. These phenomena all affect the PRHR-to-IRWST heat transfer because they influence the condition of fluid entering the PRHR system. The PRHR system inlet is connected to the ADS stage 4 line that leaves the top of one hot leg. If that hot leg voids, then steam may be passed into to the PRHR system. If noncondensible gas (hydrogen, see R4) is present in the hot leg and is passed into the PRHR system, then the PRHR system performance may be degraded or terminated (see R11).
R37	Not used.

Table D-6. (continued).

Ranking rationale for the phenomena in Tables D-1 through D-5

Code	Ranking Rationale
R38	In the IRWST, flow and temperature distributions in the PRHR bundle region, pool thermal stratification, and pool level are ranked medium during the passive decay heat removal and CMT draining-to-ADS actuation phases. These phenomena affect the PRHR-to-IRWST heat transfer that is ranked high (see R39). Flow and temperature distribution in the PRHR bundle region and pool thermal stratification affect the heat sink temperature and convective thermal resistance on the outer surfaces of the PRHR tubes. The IRWST pool level determines the PRHR tube effective heat transfer area; only tube regions below the pool level will efficiently transfer heat. The pool level response during this accident has not yet been established: The IRWST pool inventory is depleted by boil-off to the containment and is replenished by condensate from the containment shell. A significant fraction of the total PRHR heat transfer area resides in the upper horizontal region of the tube bundle, and this region is only slightly submerged below the pool level present at the time the MSLB occurs. However, the MSLB discharged virtually all of the contents of one steam generator secondary into the containment during the previous phase. A substantial return of condensate from the containment shell to the IRWST is expected, and, therefore, during this phase, the IRWST may be filled to the point of overflowing.
R39	Heat transfer between the PRHR and the IRWST is ranked high during the passive heat removal and CMT draining-to-ADS actuation phases. PRHR heat transfer represents a significant mechanism for heat removal from the RCS during these phases.
R40	In the PRHR component, differential density, voiding, and noncondensible effects are ranked medium during the passive decay heat removal and CMT draining-to-ADS actuation phases. These phenomena affect the flow through the primary side of the PRHR heat exchanger as follows: the differential density (i.e., the difference in density between the fluid in the inflow and outflow sides of the PRHR system piping) is the driving force for flow through the primary side of the PRHR system. Noncondensible effects (hydrogen, see R4) can alter the heat transfer processes on the inside of the tubes. In addition, if noncondensible gas accumulates at the high point of the PRHR inlet line (its configuration includes an inverted trap), the path for flow through the PRHR heat exchanger may be blocked by localized voiding in the inlet line.
R41	Pressurizer level and vapor space (compression) behavior are ranked medium during the passive decay heat removal phase. During this phase, the RCS pressure is determined by the behavior of the pressurizer bubble, along with any bubble present in the reactor vessel upper head.
R42	Noncondensible effects in the pressurizer are ranked medium during the passive decay heat removal phase. The composition of the gas in the pressurizer bubble that controls RCS pressure during this phase (see R41) is steam and hydrogen (see R4). The gas bubble expansion and contraction characteristics are affected by the gas composition.
R43	Steam generator primary-to-secondary heat transfer is ranked medium during the passive decay heat removal and CMT draining-to-ADS actuation phases. The affected steam generator secondary system blew down and dried out during the first phase. However, heat exchange between the RCS and unaffected steam generator remains a contributor to the RCS energy balance. The unaffected steam generator may act as an RCS heat source or sink, depending upon the relationship between the RCS and unaffected steam generator temperatures.

Table D-6. (continued).

Code	Ranking rationale for the phenomena in Tables D-1 through D-5 Ranking Rationale
R44	Steam generator secondary level and pressure are ranked low during the passive decay heat removal and CMT draining-to-ADS actuation phases. During the initial depressurization phase, a portion of the unaffected steam generator inventory was lost out the break. This loss was terminated when the main steam isolation valves closed. A low level in the unaffected steam generator can influence the heat transfer between it and the RCS (see R43) because it may reduce the effective tube heat transfer area. The unaffected steam generator secondary pressure also affects this heat transfer through its influence on the secondary system saturation temperature.
R45	Steam generator asymmetric behavior is ranked medium during the passive decay heat removal and CMT draining-to-ADS actuation phases. This asymmetry arises because the affected generator blowdown has been completed, its secondary system has dried out, and there is only limited potential for heat transfer between the RCS and this generator. On the other hand, the unaffected steam generator may continue to exchange heat with the RCS (see R44) during this phase. This thermal asymmetry, coupled with the asymmetry of the CMT and PRHR system configurations (they each are connected to only one of the two coolant loops), provide the potential for fluids of different temperature to enter the PRHR system. This behavior depends upon (among other things) which steam generator is assumed to have been connected to the broken steam line.
R46	Voiding in the upper head/upper plenum component are ranked medium during the passive decay heat removal and CMT draining-to-ADS actuation phases. This phenomenon affects the RCS pressure response. The upper head region flashed and voided during the first phase. During these two phases, the vapor bubble in the upper head affects RCS pressure in a manner similar to the bubble in the pressurizer (see R41). In addition, if the upper plenum region is voided, then void will enter the hot legs, from where it can affect both steam generator and PRHR system heat transfer.
R47	Flow split in the upper plenum is ranked medium during the initial depressurization and passive decay heat removal phases. In the first phase, this flow split affects heat removal to the affected steam generator because it determines the flow through the primary side of that steam generator. In the second phase, this flow split affects heat removal/addition to/from the unaffected steam generator (see R44 and R45) for the same reason.
R48	Containment-interior phenomena are ranked low during the passive decay heat removal and CMT draining-to-ADS actuation phases. These phenomena have only a minor effect on PRHR-to-IRWST heat transfer during these phases.
R49	Not used.
R50	Cold leg loop asymmetry effects are ranked medium during the CMT draining-to-ADS actuation phase. Only one CMT is active, and its draining along with that of its PBL are yet another source of loop asymmetry.
R51	Hot leg stored energy release is ranked low during the CMT draining-to-ADS actuation phase. Heat released from the piping walls to the RCS fluid has a minor effect on the RCS energy balance.
R52	The CMT level is ranked high during the CMT draining-to-ADS actuation phase. This phenomenon is one of the important parameters listed for this phase. Activation of the ADS is based upon the CMT level response, and this activation defines the end of this phase.

Table D-6. (continued).

Ranking rationale for the phenomena in Tables D-1 through D-5

Code	Ranking Rationale
R53	The following phenomena in the CMT are ranked low during the CMT draining-to-ADS actuation phase: condensation, flow resistance, and thermal stratification. The CMT level response is primarily determined by phenomena external to the CMT (primarily those affecting the RCS mass and energy balances and distributions). The three CMT phenomena listed above affect the manner in which the CMT drains, but do not significantly affect onset of CMT draining, and, therefore, these phenomena were ranked low. Flashing and thermal stratification in the CMT are ranked low during the ADS blowdown phase. The entire RCS flashes during this phase, and it is at this time that the CMT fluid conditions and their distributions determine the CMT behavior.
R54	The flow distribution in the downcomer/lower plenum is ranked low during the CMT draining-to-ADS actuation phase because the flow rates and temperatures of fluids in the cold legs are asymmetric. These asymmetries are related to the CMTs being connected to the cold legs of only one of the two coolant loops and the PRHR system being connected to the other loop. Downcomer flow distribution represents the fluid mixing processes that determine the RCS energy distribution, one of the important parameters listed for this phase.
R55	Horizontal fluid stratification is ranked medium and flashing and phase separation in tees are ranked low in the hot legs during the CMT draining-to-ADS actuation phase. RCS flashing is preferential (i.e., it is based on localized pressures and temperatures). Flashing affects the RCS mass distribution, one of the important parameters for this phase. The PRHR system inlet is connected to the ADS stage 4 line that exits the top of one hot leg pipe. If steam resides in the upper portion of the hot leg, it may freely enter the PRHR system; this steam flow may entrain liquid. The PIRT committee believed the hot leg, if voided, likely will be stratified during this phase. Fluid stratification and phase separation at tees were included because they affect the state of the fluid entering the PRHR system.
R56	Pressurizer level was ranked medium during the CMT draining-to-ADS actuation phase. Because the RCS is a closed system during this phase of the accident, the pressurizer may refill if the RCS fluid is reheated. In that case, the RCS pressure will be determined by compression of the bubbles inside the pressurizer and reactor vessel upper head.
R57	The pump flow resistance is ranked low for the CMT draining-to-ADS actuation phase. Here, the pump flow resistance is the locked-rotor resistance that is present following the pump coastdown period. This resistance affects natural circulation flows around the RCS loops (i.e., through the core, hot legs, steam generators, pumps, and cold legs). This resistance also affects the flow rate through the PRHR system natural circulation loop (i.e., through the core, hot leg, PRHR inlet, PRHR heat exchanger, PRHR outlet, pump, and cold leg). Flow through this loop is expected to continue throughout this phase. However, for this natural circulation loop, the pump locked rotor resistance is a small contributor to the overall loop resistance.
R58	Voiding in the steam generator tubes is ranked medium for the passive decay heat removal and CMT draining-to-ADS actuation phases. This phenomenon is the mechanism for interruption of RCS loop natural circulation flow.
R59	Noncondensible effects in the steam generator primary are ranked medium during the passive decay heat removal and CMT draining-to-ADS actuation phases. Hydrogen (see R4) may reduce the efficiency of heat transfer between RCS fluid and the inner wall of the u-tubes. In addition, sufficient quantities of hydrogen accumulated in the u-bends may interrupt loop natural circulation through the steam generators.

Table D-6. (continued).

Ranking rationale for the phenomena in Tables D-1 through D-5

Code	Ranking Rationale
R60	Containment-interior phenomena are ranked low during the CMT draining-to-ADS actuation phase. These phenomena have only a minor effect on PRHR-to-IRWST heat transfer during this phase.
R61	Noncondensible effects in the accumulators are ranked medium in the ADS blowdown phase. Expansion of the nitrogen gas bubble within the accumulators controls the differential pressure between the accumulator and RCS and, therefore, the rate at which liquid flows from the accumulator into the RCS (this flow is ranked high, see R62).
R62	The accumulator flow is ranked high during the ADS blowdown phase. This flow is a major RCS mass addition source.
R63	The ADS mass flow rate and energy release are controlling phenomena during the ADS blowdown phase of the accident and are ranked high (ADS flow rate is listed as an important parameter for this phase). The ADS flow resistance is ranked medium for the ADS blowdown phase because it affects the ADS fourth stage discharge after it unchokes (because the differential pressure between RCS and containment has been reduced). The effects of noncondensible gases are ranked medium for the ADS blowdown phase; the accumulators empty and vent a large volume of nitrogen into the RCS (note the noncondensible gas volume grows as the RCS continues depressurizing). This nitrogen can affect the ADS flow and energy release.
R64	Noncondensible effects in the cold legs are ranked low during the ADS blowdown phase. Nitrogen expelled from the accumulators accumulates in this region of the RCS and disposition of nitrogen can affect the ADS mass flow and energy release rates (see R63).
R65	Stored energy release in the following components is ranked low for the ADS blowdown phase: cold legs, core, downcomer/lower plenum, fuel rods, hot legs, pressurizer, and upper head/upper plenum. The RCS pressure and saturation temperature fall sharply during this phase. As a result, remaining heat stored in metal structures in these components is available to flow into the RCS coolant. However, this flow of heat is expected to be a minor contributor to the overall RCS energy balance; energy loss through the ADS is expected to dominate that balance.
R66	Flashing in the cold leg is ranked low during the ADS blowdown phase. Liquid volume drained from the CMT must be replaced by steam volume; flashing in this component represents one possible source of steam for that purpose. Steam produced in the cold legs (or elsewhere, and convected into the cold legs) must enter the pressure balance line to replace liquid drained from the CMT. The CMT draining process determines the actuation of the ADS fourth stage.
R67	Core two-phase mixture level is ranked high for the ADS blowdown phase. Regarding high core levels, a relationship between the core level and ADS flow rate has not been established with current evidence. However, core level behavior can dramatically affect the ADS discharge (if core level swells, an increased flow of liquid into the ADS will result). This phenomenon was ranked high pending later evidence to the contrary. Regarding low core levels, the minimum core level is attained at the end of the ADS blowdown when the onset of IRWST injection reverses the declining core level trend. Therefore, this phenomenon was also ranked high because it is an indicator of core uncovery and coolability.

Table D-6. (continued).

Ranking rationale for the phenomena in Tables D-1 through D-5

Code	Ranking Rationale
R68	The CMT level is ranked high during the ADS blowdown phase. This phenomenon is an important parameter listed for this phase because actuation of fourth stage ADS is based upon attaining a 20% CMT indicated level.
R69	Flashing, level, and noncondensible effects in the downcomer/lower plenum and noncondensible effects in the hot legs and pressurizer are ranked low during the ADS blowdown phase. Noncondensible gas is expelled from the accumulators into the RCS at the same time the fluid within the RCS is flashing. Flashing will be preferential based upon location within the plant and upon the temperature of the fluid present. The presence of noncondensible gas alters the flashing process. Therefore, during this phase, these phenomena may have some effect on the ADS flow rates and, perhaps, upon the core level.
R70	Phase separation in hot leg tees is ranked high during the ADS blowdown phase. This phenomenon controls the quality of the fluid entering ADS stages 1, 2, and 3 (via the pressurizer surge line tee) and ADS stage 4 (through the ADS-4 tees).
R71	CCFL, countercurrent flow, entrainment, flashing, and horizontal fluid stratification in the hot legs are ranked medium during the ADS blowdown phase. These phenomena control the phase separation process at the hot leg tees (see R70). The inventory, inventory distribution, and flow behavior in the hot legs determines the behavior at the pressurizer surge line and ADS stage 4 tees.
R72	In the IRWST, interphasic condensation, pool flow, and pool thermal stratification are ranked medium for the ADS blowdown phase. ADS stages 1, 2, and 3 discharge RCS fluid into the IRWST through two spargers. The fluid flowing through the spargers has a high steam content, perhaps superheated, at the near-atmospheric pressure inside the tank. However, the IRWST fluid is initially subcooled, so high interphase condensation rates are anticipated. The phenomena ranked here affect: (1) the manner in which the IRWST performs the quenching process, (2) the state of the IRWST fluid (that later is injected into the RCS), and (3) the containment pressure.
R73	The IRWST pool level is ranked low for the ADS blowdown phase. After ADS stages 1, 2, and 3 unchoke, the pool level has a minor effect upon the pressure at the ADS sparger and, therefore, upon the ADS flow rate.
R74	IRWST pool-to-tank heat transfer is ranked low for the ADS blowdown phase. Over the long term, the energy removed from the pool to its surroundings may be important, but during this phase this energy removal was judged to be significantly smaller than that introduced into the pool through the ADS.
R75	Heat transfer between the PRHR and IRWST is ranked medium during the ADS blowdown phase. The importance of PRHR heat removal during this phase has not been established. It is suspected that this heat removal may be overshadowed by ADS effects during this phase. However, PRHR heat transfer has the potential to be important, so it was ranked medium pending better information.

Table D-6. (continued).

Ranking rationale for the phenomena in Tables D-1 through D-5

Code	Ranking Rationale
R76	In the PRHR component, differential density, flashing, noncondensible effects, flow resistance, and phase separation in tees are ranked low in the ADS blowdown phase. These phenomena can affect the PRHR heat removal rate (ranked medium, see R75) and, therefore, have been ranked low. Note that this is the only instance where phase separation in tees has been ranked for the PRHR component. For normal PRHR flow situations, tee phase separation is primarily of interest at the PRHR inlet line connection on the hot leg, and this phenomenon was included in the listings for the hot leg component. However, for the ADS blowdown situation, RCS conditions are chaotic, and the question here is the manner in which the PRHR system outlet tee (on the steam generator outlet plenum) might perform under potential reverse-flow conditions. Because the PRHR inlet line is connected directly to one of the ADS fourth-stage inlet lines, reverse flow through the PRHR system is likely to develop as RCS fluid rushes out the ADS fourth stage.
R77	In the pressurizer, CCFL, entrainment/de-entrainment, and level swell are ranked medium during the ADS blowdown phase. During this phase, the ADS mass flow and energy release are ranked high (see R63). These phenomena determine the upstream conditions that control the ADS stage 1, 2, and 3 mass flow and energy release rates.
R78	Steam generator heat transfer is ranked low during the ADS blowdown phase. The RCS energy balance is controlled by decay heat addition and ADS energy removal. The steam generators are essentially thermally-decoupled from the RCS because the affected steam generator is dry and fluid in the unaffected secondary system is significantly hotter than the fluid in the RCS.
R79	In the upper plenum, entrainment/de-entrainment is ranked medium during the ADS blowdown phase. During this phase, the ADS mass flow and energy release are ranked high (see R63). This phenomenon has a major influence on the upstream conditions that control the mass flow and energy release rates from all ADS stages.
R80	Flashing in the core and upper plenum/upper head is ranked medium during the ADS blowdown phase. This flashing will affect the RCS mass and energy distributions. Flashing will be preferential and the warmest RCS fluid will reside in the core and upper head/upper plenum regions.
R81	ADS mass flow and energy release are ranked high, ADS flow resistance is ranked medium, and ADS noncondensible effects are ranked low during the IRWST and sump injection phase. The ADS mass and energy flow rates directly affect the differential pressure between the RCS and the containment. The ADS flow resistance affects the mass and energy flow rates. Noncondensibles affect the ADS mass and energy flows, but to a lesser extent than during the previous phase (where they were ranked medium, see R63). Peak flow of noncondensibles from the accumulators into the RCS occurs during the ADS blowdown phase.
R82	In the cold legs, condensation and noncondensible effects are ranked low for the IRWST and sump injection phase. The cold legs are expected to be an inactive RCS region during this phase. However, these phenomena were left on the list because of the possibility for effects due to: (1) condensation of steam (entering this region through the reactor vessel upper head/downcomer bypass path), and (2) large expansions of nitrogen (caused by total depressurization of the RCS).

Table D-6. (continued).

Ranking rationale for the phenomena in Tables D-1 through D-5

Code	Ranking Rationale
R83	Two-phase mixture level in the core is ranked high during the IRWST and sump injection phase. The two-phase mixture level determines the status of core coolability and affects the differential pressure between the RCS and the containment (see R67). The core flow resistance is ranked medium during the IRWST and sump injection phase. This resistance affects the RCS-to-containment differential pressure, but to a lesser extent than does the mixture level.
R84	Downcomer level is ranked high during the IRWST and sump injection phase. This level is the driving force for flow through the core. The static head created by this level is a significant term affecting the RCS/containment pressure balance.
R85	Condensation in the downcomer is ranked medium during the IRWST and sump injection phase. Steam may flow through the upper head/downcomer bypass path. If condensation is present, it can alter the high-ranked downcomer level (see R84).
R86	Phase separation in tees in the hot leg is ranked high during the IRWST and sump injection phase. Separation at the ADS fourth stage tees determines the energy and content of the fluid mixture that is routed through the ADS.
R87	CCFL and countercurrent flow in the hot leg are ranked medium during the ADS blowdown and IRWST and sump injection phases. These phenomena contribute to the highly-ranked hot leg phase separation process (see R86) because they affect the fluid state and flow regime in the hot leg.
R88	Horizontal fluid stratification in the hot legs is ranked medium during the IRWST and sump injection phase. Fluid conditions during this phase may be quiescent, and in that case the hot leg would stratify. Whether or not the hot leg fluid stratifies has a direct influence on the phase separation in the hot leg tees (ranked high, see R86) and the state of the mixture being passed on to the all ADS stages.
R89	Not used.
R90	IRWST pool thermal stratification, pool level, and flow resistance are ranked medium during the IRWST and sump injection phase. Stratification affects the injection temperature (the fluid present at the bottom of the tank is injected). Level provides the driving force to push the injection flow through the total resistance (the IRWST piping system flow resistance is an important part of the total). Therefore, the IRWST pool level and flow resistance directly affect the injection flow rate.
R91	Not used.
R92	Heat transfer between the PRHR and IRWST is ranked low during the IRWST and sump injection phase. The potential for this heat transfer remains, via condensation of steam on the inside of the PRHR tubes. However, the energy removal from the RCS is expected to be dominated by the ADS fourth stage during this phase.
R93	Steam generator heat transfer is ranked low during the ADS blowdown and IRWST and sump injection phases. During these phases, the RCS energy balance is controlled by decay heat addition and ADS energy removal. The steam generators are essentially thermally-decoupled from the RCS because the affected steam generator is dry and fluid in the unaffected steam generator secondary is significantly hotter than fluid in the RCS.

Table D-6. (continued).

Ranking rationale for the phenomena in Tables D-1 through D-5

Code	Ranking Rationale
R94	Sump fluid temperature, level, and flow resistance are ranked medium during the IRWST and sump injection phase. The sump fluid temperature is the RCS injection temperature (the fluid present at the bottom of the sump is injected). The sump level provides the driving force to push the injection flow through the total resistance (the sump piping system flow resistance is an important part of the total). Therefore, all these phenomena contribute to the determination of the injection flow rate and temperature.
R95	Entrainment/de-entrainment in the upper plenum is ranked high during the IRWST and sump injection phase. This phenomenon affects the state of the fluid entering the hot leg (that, in turn, affects the state of fluid entering the ADS fourth stage). It also affects the pressure drop between the core and hot legs.
R96	Not used.
R97	Condensation, natural convection, noncondensible effects, noncondensible segregation, steam-noncondensible mixing, and nonuniform air/steam distribution in the containment interior are all ranked medium during the IRWST and sump injection phase. These phenomena determine the containment pressure and the heat transfer processes on the inside of the containment shell, a phenomenon that is ranked high. Wall condensation is the primary heat transfer mechanism on the inside of the shell. Natural convection is the process inside the containment by which steam is transported from its source (i.e., the top of the IRWST, or ADS stage 4) to the shell. Noncondensible effects may impede the flow of heat from the containment atmosphere to the inner surface of the shell, and the condensation process may cause noncondensible gases to build up near the shell (noncondensible segregation), a process that may starve the shell inner wall heat transport process of steam. Steam-noncondensible mixing, and nonuniform air/steam distribution are phenomena indicating that mixture irregularities of the steam and noncondensible gases may be significant to the inner-shell heat removal processes.
R98	Condensate transport, liquid holdup, and liquid distribution in the containment interior are ranked medium during the IRWST and sump injection phase. These phenomena contribute to the disposition of liquid within the containment. Liquid that is returned to the IRWST or sump is available for injection into the RCS. Liquid escaping that return is not available for that purpose; examples include: liquid inventory stored on the containment shell during normal operation of the passive containment cooling heat removal system and liquid that becomes trapped in other containment regions (such as in the reactor vessel cavity).
R99	The passive heat sink in the containment interior is ranked medium during the IRWST and sump injection phase. The passive heat sink provided by the containment walls and interior structures represents a significant contribution to the containment energy balance during transients.
R100	PCCS evaporation, PCCS mixture convective heat transfer, PCCS water flow, air flow, and chimney effects on the containment exterior are all ranked medium during the IRWST and sump injection phase. These phenomena contribute to the containment shell exterior-to-ambient heat transfer that is ranked high (see R114). PCCS water will be sprayed on the outer containment shell surface. This water will flow downward on the outside of the shell and heat will be removed to upwardly-flowing air. Heat transfer mechanisms from the wall will include conduction and convection to water, evaporation of the water, and convection to the upward-flowing air.

Table D-6. (continued).

Ranking rationale for the phenomena in Tables D-1 through D-5

Code	Ranking Rationale
R101	In addition to the phenomena described in R100, the following containment exterior phenomena are ranked medium during the IRWST and sump injection phase: atmospheric temperature, humidity, PCCS wetting, and radiation heat transfer. These phenomena also contribute to the containment shell exterior-to-ambient heat transfer that is ranked high (see R114). The atmospheric temperature is that to which the containment shell exterior heat transfer takes place. The humidity present in the air determines the efficiency of the evaporation process. PCCS wetting effects may alter the effective heat transfer area (if water rivulets form, then evaporation may take place only on the outer shell regions covered by them). Radiation from the outer shell wall to the air and from the outer shell wall to the containment support structure (across the air-flow annulus), may be a significant heat transfer mechanism.
R102	Not used.
R103	Stored energy release in the cold legs, core (non-fuel structures), downcomer/lower plenum, fuel rods, hot legs, and upper head/upper plenum is ranked low during the initial depressurization phase. This phenomenon represents the removal, to the RCS fluid, of heat stored in the piping walls and other structures during normal reactor operation. The low ranking indicates this phenomenon has a smaller influence on the RCS energy balance than do the other contributors to that balance: core decay power (as distinguished from release of the initial fuel stored energy), steam generator heat transfer, and the PRHR-to-IRWST heat transfer.
R104	Loop asymmetry effects in the cold legs, downcomer/lower plenum, hot legs, and upper plenum are ranked medium during the passive decay heat removal phase. The rationales for these rankings are the same as described in R45 and R47.
R105	Flow resistance in the reactor coolant pumps is ranked low during both the initial depressurization and passive decay heat removal phases. Following the pump coastdown, the locked-rotor resistance of the pump is a significant portion of the total flow resistance through the RCS loops. Therefore, this resistance affects the RCS coolant loop natural circulation flow rates and, thereby, heat exchange between the RCS and the affected and unaffected steam generators. This flow resistance is also present in the PRHR system flow loop; however, total resistance through this flow loop is instead dominated in the PRHR piping and heat exchanger.
R106	Not used.
R107	The core flow resistance is ranked low during the passive residual heat removal and CMT draining-to-ADS actuation phases. This phenomenon affects PRHR-to-IRWST heat transfer through its influence on the PRHR system natural circulation flow rate. However this influence is less than that of the PRHR system flow resistance.
R108	In the CMT component, flow resistance is ranked low during the passive decay heat removal phase. This flow resistance is dominated in the CMT discharge lines, that include both orifices and check valves. This phenomenon influences the RCS energy balance through its effect on the CMT recirculation rate.
R109	Interphase condensation and pool flow in the IRWST are ranked low during the passive decay heat removal and CMT draining-to-ADS actuation phases. These phenomena affect PRHR-to-IRWST heat transfer through their influences on the flow and temperature distributions in the PRHR bundle region (this phenomenon is ranked medium, see R38).

Table D-6. (continued).

Ranking rationale for the phenomena in Tables D-1 through D-5

Code	Ranking Rationale
R110	The PRHR flow resistance is ranked medium during the passive decay heat removal and CMT draining-to-ADS actuation phases. The flow resistance through the entire PRHR primary-system cooling loop is dominated by components within the PRHR system itself (piping, fittings, and heat exchanger) and not in the associated RCS components. The PRHR flow resistance determines the PRHR system natural circulation flow rate and, thereby, affects PRHR-to-IRWST heat transfer (by influencing the tube inner surface convective thermal resistance).
R111	Not used.
R112	Discharge line flashing in the IRWST and sump injection lines is ranked medium during the IRWST and sump injection phase. The temperatures of the injection fluids will depend upon behavior within the IRWST and containment. It is not known if fluid in these lines will flash. However, if the fluid does flash, then the injection rate may be significantly affected by the increased injection-line pressure drop.
R113	Heat transfer between the IRWST fluid and the tank walls is ranked low during the IRWST and sump injection phase. The energy loss via this phenomenon is expected to be much smaller than the other terms involved in the containment energy balance.
R114	During the IRWST and sump injection phase, the overall containment shell interior and exterior heat transfer represent the removal of decay heat to the ultimate heat sink and are, therefore, ranked high.
R115	During the ADS blowdown phase, containment phenomena impact the containment pressure response, which affects the timing of IRWST injection. Little analysis is available to support the relative phenomena rankings. The PIRT committee ranked the overall heat transfer on the interior and exterior surfaces of the containment shell medium, along with the expected heat transfer processes on those surfaces (condensation on the inside and PCCS evaporative cooling on the outside). In addition, passive heat sink is ranked medium because the effects of wall heat transfer (containment shell, structural walls, and internal equipment) are expected to be important during this phase because the fluid-to-wall temperature differentials are large. The other containment-related phenomena are ranked low.

Appendix E - Detailed Results, Steam Generator Tube Rupture Without ADS PIRT

This appendix presents the detailed results of the steam generator tube rupture (SGTR) sequence without Automatic Depressurization System (ADS) activation PIRT. The detailed PIRT results are shown in Tables E-1 and E-2, and the transient description, overall phenomena ranking criteria, and specific ranking rationales are shown in Table E-3. The information in Tables E-1 and E-2 is arranged to correspond with the two phases of the accident scenario. These tables are organized in alphabetical order according to the component name. Within the listings for each component, the pertinent identified phenomena are arranged by order of ranking. The right sides of these tables contain identifier codes that refer the reader elsewhere in this report for further information:

The code labeled "Ranking Rationale" (for example, "R1") leads the reader to a description of the logic leading to the ranking of each specific phenomenon; this information is found in Table E-3 in this appendix.

The code labeled "Phenomena Description" (for example, "D1") leads the reader to a general description of each phenomenon; this information is found in Appendix G, Table G-1.

Two codes are labeled "Type Geometry" (for example "C1/G1"). The "C" code leads the reader to the physical geometries and general functions of the component under discussion; this information is found in Appendix G, Table G-2. The "G" code leads the reader to more detailed discussion of the specific phenomena associated with each of the components; this information is found in Appendix G, Table G-3.

The "Supporting Evidence" code (for example, "E1") leads the reader to references (geometrical, experimental, and analytical) that provide background and corroborating information. This information is found in Appendix G, Table G-4. It is noted that the supporting evidence is currently being developed in experimental and analytical tasks both inside and outside the PIRT task. Thus, the information in this table can be expected to increase as the supporting tasks are completed.

The "Sublevel Phenomena" code (for example, "S1") leads the reader to a list of contributing phenomena affecting the primary phenomenon. The sublevel phenomena information is found in Appendix G, Table G-5.

Table E-1. PIRT for the initial depressurization phase of a single SGTR.

			For codes shown in these columns, See Tables:				
			E-3	G-1	G-2/G-3	G-4	G-5
Component	Phenomena	Rank	Ranking Rationale	Phenomena Description	Type Geometry	Supporting Evidence	Sublevel Phenomena
Break (single SG tube, two break paths)	Choking in complex geometries	H	R11	D6	C3	E1	S66
	Mass flow	H	R1	D46	C3/G6	E1	S1
	Energy release	M	R2	D19	C3/G6	E1	S1
	Flow resistance	M	R7	D27	C3/G6	E1	S11
Fuel rods	Core power/decay heat	H	R3	D12	C8/G20	E1	S4
	Stored energy release	L	R4	D68	C8/G21	E1	S2
Pressurizer	Flashing	H	R5	D21	C14/G33	E1	S5
	Heater power	H	R5	D34	C14/G35	E1	S49
	Level (inventory)	H	R5	D39	C14/G33	E1	S13
	Vapor space behavior	H	R5	D77	C14/G33	E1	S60
	Noncondensible effects	L	R6	D50	C14	E1	S12
	Stored energy release	L	R4	D68	C14/G35	E1	S2
Steam generators	Primary to secondary heat transfer	H	R8	D33	C16/G39	E1	S53
	Secondary pressure	M	R10	D64	C16/G39	E1	S17
	SRV energy release	M	R9	D65	C16/G44	E1	S51
	SRV mass flow	M	R9	D66	C16/G44	E1	S50

Table E-2. PIRT for the passive decay heat removal phase of a single SGTR.

			For codes shown in these columns, See Tables:				
			E-3	G-1	G-2/G-3	G-4	G-5
Component	Phenomena	Rank	Ranking Rationale	Phenomena Description	Type Geometry	Supporting Evidence	Sublevel Phenomena
Break (single SG tube, two break paths)	Choking in complex geometries	H	R11	D6	C3	E1	S66
	Energy release	H	R17	D19	C3/G6	E1	S1
	Mass flow	H	R17	D46	C3/G6	E1	S1
	Flow resistance	M	R7	D27	C3/G6	E1	S11
Cold legs	Stored energy release	L	R14	D68	C4/G7	E1	S2
Core	Subcooling margin	M	R13	D69	C5	E1	S52
	Flow resistance	L	R12	D27	C5/G12	E1	S11
	Stored energy release	L	R14	D68	C5/G11	E1	S2
CMT	CMT-to-loop differential density	M	R15	D17	C6/G13	E1	S10
	Thermal stratification	M	R15	D73	C6/G14	E1	S19
	Level	M	R16	D39	C6/G14	E1	S13
	Flow resistance	L	R31	D27	C6/G13	E1	S11
Downcomer/ lower plenum	Stored energy release	L	R14	D68	C7/G15	E1	S2
Fuel rods	Decay heat	H	R18	D12	C8/G20	E1	S4
	Stored energy release	L	R14	D68	C8/G21	E1	S2
Hot legs	Flashing	M	R19	D21	C9	E1	S5
	Loop asymmetry effects	M	R19	D45	C9/G23		S9
	Voiding	M	R19	D78	C9/G25	E1	S54
	Stored energy release	L	R14	D68	C9/G22	E1	S52
IRWST	Flow & temperature distribution in PRHR bundle region	M	R20	D23	C10/G26	E1	S24
	Pool level	M	R20	D58	C10/G26	E1	S25
	Pool thermal stratification	M	R20	D59	C10/G26	E1	S19
	Interphasic condensation	L	R32	D37	C10/G29	E1	S18

Table E-2. (continued).

			For codes shown in these columns, See Tables:				
			E-3	G-1	G-2/G-3	G-4	G-5
Component	Phenomena	Rank	Ranking Rationale	Phenomena Description	Type Geometry	Supporting Evidence	Sublevel Phenomena
IRWST, Continued	Pool flow	L	R32	D57	C10/G26	E1	S24
Pressurizer	Flashing	M	R38	D21	C14/G33	E1	S5
	Level (inventory)	M	R38	D39	C14/G33	E1	S13
	Noncondensible effects	L	R6	D50	C14	E1	S12
PRHR	Heat transfer between PRHR and IRWST	H	R23	D32	C12/G30	E1	S28
	Condensation	M	R20	D9	C12/G30	E1	S18
	Differential density	M	R20	D17	C12/G30	E1	S10
	Flow resistance	M	R20	D27	C12/G30	E1	S11
	Noncondensible effects	M	R25	D50	C12/G31	E1	S12
	Voiding	M	R20	D78	C12/G31	E1	S54
Pumps	Coastdown performance	L	R33	D7	C15/G37	E1	S14
	Flow resistance	L	R26	D27	C15/G38	E1	S15
Steam generators	Primary to secondary heat transfer	H	R28	D33	C16/G39	E1	S53
	SRV energy release	H	R27	D65	C16/G44	E1	S51
	SRV mass flow	H	R27	D66	C16/G44	E1	S50
	Secondary level	M	R29	D63	C16/G39	E1	S7
	Secondary pressure	M	R29	D64	C16/G39	E1	S17
	Tube voiding	M	R29	D75	C16/G39	E1	S16
	Condensation in U-tubes	L	R24	D9	C16/G39	E1	S18
Upper head / upper plenum	Flashing	M	R30	D21	C18/G45	E1	S5
	Loop asymmetry effects	M	R34	D45	C18/G46	E1	S9
	Stored energy release	L	R14	D68	C18/G47	E1	S2

Table E-2. (continued).

			For codes shown in these columns, See Tables:				
			E-3	G-1	G-2/G-3	G-4	G-5
Component	Phenomena	Rank	Ranking Rationale	Phenomena Description	Type Geometry	Supporting Evidence	Sublevel Phenomena
Containment (interior)	Interior to wall heat transfer	H	R36	D86	C19/G48	E1	S72
	Condensate transport	M	R35	D8	C19/G48	E1	S37
	Condensation	M	R35	D9	C19/G48	E1	S18
	Liquid distribution	M	R35	D43	C19/G48	E1	S38
	Liquid holdup	M	R35	D44	C19/G48	E1	S38
	Natural convection	M	R36	D48	C19/G48	E1	S12
	Noncondensible effects	M	R36	D50	C19/G49	E1	S12
	Noncondensible segregation	M	R36	D84	C19/G49	E1	S71
	Nonuniform steam/air distribution	M	R36	D51	C19/G49	E1	S35
	Steam-noncondensible mixing	M	R36	D67	C19/G49	E1	S68
	Passive heat sink	M	R36	D81	C19/G48	E1	S67
Containment (exterior)	Exterior to ambient heat transfer	H	R37	D83	C20/G50	E1	S70
	Air flow	M	R37	D82	C20/G50	E1	S69
	Atmospheric temperature	M	R37	D2	C20/G50	E1	S43
	Chimney effects	M	R37	D5	C20/G50	E1	S41
	Humidity		R37	D36	C20/G50	E1	S46
	PCCS evaporation	M	R37	D52	C20/G50	E1	S39
	PCCS mixture convective heat transfer	M	R37	D54	C20/G50	E1	S30
	PCCS water flow	M	R37	D53	C20/G50	E1	S40
	PCCS wetting	M	R37	D55	C20/G50	E1	S42
	Radiation heat transfer	M	R37	D62	C20/G50	E1	S45

Table E-3. Transient description and ranking rationale for the single-SGTR PIRT.

Overall Transient Description and Top-level Ranking Rationale

This sequence is initiated by a double-ended rupture of a single steam generator (SG) tube at the tubesheet, with no additional failures. Subsequent plant response is assumed to be within the design goal that the active fuel remains covered throughout the transient with eventual recovery to a long term quasi-steady condition that does not require ADS actuation. The availability only of safety-grade plant systems is assumed. Although core uncovery is assumed to be avoided, a radioactive release to the atmosphere occurs through the SG secondary safety relief valves (SRVs). One of the primary purposes of the PIRT is to ensure that the analysis code(s) have adequate modeling capabilities for simulating the vessel inventory and release responses. The important hierarchical elements in the code assessment structure are those affecting vessel inventory and release rate as described below.

Phase Descriptions and Medium-level Ranking Rationales

Initial Depressurization Phase:

Description - This phase begins at the time of the tube rupture, when two break paths are opened between the RCS and the affected SG secondary system. The flow through the tubesheet-side break is much larger than that through the longer tube-side break. The feedwater control system reduces the feedwater flow rate to compensate for the break flow, and initially the affected SG secondary level does not increase. The pressurizer heater power increases to compensate for declining RCS pressure, and this effect slows the rate of RCS depressurization. The break in the RCS boundary causes the pressurizer level to decline and the pressurizer gas bubble to expand. The RCS pressure eventually falls to the reactor trip low setpoint pressure. This occurrence results in scram control rod insertion and turbine stop valve closure. Reactor power is quickly reduced to the decay heat rate, causing RCS temperatures to fall, its fluid to shrink and, therefore, its depressurization rate to increase. Affected SG SRV opening causes a release of radioactivity to the atmosphere, and elimination of this release is the key to a satisfactory outcome for this event sequence. Break flow and fluid shrinkage effects cause the RCS pressure to continue falling to the S signal setpoint pressure; this occurrence marks the end of this phase.

Important parameters and dominant processes - RCS pressure is judged to be the parameter of primary importance for this phase because it determines the flow rate from the RCS to the affected SG secondary system through the ruptured tube. The processes important for accurate simulation of this parameter are: gas bubble expansion, net RCS mass and energy balances, critical flow through the broken SG tube, and transient pressurizer inventory.

Passive Decay Heat Removal Phase:

Description - This phase begins at the time of the S signal, an occurrence that causes PRHR and CMT system actuations, reactor coolant pump trip, and feedwater isolation. The RCS loop flows decline rapidly from a forced-circulation to a natural-circulation condition. The affected SG inventory increases as a result of flow through the ruptured tube; this flow also sustains the affected SG secondary pressure near the SRV opening setpoint pressure. The combination of CMT system recirculation, energy release through the affected SG SRVs, and PRHR system operation removes core decay heat from the RCS. The performance of the CMT system eventually degrades as fluid in the CMT tanks is warmed. Eventually, CMT recirculation may be interrupted by flashing in the CMT or its inlet line. However, CMT levels are assumed not to decline significantly, and, therefore, ADS is assumed not initiated for this event sequence. The PRHR system eventually becomes the sole RCS core decay heat removal mechanism. IRWST tank thermal stratification has the potential to degrade PRHR performance. When the PRHR system is capable of removing all core decay heat at an RCS pressure below the opening set-point pressure of the affected

Table E-3. (continued).

SG SRVs, the break and SRV flows cease. Afterward, the SRVs remain closed, and the radiation release is terminated. Long-term decay heat removal from the containment to environment is accomplished across the containment shell. Steam boiled off from the IRWST is returned to the IRWST as condensate from the containment shell.

Important parameters and dominant processes - RCS pressure is judged to be the parameter of primary importance for this phase because it determines the duration and magnitude of the atmospheric release through the SG SRVs. The processes important for accurate simulation of this parameter are: core, SG, PRHR, and containment shell heat transfer, natural circulation flow in the RCS coolant loops, loop asymmetries, and SG SRV critical flow.

Detailed Phenomena Ranking Rationales

Ranking rationale for the phenomena in Tables E-1 and E-2

Code	Ranking Rationale
R1	Break mass flow is ranked high during the initial depressurization phase. This phenomenon is the outflow term in the RCS mass balance. The pressurizer level falls because of the net outflow of coolant from the RCS. The expansion of the pressurizer gas bubble determines the RCS pressure, the parameter of primary importance during this phase.
R2	Break energy release is ranked medium during the initial depressurization phase. The break energy release was judged less significant than the break mass flow (see R1). While energy is removed at the break, for a SGTR, the break size is small, and the influence of the break on the RCS energy balance is smaller than other contributors (heat addition from the core fuel rods and heat removal to the steam generators, see R3 and R8).
R3	Fuel rod core power/decay heat is ranked high during the initial depressurization phase. This phenomenon is the major heat addition term in the RCS energy balance. In addition, removal of this heat is a basic safety issue.
R4	Stored energy releases to RCS fluid from the fuel rods and pressurizer tank wall are ranked low during the initial depressurization phase. Significant energy is stored in the fuel rods during normal reactor operation. This energy is retained in the fuel rods prior to the time of reactor trip. After reactor trip, most of the initial fuel rod stored energy is quickly removed to the RCS coolant. Since this effect is temporary, fuel rod stored energy release was judged less significant to the RCS energy balance than the continuous fuel rod core power/decay heat phenomenon (that is ranked high, see R3). Stored energy release from the pressurizer vessel wall to fluid inside the pressurizer has a minor influence on the pressurizer gas bubble expansion process that controls RCS pressure during this phase.
R5	Not used.
R6	Noncondensible effects in the pressurizer are ranked low during the initial depressurization and passive decay heat removal phases. Hydrogen gas will evolve from solution during depressurization of the RCS. Accumulations of hydrogen in the pressurizer affect the species of gas in the pressurizer bubble; expansion/contraction of this bubble controls the RCS pressure.

Table E-3. (continued).

Ranking rationale for the phenomena in Tables E-1 and E-2

Code	Ranking Rationale
R7	Break flow resistance is ranked medium during the initial depressurization and passive decay heat removal phases. This phenomenon affects the highly-ranked break mass flow. Flow through both break paths is at first dominated by critical flow (see R11). The flow resistance affects the critical flow, particularly through the longer break path. As the RCS depressurizes and the affected SG secondary system pressurizes, flows through these break paths unchoke and become dominated by frictional flow resistance considerations.
R8	Steam generator primary-to-secondary heat transfer is ranked high during the initial depressurization phase. This phenomenon is the major heat removal term in the RCS energy balance.
R9	Steam generator safety relief valve (SRV) mass flow and energy release are ranked medium during the initial depressurization phase. Existing analyses are insufficient to indicate whether the SRVs will be opened during this phase. While awaiting this indication, these phenomena are assigned a medium ranking to show their potential importance.
R10	Steam generator secondary pressure is ranked medium during the initial depressurization phase. The break flow is delivered against the affected steam generator secondary pressure, and this pressure also determines if the safety relief valves are opened. The pressures in the steam generator secondary systems determine the secondary-side saturation temperatures affecting heat exchange between the RCS and the steam generators.
R11	Choking in complex geometries is ranked high during the initial depressurization and passive decay heat removal phases. This phenomenon determines the highly-ranked break mass flow for both break flow paths prior to the time when these paths unchoke (see R7). Choking was ranked high (in comparison with the frictional resistance that is ranked medium) because the modeling of critical flow processes in the unique geometries associated with broken steam generator tubes is particularly uncertain.
R12	Core flow resistance is ranked low during the passive decay heat removal phase. A large portion of the total resistance to RCS loop natural circulation flow resides in the core. This phenomenon therefore affects the RCS loop flow rate. Although this resistance is also present for PRHR system loop flow, the resistance for that loop is dominated within the PRHR system itself (the PRHR system has a much lower design flow rate than do the RCS loops).
R13	Subcooling margin is ranked medium during the passive decay heat removal phase. This ranking indicates the importance of: (1) core coolability and (2) the effects of core void generation on PRHR system heat removal and RCS depressurization.
R14	Stored energy release to the RCS fluid from structures in the core, fuel rods, cold legs, downcomer/lower plenum, hot legs, and upper head/upper plenum is ranked low during the passive decay heat removal phase. Heat that is initially stored in these structures during normal reactor operation is released into the RCS as it depressurizes and cools. However, these releases are judged to be less significant contributors to the RCS energy balance than are the core decay power heat source and the CMT, steam generator, and PRHR system heat sinks (see R18, R15, R28, and R23, respectively).

Table E-3. (continued).

Ranking rationale for the phenomena in Tables E-1 and E-2

Code	Ranking Rationale
R15	In the CMT component, CMT-to-loop differential density and thermal stratification are ranked medium during the passive decay heat removal phase. These phenomena directly influence CMT recirculation and its effectiveness as an RCS heat sink. This heat sink is an important contributor to the RCS energy balance until the time when CMT recirculation is interrupted. The differential density is the driving force for CMT recirculation. Thermal stratification affects this driving force, the manner in which CMT recirculation is interrupted, and the temperature of fluid discharged from the CMTs.
R16	CMT level is ranked medium during the passive decay heat removal phase. This SGTR accident scenario assumes the CMT level will not fall to the low-level setpoint that initiates ADS. This phenomenon is included here only to assure that the appropriateness of this assumption is later considered.
R17	Break energy release and mass flow are ranked high during the passive decay heat removal phase. These phenomena affect the RCS pressure response. Flow from the RCS to affected steam generator secondary system through the two break paths may be dominated by critical or friction-dominated processes (see R7 and R11).
R18	Fuel rod decay heat is ranked high during the passive decay heat removal phase. This phenomenon is the major heat addition term in the RCS energy balance, and removal of this heat is a basic safety issue.
R19	Flashing, loop asymmetry effects, and voiding in the hot legs are ranked medium during the passive decay heat removal phase. Hot leg behavior is of significance because fluid conditions in this component determine the conditions of fluids entering the break, steam generators, and PRHR system. Of particular importance is the steam content of the hot leg fluid, as this affects break flow and PRHR heat removal. Steam may be produced in the core and passed into the hot leg, or it may be generated by flashing within the hot legs. If the hot legs become sufficiently voided, then pure steam may be passed to the steam generators and PRHR system. Loop asymmetry effects may be present because the break, PRHR system, and CMT system each are located on only one coolant loop. Therefore, plant response may be sensitive to which steam generator is assumed to contain the tube rupture. Existing analyses are insufficient to indicate whether these phenomena will be important during this phase. While awaiting this indication, these phenomena are assigned a medium ranking to show their potential importance.

Table E-3. (continued).

Ranking rationale for the phenomena in Tables E-1 and E-2

Code	Ranking Rationale
R20	In the IRWST component, pool level, flow and temperature distribution in the PRHR bundle region, and pool thermal stratification are ranked medium during the passive decay heat removal phase. In the PRHR component, condensation, differential density, flow resistance, and voiding are ranked medium during the passive decay heat removal phase. These phenomena all contribute to the PRHR-to-IRWST heat transfer process. The convective thermal resistance on the PRHR tube inner surface is sensitive to (among other things) the presence or absence of the condensation process. On the PRHR tube outer surface, the convective thermal resistance is sensitive to the flow rate through the PRHR tube bundle region in the IRWST. Reduced IRWST pool levels (due to boil-off) can lower the usable PRHR bundle heat transfer area; the initial IRWST pool level is only slightly above the elevation span of the upper horizontal PRHR tube bundle region. Pool thermal stratification affects the heat sink temperature for the PRHR tube outer surface and the vertical distribution of that temperature. The differential density (i.e., the difference in density between the fluid in the inflow and outflow sides of the PRHR system piping) is the driving force for flow through the primary side of the PRHR system. The flow resistance of the PRHR system (including the entire flow loop through the core) balances the driving force created by the differential density. The voiding from noncondensible gas (see R25) accumulated at the high point of the PRHR inlet line (it is an inverted trap configuration) may block the path for flow through the PRHR heat exchanger.
R21	Not used.
R22	Not used.
R23	Heat transfer between the PRHR and IRWST is ranked high during the passive decay heat removal phase. This phenomenon represents the only means by which decay heat may be removed from the RCS to the containment. PRHR heat transfer also is the only continuous RCS decay heat removal mechanism during this phase.
R24	Condensation in the steam generator U-tubes is ranked low during the passive decay heat removal phase. This phenomenon can remove steam void from the U-tubes (see R29). Wall condensation inside the tubes can be caused by heat transfer to the steam generator secondary. Interphase condensation inside the tubes can be caused by flow of cold water into the U-tubes from the PRHR discharge.
R25	Noncondensible effects in the PRHR are ranked medium during the passive decay heat removal phase. Hydrogen gas will evolve from solution during the depressurization of the RCS. The presence of this gas inside the PRHR tube can degrade the heat transfer process on the tube inner surface. Voiding from noncondensible gas accumulated at the high point of the PRHR inlet line (its configuration includes an inverted trap) may block the path for flow through the PRHR heat exchanger.

Table E-3. (continued).

Ranking rationale for the phenomena in Tables E-1 and E-2

Code	Ranking Rationale
R26	The pump flow resistance is ranked low during the passive decay heat removal phase. Here the pump flow resistance is the locked-rotor resistance that is present following the pump coastdown period (see R33). The pump resistance influences steam generator heat transfer through its effect on the natural circulation flows through the RCS loops (i.e., through the core, hot legs, steam generators, pumps, and cold legs). For the RCS loops, the pump flow resistance is a significant fraction of the total loop resistance. The pump resistance also influences PRHR-to-IRWST heat transfer through its effect on the flow through the PRHR system natural circulation loop (i.e., through the core, hot leg, PRHR inlet, PRHR heat exchanger, PRHR outlet, pump, and cold leg). For the PRHR system loop, the pump resistance is only a small fraction of the total loop resistance.
R27	Steam generator safety relief valve (SRV) energy release and mass flow are ranked high during the passive decay heat removal phase. When the SRVs are open, fluid is released from the affected steam generator secondary system to the atmosphere. This fluid contains radioactivity that was previously passed from the RCS into the affected secondary system through the break. To terminate the atmospheric release, the RCS pressure must, therefore, be maintained below the lowest SRV opening setpoint pressure. SRV flow removes both mass and energy from the coupled RCS-affected steam generator system. Because the SRV downstream pressure is atmospheric, flow through this path will be dominated by critical flow processes.
R28	Steam generator primary-to-secondary heat transfer is ranked high during the passive decay heat removal phase. Heat exchanges between the RCS and both steam generators influence the RCS pressure because they are major terms in the RCS energy balance. The possibility exists for reverse (i.e., secondary-to-primary) heat transfer.
R29	Steam generator secondary level and pressure, and voiding inside u-tubes, are ranked medium during the passive decay heat removal phase. Steam generator secondary pressure determines the saturation temperature that is the heat sink for primary-to-secondary heat transfer (see R28). Steam generator secondary level influences that heat transfer through its effect on the convective thermal resistance on the outside of the u-tubes. Tube regions not submerged under the level do not efficiently transfer heat. The level response in the affected steam generator is particularly uncertain because its inventory is gained through the two break paths but may be lost through the safety relief valves. Voiding inside the u-tubes influences primary-to-secondary heat transfer through its effect on the convective thermal resistance on the inside of the u-tubes. If the void is from steam, then the resistance may be low, due to wall condensation heat transfer (also see R24). However, if the void is from noncondensible gas, the resistance may be high. Hydrogen gas evolves from solution in the RCS fluid during depressurization; this gas can degrade the heat transfer process on the inner u-tube walls. Voiding from noncondensible gas accumulated at the u-tube high points may block the path for flow through the tubes.
R30	Flashing in the reactor vessel upper head is ranked medium during the passive decay heat removal phase. This region is prone to flash as the RCS is depressurized, and the bubble created there cannot be readily collapsed. This phenomenon therefore affects the RCS pressure response.

Table E-3. (continued).

Ranking rationale for the phenomena in Tables E-1 and E-2

Code	Ranking Rationale
R31	The CMT flow resistance is ranked low during the passive decay heat removal phase. This phenomenon affects the CMT recirculation rate and, therefore, the period when the CMTs are effective RCS heat sinks. Following termination of recirculation and if draining occurs, this phenomenon affects the CMT draining rate. See R15 and R16 for more discussion of CMT behavior.
R32	Interphasic condensation and pool flow in the IRWST are ranked low during the passive decay heat removal phase. These phenomena affect the flow and temperature distributions in the PRHR bundle region of the IRWST (ranked medium, see R20). IRWST pool flow refers to natural convection flows in the large tank region away from the PRHR bundle. Interphasic condensation refers to the collapse of bubbles formed due to boiling on the outside of the PRHR tubes. This condensation may take place either in the pool bundle region or elsewhere in the pool.
R33	Pump coastdown performance is ranked low during the passive decay heat removal phase. The reactor coolant pump coastdown behavior influences the RCS energy balance because it determines flows through the steam generator and PRHR system tubes. However, this effect is limited because of the short coastdown period (about 2 minutes).
R34	Loop asymmetry effects in the upper plenum are ranked medium during the passive decay heat removal phase. Loop asymmetry effects may be present because the break, PRHR system, and CMT system each are located on only one coolant loop. Therefore, plant response may be sensitive to which steam generator is assumed to contain the tube rupture. Existing analyses are insufficient to indicate whether these phenomena will be important during this phase. While awaiting this indication, this phenomenon is assigned a medium ranking to show its potential importance.
R35	Condensate transport, condensation, liquid distribution, and liquid holdup in the containment interior are ranked medium during the passive decay heat removal phase. These phenomena influence PRHR-to-IRWST heat transfer (ranked high, see R23) through their effect on the IRWST pool level (see R20).
R36	Containment interior-to-wall heat transfer is ranked high during the passive decay heat removal phase. This phenomenon represents the removal of the reactor decay power from the containment atmosphere to the containment shell. Natural convection, noncondensible segregation, noncondensible effects, nonuniform steam/air distribution, steam-noncondensible mixing, and passive heat sink in the containment interior are ranked medium during the passive decay heat removal phase. These phenomena affect heat transfer processes on the inside surface of the containment shell.
R37	Containment exterior-to ambient heat transfer is ranked high during the passive decay heat removal phase. This phenomenon represents the removal of the reactor decay power from the outer containment shell wall to its ultimate heat sink. The nine other containment-exterior phenomena are ranked medium during the passive decay heat removal phase. These phenomena control the heat transfer processes on the containment shell exterior.
R38	Pressurizer flashing and level (inventory) are ranked medium during the passive decay heat removal phase. These phenomena influence RCS pressure. Flashing affects the pressurizer level and slows RCS depressurization.

Appendix F - Detailed Results, Steam Generator Tube Rupture With ADS PIRT

This appendix presents the detailed results of the steam-generator tube rupture (SGTR) with Automatic Depressurization System (ADS) activation PIRT. The detailed PIRT results are shown in Tables F-1 through F-5, and the transient description, overall phenomena ranking criteria, and specific ranking rationales are shown in Table F-6. The information in Tables F-1 through F-5 is arranged to correspond with the five phases of the accident scenario. These tables are organized in alphabetical order according to the component name. Within the listings for each component, the pertinent identified phenomena are arranged by order of ranking. The right sides of these tables contain identifier codes that refer the reader elsewhere in this report for further information:

The code labeled "Ranking Rationale" (for example, "R1") leads the reader to a description of the logic leading to the ranking of each specific phenomenon; this information is found in Table F-6 in this appendix.

The code labeled "Phenomena Description" (for example, "D1") leads the reader to a general description of each phenomenon; this information is found in Appendix G, Table G-1.

Two codes are labeled "Type Geometry" (for example "C1/G1"). The "C" code leads the reader to the physical geometries and general functions of the component under discussion; this information is found in Appendix G, Table G-2. The "G" code leads the reader to more detailed discussion of the specific phenomena associated with each of the components; this information is found in Appendix G, Table G-3.

The "Supporting Evidence" code (for example, "E1") leads the reader to references (geometrical, experimental, and analytical) that provide background and corroborating information. This information is found in Appendix G, Table G-4. It is noted that the supporting evidence is currently being developed in experimental and analytical tasks both inside and outside the PIRT task. Thus, the information in this table can be expected to increase as the supporting tasks are completed.

The "Sublevel Phenomena" code (for example, "S1") leads the reader to a list of contributing phenomena affecting the primary phenomenon. The sublevel phenomena information is found in Appendix G, Table G-5.

Table F-1. PIRT for the initial depressurization phase of a SGTR with ADS.

			For codes shown in these columns, See Tables:				
			F-6	G-1	G-2/G-3	G-4	G-5
Component	Phenomena	Rank	Ranking Rationale	Phenomena Description	Type Geometry	Supporting Evidence	Sublevel Phenomena
Break (single SG tube, two break paths)	Choking in complex geometries	H	R11	D6	C3	E1	S66
	Mass flow	H	R1	D46	C3/G6	E1	S1
	Energy release	M	R2	D19	C3/G6	E1	S1
	Flow resistance	M	R7	D27	C3/G6	E1	S11
Fuel rods	Core power/decay heat	H	R3	D12	C8/G20	E1	S4
	Stored energy release	L	R4	D68	C8/G21	E1	S2
Pressurizer	Flashing	H	R5	D21	C14/G33	E1	S5
	Heater power	H	R5	D34	C14/G35	E1	S49
	Level (inventory)	H	R5	D39	C14/G33	E1	S13
	Vapor space behavior	H	R5	D77	C14/G33	E1	S60
	Noncondensible effects	L	R6	D50	C14	E1	S12
	Stored energy release	L	R4	D68	C14/G35	E1	S2
Steam generators	Primary to secondary heat transfer	H	R8	D33	C16/G39	E1	S53
	Secondary pressure	M	R10	D64	C16/G39	E1	S17
	SRV energy release	M	R9	D65	C16/G44	E1	S51
	SRV mass flow	M	R9	D66	C16/G44	E1	S50

Table F-2. PIRT for the passive decay heat removal phase of a SGTR with ADS.

			For codes shown in these columns, See Tables:				
			F-6	G-1	G-2/G-3	G-4	G-5
Component	Phenomena	Rank	Ranking Rationale	Phenomena Description	Type Geometry	Supporting Evidence	Sublevel Phenomena
Break (single SG tube, two break paths)	Choking in complex geometries	H	R11	D6	C3	E1	S66
	Energy release	H	R89	D19	C3/G6	E1	S1
	Mass flow	H	R89	D46	C3/G6	E1	S1
	Flow resistance	M	R7	D27	C3/G6	E1	S11
Cold legs	Phase separation in tees	H	R12	D56	C4/G8	E1	S8
	Stored energy release	L	R16	D68	C4/G7	E1	S2
Core	Subcooling margin	M	R14	D69	C5	E1	S52
	Flow resistance	L	R13	D27	C5/G12	E1	S11
	Loop asymmetry effects	L	R15	D45	C5	E1	S9
	Stored energy release	L	R16	D68	C5/G11	E1	S2
CMT	CMT-to-loop differential density	H	R17	D17	C6/G13	E1	S10
	Flow resistance	M	R17	D27	C6/G13	E1	S11
	Thermal stratification	M	R17	D73	C6/G14	E1	S19
Downcomer/ lower plenum	Loop asymmetry effects	M	R15	D45	C7/G16	E1	S9
	Condensation	L	R81	D9	C7/G18	E1	S18
	Stored energy release	L	R16	D68	C7/G15	E1	S2
Fuel rods	Decay heat	H	R18	D12	C8/G20	E1	S4
	Stored energy release	L	R16	D68	C8/G21	E1	S2
Hot legs	Flashing	M	R19	D21	C9	E1	S5
	Loop asymmetry effects	M	R15	D45	C9/G23	E1	S9
	Voiding	M	R19	D78	C9/G25	E1	S54
	Stored energy release	L	R16	D68	C9/G22	E1	S2

Table F-2. (continued).

			For codes shown in these columns, See Tables:				
			F-6	G-1	G-2/G-3	G-4	G-5
Component	Phenomena	Rank	Ranking Rationale	Phenomena Description	Type Geometry	Supporting Evidence	Sublevel Phenomena
IRWST	Flow & temperature distribution in PRHR bundle region	M	R82	D23	C10/G26	E1	S24
	Pool thermal stratification	M	R82	D59	C10/G26	E1	S19
	Interphasic condensation	L	R83	D37	C10/G29	E1	S18
	Pool flow	L	R83	D57	C10/G26	E1	S24
Pressurizer	Flashing	M	R90	D21	C14/G33	E1	S5
	Level (inventory)	M	R90	D39	C14/G33	E1	S13
	Noncondensible effects	L	R6	D50	C14	E1	S12
PRHR	Heat transfer between PRHR and IRWST	H	R22	D32	C12/G30	E1	S28
	Condensation	M	R20	D9	C12/G30	E1	S18
	Differential density	M	R20	D17	C12/G30	E1	S10
	Flow resistance	M	R20	D27	C12/G30	E1	S11
	Noncondensible effects	M	R24	D50	C12/G31	E1	S12
	Voiding	M	R20	D78	C12/G31	E1	S54
Pumps	Coastdown performance	L	R84	D7	C15/G37	E1	S14
	Flow resistance	L	R25	D27	C15/G38	E1	S15
Steam generators	Primary to secondary heat transfer	H	R27	D33	C16/G39	E1	S53
	SRV energy release	H	R26	D65	C16/G44	E1	S51
	SRV mass flow	H	R26	D66	C16/G44	E1	S50
	Secondary level	M	R28	D63	C16/G39	E1	S7
	Secondary pressure	M	R28	D64	C16/G39	E1	S17
	Tube voiding	M	R28	D75	C16/G39	E1	S16
	Condensation in U-tubes	L	R29	D9	C16/G39	E1	S18

Table F-2. (continued).

			For codes shown in these columns, See Tables:				
			F-6	G-1	G-2/G-3	G-4	G-5
Component	Phenomena	Rank	Ranking Rationale	Phenomena Description	Type Geometry	Supporting Evidence	Sublevel Phenomena
Upper head / upper plenum	Flashing	M	R30	D21	C18/G45	E1	S5
	Loop asymmetry effects	M	R85	D45	C18/G46	E1	S9
	Stored energy release	L	R16	D68	C18/G47	E1	S2

Table F-3. PIRT for the CMT draining to ADS actuation phase of a SGTR with ADS.

			For codes shown in these columns, See Tables:				
			F-6	G-1	G-2/G-3	G-4	G-5
Component	Phenomena	Rank	Ranking Rationale	Phenomena Description	Type Geometry	Supporting Evidence	Sublevel Phenomena
Break (single SG tube, two break paths)	Energy release	H	R36	D19	C3/G6	E1	S1
	Mass flow	H	R36	D46	C3/G6	E1	S1
	Choking in complex geometries	M	R36	D6	C3	E1	S66
	Flow resistance	M	R36	D27	C3/G6	E1	S11
Cold legs	PBL-to-cold leg tee phase separation	H	R31	D56	C4/G8	E1	S8
	Loop asymmetry effects	M	R42	D45	C4/G9	E1	S9
	Flashing	L	R32	D21	C4	E1	S5
Core	Flashing	L	R32	D21	C5/G12	E1	S5
	Flow resistance	L	R13	D27	C5/G12	E1	S11
	Loop asymmetry effects	L	R42	D45	C5	E1	S9
	Mass flow, including bypass	L	R33	D46	C5/G10	E1	S3
CMT	Level	H	R34	D39	C6/G14	E1	S13
	Flashing	M	R35	E21	C6/G14	E1	S5
	Condensation	L	R35	D9	C6/G14	E1	S18
	Flow resistance	L	R35	D27	C6/G13	E1	S11
	Thermal stratification	L	R35	D73	C6/G14	E1	S19
Downcomer/ lower plenum	Loop asymmetry effects	M	R42	E45	C7/G16	E1	S9
	Condensation	L	R81	E9	C7/G18	E1	S18
	Level	L	R37	D39	C7/G17	E1	S13
Fuel rods	Decay heat	H	R18	D12	C8/G20	E1	S4
Hot legs	Horizontal fluid stratification	M	R39	D35	C9/G25	E1	S33
	Flashing	L	R32	D21	C9	E1	S5
	Phase separation in tees	L	R39	D56	C9/G24	E1	S8

Table F-3. (continued).

			For codes shown in these columns, See Tables:				
			F-6	G-1	G-2/G-3	G-4	G-5
Component	Phenomena	Rank	Ranking Rationale	Phenomena Description	Type Geometry	Supporting Evidence	Sublevel Phenomena
IRWST	Flow & temperature distribution in PRHR bundle region	M	R82	D23	C10/G26	E1	S24
	Pool thermal stratification	M	R82	D59	C10/G26	E1	S19
	Interphasic condensation	L	R83	D37	C10/G29	E1	S18
	Pool flow	L	R83	D57	C10/G26	E1	S24
PRHR	Heat transfer between PRHR and IRWST	H	R22	D32	C12/G30	E1	S28
	Condensation	M	R20	D9	C12/G30	E1	S18
	Differential density	M	R20	D17	C12/G30	E1	S10
	Flow resistance	M	R20	D27	C12/G30	E1	S11
	Noncondensible effects	M	R24	D50	C12/G31	E1	S12
	Voiding	M	R20	D78	C12/G31	E1	S54
Pumps	Flow resistance	L	R41	D27	C15/G38	E1	S15
Steam generators	Primary to secondary heat transfer	H	R38	D33	C16/G39	E1	S53
	SRV energy release	H	R38	D65	C16/G44	E1	S51
	SRV mass flow	H	R38	D66	C16/G44	E1	S50
	Secondary level	M	R40	D63	C16/G39	E1	S7
	Secondary pressure	M	R40	D64	C16/G39	E1	S17
	Tube voiding	M	R40	D75	C16/G39	E1	S16
	Condensation in U-tubes	L	R29	D9	C16/G39	E1	S18
Upper head / upper plenum	Flashing	L	R32	D21	C18/G45	E1	S5

Table F-4. PIRT for the ADS blowdown phase of a SGTR with ADS.

			For codes shown in these columns, See Tables:				
			F-6	G-1	G-2/G-3	G-4	G-5
Component	Phenomena	Rank	Ranking Rationale	Phenomena Description	Type Geometry	Supporting Evidence	Sublevel Phenomena
Accumulators	Flow	H	R44	D46	C1/G2	E1	S20
	Noncondensible effects	M	R43	D50	C1/G1	E1	S12
ADS	Energy release	H	R45	D19	C2/G3	E1	S21
	Mass flow	H	R45	D46	C2/G3	E1	S21
	Flow resistance	M	R45	D27	C2/G3	E1	S11
	Noncondensible effects	M	R45	D50	C2/G3	E1	S12
Break (single SG tube, two break paths)	Choking in complex geometries	M	R47	D6	C3	E1	S66
	Energy release	M	R47	D19	C3/G6	E1	S1
	Mass flow and direction	M	R47	D46	C3/G6	E1	S1
	Flow resistance	L	R46	D27	C3/G6	E1	S11
Cold legs	Flashing	L	R32	D21	C4	E1	S5
	Noncondensible effects	L	R49	D50	C4	E1	S12
	PBL-to-cold leg tee phase separation	L	R86	D56	C4/G8	E1	S8
	Stored energy release	L	R48	D68	C4/G7	E1	S2
Core	Two-phase mixture level	H	R50	D39	C5	E1	S31
	Flashing	M	R62	D21	C5/G12	E1	S5
	Stored energy release	L	R48	D68	C5/G11	E1	S2
CMT	Level	H	R51	D39	C6/G14	E1	S13
	Flashing	L	R91	D21	C6/G14	E1	S5
	Thermal stratification	L	R91	D73	C6/G14	E1	S19
Downcomer/ lower plenum	Condensation	L	R81	D9	C7/G18	E1	S18
	Flashing	L	R52	D21	C7	E1	S5
	Level	L	R37	D39	C7/G17	E1	S13
	Noncondensible effects	L	R52	D50	C7	E1	S12
	Stored energy release	L	R48	D68	C7/G15	E1	S2

Table F-4. (continued).

			For codes shown in these columns, See Tables:				
			F-6	G-1	G-2/G-3	G-4	G-5
Component	Phenomena	Rank	Ranking Rationale	Phenomena Description	Type Geometry	Supporting Evidence	Sublevel Phenomena
Fuel rods	Decay heat	H	R92	D12	C8/G20	E1	S4
	Stored energy release	L	R48	D68	C8/G21	E1	S2
Hot legs	Phase separation in tees	H	R53	D56	C9/G24	E1	S8
	CCFL	M	R54	D14	C9/G25	E1	S27
	Countercurrent flow	M	R54	D13	C9/G25	E1	S32
	Entrainment	M	R54	D20	C9/G25	E1	S23
	Flashing	M	R54	D21	C9	E1	S5
	Horizontal fluid stratification	M	R54	D35	C9/G25	E1	S33
	Noncondensible effects	L	R54	D50	C9	E1	S12
	Stored energy release	L	R48	D68	C9/G22	E1	S2
IRWST	Interphasic condensation	M	R55	D37	C10/G29	E1	S18
	Pool flow	M	R55	D57	C10/G26	E1	S24
	Pool thermal stratification	M	R55	D59	C10/G26	E1	S19
	Pool level	L	R56	D58	C10/G26	E1	S25
	Pool to tank structure heat transfer	L	R56	D60	C10/G28	E1	S26
Pressurizer	CCFl	M	R57	D14	C14/G34	E1	S27
	Entrainment-De-entrainment	M	R57	D20	C14/G36	E1	S23
	Level swell	M	R57	D40	C14/G36	E1	S13
	Noncondensible effects	L	R57	D50	C14	E1	S12
	Stored energy release	L	R48	D68	C14/G35	E1	S2
PRHR	Heat transfer between PRHR and IRWST	M	R58	D32	C12/G30	E1	S28
	Differential density	L	R59	D17	C12/G30	E1	S10
	Flashing	L	R59	D21	C12	E1	S5
	Flow resistance	L	R59	D27	C12/G30	E1	S11
	Noncondensible effects	L	R59	D50	C12/G31	E1	S12

Table F-4. (continued).

			For codes shown in these columns, See Tables:				
			F-6	G-1	G-2/G-3	G-4	G-5
Component	Phenomena	Rank	Ranking Rationale	Phenomena Description	Type Geometry	Supporting Evidence	Sublevel Phenomena
PRHR, Continued	Phase separation in tees	L	R59	D56	C12/G31	E1	S8
Steam generators	Primary to secondary heat transfer	L	R60	D33	C16/G39	E1	S53
	Secondary level	L	R61	D63	C16/G39	E1	S7
	Secondary pressure	L	R61	D64	C16/G39	E1	S17
Upper head / upper plenum	Entrainment/De-entrainment	M	R57	D20	C18/G46	E1	S23
	Flashing	M	R62	D21	C18/G45	E1	S5
	Stored energy release	L	R48	D68	C18/G47	E1	S2
	Voiding	L	R57	D78	C18/G45	E1	S54
Containment (interior)	Condensation	M	R63	D9	C19/G48	E1	S18
	Interior to wall heat transfer	M	R63	D86	C19/G48	E1	S72
	Passive heat sink (stored energy)	M	R63	D81	C19/G48	E1	S67
	Condensate transport	L	R63	D8	C19/G48	E1	S37
	Liquid distribution	L	R63	D43	C19/G48	E1	S38
	Liquid holdup	L	R63	D44	C19/G48	E1	S38
	Natural convection	L	R63	D48	C19/G48	E1	S36
	Noncondensible effects	L	R63	D50	C19/G49	E1	S12
	Noncondensible segregation	L	R63	D84	C19/G49	E1	S71
	Nonuniform steam/air distribution	L	R63	D51	C19/G49	E1	S35
	Steam-noncondensible mixing	L	R63	D67	C19/G49	E1	S68
Containment (exterior)	Exterior to ambient heat transfer	M	R63	D83	C20/G50	E1	S70
	PCCS evaporation	M	R63	D52	C20/G50	E1	S39
	Air flow	L	R63	D82	C20/G50	E1	S69
	Atmospheric temperature	L	R63	D2	C20/G50	E1	S43
	Chimney effects	L	R63	D5	C20/G50	E1	S41

Table F-4. (continued).

			For codes shown in these columns, See Tables:				
			F-6	G-1	G-2/G-3	G-4	G-5
Component	Phenomena	Rank	Ranking Rationale	Phenomena Description	Type Geometry	Supporting Evidence	Sublevel Phenomena
Containment (exterior), Continued	Humidity	L	R63	D36	C20/G50	E1	S46
	PCCS mixture convective heat transfer	L	R63	D54	C20/G50	E1	S30
	PCCS water flow	L	R63	D53	C20/G50	E1	S40
	PCCS wetting	L	R63	D55	C20/G50	E1	S42
	Radiation heat transfer	L	R63	D62	C20/G50	E1	S45

Table F-5. PIRT for the IRWST and sump injection phase of a SGTR with ADS.

			For codes shown in these columns, See Tables:				
			F-6	G-1	G-2/G-3	G-4	G-5
Component	Phenomena	Rank	Ranking Rationale	Phenomena Description	Type Geometry	Supporting Evidence	Sublevel Phenomena
ADS	Energy release	H	R94	D19	C2/G3	E1	S21
	Mass flow	H	R94	D46	C2/G3	E1	S21
	Flow resistance	M	R94	D27	C2/G3	E1	S11
	Noncondensible effects	L	R94	D50	C2/G3	E1	S12
Break (single SG tube, two break paths)	Choking in complex geometries	M	R47	D6	C3	E1	S66
	Energy release	M	R47	D19	C3/G6	E1	S29
	Mass flow and direction	M	R47	D46	C3/G6	E1	S29
	Flow resistance	L	R46	D27	C3/G6	E1	S11
Cold legs	Condensation	L	R65	D9	C4	E1	S18
	Noncondensible effects	L	R65	D50	C4	E1	S12
Core	Two-phase mixture level	H	R66	D76	C5	E1	S31
	Flow resistance	M	R66	D27	C5/G12	E1	S11
Downcomer/ lower plenum	Level	H	R68	D39	C7/G17	E1	S13
	Condensation	M	R69	D9	C7/G18	E1	S18
Fuel rods	Decay heat	H	R92	D12	C8/G20	E1	S4
Hot legs	Phase separation in tees	H	R70	D56	C9/G24	E1	S8
	CCFL	M	R71	D14	C9/G25	E1	S27
	Countercurrent flow	M	R71	D13	C9/G25	E1	S32
	Horizontal fluid stratification	M	R72	D35	C9/G25	E1	S33
IRWST	Discharge line flashing	M	R87	D21	C10/G27	E1	S5
	Flow resistance	M	R74	D27	C10/G27	E1	S11
	Pool level	M	R74	D58	C10/G26	E1	S25
	Pool thermal stratification	M	R74	D59	C10/G26	E1	S19
	Pool to tank structure heat transfer	L	R75	D60	C10/G28	E1	S26
PRHR	Heat transfer between PRHR and IRWST	L	R76	D32	C12/G30	E1	S28

Table F-5. (continued).

			For codes shown in these columns, See Tables:				
			F-6	G-1	G-2/G-3	G-4	G-5
Component	Phenomena	Rank	Ranking Rationale	Phenomena Description	Type Geometry	Supporting Evidence	Sublevel Phenomena
Steam generators	Primary to secondary heat transfer	L	R60	D33	C16/G39	E1	S53
	Secondary level	L	R61	D63	C16/G39	E1	S7
	Secondary pressure	L	R61	D64	C16/G39	E1	S17
Sump	Discharge line flashing	M	R87	D21	C17	E1	S5
	Flow resistance	M	R77	D27	C17	E1	S11
	Fluid temperature	M	R77	D29	C17	E1	S34
	Level	M	R77	D39	C17	E1	S13
Upper head / upper plenum	Entrainment/De-entrainment	H	R57	D20	C18/G46	E1	S23
	Voiding	M	R57	D78	C18/G45	E1	S54
Containment (interior)	Interior to wall heat transfer	H	R88	D86	C19/G48	E1	S72
	Condensate transport	M	R88	D8	C19/G48	E1	S37
	Condensation	M	R88	D9	C19/G48	E1	S18
	Liquid distribution	M	R88	D43	C19/G48	E1	S38
	Liquid holdup	M	R88	D44	C19/G48	E1	S38
	Natural convection	M	R88	D48	C19/G48	E1	S36
	Noncondensible effects	M	R88	D50	C19/G49	E1	S12
	Noncondensible segregation	M	R88	D84	C19/G49	E1	S71
	Nonuniform steam/air distribution	M	R88	D51	C19/G49	E1	S35
	Passive heat sink	M	R88	D81	C19/G48	E1	S67
	Steam-noncondensible mixing	M	R88	D67	C19/G49	E1	S68

Table F-5. (continued).

			For codes shown in these columns, See Tables:				
			F-6	G-1	G-2/G-3	G-4	G-5
Component	Phenomena	Rank	Ranking Rationale	Phenomena Description	Type Geometry	Supporting Evidence	Sublevel Phenomena
Containment (exterior)	Exterior to ambient heat transfer	H	R88	D83	C20/G50	E1	S70
	Atmospheric temperature	M	R88	D2	C20/G50	E1	S43
	Air flow	M	R88	D82	C20/G50	E1	S69
	Chimney effects	M	R88	D5	C20/G50	E1	S41
	Humidity	M	R88	D36	C20/G50	E1	S46
	PCCS evaporation	M	R88	D52	C20/G50	E1	S39
	PCCS mixture convective heat transfer	M	R88	D54	C20/G50	E1	S30
	PCCS water flow	M	R88	D53	C20/G50	E1	S40
	PCCS wetting	M	R88	D55	C20/G50	E1	S42
	Radiation heat transfer	M	R88	D62	C20/G50	E1	S45

Table F-6. Transient description and ranking rationale for the SGTR with single failure leading to ADS PIRT.

Overall Transient Description and Top-level Ranking Rationale

Current knowledge is not sufficient to indicate with certainty whether automatic depressurization system (ADS) actuation will occur following a steam generator tube rupture (SGTR) event involving a reasonable number of u-tubes. This PIRT assumes the double-ended rupture of a single steam generator tube at the tubesheet, with an additional single failure that tends to promote ADS actuation. Regarding that failure: A main steam line break (MSLB) combined with the SGTR could be lead to sufficient additional reactor coolant system (RCS) cooldown and shrinkage to result in ADS actuation. However, this sequence represents a double-failure event. The ADS also could be inadvertently actuated by an operator; however, this approach requires operator actions to be considered, and this was not desired. RCS inventory loss can be increased (potentially leading to ADS actuation) if the RCS pumps failed to trip automatically. Again, this approach was not desired because it requires operator action (the operators could manually trip the pumps after the automatic trip function failed). The single-failure assumed in this PIRT is the failure of one CMT discharge line check valve to open. This approach features an increased level reduction in the unaffected CMT, thereby promoting ADS actuation. The operators could not correct this failure.

As described in the previous paragraph, this sequence is initiated by the double-ended rupture of a single steam generator tube at the tubesheet with an additional failure of the check valve on one CMT discharge line to open. The availability only of safety-grade plant systems is assumed. Subsequent plant response is assumed to lead to ADS actuation and the fuel is assumed to remain covered throughout the transient. Although the basic plant design objective of no core uncovery is assumed to be satisfied, this sequence also involves a radioactive release to the atmosphere through the steam generator (SG) safety relief valves (SRVs). One of the primary purposes of the PIRT is to ensure that the analysis code(s) have adequate modeling for simulating the vessel inventory and release rate. The important hierarchical elements in the code assessment structure are those affecting vessel inventory and release rate as described below.

Phase Descriptions and Medium-level Ranking Rationales

Initial Depressurization Phase:

Description - This phase begins at the time of the tube rupture, when two break paths are opened between the RCS and the affected SG secondary system. The flow through the tubesheet-side break is much larger than that through the longer tube-side break. The feedwater control system reduces the feedwater flow rate to compensate for the break flow, and, initially, the affected SG levels do not increase. The pressurizer heater power increases to compensate for declining RCS pressure, and this effect slows the rate of RCS depressurization. The RCS mass loss causes the pressurizer level to decline and the pressurizer gas bubble expands. The RCS pressure eventually reaches the reactor trip low setpoint pressure. This occurrence results in scram control rod insertion and turbine stop valve closure. Reactor power is quickly reduced to the decay heat rate, causing RCS temperatures to fall, its fluid to shrink, and, therefore, its depressurization rate to increase. Affected SG SRV opening causes a release of radioactivity to the atmosphere, and elimination of this release is the key to a satisfactory outcome for this event sequence. Break flow and fluid shrinkage effects cause the RCS pressure to continue falling to the S signal setpoint pressure; this occurrence marks the end of this phase.

Important parameters and dominant processes - RCS pressure is judged to be the parameter of primary importance because it determines the tube rupture and atmospheric release rates. The processes important for accurate simulation of this parameter are: net RCS mass and energy balances, critical flow through the broken SG generator tube, and transient pressurizer inventory and gas bubble expansion.

Table F-6. (continued).

Passive Decay Heat Removal Phase:

Description - This phase begins at the time of the S signal, an occurrence that causes PRHR and CMT system actuations, reactor coolant pump trip, and feedwater isolation. The RCS loop flows decline rapidly from a forced-circulation to a natural-circulation condition. The affected SG inventory increases as a result of flow through the ruptured tube; this flow also sustains the affected SG secondary pressure near the SRV opening setpoint pressure. The combination of unaffected CMT recirculation, energy release through the affected SG SRVs, and PRHR system operation removes core decay heat from the RCS. The performance of the CMT system eventually degrades as fluid in the CMT tank is warmed. This event sequence assumes that, eventually, CMT recirculation is interrupted (and afterwards the unaffected CMT level may begin declining). The loss of recirculation event marks the end of this phase.

Important parameters and dominant processes - RCS pressure is judged to be the parameter of primary importance because it determines the duration of the radioactive release to the atmosphere through the steam generator SRVs. The processes important for accurate simulation of this parameter are: core, SG, and PRHR heat transfer, natural circulation in the RCS coolant loops, loop asymmetries, and SG SRV critical flow.

CMT Draining to ADS Actuation Phase:

Description - This phase begins at the time unaffected CMT recirculation is interrupted. Plant behavior during this phase is dominated by unaffected CMT draining and the phenomena that influence it: PRHR heat transfer, break mass flow rate, and flashing and voiding within the RCS. During this period, the break may transition from choked to friction-dominated flow, depending upon how closely the RCS pressure approaches the affected steam generator secondary pressure. This phase ends when the level in the unaffected CMT has declined to 67.5%.

Important parameters and dominant processes - The unaffected CMT level and RCS mass and energy distributions are judged to be the parameters of primary importance because they determine the timing of ADS stage 1 actuation. The processes important for accurate simulation of these parameters are: core, steam generator and PRHR heat transfer, and natural circulation in the RCS coolant loops, including asymmetries.

ADS Blowdown Phase:

Description - This phase begins when the level in the unaffected CMT declines to 67.5%. This occurrence produces an ADS actuation signal and, after a time delay, the ADS first stage is actuated (see Reference 6, Table H-2, for details of the sequencing of ADS operation). ADS actuation results in a blowdown of the RCS; ADS first, second, and third stages discharge through spargers submerged under water in the IRWST. As the RCS pressure declines, regions with the warmest fluid and those at the lowest pressure preferentially flash first, followed by cooler and higher-pressure regions. Actuations of ADS second and third stages occur at specified time intervals following ADS first stage actuation. Actuation of ADS fourth stage occurs upon attaining a level in either CMT of 20%, with an additional time-delay requirement. Unlike the other stages, ADS fourth stage discharges directly into the containment loop compartments. Plant behavior during this phase is dominated by the RCS blowdown, and this is determined by the RCS mass and energy distributions, especially as they affect the break and ADS flow rates and the CMT level. Accumulator injection begins when the RCS pressure has fallen to the initial accumulator pressure. Accumulator levels fall, and, eventually, nitrogen is injected from the accumulators into the RCS. As the RCS pressure approaches that in the containment, flows through the ADS change from choked to friction dominated. Break flow reverses during this phase because the affected SG secondary pressure becomes higher than that in the RCS; the atmospheric release through the SG secondary SRVs ceases. The RCS

Table F-6. (continued).

inventory declines after accumulator injection ends, and it is critical that the core remains covered until IRWST injection begins. This phase ends when the differential pressure between the RCS and the containment has been reduced to 12.1 psi. This pressure difference is equivalent to the 28-ft static head available for driving fluid from the IRWST into the reactor vessel. Onset of IRWST injection marks the end of the ADS blowdown phase.

Important parameters and dominant processes - The unaffected CMT level and ADS flow rate are judged to be the parameters of primary importance because they determine ADS staging and RCS depressurization rate. The processes important for accurate simulation of these parameters are: discharge flow (critical- and friction-dominated) and RCS mass and energy balances.

IRWST and Sump Injection Phase:

Description - This phase begins when flow commences from the IRWST, through the direct vessel injection lines, into the downcomer of the reactor vessel. This flow replenishes RCS inventory and reverses the downward core level trend. Steam produced in the core is passed out the ADS valves into the containment. In the containment, steam is condensed on the inside of the containment shell, and the condensate is returned via gutters to the IRWST, where it is available as a core injection source. Core decay heat is removed through the containment shell to its ultimate heat sink (the environment) via evaporative, convective, and radiative heat transfer on the outside of the containment shell. The IRWST injection rate may be unsteady. Increased injection rates may lead to decreased core steam production, decreased quality and volumetric flow at the fourth stage ADS and, therefore, RCS repressurization which results in a decreased injection rate. Most liquid that escapes returning to the IRWST (for example, that flowing from the ADS fourth stage) is collected in the containment sump which, like the IRWST, is elevated above the elevation span of the core. Some liquid may be trapped in locations where it cannot return to the IRWST or sump. Gravity-driven injection from the sump, similar to that from the IRWST, returns liquid to the reactor vessel downcomer. The plant end-state for this accident includes: (1) no atmospheric release through the affected SG SRVs, (2) core inventory maintenance from IRWST and/or sump injections, and (3) decay heat removal, across the containment shell, to the atmosphere.

Important parameters and dominant processes - The RCS-to-containment differential pressure is judged to be the parameter of primary importance because it determines the magnitude of the IRWST and sump flow rates. The processes important for accurate simulation of this parameter are: ADS flow and pressure drop, transient IRWST inventory, transient sump inventory, and containment and RCS mass and energy balances.

Detailed Phenomena Ranking Rationales

Ranking rationales for the phenomena in Tables F-1 through F-5

Code	Ranking Rationale
R1	Break mass flow is ranked high during the initial depressurization phase. This phenomenon is the outflow term in the RCS mass balance. The pressurizer level falls because of the net outflow of coolant from the RCS. The expansion of the pressurizer gas bubble determines the RCS pressure, the parameter of primary importance during this phase.

Table F-6. (continued).

Ranking rationales for the phenomena in Tables F-1 through F-5

Code	Ranking Rationale
R2	Break energy release is ranked medium during the initial depressurization phase. The break energy release was judged less significant than the break mass flow (see R1). While energy is removed at the break, for a SGTR, the break size is small and the influence of the break on the RCS energy balance is smaller than other contributors (heat addition from the core fuel rods and heat removal to the steam generators, see R3 and R8).
R3	Fuel rod core power/decay heat is ranked high during the initial depressurization phase. This phenomenon is the major heat addition term in the RCS energy balance. In addition, removal of this heat is a basic safety issue.
R4	Stored energy releases to RCS fluid from the fuel rods and pressurizer tank wall are ranked low during the initial depressurization phase. Significant energy is stored in the fuel rods during normal reactor operation. This energy is retained in the fuel rods prior to the time of reactor trip. After reactor trip, most of the initial fuel rod stored energy is quickly removed to the RCS coolant. Since this effect is temporary, fuel rod stored energy release was judged less significant to the RCS energy balance than the continuous fuel rod core power/decay heat phenomenon (that is ranked high, see R3). Stored energy release from the pressurizer vessel wall to fluid inside the pressurizer has a minor influence on the pressurizer gas bubble expansion process that controls RCS pressure during this phase.
R5	Not used.
R6	Noncondensible effects in the pressurizer are ranked low during the initial depressurization and passive decay heat removal phases. Hydrogen gas will evolve from solution during depressurization of the RCS. Accumulations of hydrogen in the pressurizer affect the species of gas in the pressurizer bubble; expansion/contraction of this bubble controls the RCS pressure.
R7	Break flow resistance is ranked medium during the initial depressurization and passive decay heat removal phases. This phenomenon affects the highly-ranked break mass flow. Flow through both break paths is at first dominated by critical flow (see R11). The flow resistance affects the critical flow, particularly through the longer break path. As the RCS depressurizes and the affected SG secondary system pressurizes, flows thorough these break paths unchoke and become dominated by frictional flow resistance considerations.
R8	Steam generator primary-to-secondary heat transfer is ranked high during the initial depressurization phase. This phenomenon is the major heat removal term in the RCS energy balance.
R9	Steam generator safety relief valve (SRV) mass flow and energy release are ranked medium during the initial depressurization phase. Existing analyses are insufficient to indicate whether the SRVs will be opened during this phase. While awaiting this indication, these phenomena are assigned a medium ranking to show their potential importance.
R10	Steam generator secondary pressure is ranked medium during the initial depressurization phase. The break flow is delivered against the affected steam generator secondary pressure, and this pressure also determines if the safety relief valves are opened. The pressures in the steam generator secondary systems determine the secondary-side saturation temperatures affecting heat exchange between the RCS and the steam generators.

Table F-6. (continued).

Ranking rationales for the phenomena in Tables F-1 through F-5

Code	Ranking Rationale
R11	Choking in complex geometries is ranked high during the initial depressurization and passive decay heat removal phases. This phenomenon determines the highly-ranked break mass flow for both break flow paths prior to the time when these paths unchoke (see R7). Choking was ranked high (in comparison with the frictional resistance that is ranked medium) because the modeling of critical flow processes in the unique geometries associated with broken steam generator tubes is particularly uncertain.
R12	Phase separation at the cold leg-to-PBL tee is ranked high for the passive decay heat removal phase. This phase is defined to end when CMT recirculation is interrupted by accumulation of void at the top of one or both PBLs. Three mechanisms are postulated for this accumulation of void: (1) flashing within the PBL, (2) flashing inside the CMT, with vapor flowing into the PBL, and (3) convection of void from the cold leg into the PBL. This phenomenon was ranked high because it controls mechanism (3).
R13	Core flow resistance is ranked low during the passive decay heat removal and CMT draining-to-ADS actuation phases. A large portion of the total resistance to RCS loop natural circulation flow resides in the core. This phenomenon, therefore, affects the RCS loop flow rate. Although this resistance is also present for PRHR system loop flow, the resistance for that loop is dominated within the PRHR system itself (the PRHR system has a much lower design flow rate than do the RCS loops).
R14	Subcooling margin is ranked medium during the passive decay heat removal phase. This ranking indicates the importance of: (1) core coolability and (2) the effects of core void generation on PRHR system heat removal and RCS depressurization.
R15	Loop asymmetric effects in the core, downcomer/lower plenum and hot legs are ranked low during the passive decay heat removal phase. This phenomenon is included to highlight that the assumed failure of the check valve in one CMT discharge line to open represents a source of additional asymmetry.
R16	Stored energy release to the RCS fluid from structures in the core, fuel rods, cold legs, downcomer/lower plenum, hot legs, and upper head/upper plenum is ranked low during the passive decay heat removal phase. Heat that is initially stored in these structures during normal reactor operation is released into the RCS as it depressurizes and cools. However, these releases are judged to be less significant contributors to the RCS energy balance than are the core decay power, and the CMT, steam generator, and PRHR system heat sinks (see R18, R17, R27, and R22, respectively).
R17	In the CMT component, CMT-to-loop differential density is ranked high and thermal stratification and flow resistance are ranked medium during the passive decay heat removal phase. These phenomena influence CMT recirculation and its effectiveness as an RCS heat sink. This heat sink is an important contributor to the RCS energy balance until the time when CMT recirculation is interrupted. The differential density is the driving force for CMT recirculation. Thermal stratification affects this driving force, the manner in which CMT recirculation is interrupted, and the temperature of fluid discharged from the CMT. The CMT flow resistance affects the CMT recirculation rate and, thereby, the period when the CMT is an effective RCS heat sink.
R18	Fuel rod decay heat is ranked high during the passive decay heat removal and CMT draining-to-ADS actuation phases. This phenomenon is the major heat addition term in the RCS energy balance, and removal of this heat is a basic safety issue.

Table F-6. (continued).

Ranking rationales for the phenomena in Tables F-1 through F-5

Code	Ranking Rationale
R19	Flashing and voiding in the hot legs are ranked medium during the passive decay heat removal phase. Hot leg behavior is of significance because fluid conditions in this component determine the conditions of fluids entering the intact and broken steam generator u-tubes and the PRHR system. Of particular importance is the steam content of the hot leg fluid, as this affects break flow and PRHR heat removal. Steam may be produced in the core and passed into the hot leg, or it may be generated by flashing within the hot legs. If the hot legs become sufficiently voided, then pure steam may be passed to the steam generators and PRHR system.
R20	In the PRHR component, condensation, differential density, flow resistance, and voiding are ranked medium during the passive decay heat removal and CMT draining-to-ADS actuation phases. These phenomena all contribute to the PRHR-to-IRWST heat transfer process. The convective thermal resistance on the PRHR tube inner surface is sensitive to (among other things) the presence or absence of the condensation process. The differential density (i.e., the difference in density between the fluid in the inflow and outflow sides of the PRHR system piping) is the driving force for flow through the primary side of the PRHR system. The flow resistance of the PRHR system (including the entire flow loop through the core) balances the driving force created by the differential density. The voiding from noncondensible gas (hydrogen, see R6) accumulated at the high point of the PRHR inlet line (it is an inverted trap configuration) may block the path for flow through the PRHR heat exchanger.
R21	Not used.
R22	Heat transfer between the PRHR and IRWST is ranked high during the passive decay heat removal and CMT draining-to-ADS actuation phases. This phenomenon represents the only means by which decay heat may be removed from the RCS to the containment during these phases.
R23	Not used.
R24	Noncondensible effects in the PRHR are ranked medium during the passive decay heat removal and CMT draining-to-ADS actuation phases. Hydrogen gas will evolve from solution during the depressurization of the RCS. The presence of this gas inside the PRHR tube can degrade the heat transfer process on the tube inner surface. Voiding from noncondensible gas accumulated at the high point of the PRHR inlet line (its configuration includes an inverted trap) may block the path for flow through the PRHR heat exchanger.
R25	The pump flow resistance is ranked low during the passive decay heat removal phase. Here, the pump flow resistance is the locked-rotor resistance that is present following the pump coastdown period. The pump resistance influences steam generator heat transfer through its effect on the natural circulation flows through the RCS loops (i.e., through the core, hot legs, steam generators, pumps, and cold legs). For the RCS loops, the pump flow resistance is a significant fraction of the total loop resistance. The pump resistance also influences PRHR-to-IRWST heat transfer through its effect on the flow through the PRHR system natural circulation loop (i.e., through the core, hot leg, PRHR inlet, PRHR heat exchanger, PRHR outlet, pump, and cold leg). For the PRHR system loop, the pump resistance is only a small fraction of the total loop resistance.

Table F-6. (continued).

Ranking rationales for the phenomena in Tables F-1 through F-5

Code	Ranking Rationale
R26	Steam generator safety relief valve (SRV) energy release and mass flow are ranked high during the passive decay heat removal phase. When the SRVs are open, fluid is released from the affected steam generator secondary system to the atmosphere. This fluid contains radioactivity that was previously passed from the RCS into the affected secondary system through the break. To terminate the atmospheric release, the RCS pressure must, therefore, be maintained below the lowest SRV opening setpoint pressure. SRV flow removes both mass and energy from the coupled RCS-affected steam generator system. Because the SRV downstream pressure is atmospheric, flow through this path will be dominated by critical flow processes.
R27	Steam generator primary-to-secondary heat transfer is ranked high during the passive decay heat removal phase. Heat exchanges between the RCS and both steam generators influence the RCS pressure because they are major terms in the RCS energy balance. The possibility exists for reverse (i.e., secondary-to-primary) heat transfer.
R28	Steam generator secondary level and pressure, and voiding inside u-tubes, are ranked medium during the passive decay heat removal phase. Steam generator secondary pressure determines the saturation temperature that is the heat sink for primary-to-secondary heat transfer (see R27). Steam generator secondary level influences that heat transfer through its effect on the convective thermal resistance on the outside of the u-tubes. Tube regions not submerged under the level do not efficiently transfer heat. The level response in the affected steam generator is particularly uncertain because its inventory is gained through the two break paths but may be lost through the safety relief valves. Voiding inside the u-tubes influences primary-to-secondary heat transfer through its effect on the convective thermal resistance on the inside of the u-tubes. If the void is from steam, then the resistance may be low, due to wall condensation heat transfer (also see R29). However, if the void is from noncondensible gas, the resistance may be high. Hydrogen gas evolves from solution in the RCS fluid during depressurization; this gas can degrade the heat transfer process on the inner u-tube walls. Voiding from noncondensible gas accumulated at the u-tube high points may block the path for flow through the tubes.
R29	Condensation in the steam generator U-tubes is ranked low during the passive decay heat removal and CMT draining-to-ADS actuation phases. This phenomenon can remove steam void from the U-tubes (see R28). Wall condensation inside the tubes can be caused by heat transfer to the steam generator secondary. Interphase condensation inside the tubes can be caused by flow of cold water into the U-tubes from the PRHR discharge.
R30	Flashing in the reactor vessel upper head is ranked medium during the passive decay heat removal phase. This region is prone to flash as the RCS is depressurized, and the bubble created there cannot be readily collapsed. This phenomenon, therefore, affects the RCS pressure response.
R31	Phase separation in the cold leg-to-pressure balance line tee is ranked high during the CMT draining-to-ADS actuation phase. As the CMT drains, void may be convected into the pressure balance line through this tee, and this process has a direct effect upon the CMT level that is one of the important parameters for this phase.

Table F-6. (continued).

Ranking rationales for the phenomena in Tables F-1 through F-5

Code	Ranking Rationale
R32	Flashing in the cold legs, core, hot legs, and upper head/upper plenum is ranked low during the CMT draining-to-ADS actuation phase. Flashing in the cold legs is ranked low during the ADS blowdown phase. Liquid volume drained from the CMT must be replaced by gas volume; flashing in these components represents one possible source of steam for that purpose. Steam produced in the cold legs (or elsewhere, and convected into the cold legs) must enter the pressure balance line to replace liquid drained from the CMT. The CMT draining process determines the staging of ADS. See R62 for additional discussion of flashing in RCS components during the ADS blowdown phase.
R33	Core mass flow (including bypass) is ranked low during the CMT draining-to-ADS actuation phase. Although this phenomenon affects the coolant loop differential pressures, it has a minimal influence on the RCS mass and energy distributions, as compared with the other ranked phenomena in the break, core, PRHR, and steam generator components.
R34	The CMT level is ranked high during the CMT draining-to-ADS actuation phase. This phenomenon is one of the important parameters listed for this phase. Activation of the ADS is based upon the CMT level response, and this activation defines the end of this phase.
R35	CMT flashing is ranked medium and CMT condensation, flow resistance, and thermal stratification are ranked low during the CMT draining-to-ADS actuation phase. The CMT level response (see R34) is primarily determined by phenomena external to the CMT (primarily those affecting the RCS mass and energy balances and distributions). While CMT flashing affects the onset of CMT draining, the other three phenomena affect only the manner in which the CMT drains.
R36	Break energy release and mass flow are ranked high, and choking in complex geometries and flow resistance are ranked medium, during the CMT draining-to-ADS actuation phase. The break mass flow and energy release directly affect the CMT level and RCS mass and energy distributions. Choking and flow resistance determine the break flow.
R37	The reactor vessel downcomer level is ranked low during the CMT draining-to-ADS actuation and ADS blowdown phases. A downcomer level may form during these phases because of steam flow (from the upper head into the upper downcomer through the bypass nozzles), flashing, and asymmetries in the cold leg fluid conditions between the CMT and pressurizer loops. However, the downcomer level has only a minimal effect on the CMT level and RCS mass and energy distributions, the important parameters for this phase.
R38	Steam generator primary-to-secondary heat transfer is ranked high during the CMT draining-to-ADS actuation phase. Heat exchanges between the RCS and both steam generators influence the RCS pressure because they are major terms in the RCS energy balance. The possibility exists for reverse (i.e., secondary-to-primary) heat transfer. Steam generator safety relief valve (SRV) energy release and mass flow are ranked high during the CMT draining-to-ADS actuation phase. When the SRVs are open, fluid is released from the affected steam generator secondary system to the atmosphere. This fluid contains radioactivity that was previously passed from the RCS into the affected secondary system through the break. To terminate the atmospheric release, the RCS pressure must, therefore, be maintained below the lowest SRV opening setpoint pressure. SRV flow removes both mass and energy from the coupled RCS-affected steam generator system. Because the SRV downstream pressure is atmospheric, flow through this path will be dominated by critical flow processes.

Table F-6. (continued).

Ranking rationales for the phenomena in Tables F-1 through F-5

Code	Ranking Rationale
R39	Phase separation in hot leg tees is ranked low and horizontal fluid stratification is ranked medium during the CMT draining-to-ADS actuation phase. The PRHR system inlet is connected to the ADS stage 4 line that exits the top of one hot leg pipe. If steam resides in the upper portion of the hot leg, then it may freely enter the PRHR system; this steam flow may entrain liquid. The PIRT committee believed the hot leg likely will be stratified during this phase. These phenomena were included because they affect the state of the fluid entering the PRHR system.
R40	Steam generator secondary level and pressure and voiding inside u-tubes are ranked medium during the CMT draining-to-ADS actuation phase. Steam generator secondary pressure determines the saturation temperature that is the heat sink for primary-to-secondary heat transfer (see R38). Steam generator secondary level influences that heat transfer through its effect on the convective thermal resistance on the outside of the u-tubes. Tube regions not submerged under the level do not efficiently transfer heat. The level response in the affected steam generator is particularly uncertain because its inventory is gained through the two break paths but may be lost through the safety relief valves. Voiding inside the u-tubes influences primary-to-secondary heat transfer through its effect on the convective thermal resistance on the inside of the u-tubes. If the void is from steam, then the resistance may be low, due to wall condensation heat transfer (also see R29). However, if the void is from noncondensible gas, the resistance may be high. Hydrogen gas evolves from solution in the RCS fluid during depressurization; this gas can degrade the heat transfer process on the inner u-tube walls. Voiding from noncondensible gas accumulated at the u-tube high points may block the path for flow through the tubes.
R41	The pump flow resistance is ranked low for the CMT draining-to-ADS actuation phase. Here, the pump flow resistance is the locked-rotor resistance that is present following the pump coastdown period. This resistance affects natural circulation flows around the RCS loops (i.e., through the core, hot legs, steam generators, pumps, and cold legs). This resistance also affects the flow rate through the PRHR system natural circulation loop (i.e., through the core, hot leg, PRHR inlet, PRHR heat exchanger, PRHR outlet, pump, and cold leg). However, for this natural circulation loop, the pump locked-rotor resistance is a small contributor to the overall loop resistance.
R42	Loop asymmetry effects were ranked medium in the cold leg and downcomer/lower plenum components and low in the core component during the CMT draining-to-ADS actuation phase. Asymmetric conditions (pressures, temperatures, flow rates) within and/or between RCS components may be present. The sources of these asymmetries are the break location (e.g., it is located in only one of the two steam generators) and the plant configuration (the pressurizer and PRHR system are connected on one coolant loop while the CMTs are connected on the other). The importance of these asymmetry effects cannot be determined until confirmation calculations are completed. In general, the PIRT committee judged that asymmetric effects may significantly influence the progression of the SGTR transient.
R43	Noncondensible effects in the accumulators are ranked medium in the ADS blowdown phase. Expansion of the nitrogen gas bubbles within the accumulators controls the differential pressure between the accumulator and RCS and, therefore, the rate at which liquid flows from the accumulator into the RCS (this flow is ranked high, see R44).
R44	The accumulator flow is ranked high during the ADS blowdown phase. This flow is a major RCS mass addition source.

Table F-6. (continued).

Ranking rationales for the phenomena in Tables F-1 through F-5

Code	Ranking Rationale
R45	The ADS mass flow rate and energy release are controlling phenomena during the ADS blowdown phase of the accident and are ranked high (ADS flow rate is listed as an important parameter for this phase). The ADS flow resistance is ranked medium for the ADS blowdown phase because it affects the ADS fourth stage discharge after it unchokes (because the differential pressure between RCS and containment has been reduced). The effects of noncondensible gases are ranked medium for the ADS blowdown phase; the accumulators empty and vent a large volume of nitrogen into the RCS (note the noncondensible gas volume grows as the RCS continues depressurizing). This nitrogen can affect both the flows and energy releases of the break and ADS.
R46	The break flow resistance is ranked low during the ADS blowdown phase. Break flow will reverse because the RCS pressure falls below the affected SG pressure after ADS is opened. For most of this phase, the pressure difference across the break path is expected to be large enough for these reverse flows to choke (see R47). However, the break will be dominated by friction during at least a portion of this phase.
R47	In the break component, choking in complex geometries, energy release, and mass flow and direction are ranked medium during the ADS blowdown and IRWST and sump injection phases. Break flow will reverse during the blowdown phase because the RCS pressure falls below that in the affected SG after ADS is opened. During most of these phases, the pressure difference across the break path is expected to be large enough to cause the broken tube flows to be dominated by critical flow processes. The break flow and energy release are contributors to the RCS mass and energy balances. However, these balances are controlled by mass flow and energy release through the ADS.
R48	Stored energy release in the following components is ranked low for the ADS blowdown phase: cold legs, core, downcomer/lower plenum, fuel rods, hot legs, pressurizer, and upper head/upper plenum. The RCS pressure and saturation temperature fall sharply during this phase. As a result, remaining heat stored in metal structures in these components is available to flow into the RCS coolant. However, this flow of heat is expected to be a minor contributor to the overall RCS energy balance; energy loss through the ADS is expected to dominate that balance.
R49	Noncondensible effects in the cold legs are ranked low during the ADS blowdown phase. Noncondensible gas expelled from the accumulators during this phase are expected to preferentially reside within the cold legs and therefore alter the distribution of RCS fluid.
R50	Core two-phase mixture level is ranked high for the ADS blowdown phase. Regarding high core levels, a relationship between the core level and ADS flow rate has not been established with current evidence. However, core level behavior can dramatically affect the ADS discharge (if core level swells, then an increased flow of liquid into the ADS will result). This phenomenon was ranked high pending later evidence to the contrary. Regarding low core levels, for a SBLOCA, the minimum core level is attained at the end of the ADS blowdown when the onset of IRWST injection reverses the declining core level trend. This trend is believed to apply for the SGTR accident as well. Therefore, this phenomenon was also ranked high because it is an indicator of core uncovery and coolability.
R51	The CMT level is ranked high during the ADS blowdown phase. This phenomenon is an important parameter listed for this phase because initiation of fourth stage ADS is based upon attaining a 20% CMT indicated level.

Table F-6. (continued).

Ranking rationales for the phenomena in Tables F-1 through F-5

Code	Ranking Rationale
R52	Flashing and noncondensible effects in the downcomer/lower plenum are ranked low in the ADS blowdown phase. Prior to opening the ADS, the regions of the downcomer above the water level will be filled with nitrogen that was previously expelled from the accumulators. The opening of the ADS will cause fluid everywhere in the RCS to flash. Flashing will be preferential based upon location within the plant and upon the temperature of fluid present. Therefore, during this phase, these phenomena may have some effect on the ADS and break flow rates and, perhaps, upon the core level.
R53	Phase separation in hot leg tees is ranked high during the ADS blowdown phase. Phase separation in hot leg tees controls the quality of the fluid entering ADS stages 1, 2, and 3 (via the pressurizer surge line tee) and ADS stage 4 (through the ADS-4 tees).
R54	CCFL, countercurrent flow, entrainment, flashing, and horizontal fluid stratification are ranked medium and noncondensible effects are ranked low during the ADS blowdown phase. These phenomena control the phase separation process at the hot leg tees (see R53). The inventory, inventory distribution, and flow behavior in the hot legs determines the behavior at the pressurizer surge line and ADS stage 4 tees.
R55	In the IRWST, interphasic condensation, pool flow, and pool thermal stratification are ranked medium during the ADS blowdown phase. ADS stages 1, 2, and 3 discharge RCS fluid into the IRWST through two spargers. The fluid flowing through the spargers has a high steam content, perhaps superheated, at the near-atmospheric pressure inside the tank. However, the IRWST fluid is initially subcooled, so high interphase condensation rates are anticipated. The phenomena ranked here affect: (1) the manner in which the IRWST performs the quenching process, (2) the state of the IRWST fluid (that later is injected into the RCS), and (3) the containment pressure.
R56	The IRWST pool level and pool-to-tank structure heat transfer are ranked low for the ADS blowdown phase. After ADS stages 1, 2, and 3 unchoke, the pool level has a minor effect upon the pressure at the ADS sparger and, therefore, upon the unchoked ADS flow rate. Over the long term, the energy removed from the pool to its surroundings may be important, but during this phase this energy removal was judged to be significantly smaller than that introduced into the pool through the ADS.
R57	In the pressurizer, CCFL, entrainment/de-entrainment, and level swell are ranked medium during the ADS blowdown phase. The ADS mass flow and energy release are ranked high during this phase (see R45). These phenomena determine the upstream fluid conditions for the ADS stage 1, 2, and 3 mass flow and energy release rates. Noncondensible effects in the pressurizer are ranked low during the ADS blowdown phase. Noncondensible gas is expelled from the accumulators into the RCS, and this gas will find its way into the pressurizer as it flows out ADS stages 1, 2, and 3 (see R45). Upper plenum entrainment/de-entrainment is ranked medium during the ADS blowdown phase and high during the IRWST and sump injection phase. The process of separating liquid from steam in the upper plenum directly affects the state of fluid passed to the ADS. Upper head voiding is ranked low during the ADS blowdown phase and medium during the IRWST and sump injection phase. Expansion of the bubble in this region affects the RCS pressure response during the blowdown period. During the final phase, the upper head may refill, and this affects RCS fluid distribution.

Table F-6. (continued).

Ranking rationales for the phenomena in Tables F-1 through F-5

Code	Ranking Rationale
R58	Heat transfer between the PRHR and IRWST is ranked medium during the ADS blowdown phase. The importance of PRHR heat removal during this phase has not been established. It is suspected that this heat removal may be overshadowed by ADS effects during this phase. However, PRHR heat transfer has the potential to be important, so it was ranked medium pending better information.
R59	In the PRHR component, differential density, flashing, noncondensible effects, flow resistance, and phase separation in tees are ranked low in the ADS blowdown phase. These phenomena can affect the PRHR heat removal rate (ranked medium, see R58) and, therefore, they have been ranked low. Note that this is the only instance where phase separation in tees has been ranked for the PRHR component. For normal PRHR flow situations, tee phase separation is primarily of interest at the PRHR inlet line connection on the hot leg, and this phenomenon was included in the listings for the hot leg component. However, for the ADS blowdown situation, RCS conditions are chaotic, and the question here is the manner in which the PRHR system outlet tee (on the steam generator outlet plenum) might perform under potential reverse-flow conditions. Because the PRHR inlet line is connected directly to one of the ADS fourth-stage inlet lines, reverse flow through the PRHR system is likely to develop as fluid rushes out the ADS fourth stage.
R60	Steam generator heat transfer is ranked low during the ADS blowdown and IRWST and sump injection phases. During these phases, the RCS energy balance is controlled by decay heat addition, energy addition from the break (reverse flow), and ADS energy removal. The steam generators are essentially thermally-decoupled from the RCS because fluid in the secondary system is significantly hotter than in the RCS (see R28).
R61	Steam generator secondary level and pressure are ranked low during the ADS blowdown and IRWST and sump injection phases. These phenomena affect both primary-to-secondary heat transfer and the steam generator secondary safety relief valve flow.
R62	Flashing in the core and upper plenum/upper head are ranked medium during the ADS blowdown phase. This flashing will affect the RCS mass and energy distributions. Flashing will be preferential (see R72), and the warmest RCS fluid will reside in the core and upper head/upper plenum regions.
R63	Containment phenomena first appear of significance during this phase because of their impact on the containment pressure response, which affects the timing of IRWST injection. Little analysis is available to support the relative phenomena rankings. The PIRT committee ranked the overall heat transfer on the interior and exterior surfaces of the containment shell medium, along with the expected heat transfer processes on those surfaces (condensation on the inside and PCCS evaporative cooling on the outside). In addition, passive heat sink is ranked medium because the effects of wall heat transfer (containment shell, structural walls, and internal equipment) are expected to be greatest during this phase, when the fluid-to-wall temperature differentials are the largest. The other phenomena are ranked low.
R64	Break flow resistance is ranked low during the IRWST and sump injection phase. This phenomenon influences the break flow, but only during periods when the break is unchoked (see R47).

Table F-6. (continued).

Ranking rationales for the phenomena in Tables F-1 through F-5

Code	Ranking Rationale
R65	In the cold legs, condensation and noncondensible effects are ranked low during the IRWST and sump injection phase. The cold legs are expected to be an inactive RCS region during this phase. However, these phenomena were left on the list because of the possibility for effects due to: (1) condensation of steam (entering this region through the reactor vessel upper head/downcomer bypass path) and (2) large expansions of nitrogen (caused by total depressurization of the RCS).
R66	Two-phase mixture level in the core is ranked high during the IRWST and sump injection phase. The two-phase mixture level determines the status of core coolability and affects the differential pressure between the RCS and the containment. The core flow resistance is ranked medium during the IRWST and sump injection phase. This resistance affects the RCS-to-containment differential pressure, but to a lesser extent than does the mixture level.
R67	Not used.
R68	Downcomer level is ranked high during the IRWST and sump injection phase. This level is the driving force for flow through the core. The static head created by this level is a significant term affecting the RCS/containment pressure balance.
R69	Condensation in the downcomer is ranked medium during the IRWST and sump injection phase. Steam may flow through the upper head/downcomer bypass path (also see R81). If condensation is present, it can alter the high-ranked downcomer level (see R68).
R70	Phase separation in tees in the hot leg is ranked high during the IRWST and sump injection phase. Separation at the ADS fourth-stage tees determines the energy and content of the fluid mixture that is routed through the ADS to containment.
R71	CCFL and countercurrent flow in the hot leg are ranked medium during the IRWST and sump injection phase. These phenomena contribute to the highly-ranked hot leg phase separation process (see R70) because they affect the fluid state and flow regime in the hot leg.
R72	Horizontal fluid stratification in the hot legs is ranked medium during the IRWST and sump injection phase. Fluid conditions during this phase may be quiescent, and in that case the hot leg would stratify. Whether or not the hot leg fluid stratifies has a direct influence on the phase separation in the hot leg tees (ranked high, see R70) and the state of the mixture being passed on to the ADS.
R73	Not used.
R74	IRWST pool thermal stratification, pool level, and flow resistance are ranked medium during the IRWST and sump injection phase. Stratification affects the injection temperature (the fluid present at the bottom of the tank is injected). Level provides the driving force to push the injection flow through the total resistance (the IRWST piping system flow resistance is an important part of the total). Therefore, the IRWST pool level and flow resistance directly affect the injection flow rate.
R75	Heat transfer between the IRWST fluid and the tank walls is ranked low during the IRWST and sump injection phase. The energy loss via this phenomenon is expected to be much smaller than the other terms involved in the containment energy balance.

Table F-6. (continued).

Ranking rationales for the phenomena in Tables F-1 through F-5

Code	Ranking Rationale
R76	Heat transfer between the PRHR and IRWST is ranked low during the IRWST and sump injection phase. The potential for this heat transfer remains, via condensation of steam on the inside of the PRHR tubes. However, the energy removal from the RCS is expected to be dominated by the ADS fourth stage during this phase.
R77	Sump fluid temperature, level, and flow resistance are ranked medium during the IRWST and sump injection phase. The sump fluid temperature is the RCS injection temperature (the fluid present at the bottom of the sump is injected). The sump level provides the driving force to push the injection flow through the total resistance (the sump piping system flow resistance is an important part of the total). Therefore, all these phenomena contribute to the determination of the injection flow rate and temperature.
R78	Not used.
R79	Not used.
R80	Not used.
R81	Condensation in the downcomer is ranked low during the passive decay heat removal, CMT draining-to-ADS actuation, and ADS blowdown phases. RELAP5 SBLOCA simulations (see Reference 8) have shown that interphasic condensation of steam flowing from the upper head through the bypass into the upper portion of the reactor vessel downcomer can alter the break flow and progression of a SBLOCA sequence. Condensation effects for the SGTR accident are expected to be similar to those in the SBLOCA (also see R69).
R82	In the IRWST component, flow and temperature distribution in the PRHR tube bundle region and pool thermal stratification are ranked medium during the passive decay heat removal and CMT draining-to-ADS actuation phases. These phenomena are major contributors (others are listed in R83) to PRHR-to-IRWST heat transfer that is ranked high (see R22). The convective thermal resistance on the outside of the PRHR tubes is sensitive to the flow rate through the tube bundle. Pool thermal stratification affects the heat sink temperature on the outside of the PRHR tubes and the vertical distribution of that sink temperature.
R83	IRWST pool flow and interphasic condensation are ranked low in the passive decay heat removal and CMT draining-to-ADS actuation phases. The flow and temperature distributions in the PRHR bundle region are ranked medium during these phases (see R82). IRWST pool flow and interphasic condensation affect those distributions and are, therefore, ranked low. IRWST pool flow refers to natural convection flows in the large tank region away from the PRHR bundle. Interphasic condensation here refers to the collapse of bubbles that may be formed due to boiling on the outside of the PRHR tubes. This condensation may take place either in the pool bundle region or elsewhere in the pool.
R84	Pump coastdown performance is ranked low for the passive decay heat removal phase. The reactor coolant pump coastdown behavior will influence the primary-to-secondary heat transfer because it determines the flow rates inside the steam generator and PRHR system tubes. However, this effect is limited because of the short time duration of the coastdown (about 2 minutes) and its decaying nature.

Table F-6. (continued).

Ranking rationales for the phenomena in Tables F-1 through F-5

Code	Ranking Rationale
R85	Asymmetric conditions (pressures, temperatures, flow rates) within and/or between RCS components may be present. The sources of these asymmetries are the break location (i.e., it is situated in only one of the two steam generators) and the plant configuration (the pressurizer and PRHR system are connected on one coolant loop, while the CMTs are connected on the other). The importance of these asymmetry effects cannot be determined until confirmation calculations are completed. In general, the PIRT committee judged that asymmetric effects will influence the progression of the SGTR transient. Asymmetric effects in the upper plenum are, therefore, ranked medium during the passive decay heat removal phase.
R86	Phase separation at the cold leg-to-PBL tee is ranked low during the ADS blowdown phase. Fluid behavior is very dynamic during this phase, and the behavior at this tee will affect the CMT level response and, therefore, the ADS sequencing behavior.
R87	Discharge line flashing in the IRWST and sump injection lines is ranked medium during the IRWST and sump injection phase. The temperatures of the injection fluids will depend upon behavior within the IRWST and containment. It is not known if fluid in these lines will flash. However, if the fluid does flash, then the injection rate may be significantly affected by the increased injection-line pressure drop.
R88	Containment interior and exterior phenomena are ranked as follows during the IRWST and sump injection phase: The containment shell interior and exterior heat transfer represent the decay heat removal to the ultimate heat sink and, therefore, are ranked high. Condensation, natural convection, noncondensible effects, noncondensible segregation, steam-noncondensible mixing, and nonuniform air/steam distribution in the containment interior are all ranked medium because they contribute to the determination of the containment pressure. Condensate transport, liquid holdup, and liquid distribution in the containment interior are ranked medium because they contribute to the determination of the containment pressure. The passive heat sink provided by the containment walls and interior structures represents a significant contribution to the containment energy balance and is, therefore, ranked medium. PCCS evaporation, PCCS mixture convective heat transfer, PCCS water flow, air flow, and chimney effects on the containment exterior are all ranked medium because they affect decay heat removal to the ultimate heat sink during this phase. Containment exterior atmospheric temperature, humidity, PCCS wetting, and radiation heat transfer are all ranked medium because they affect decay heat removal to the ultimate heat sink.

Table F-6. (continued).

Ranking rationales for the phenomena in Tables F-1 through F-5

Code	Ranking Rationale
R89	Break energy release and mass flow are ranked high during the passive decay heat removal phase. The break mass flow and energy release directly affect the RCS mass and energy distributions.
R90	Pressurizer flashing and level (inventory) are ranked medium during the passive decay heat removal phase. These phenomena influence RCS pressure through their effect on the pressurizer bubble expansion process. However, these effects are smaller than during the previous phase because other RCS regions also flash during this phase (see R19 and R30).
R91	Flashing and thermal stratification in the CMT are ranked low during the ADS blowdown phase. These phenomena determine the CMT emptying behavior during the blowdown; ADS fourth stage actuation is based upon CMT level attaining a low-level setpoint.
R92	Fuel rod decay heat is ranked high during the ADS blowdown and IRWST and sump injection phases. This phenomenon represents the major RCS energy source; this heat must be removed to the ultimate heat sink.
R93	Not used.
R94	ADS mass flow and energy release are ranked high, ADS flow resistance is ranked medium, and ADS noncondensible effects are ranked low during the IRWST and sump injection phase. The ADS mass and energy flow rates directly affect the differential pressure between the RCS and the containment. The ADS flow resistance affects the mass and energy flow rates. Noncondensible gases affect the ADS mass and energy flows, but to a lesser extent than during the previous phase (where noncondensible effects were ranked medium, see R45). Peak flow of noncondensibles from the accumulators into the RCS occurs during the ADS blowdown phase.

Appendix G - Common Supporting Documentation

The tables provided in this appendix provide descriptive supporting information for the individual PIRTs in Appendixes B through F. The identifier "codes" shown in these tables are those referenced within the individual detailed PIRTs. Table G-1 provides brief descriptions of the general phenomena. Table G-2 describes the physical geometries and general functions of the AP600 components. Table G-3 provides more detailed discussions regarding the specific phenomena associated with each of the components. Table G-4 provides supporting references. Table G-5 describes pertinent sublevel phenomena related to each of the primary phenomena.

Table G-1. Phenomena descriptions for the PIRTS.

The phenomena identified and ranked in the PIRTs are defined here. The "code" column shows the indicator used in the master PIRTs to reference the information given in this table.

Code	Phenomena	Description
D1	Not used	
D2	Atmospheric temperature	The temperature of the atmosphere surrounding the containment exterior. This temperature effects the heat transfer from the containment exterior to the surrounding environment.
D3	Boron reactivity feedback	The change in core reactivity due to an increase or decrease of boron concentration in the moderating fluid.
D4	Channeling	Concurrent, non-uniform flow of fluids with different properties (temperature, density, boron concentration).
D5	Chimney effects	The process wherein wind flowing over the top of the containment gap reduces the local static pressure, drawing air out of the gap to be replaced by air drawn into the bottom. Air in the gap between the containment exterior and its shroud is also heated on the containment exterior, lowering its density and causing it to rise and flow out of the top of the gap. Eddies can form on the downwind side of the containment exterior, causing the heated air to recirculate through the containment gap.
D6	Choking in complex geometries	The process wherein the critical flow out of a component is significantly affected by the geometry of the component. For example, the critical flow out of a sheared steam generator tube is significantly affected by the large length-to-diameter ratio on the tube-side break.
D7	Coastdown performance	The pump head and flow reductions that occur as the shaft and impeller coast to a stop following disconnection of the motor electrical power.
D8	Condensate transport	The process of delivering the steam condensed on the containment interior to the IRWST.
D9	Condensation	The process where steam is cooled due to contact with a colder substance, resulting in change of phase from vapor to liquid.
D10	Convective heat transfer	The transport of energy to or from a surface by gross fluid movement.

Table G-1. (continued).

Code	Phenomena	Description
D11	Core channeling	Concurrent, non-uniform flow of fluids with different properties (temperature, density, boron concentration) in the core.
D12	Core power/decay heat	The power generated in the fuel rods due to either nuclear fission, or decay of the fission products, and including the heat conduction through the fuel, convection and radiation across the gap, conduction through the clad, and convection to the coolant.
D13	Countercurrent flow	The process whereby liquid flows opposite (counter) to the gas flow direction.
D14	Countercurrent flow limiting (CCFL)	The process by which interfacial drag and/or entrainment prevents or limits liquid flow opposite (counter) to the gas flow direction.
D15	Critical heat flux (CHF)/Dryout	CHF refers to a departure from nucleate boiling that causes a sudden deterioration in heat transfer and results in a temperature excursion of the heated surface and potential burnout. Dryout refers to a temperature excursion of the heated surface due to starvation of liquid.
D16	Not used	
D17	Differential density	The difference between the cold and hot side average densities for buoyancy driven flow circuits. This determines the driving potential for the flow.
D18	Not used	
D19	Energy Release	The transfer of energy associated with the flow of fluid mass out of a system or component.
D20	Entrainment/de-entrainment	Entrainment is the process whereby liquid is captured (entrained) by a high-velocity steam flow.
D21	Flashing	The process whereby fluid changes from the liquid state to the vapor state due to a reduction in the fluid pressure (that lowers the saturation temperature).
D22	Not used	
D23	Flow & temperature distribution in PRHR bundle region	Local fluid flow and temperature in the IRWST region containing the PRHR tube bundle.
D24	Fluid distribution	Fluid flow profiles within a component.
D25	Break (flow limiter) energy release	The energy transfer associated with fluid flow out of the steam line flow limiter.
D26	Break (flow limiter) mass flow	The mass transfer associated with single and two-phase flow out of the steam line flow limiter.
D27	Flow resistance	The hydraulic resistance to flow due to form and wall viscous losses. These losses result in frictional pressure drops, which impede the flow.
D28	Flow split	The distribution of fluid flows in dividing flow circuits. This phenomenon also considers a potential temperature difference between the dividing flows.
D29	Fluid temperature	A basic fluid thermodynamic property.

Table G-1. (continued).

Code	Phenomena	Description
D30	Fouling	The process whereby contaminants, such as oxides, organic matter, etc., build up on the surface of a structure, impeding the heat transfer to or from the structure.
D31	Heat transfer	The process whereby energy is transferred from a hot source to a colder sink by virtue of their temperature difference.
D32	Heat transfer between PRHR and IRWST	The process whereby energy is transferred between the PRHR fluid and tubes and the IRWST pool fluid by virtue of their temperature difference.
D33	Heat transfer between primary and secondary	The process in the steam generator whereby energy is transferred from the primary coolant system fluid, through the steam generator tubes, to the secondary coolant system fluid by virtue of the difference in temperatures between fluids in the two systems.
D34	Heater power	The electrical power applied to heating elements (rods located near the bottom of the pressurizer).
D35	Horizontal fluid stratification	The process whereby gravity forces produce vertical fluid temperature and density gradients within a horizontal pipe. The phenomena can include separated flow of hot and cold fluid regions.
D36	Humidity	A measure of the quantity of water vapor contained in air. This parameter affects heat transfer from a component surface to a surrounding air environment.
D37	Interphasic condensation	The process where steam is cooled due to contact with a colder liquid, resulting in change of phase from a vapor to a liquid state at the interface between the two phases.
D38	Inventory (Steam volume expansion)	The depressurization process in a region containing steam and liquid, whereby the volume of steam expands as the liquid inventory (and level) are reduced.
D39	Level	For the CMT, "level" refers to the volume fraction (specified in percent) of the tank occupied by liquid (see page 3). For all other components, "level" is the vertical height of a column of single or two-phase fluid.
D40	Level swell	The process whereby the two-phase fluid level increases as the fluid density decreases. The phenomena can be caused by flashing, boiling, or convection of vapor into the component.
D41	Level swell & depletion	The process whereby the two-phase fluid level first increases as the fluid density decreases (see D40), but later falls because of a loss of fluid mass out the top of the component.
D42	Liquid carry-over	The process whereby liquid separation is not complete within a component, and liquid is carried out with the steam.
D43	Liquid distribution	The quantity and location of liquid outside the reactor coolant system (containment steam, inner wall condensate, IRWST, sump, and lower containment compartments).

Table G-1. (continued).

Code	Phenomena	Description
D44	Liquid holdup	The process whereby liquid flow is delayed or prevented due to trapping or storage.
D45	Loop asymmetry	A difference in thermal-hydraulic behavior that can be attributed to the geometrically asymmetric arrangement of the PRHR, CMTs, pressurizer, and postulated break location.
D46	Mass flow	The mass transfer (single and two-phase) into, within, or out of a component or system.
D47	Moderator temperature feedback	The change in core reactivity due to an increase or decrease in the temperature of the moderating fluid.
D48	Natural convection	The process whereby energy is transported between a solid surface and a liquid or gas by the combined action of heat conduction, energy storage and mixing motion, where the mixing motion is due solely to density differences caused by fluid temperature gradients.
D49	Not used	
D50	Noncondensible effects	The degree to which the presence of noncondensible gases impedes the heat transfer in any heat exchanger (PRHR, core, or steam generator) or directly affects the response of other phenomena, such as mass flow, condensation, flashing, and vapor volume expansion.
D51	Nonuniform steam/air distribution	The process whereby steam entering the containment interior at various locations mixes with air while gravity effects tend to cause steam/air mixtures to separate. This produces nonuniform steam/air mixture ratios within the containment interior. This phenomena can effect the heat transfer to the containment shell.
D52	PCCS evaporation	The process whereby fluid on the containment exterior surface undergoes a change of state from liquid to vapor due to the partial pressure of the vapor in the containment air gap being below the saturation pressure of the liquid. This phenomena affects the heat transfer from the containment exterior to the surrounding environment.
D53	PCCS water flow	The flow of liquid over the outer surface of the containment shell. This phenomena affects the heat transfer from the containment exterior to the surrounding environment.
D54	PCCS mixture convective heat transfer	The transport of energy from the containment exterior surface by gross fluid movement on the containment exterior surface and in the containment air gap.
D55	PCCS wetting	The extent and pattern of liquid coverage on the containment shell exterior surface. This phenomena affects the heat transfer from the containment shell exterior to the surrounding environment, since wetted surfaces exhibit greater convective heat transfer than dry surfaces.

Table G-1. (continued).

Code	Phenomena	Description
D56	Phase separation in tees	The separation of liquid from vapor in a two-phase mixture undergoing acceleration due to changing flow direction. Vapor accommodates the change in flow direction more readily than liquid due to its lower momentum. Thus, vapor prefers to take the branch while liquid prefers to take the run of a diverging tee.
D57	Pool flow	Local fluid flow in a pool.
D58	Pool level	The vertical height of the fluid in a pool.
D59	Pool thermal stratification	The process whereby buoyancy effects produce and/or sustain vertical fluid temperature and density gradients in a pool.
D60	Pool to tank structure heat transfer	The energy transferred from the hotter liquid in a pool to the colder surrounding tank walls, floor, and other structures.
D61	Preferential loop cooldown	The tendency of one RCS loop to cool faster than the other due to asymmetric conditions (for example as would be caused by one steam generator blowing down to containment while the other is isolated).
D62	Radiation heat transfer	The process whereby heat flows from a high temperature body to a body at a lower temperature when the bodies are separated in space. The region separating the bodies can contain some medium or a vacuum.
D63	Secondary level	The steam generator downcomer level as measured by plant instruments. This level actuates various trips and indicates the liquid mass available in the steam generator secondary.
D64	Secondary pressure	The absolute pressure measured in the steam generator above the separator/dryer region.
D65	SRV energy release	The energy convection associated with a mass flow out of the steam generator secondary via the safety relief valves.
D66	SRV mass flow	The mass transfer associated with a single- or two-phase mass flow out of the steam generator secondary through the safety relief valves.
D67	Steam-noncondensible mixing	The degree to which steam and noncondensible gases mix.
D68	Stored energy release	The rate at which energy is released from warm metal structures to the surrounding fluid.
D69	Subcooling margin	The difference between the fluid saturation temperature (function of the fluid pressure) and the subcooled fluid temperature. Provides a measure of the relative proximity to saturation conditions and the associated heat transfer regimes.
D70	Not used	
D71	Not used	
D72	Thermal driving head	The vertical fluid density gradients caused by the differences in fluid temperatures result in a buoyancy-related potential to drive fluid flow.

Table G-1. (continued).

Code	Phenomena	Description
D73	Thermal stratification and mixing	The process whereby gravity forces produce a vertical density gradient in a component, resulting in a corresponding temperature gradient. This effect is reduced by mixing due to flow within the component caused by other phenomena.
D74	Tube dryout	The process whereby the local outer surface of a steam generator tube becomes completely dry due to a lack of liquid inventory in the secondary.
D75	Tube voiding	The process wherein gas and/or vapor is trapped and accumulates in steam generator tubes as the system liquid inventory is depleted. This phenomena causes a decoupling of the primary and secondary systems, reducing the energy transfer between them.
D76	Two-phase mixture level	The vertical height of a continuous column of two-phase mixture which results from the mixture volume (inventory) being less than the component volume.
D77	Vapor space behavior	The process whereby a vapor space volume expands or compresses as the liquid inventory changes below the vapor space, resulting in pressure reduction or increase in the vapor space.
D78	Voiding	The process whereby gas and/or vapor is transported through or accumulates in a component.
D79	Not used	
D80	Not used	
D81	Passive heat sink	Heat transfer from fluids to structures and water pools. Typically, this phenomena refers to the containment.
D82	Air flow	Buoyancy-driven movement of air on the outside of the containment shell.
D83	Exterior-to-ambient heat transfer	The exchange of heat from the outside wall of the containment shell to the atmosphere, via a combination of convective, evaporative, and radiative heat transfer processes.
D84	Noncondensible segregation	The process whereby the water content of a steam-air mixture is removed or reduced via wall condensation heat and mass transfer. The resulting mixture next to the wall has a lower, or no, steam content, and this reduces or terminates the condensation process.
D85	Steam generator asymmetric behavior	The differing responses of the two steam generators, arising from differences in heat transfer. The asymmetric behavior can manifest itself as differences in fluid temperatures, flow rates, or voiding.
D86	Interior-to-wall heat transfer	The exchange of heat from the containment interior atmosphere to the inside wall of the containment shell via condensation, convection, and radiation heat transfer processes.

Table G-1. (continued).

Code	Phenomena	Description
D87	Condensation in ADS stages 1, 2, and 3 and spargers in IRWST	Condensation (see D9) processes within the ADS stage 1, 2, and 3 piping network from the top of the pressurizer to the spargers. Condensation may be interfacial (subcooled water may be available from the IRWST) or wall (a portion of the discharge lines and the spargers are submerged under water in the IRWST)
D88	CMT-to-IRWST differential head	The difference in static heads between water standing in the CMT (and its discharge line) and in the IRWST (and its discharge line). The connection point between these two systems is in the direct vessel injection line.
D89	Sparger pipe level	The water level in the ADS stage 1, 2, and 3 discharge line. This line initially is submerged under water in the IRWST. This level must be depressed to the spargers in order to support flow into the IRWST.
D90	Mixing	Interactions between cold liquid and warm liquid fluid regions.
D91	Upper head-to-downcomer bypass flow	During normal plant operation, this flow path passes water from the top of the reactor vessel downcomer into the reactor vessel upper head. The initial fluid temperature in the head is determined by this flow rate (and that of the guide tube path; these two flows are mixed in the upper head). Following reactor coolant pump trip, communication through this flow path may be in either direction. In this PIRT, this phenomena generally is of interest following pump trip, when steam may flow from the reactor vessel upper head into the downcomer. Disposition of this steam can affect plant response in many ways (its condensation affects the local pressure, may alter distribution of the RCS inventory, and may alter the break flow - especially for cold leg and direct vessel injection line breaks.
D92	Critical heat flux/dryout	Critical heat flux/dryout (see D15) relates to core cooling during the ADS blowdown period. RCS fluid conditions are chaotic, with flashing and boiling widespread. This phenomena is included to address the possibility that liquid starvation in the core region may result in a fuel rod heatup during the blowdown.
D93	Containment pressure	The thermodynamic total vapor pressure in the containment region surrounding the RCS piping and vessels.
D94	Boiling	The process whereby fluid changes from the liquid state to the vapor state due to wall heat addition.
D95	Two-phase level in upper plenum	The vertical height of the column of water (or two-phase fluid) within the reactor vessel upper plenum region (in particular, as it compares with the elevation span of the hot leg connections).
D96	Liquid distribution	The quantity and location of water within the various compartments and regions of the containment.
D97	Liquid subcooling	The difference between the local saturation temperature and fluid temperature within the various compartments and regions of the containment.

Table G-2. Component related geometric descriptions[1].

Code	Component	Description
C1	Accumulator	The accumulator is a large-radius, thick-walled, spherical tank. AP600 contains two accumulators, each connected via a medium-diameter injection line, containing a check valve, to a passive safety injection system line. The accumulator is not an active component during normal plant operation, when it is partially-filled with borated water (at the containment temperature) and pressurized (at a constant moderate pressure with nitrogen). If, during an accident, the primary coolant system pressure falls below the initial nitrogen pressure, water is injected from the accumulator into the primary coolant system. This depressurization might be caused unintentionally, such as by a break in the primary coolant system or intentionally, such as by the operation of the ADS. Note that in existing pressurized water reactors, the accumulators are cylindrical with spherical heads; the spherical AP600 accumulator, therefore, provides different relationships between the gas bubble volume, the gas/liquid interface contact area, and the depth of liquid in the tank than those in the accumulators of existing plants. If the depressurization of the primary coolant system is extensive, such as is the case with ADS operation, and all the water is expelled from the accumulator, then nitrogen is injected into the primary coolant system. If the primary coolant system repressurizes, then accumulator flow is terminated; in this situation, reverse flow into the accumulator is prevented by the action of the check valve. If the primary coolant system subsequently depressurizes again, then accumulator injection recommences whenever the primary coolant system pressure falls below the nitrogen pressure.
C2	ADS	The purpose of the Automatic Depressurization System (ADS) is to depressurize the primary coolant system sufficiently so that borated water can drain by gravity from the In Containment Refueling Water Storage Tank (IRWST) into the primary coolant system. This injection is only possible if the static head available from water in the IRWST is greater than the differential pressure created by fluid escaping from the primary coolant system into the containment. The principal flow path for this fluid escape is through the ADS (note, for accidents involving breaks between the primary coolant system and containment, the break path is in parallel with the ADS path). Therefore, the flow characteristics of the ADS are of great importance to overall safety of AP600. The ADS system is composed of four stages. Stages 1, 2, and 3 pass fluid from the top of the pressurizer, through an intricate network of medium-diameter valves, and discharge lines to spargers submerged under water in the IRWST. Stage 4 passes fluid from the hot leg, through a simple network of large-diameter pipes, directly into the containment atmosphere. Each ADS stage consists of two virtually-identical and completely-redundant trains (piping, valves, spargers, etc.). The ADS is activated upon an indication of declining primary coolant system inventory (a level in either core makeup tank that is less than 67%). The relatively small valves in ADS Stage 1 are activated first. The progressively larger valves in ADS Stages 2 and 3 are then opened sequentially based upon time delays after Stage activation. The largest valves are located in ADS stage 4, and these are opened upon an indication of a core makeup tank level below 20%.

[1]Within each accident category, the PIRTs subdivide the behavior according to the plant components. For the PIRTs, the AP600 system has been divided into 20 components and this table summarizes the functions and geometries of these components. The "code" column shows the indicator used in the master PIRTs to reference the information in this table.

Table G-2. (continued).

Code	Component	Description
C3	Break	The break component refers to a rupture in the pressure boundary of the primary or secondary coolant system that is assumed to open instantaneously. The definition of the break is different for the small break loss-of-coolant accident, main steam line break, and steam generator tube rupture accidents: Small Break LOCA The break is an unisolable opening in the pressure boundary between the primary coolant system and containment. The break location is assumed to be in any one of the four cold legs. For convenience, the break is assumed to be a circular hole, but breaks of irregular shape are not excluded. The size of the break is assumed to be 2-inch in diameter or smaller. A break of this size is not sufficiently large to remove the full core decay heat. The break may be located in any orientation on the pipe. Main Steam Line Break The break is assumed to be the double-ended rupture of the main steam line from one steam generator. This break opens two separate paths between fluid in the secondary coolant system and the containment atmosphere. One of these paths is shorter and cannot be isolated; it represents flow that exits the affected steam generator (i.e., the one whose steam line was assumed to be ruptured) into the containment. The other path is much longer, representing flow that exits the unaffected steam generator through its steam line, the turbine inlet common to both steam lines, and then backward through the steam line of the affected steam generator to the pipe rupture. This longer path is isolated within a few seconds of the break opening by closure of the main steam isolation valves. The broken piping has a diameter of several feet, however the break flow through both paths is effectively restricted to that allowed by the flow limiter that is located at the entrance from the steam dome of each steam generator to the main steam line. The flow limiter has a flow area smaller than the full flow area of the ruptured steam line pipe. Steam Generator Tube Rupture This unisolable break is assumed to result from a clean double-ended rupture of one steam generator tube at the tube sheet; the tube diameter is less than one inch. Whether the rupture occurs at the hot or cold end of the tube is not specified. The break opens two separate flow paths between fluid in the primary and secondary coolant systems. One of these paths is shorter, representing flow that exits from the steam generator inlet or outlet plenum through the tube sheet (the tubesheet side break). The other path is approximately 40 times longer than the first and represents flow that exits from the other plenum through the full length of the broken tube (the tube side break).

Table G-2. (continued).

Code	Component	Description
C4	Cold Legs	The cold legs are four large-diameter pipes that carry primary coolant from the discharges of the coolant pumps to the reactor vessel downcomer during normal operation. The cold leg piping runs are horizontal throughout their entire lengths, and these runs contain several large-radius, small-angle bends. The diameters, lengths, and arrangement of the four cold legs are virtually identical. However, there are several asymmetries among the cold legs that are related to piping penetrations (only the major penetrations are discussed here). The two cold legs on loop 1 (defined to be the one that the pressurizer is connected to) both contain small-diameter pressurizer spray penetrations located near the pump discharges. These nozzles are oriented 30° above the horizontal. In loop 2 (the non-pressurizer loop), the medium-diameter core makeup tank pressure balance lines are connected to the tops of both cold legs.
C5	Core	The reactor core is an arrangement of more than one hundred fuel assemblies, each composed of more than two hundred vertical, small-diameter fuel rods (see C8). The fuel assemblies each also contain more than 20 guide tubes and one instrument tube. The fuel rods are held in place by plates at their upper and lower ends, and by grid spacers at many intermediate locations. The height of the heated core is 12 ft., as is common to most commercial power reactors. Coolant flows upward through the core; the flow areas through the bottom and top core plates and through the grid spacers are smaller than the open flow area within the fuel rod bundle.
C6	Core Makeup Tanks	The two core makeup tanks (CMTs) are large thick-walled cylindrical vessels with spherical upper and lower heads. These tanks are elevated above the cold legs and are completely filled with borated water at the containment temperature during normal operation. A large-diameter discharge line is connected from the bottom head of each CMT. This discharge line contains a normally-closed CMT actuation valve and an orifice to limit the rate of flow out of the CMT; the discharge line delivers flow to the reactor vessel downcomer via the passive safety injection system line. A large-diameter pressure balance line is connected to the upper head of each CMT. The pressure balance lines are the inlets to the two CMTs; they deliver flow from the two cold legs (see C4) of loop 2 (the non-pressurizer loop).
C7	Downcomer/Lower Plenum	The reactor vessel downcomer is an annular fluid region, several inches thick, between the core barrel and reactor vessel wall. During normal operation, core coolant flows from the four cold legs, downward through the downcomer, and into the lower plenum. Fluid entering the lower plenum is turned upward to the inlet of the core. The AP600 lower plenum arrangement differs significantly from those of existing plants; the AP600 lower plenum is relatively open, with little resistance to flow, and contains a vortex suppression plate to stabilize the flow before it enters the core. The Passive Safety Injection System terminates at two large-diameter Direct Vessel Injection Nozzles on the downcomer.
C8	Fuel Rods	The core (see C5) is composed of thousands of fuel rods; the core heated length is 12 ft. The fuel rods are constructed from small-diameter, thin-wall zirconium tubes. Each fuel rod is loaded with hundreds of uranium dioxide fuel pellets that are axially restrained with springs. There is a small radial gap between the outer radius of the pellet and the inner radius of the tube; this gap is filled with an inert noncondensible gas.

Table G-2. (continued).

Code	Component	Description
C9	Hot Legs	The hot legs are two large-diameter pipes that carry primary coolant from the reactor vessel upper plenum to the steam generator inlet plena during normal operation. The hot leg piping runs are horizontal as they leave the reactor vessel; each hot leg has a single medium-angle, large radius bend that turns the pipe upward for several feet to meet the steam generator inlet plenum. The diameters, lengths, and arrangement of the two hot legs are virtually identical. However, there are several asymmetries between the hot legs that are related to piping penetrations (only the major penetrations are discussed here). The hot leg on loop 1 contains a large-diameter penetration for the pressurizer surge line; this nozzle is located on the top of the hot leg, about midway between the hot leg bend and the steam generator inlet plenum, and leaves the hot leg at a right angle. The loop 1 hot leg also contains a penetration for the PRHR inlet; this medium-diameter nozzle is located on top of the horizontal hot leg. The hot legs of both loops also contain large-diameter nozzles for the ADS fourth stage; these penetrations are on the tops of the horizontal hot legs near the bend.
C10	IRWST	The In-Containment Refueling Water Storage Tank (IRWST) is a very large irregularly-shaped compartment located around about one half of the AP600 containment periphery. The functions of the IRWST are to: provide the heat sink for the PRHR system (the PRHR heat exchanger is immersed in the IRWST), provide the discharge sink for ADS stages 1, 2, and 3 (two ADS spargers are located within the IRWST), and provide the source of safety-grade injection water following ADS blowdown. The geometries of the PRHR heat exchanger and ADS spargers are described, respectively, in C12 and C2. The IRWST injection lines are two medium-diameter pipes that carry fluid from the bottom of the IRWST tank downward several feet to the Passive Safety Injection System lines for injection into the reactor vessel. The IRWST is nearly filled with water at the containment temperature during normal operation; the normal water level is above the upper horizontal tube bundle section of the PRHR heat exchanger. However, the pool level can vary, decreasing as water is boiled off or evaporated and increasing as a result of ADS sparger discharge or condensate return from the containment interior (see C19).
C11	Not used	

Table G-2. (continued).

Code	Component	Description
C12	PRHR	The function of the Passive Residual Heat Removal (PRHR) system is safety-grade decay heat removal. The main feature of the PRHR system is its heat exchanger. The heat exchanger primary system is plumbed to the primary coolant system and the heat exchanger secondary system is the water inside the In-Containment Refueling Water Storage Tank (IRWST, see C10). The PRHR primary-side inlet piping begins at a medium-diameter nozzle on the top of the loop-1 (pressurizer-loop) horizontal hot leg section. The inlet piping is a medium-diameter line that contains a normally-open isolation valve. The inlet line contains an inverted trap (i.e., the inlet line rises to an elevation above that of the PRHR heat exchanger inlet). The heat exchanger consists of an inlet plenum, hundreds of long, small-diameter, thin-wall tubes, and an outlet plenum. The tube configuration is roughly "C"-shaped. From the inlet plenum, the tubes run horizontally into the IRWST, turn downward, and then horizontally again, to the outlet plenum that is located directly below the inlet plenum on the IRWST wall. The tube lengths encompassed by the vertical and horizontal sections are approximately the same. The tubes in the horizontal sections are on a square pitch; however, in the vertical section, this changes to a rectangular pitch. In the vertical section, the flow area into the tube bundle region in a direction parallel to the IRWST wall is significantly larger than the flow area normal to the IRWST wall. The medium-diameter pipe from the heat exchanger outlet plenum contains two normally-closed PRHR actuation valves in parallel. Downstream from these valves, the outlet pipe from the heat exchanger connects to the loop-1 steam generator outlet plenum.
C13	Not used	
C14	Pressurizer	The pressurizer is a large thick-walled cylindrical tank, with spherical upper and lower heads, that is elevated above the hot legs. During normal operation, the pressurizer contains well-separated saturated water and steam. Primary coolant system pressure control is attained by the combined actions of pressurizer spray and heater power. The spray nozzles are located in the steam space at the top of the tank and the heaters are located in the water space at the bottom of the tank. The spray function is lost if the primary coolant pumps are tripped, and powering of the heaters is prevented if a low pressurizer level is sensed. Pressures above the desired range result in the opening of the spray valves, admitting water at the cold leg temperature (see C4 for geometry of pressurizer spray piping) as a mist into the pressurizer steam space. Pressures below the desired range result in powering of the heaters. For pressures within the desired range, both the spray and heaters are inactive. The pressurizer surge line is a large-diameter pipe from the bottom of the pressurizer to the loop-1 hot leg (see C9). The inlet lines for ADS stages 1, 2, and 3 (see C2) are connected to the top of the pressurizer.
C15	Reactor Coolant Pumps	The four reactor coolant pumps function to circulate flow through the core and coolant loops during normal plant operation. Two pumps are located at the outlet plenum of each steam generator, and each pump directs flow into one of the two cold legs on each loop. The energy added to the primary system coolant when the pump motors are powered is significant.

Table G-2. (continued).

Code	Component	Description
C16	Steam Generator	The function of the two AP600 steam generators is to remove the core heat during normal operation. Each steam generator primary system consists of a thick-wall half-hemispherical inlet plenum (to which the hot leg is connected, see C9), a thick steel tubesheet, thousands of long, small-diameter, thin-wall, u-shaped tubes, and a thick-wall half-hemispherical outlet plenum (to which two reactor coolant pumps are connected, see C15). Each steam generator secondary system consists of a thick-walled cylindrical vessel with a large hemispherical upper head, an internal downcomer arrangement, centrifugal steam separators, impingement steam dryers, and major nozzle penetrations for feedwater inlet and steam line outlet. The separators are cylinders, with internals shaped so that fluid passing through them is forced to negotiate a swirling flow path. Swirling the flow separates the high-density fluid droplets from the low-density steam. The dryers are arrangements of multiple vanes, designed to separate water droplets from steam by impingement as fluid passes through them. The steam lines are large-diameter pipes, and a flow limiter is located at the steam line nozzles to restrict the flow rate out of the steam generator in the event of a large steam line rupture. The steam generator safety relief valves discharge fluid from the steam region to atmosphere.
C17	Sump	The sump is a compartment within the containment into which liquid may collect. Two medium-diameter injection lines, each containing a check valve, connect the bottom of the sump to the passive safety injection system lines. The function of the sump is to collect effluent from a pipe break so that it is available for injection into the primary coolant system. This function in many ways is comparable to that of the In-Containment Refueling Water Storage Tank (IRWST, see C10). However, the sump and IRWST differ in several ways: During normal operation, the sump is empty while the IRWST is nearly filled with water. The IRWST inventory can be increased due to ADS blowdown (through the spargers) or due to condensate returning from the containment heat removal system (see C19) but the sump level can only be increased by flow from a pipe break. The water in the IRWST initially is cold, and may be heated toward the containment saturation temperature by PRHR and ADS operation. Any water present in the sump comes from break effluent and therefore can be expected to be hot (perhaps at the containment saturation temperature) unless cooled by ambient heat loss. The actual geometry of the sump is not yet known, but it is assumed the sump floor elevation is below the elevation of the IRWST floor and above the direct vessel injection nozzles on the reactor vessel downcomer. This assumption is reasonable because the sump must be located lower than the hot and cold leg pipes in order to collect the effluent from a pipe break, yet must be high enough to allow gravity flow into the downcomer. Therefore sump injection involves a lower gravity driving head and a higher temperature liquid than does IRWST injection. Further, due to elevation considerations, sump injection cannot occur until the IRWST level falls below that in the sump, and this condition is not expected until very late (perhaps days or weeks) into an accident scenario. For the IRWST level to be depleted, its injection rate must exceed its replenishment rate (from the containment cooling system condensate). This condition can occur only if a long time has elapsed since the reactor scram so that the total steam flow to the containment and resulting condensate return rate are reduced. Therefore, sump injection can occur only during the very late stages of an accident.

Table G-2. (continued).

Code	Component	Description
C18	Upper Head/Upper Plenum	The reactor vessel upper head and upper plenum are two large fluid regions near the top of the reactor vessel. The upper plenum is located atop the core, and during normal operation functions to route coolant at the core outlet temperature from the core to the two hot legs. Coolant exiting the core is turned 90° to meet the hot legs, and to reach them must flow around multiple internal structures. The upper head is located above the upper plenum. Flow entering the upper head comes upward from the core through the guide tubes and upward through the bypass path from the upper annulus of the downcomer. Flow leaves the upper head downward through a support plate into the upper plenum. The guide tube flow rate is higher than that of the bypass path, and therefore during normal operation the upper head fluid temperature is below, but near the core outlet temperature. Both the upper plenum and upper head contain very thick steel structures, many of which have small surface areas.
C19	Containment Interior	The containment is a large free-standing medium-thickness steel shell that contains all of the components described in C1 through C18. The steel shell is cylindrical, with a hemispherical upper head. The function of the containment is to confine any fission products that may be released during an accident. To succeed at this function, the containment must remain leak free, even when pressurized above atmospheric pressure as can occur during many accidents. Despite containing many components, the containment interior has a very large free volume that is filled with air during normal operation. The containment diameter is more than 100 ft. In addition to its steel shell and internal components, the containment contents also include many thick reinforced concrete structures. The safety-grade containment heat removal mechanism involves transferring heat from the containment atmosphere, across the steel shell, to the environmental atmosphere.
C20	Containment Exterior	The containment exterior consists of a large reinforced concrete structure that surrounds the free-standing containment steel shell (see C19). The concrete structure acts as a missile barrier, but also functions to direct air flow to the outside surface of the containment shell. The air intakes are large openings near the top of the concrete structure. Air flows downward in an annular space inside the structure, turns and is drafted upward in another annular space that has the containment shell as an inner wall, and finally is discharged back to the environmental atmosphere near the top of the concrete structure. Heat transfer on the outside of the containment shell is aided by the Passive Containment Cooling System (PCCS) that sprays water on the top of the containment shell hemispherical head. This water flows downward on the outside of the shell, and its evaporation, caused by heat removed across the shell wall, aids the heat transfer process on the outside of the shell wall.

Table G-3. Phenomena related geometric and function descriptions.[2]

Code	Component-Specific Phenomena	Description
G1	Accumulator/ Noncondensible Effects	The accumulator injection behavior is primarily determined by the expansion characteristics of its noncondensible gas (nitrogen) bubble. Initially, the accumulator gas and liquid are isothermal at the containment temperature. If accumulator injection occurs (see C1), the accumulator pressure falls, and the gas bubble volume expands at the same volumetric rate at which liquid is expelled from the tank. This gas expansion is accompanied by a cooling of the gas, and subsequent flows of heat from the accumulator liquid and tank walls into the gas that tend to reheat the gas. The accumulator pressure is important because the difference between it and the primary coolant system pressure is what drives the accumulator injection flow. The accumulator pressure is determined by the gas bubble volume and the gas temperature.
G2	Accumulator/Flow	The driving force for accumulator injection flow (see C1 and G1) is the differential pressure between the accumulator gas bubble and the primary coolant system. The flow obtained with this driving force is that allowed by the flow resistances of the system, including the form losses at the tank exit and valve, and the frictional losses in the injection line. As discussed in C1, the accumulator will inject nitrogen into the primary coolant system once all of its water inventory has been expelled. Further, accumulator injection will be terminated if the primary coolant system is repressurized and the possibility exists for an intermittent accumulator injection mode.
G3	ADS/Flow Resistance, Mass Flow, Energy Release, Noncondensible Effects, and Choking in Complex Geometry	The flow characteristics of the ADS determine both the timing of the primary coolant system blowdown and the IRWST injection response following the blowdown. These flow characteristics include the mass flow rate of the coolant leaving the primary coolant system, its energy content, and the resistance to flow through the ADS system piping and valves. The presence of noncondensible gas in the fluid flowing through the ADS can alter the behavior of that flow. The ADS blowdown phase is controlled by the flow characteristics of ADS Stages 1, 2, and 3 that determine the rate at which mass and energy is expelled from the primary coolant system. Flows through these paths are driven by the pressure difference between the pressurizer and the spargers in the IRWST. The fluid entering the ADS lines may be single-phase liquid, single phase steam, or a two-phase mixture. During the blowdown phase, the differential pressure across the ADS is large, and its performance will be determined by choking (critical flow). Therefore, only the geometry of the ADS (see C2) upstream of the choked location will be pertinent.

[2]This table describes the phenomena related geometric and function considerations applicable to a specific component. The component related geometric and function descriptions are given in Table G-2. The "code" column shows the indicator used in the master PIRTs to reference the information given in this table.

Table G-3. (continued).

Code	Component-Specific Phenomena	Description
G3 Cont.		During injection phases (following an ADS blowdown) the ADS stages 1, 2, and 3 are inactive because the pressure difference between the primary coolant system and containment is low, and the ADS spargers in the IRWST are likely to be covered with water. Therefore, only ADS stage 4 may be active during the injection phase and its flow characteristics are important because it is the principal mechanism for primary coolant system decay heat removal. Fluid is expelled through ADS stage 4 by the pressure difference between the hot leg regions of the primary coolant system and the containment atmosphere. As with the earlier ADS stages, the fluid entering the ADS stage 4 lines may be single-phase liquid, single-phase steam, or a two-phase mixture. The differential pressure across ADS stage 4 is small, and its performance will be determined by subsonic, friction-dominated phenomena through the resistance of the entire length of its piping network (see C2). Because the ADS stage 4 operates at a low pressure, steam densities are low, fluid void fractions are high, and the system may be required to pass significant quantities of noncondensible gas (released by the accumulators during ADS blowdown, see C1). These factors affect the flow resistance and performance of the stage 4 ADS.
G4	Break (SBLOCA)/Mass Flow, Energy Release, Flow Resistance Noncondensible Effects	Fluid in the primary coolant system is accelerated out the break because the pressure in the containment is lower than that in the primary coolant system (see C3). This fluid can be single-phase liquid or steam, two-phase liquid and steam, with or without noncondensible gas. As the fluid is accelerated, its pressure falls and localized fluid flashing chokes the flow (usually at the break plane). The mass flow rate through the break typically is limited by critical flow until the ratio of the primary coolant system to containment pressure falls below about 2. For lower pressure ratios, the break flow is determined by the flow resistance resulting from frictional flow losses. The energy release at the break results from fluid at the upstream enthalpy being convected out of the primary coolant system by the break flow rate. Noncondensible gases present at the break have the potential to alter the critical flow rate, the frictional pressure drop, and the break energy release rate.
G5	Break (MSLB)/Flow Limiter Mass Flow, Flow Limiter Energy Release, Flow Resistance	Fluid in the secondary coolant system is accelerated out the break because the pressure in the containment is lower than that in the secondary coolant system. This fluid can be single-phase steam or liquid, or two-phase steam and liquid. The mass flow rate through the break typically is limited by critical flow at the flow limiter (see C3) until the ratio of the pressures in the secondary coolant system and containment falls below about 2. For lower pressure ratios, the break flow is determined by the flow resistance resulting from frictional flow losses (of which the flow limiter is only one component). The energy release at the break results from fluid at the upstream enthalpy being convected out of the secondary coolant system by the break flow.

Table G-3. (continued).

Code	Component-Specific Phenomena	Description
G6	Break (SGTR)/Mass Flow, Energy Release, Flow Resistance	Fluid in the primary coolant system is accelerated out the break because the pressure in the secondary coolant system is lower than that in the primary coolant system (see C3). This fluid can be single-phase liquid or steam, or two-phase liquid and steam. The break flow initially may be choked. However, the ratio of primary to secondary system pressures initially is only slightly above 2, and this ratio falls rapidly during the course of a steam generator tube rupture event (because the primary system pressure falls and the secondary system pressure rises). Therefore, the break mass flow is more often determined by the flow resistance caused by frictional pressure drop than it is by critical flow. The mass flow rate through the tubesheet side break is markedly larger than that through the tube side break because of the much larger frictional pressure drop associated with flow through the long tube. The energy release at the break results from fluid at the upstream enthalpy being convected out of the primary coolant system by the break flow.
G7	Cold Legs/Stored Energy Release	During normal operation, the cold legs carry fluid that is at the core inlet temperature. The heat stored in the pipe walls (that are fabricated from carbon steel, several inches thick, with a stainless steel cladding) is available to flow out into the primary coolant, that may be at significantly reduced temperatures during accidents.
G8	Cold Legs/PBL-to-Cold Leg Tee Phase Separation, Voiding	The core makeup tank (CMT) pressure balance lines penetrate the tops of the two loop 2 cold legs (see C4). These lines are the paths by which fluid enters the CMTs during their recirculation phase. Recirculation through a CMT stops when the associated cold leg saturates and voids. Under these conditions, steam may be admitted into the CMT pressure balance line. This steam can collect at the top of the pressure balance line, blocking the flow of liquid to the CMT. However, it is the flow of steam into the pressure balance line that leads to the blocked condition, and this steam flow is controlled by the processes occurring at the cold leg/pressure balance line tee.
G9	Cold Legs/Loop Asymmetric Effects	The lengths, diameters, and arrangements of the four cold legs are virtually identical. There are, however, two asymmetries related to their penetrations (see C4): the two cold legs on loop 1 (the pressurizer loop) have nozzles for pressurizer spray, while the two cold legs on loop 2 (the non-pressurizer loop) have nozzles for the core makeup tank pressure balance lines. In general, the pressurizer spray function is immaterial to accident simulations, and therefore asymmetries associated with pressurizer spray nozzles are not significant. However, considerable asymmetry in the conditions between the loop-1 and loop-2 cold legs is expected because of the CMT pressure balance line configuration. In addition, there is a potential for asymmetric cold leg conditions because the passive residual heat removal system is connected only to one loop (specifically, from the loop 1 hot leg to the loop 1 steam generator outlet plenum).
G10	Core/Mass Flow Including Bypass	The core coolant flow is responsible for removing the heat generated within the fuel rods; this typically results in an increasing fluid temperature from the bottom to the top of the core. A small fraction of the total core flow is bypassed around the core fuel assemblies and is used to cool ancillary regions within the reactor vesse

Table G-3. (continued).

Code	Component-Specific Phenomena	Description
G11	Core/Stored Energy Release	During normal operation, the fluid and structure temperatures are high. The heat stored in the structures is available to flow into the primary coolant. Since most accident sequences result in significantly reduced core fluid temperatures, the structure temperatures generally lag those of the adjacent fluid. During most accidents the structures tend to function as heat sources to the fluid; initial structure temperatures typically are the same as the adjacent fluid and the energy stored in the structures is released into the fluid as it cools. This description covers the stored energy release from core structures (such as the support plates); the fuel rods are treated elsewhere.
G12	Core/Flashing, Flow Resistance, Voiding	Because the total of the wetted perimeters of the fuel rods is so large, the hydraulic diameter of the core is quite small, and therefore its flow resistance is relatively high (as compared with that of other features in the primary coolant system flow loop). The flow restrictions at the core support plates and grid spacers result in lumped flow losses that are added to the distributed wall friction loss. These flow resistances determine the total core pressure drop and the pressure distribution throughout the core. The accidents investigated generally include a primary coolant system depressurization, and the flashing behavior within the core is determined by the local fluid temperature and pressure distributions. The voiding caused by flashing tends to increase the flow resistance.
G13	Core Makeup Tanks/CMT-to-Loop Differential Density, Flow Resistance, Voiding	When the CMTs are actuated, a recirculation flow is established. The flow loop is from the CMT discharge, through the reactor vessel, cold leg, and pressure balance line, and back to the CMT. The distribution of fluid temperatures around this flow loop provides a buoyancy driving force for flow through the loop. This driving force is opposed by the flow losses around this loop. The major loop flow resistances are associated with the reactor vessel, especially within the core, and the orifice in the CMT discharge line. The tall pressure balance lines fill with hot water, and the density difference between water in these lines and in the CMTs provides a continual driving force for the recirculation flow. Voiding within the pressure balance line (especially at the top bend) can terminate CMT recirculation.
G14	Core Makeup Tank/Level, Thermal Stratification, Flashing, Condensation, Noncondensible Effects	Following CMT actuation, the recirculation flow (see C6) continually delivers warmer water to the top of the CMT. While some mixing between the inlet and tank water may occur, the warm water entering the tank is expected to remain near the top of the tank, thermally-stratifying the fluid in the tank. CMT thermal stratification affects the temperature of the fluid injected from the bottom of the tank, but more importantly the thermal distribution of the fluid in the tank affects the response of the tank level both during the CMT draining phase and during the ADS blowdown phase. During the draining phase, steam may be passed through the CMT pressure balance line into the top of the tank. If the tank water is thermally stratified, then the warm water residing near the tank level places a buffer between steam and the cold water that represents a condensation sink. Noncondensibles convected into the CMT or generated within the CMT as dissolved gas comes out of solution affects the condensation. During the ADS blowdown phase, the CMT flashing behavior is affected by the thermal distribution of the liquid within the CMT. All of these phenomena are of significance because they affect the indicated CMT level, upon which the ADS actuation is based.

Table G-3. (continued).

Code	Component-Specific Phenomena	Description
G15	Downcomer/Lower Plenum Stored Energy Release	The structures in the downcomer and lower plenum generally are thick, but with relatively small heat transfer areas. In an accident situation, the release of energy stored in these structures during normal operation can be significant and extend over long periods.
G16	Downcomer/Lower Plenum/Asymmetric Effects, Flow Distribution	There may be nonuniform fluid temperature distributions in the downcomer during accident sequences because of the potential for different temperature fluids entering the downcomer from the cold leg and the Direct Vessel Injection nozzles.
G17	Downcomer/Lower Plenum/Level	The static head created by the liquid level standing in the downcomer is the driving force to push fluid through the core during phases with CMT, accumulator, or IRWST injection.
G18	Downcomer/Lower Plenum/ Condensation, Flashing	The flow of steam from the upper head, through the bypass, into the upper regions of the downcomer can result in condensation. The condensation of steam on cold walls and liquid within the downcomer affects downcomer level and temperature. Flashing in the downcomer and lower plenum will occur during ADS blowdown.
G19	Downcomer/Lower Plenum/ Noncondensible Effects	This specific phenomena applies only following discharge of nitrogen from the accumulators (for the accidents considered, this discharge will occur only during ADS blowdown). A very large volume of nitrogen will be released into the downcomer through the Direct Vessel Injection nozzles. Noncondensible gas may alter flashing and condensation processes or the distribution of liquid.
G20	Fuel Rods/Core Power, Decay Heat, CHF, and dryout	During operation, the nuclear heat is released mainly within the fuel pellets, although minor fractions of the heat are deposited elsewhere (in the nearby structures and fluids). Following a reactor scram, the rate at which heat is produced is quickly reduced to about 93% of its initial rate because the nuclear fission process is terminated. After scram, the core power is due mainly to fission product decay heat. The decay heat rate initially is about 7% of the pre-scram core power, and its rate of decline is slow. A main safety concern is that both the fission and decay heat be continuously removed from the fuel rods.
G21	Fuel Rods/Stored Energy Release	The nuclear heat, deposited mainly within the fuel pellet, must flow radially outward through the fuel pellet, gas-filled gap, and cladding to reach the core coolant on the outside of the zirconium fuel rod tube. The thermal conductivity of the pellet is low, and that of the gap is even lower. During operation, the fuel pellet temperatures are very high (thousands °F). The heat stored within the fuel rods therefore is very high, and its release into the coolant can be a significant phenomena.
G22	Hot Legs/Stored Energy Release	During normal operation, the hot legs carry fluid that is at the core outlet temperature. The heat stored in the pipe walls (that are fabricated from carbon steel, several inches thick, with a stainless steel cladding) is available to flow out into the primary coolant, that may be at significantly reduced temperatures during accidents.

Table G-3. (continued).

Code	Component-Specific Phenomena	Description
G23	Hot Legs/Loop Asymmetric Effects	The lengths, diameters, and arrangements of the two hot legs are virtually identical. There are, however, two asymmetries related to their penetrations (see C9): only the hot leg on loop 1 has penetrations for the pressurizer surge line and PRHR inlet line. Asymmetric responses between the loop 1 and 2 hot legs may be expected due to pressurizer draining effects, early ADS effects (stages 1, 2, and 3 discharge from the top of the pressurizer), and PRHR effects.
G24	Hot Legs/Phase Separation in Tees	Phase separation at the hot leg/pressurizer surge line tee controls the state of the fluid passed to the pressurizer, and this affects ADS stage 1, 2, and 3 performance. Phase separation at the hot leg/ADS stage 4 tees controls the state of the fluid passed out ADS stage 4 to the containment. Phase separation at the hot leg/PRHR inlet line tee controls the state of the fluid entering the PRHR system. All of these effects have the potential to be significant.
G25	Hot Legs/Entrainment, CCFL, Horizontal Fluid Stratification, Voiding, Countercurrent Flow	These phenomena address the interactions between liquid and vapor within the hot leg and are important because of their effect upon ADS and PRHR performance (see G24). Specifically, the fluid state and flow velocities of liquid and vapor within the hot legs determine the behavior at the pressurizer surge line, ADS stage 4, and PRHR inlet tees. If the hot leg fluid is stratified (steam over liquid), then the fluid passing out these tees will be primarily steam and its energy content will be high. If the steam flow rate is high enough, then liquid droplets will be entrained by the steam flow and be carried out the tees. The CCFL (countercurrent flow limiting) and countercurrent flow phenomena are listed to address behavior where liquid may be stored within the hot legs. CCFL may prevent fallback of liquid from the hot leg into the reactor vessel upper plenum. Countercurrent flow may be encountered in a reflux cooling situation.
G26	IRWST/Pool Level, Pool Flow and Temperature Distribution, Thermal Driving Head, Thermal Stratification	The pool level and temperature determine the static head available for injecting coolant into the reactor vessel. The pool level also determines the extent to which the outside of the PRHR heat exchanger tubes are covered and capable of removing heat. The pool flow and temperature distributions determine the heat transfer coefficients and sink temperatures applicable on the outside of the PRHR heat exchanger tubes. These flow and temperature distributions can vary with location within the tank, and are expected to be considerably different in the free tank, near the PRHR heat exchanger tube bundle, and near the ADS spargers. In IRWST regions with little induced or convected flow, the tank water is expected to thermally stratify (warm water residing over cooler water).
G27	IRWST/Flow Resistance, Discharge Line Flashing	The flow resistance of the IRWST discharge piping, fittings, and check valves can be a significant factor in determining the injection flow rate. Flashing in the IRWST discharge line may occur if the IRWST fluid becomes hot enough, and in that event, the two phase flow in the discharge line can reduce the injection flow rate.
G28	IRWST/Pool-to-Tank Wall Heat Transfer, Ambient Heat Loss	The boundaries of the IRWST are thick steel-lined concrete containment walls. These walls have the potential to be significant heat sinks for water in the tank. In addition, ambient heat loss to these walls and from the pool free surface can be a significant fraction of the IRWST heat load.

Table G-3. (continued).

Code	Component-Specific Phenomena	Description
G29	IRWST/Interphase Condensation	The interphase condensation phenomena for the IRWST regards the discharge of steam or two-phase mixture from the ADS spargers into IRWST pool or the condensation of steam generated by PRHR heat transfer. The sparger holes are of small diameter. The sparging process generally is expected to result in complete condensation of the steam flow.
G30	PRHR/Differential Density, Flow Resistance, PRHR-to-IRWST Heat Transfer, Condensation	The PRHR-to-IRWST heat removal is the primary phenomena of interest for the PRHR system. Flow through the PRHR primary side may be forced if the reactor coolant pumps are operating. However, in most accident sequences the primary coolant pumps will be tripped, and therefore flow through the PRHR primary side must be driven by natural-circulation buoyancy forces. These buoyancy forces are generated by the difference in density between fluids in vertical sections of the PRHR inlet and outlet flow paths. Most of the elevation change in the PRHR flow loop is found over the elevation span of the PRHR heat exchanger tube bundle vertical section. Therefore, the difference in density between fluid in the PRHR inlet piping and that in the PRHR heat exchanger tubes is the main driving force for flow through the PRHR primary system. This flow equilibrates at a rate such that the buoyancy driving force is balanced by the flow resistances around the PRHR primary-side loop.
G31	PRHR/Phase Separation in Tees, Noncondensible Effects, Voiding	In general, voiding of the PRHR inlet line improves the PRHR primary-loop natural circulation driving force. However, because the PRHR inlet piping contains an inverted trap at its high point, the collection of void (steam or noncondensible gas) at that point can interrupt PRHR primary-side flow. See discussions in C9, C12, G24, and G25.
G32	Not used	
G33	Pressurizer/Level (Inventory), Vapor Space Behavior, Flashing	Most accidents result in declining pressurizer level and pressure. The pressurizer is the only region in the primary coolant system containing saturated water during normal operation. Therefore, declining pressurizer level and pressure results in expansion of the pressurizer vapor space and flashing of the saturated water to steam. This pressurizer behavior generally controls the depressurization rate of the primary coolant system during the initial phases of most accidents.
G34	Pressurizer/CCFL	Countercurrent Flow Limiting (CCFL) phenomena may occur at the pressurizer/surge line junction during phases where the ADS stages 1, 2, and 3 are active.
G35	Pressurizer/Stored Energy Release, Heater Power	During normal operation, the pressurizer fluid is at saturation for the primary coolant system pressure. The heat stored in the tank wall (that is fabricated from carbon steel, several inches thick, with a stainless steel cladding) is available to flow out into the primary coolant, that may be at significantly reduced temperatures during accidents. In addition, heat may be added to the primary coolant by the pressurizer heaters.

Table G-3. (continued).

Code	Component-Specific Phenomena	Description
G36	Pressurizer/Level Swell, Entrainment, Thermal Stratification, Mixing	These phenomena relate generally to pressurizer behavior during operation of ADS stages 1, 2, and 3. Specifically, opening of the ADS valves causes a blowdown of the primary coolant system through the nozzle on the top of the pressurizer. In this condition, the pressurizer fluid flashes, and the addition of this vapor swells the mixture level upward in the tank. The location of the flashing will be determined by the thermal distribution of liquid within the pressurizer. The steam flow rates may be high enough to entrain water droplets, and these may impinge upon the pressurizer dome and be deentrained, instead of being carried out the ADS line. The steam flows affecting this behavior may be generated internally, due to flashing within the pressurizer, or externally, due to flashing elsewhere in the primary coolant system and convected into the pressurizer via the surge line. CCFL may occur at the surge line nozzle (see G34).
G37	Reactor Coolant Pumps/ Coastdown Performance	The mechanical energy stored in each reactor coolant pump flywheel (on the pump shaft) is considerable. When power to the pump motor is interrupted, the coastdown of pump impeller, shaft, and motor requires several minutes. This effect can be significant, because the pump continues to generate positive head and coolant loop flows during the coastdown period. Many plant system actuations are expected to occur during the coastdown period, and therefore pump coastdown behavior can affect behavior of these systems during their initiation periods.
G38	Reactor Coolant Pumps/Flow Resistance	When power to the pump motor has been cut and the pump coastdown is complete, the pump impeller effectively represents a blockage that natural circulation flow through the coolant loop must negotiate. The blockage is so large that the pump resistance to flow can represent a very large part of the total loop flow resistance. The pump flow resistance is a strong function of the impeller status during natural loop circulation. If the loop circulation rate is high, the impeller might turn slowly in the loop flow, while if the loop recirculation rate is low the impeller might not turn at all, due to pump shaft friction considerations. This distinction is significant because the flow resistance through a slowly-turning impeller is much lower than that through a stopped impeller.
G39	Steam Generator/Primary-to-Secondary Heat Transfer, Secondary Level, Secondary Pressure, Tube Voiding, Noncondensible Effects	These steam generator-related phenomena pertain to the small break LOCA and steam generator tube rupture accidents. Steam generator primary-to-secondary heat transfer is controlled by the fluid state and flow conditions on the primary and secondary sides of the tubes. Initially, the primary side pressures and temperatures are higher than those on the secondary side, and heat transfer is from the primary to the secondary. However, during the accident progression the primary side pressure and temperature tend to fall below those of the secondary. The heat transfer in either direction can be adversely affected by voiding on either side of the tubes: Primary-to-secondary heat transfer can boil off secondary inventory and in the process void the outside of the tubes. Conversely, secondary-to-primary heat transfer can boil water inside the tubes, and once this has occurred, the heat sink on the primary side is lost. Heat transfer in either direction also can be adversely affected if noncondensible gas accumulates within the steam generator tubes.

Table G-3. (continued).

Code	Component-Specific Phenomena	Description
G40	Steam Generator/Preferential Loop Cooldown, Asymmetric Behavior	These phenomena pertain to the main steam line break accident. The double ended rupture of one steam line initially results in a blowdown of both steam generators; however, the main steam line isolation valves soon close, effectively limiting further blowdown only to the steam generator with the ruptured steam line. Blowdown of the affected steam generator continues until the secondary pressure in that steam generator reaches the containment pressure. Heat removal through the affected steam generator is at a very high rate, and this results in an asymmetric preferential primary system cooldown in the coolant loop with the affected steam generator. The cooldown of the affected steam generator results in the unaffected steam generator becoming a heat source, with possible voiding of the u-tubes and interruption of natural circulation in the unaffected loop. After the blowdown of the affected steam generator ends, the unaffected steam generator may become a heat sink again, depending on the amount of cooling provided by the PRHR. The asymmetric behavior of the loops arises from the asymmetric heat transfer to the steam generators.
G41	Steam Generator/Thermal Driving Head	This phenomena pertains to the affected steam generator primary side during a main steam line break accident. The high heat transfer rate from the primary coolant system to the affected steam generator results in a large differential temperature between the hot and cold legs on that loop. The large hot-to-cold density difference drives natural circulation loop flow through the affected loop at a high rate.
G42	Steam Generator/ Entrainment, Flashing, Level Swell and Depletion, Tube Dryout	These phenomena pertain to the affected steam generator secondary side during a main steam line break accident. The rapid blowdown of the affected secondary side at first causes its water to flash to steam, and this added steam both entrains liquid and swells the secondary level upward. As the blowdown continues, the affected steam generator inventory is depleted as steam and liquid escape out the broken steam line. Eventually, this inventory depletion lowers the secondary level and dries out the outer surface of the steam generator tubes. Tube dryout significantly reduces the primary-to-secondary heat transfer.
G43	Steam Generator/Separator and Dryer Liquid Carryover	These phenomena pertain to the affected steam generator secondary side during a main steam line break accident. Both the separators and dryers are designed to remove trace amounts of liquid present in the fluid passing through them during normal operation (see C16). During the initial portions of the blowdown of the affected secondary, liquid is both raised upward and entrained by the high steam flow rate (see G42). These processes generally flood the separator and dryer regions with water and under these conditions both the separators and dryers may be expected to pass significant quantities of water. These phenomena are significant because the water passed will escape the affected steam generator out the broken steam line. The affected steam generator primary-to-secondary heat transfer controls the plant response during a main steam line break accident, and water passed out the steam line is not available to remove heat from the primary coolant system.

Table G-3. (continued).

Code	Component-Specific Phenomena	Description
G44	Steam Generator/Safety Relief Valve Mass and Energy Flows	These phenomena pertain to the affected steam generator secondary side during a steam generator tube rupture accident. The broken tube communicates primary coolant system pressure to the secondary side and pressurization of the secondary side results in opening the safety relief valves. The passage of fluid out the safety relief valves to the atmosphere removes both mass and energy from the combined (i.e., primary and affected steam generator) system.
G45	Upper Plenum, Upper Head/ Flashing, Voiding, Vapor Space Compression	The upper plenum and upper head regions contain hot fluid and are elevated high in the reactor vessel, and therefore during depressurization events the fluid there is among the first in the coolant system to flash. Upper plenum and upper head flashing cause these regions to void, and this voiding has the potential for displacing water to elsewhere in the coolant system. For example, this displacement has been shown to cause a refilling of the pressurizer after it has first emptied. Once the upper head fluid has flashed and this region voided, interphase condensation is unlikely to collapse the voids. The fluid there tends to stratify (into a steam region located over a liquid region) with a small interphase heat transfer area that limits the interphase condensation rate. A subsequent repressurization of the primary coolant system thus results in a simple compression of the upper head steam space.
G46	Upper Plenum, Upper Head/ Loop Asymmetric Effects, Flow Split, Entrainment, De-entrainment	These phenomena pertain primarily to the upper plenum region. Flow behavior in the upper plenum determines the proportions of the total core outlet flow that is routed to each hot leg. An asymmetry in the core outlet fluid conditions (for example, colder water on the side of the core adjacent to the affected loop during a main steam line break accident) can be propagated through the upper plenum to the hot legs. Mixing of the core outlet fluid within the upper plenum reduces the asymmetry. Given the complexity of the internal structures in the upper plenum, entrainment and de-entrainment phenomena can be important both to the pressure drop through the upper plenum, and the conditions of the fluids passed to the hot legs.
G47	Upper Plenum, Upper Head/ Stored Energy Release	During normal operation, the upper plenum and head contain fluid that is near the core outlet temperature. The heat stored in the structures (that generally are fabricated from carbon steel, several inches thick, with a stainless steel cladding) is available to flow out into the primary coolant, that may be at significantly reduced temperatures during accidents. Stored energy release in the upper head region is more important than in other regions because heat added to the fluid here tends to sustain a voided upper head (see G45).

Table G-3. (continued).

Code	Component-Specific Phenomena	Description
G48	Containment Interior/ Condensation, Condensate Transport, Liquid Distribution, Liquid Holdup, Natural Convection, Passive Heat Sink, and Interior to Wall Heat Transfer	The safety-grade containment heat removal mechanism involves transferring heat from the containment atmosphere, across the steel containment shell, to the environmental atmosphere. On the inside surface of the shell, heat transfer is by condensation of steam (flowing from ADS stage 4 and any breaks in the primary coolant system) on the cooler shell. For this process to be continuous, natural convection air flows within the containment must circulate the containment atmosphere, and this circulation is set up by the thermal effects of cooling on the containment shell wall. The containment design calls for the condensate to flow downward on the shell to a location above the IRWST (see C10). There, a series of gutters collects the condensate and returns it to the IRWST, where it is available for injection into the primary coolant system. Liquid holdup refers to the inventory of condensate that at any time is not in the IRWST: in other words, the condensate flowing on the inside of the shell plus that trapped in locations where it cannot return to the IRWST. The passive heat sink refers to energy transferred to and stored in structures without being transferred to the environment.
G49	Containment Interior/ Noncondensible Effects, Nonuniform Distributions of Steam and Air, Noncondensible Segregation, Steam-Noncondensible Mixing	Noncondensible gas has the potential to affect the condensation heat transfer process on the inside of the containment shell (see C19 and G48) in two important ways. First, the containment atmosphere will be a mixture of air and steam, and wall condensation heat transfer is degraded by the presence of the air. Since the containment is initially air-filled, the air fractions of the containment atmosphere during accidents can be expected to be large. Second, nonuniform distributions of air/steam mixtures may be expected within the containment. Steam will be evolving from a few localized sites (at the ADS stage 4 discharges and any assumed pipe break). Steam and air will be mixed and convected upward to reach the condensing surfaces. Once there, the steam will be condensed out of the mixture, leaving pure air at the condensation site. The effects of these nonuniform distribution issues are not known.
G50	Containment Exterior/Air Flow, PCCS Evaporation, PCCS Water Flow, PCCS Mixture Convective Heat Transfer, PCCS Wetting, Chimney Effects, Humidity, Atmospheric Temperature, Radiation Heat Transfer, Exterior-to-Ambient Heat Transfer	Heat transfer on the outside of the containment steel shell is by evaporation of liquid deposited upon the shell by the Passive Containment Cooling System, and by convection to air flow upon the shell. The phenomena that are termed PCCS-related regard the behavior of the liquid on the containment shell outer surface. The other phenomena regard the condition of the ambient environment, and the manner in which the atmosphere is drawn into and discharged from the containment structure.

Table G-4. Evidence supporting the PIRT phenomena ranks.

In Revision 0 of this report, the perceptions regarding the phenomena and their ranking resulted from the individual and collective knowledge of the PIRT development team members and reviewers and limited AP600 analytical and experimental information. The phenomena and rankings existing by the third quarter of CY-1994 (Revision 0 of this report) were based upon the information shown under code E1. The additional information used to develop Revision 1 of this report is shown under code E2.

Code	Reference
E1	P. A. Roth and M. G. Ortiz, *Effects of Containment Back Pressure on the Long-Term Coolability of the AP600 Design*, Letter Report PDB-18-93, EG&G Idaho, Inc., December 24, 1993.
	M. G. Ortiz, et al., *Investigation of the Applicability and Limitations of the ROSA-IV Large Scale Test Facility for AP600 Safety Assessment*, NUREG/CR-5863, December 1992.
	Y. Kukita, et al., "ROSA-AP600 Program: Confirmatory Testing of AP600 Design at the ROSA-V Large Scale Test Facility", *Proceedings of 20th Water Reactor Safety Information Meeting*, NUREG/CP-0126, October 1992.
	J. E. Fisher, S. M. Sloan, and M. G. Ortiz, *Preliminary RELAP5 Scoping Calculations for the Westinghouse AP600 Design* (Draft), EGG-2687, EG&G Idaho, Inc., September 1992.
	S. M. Sloan, "Code Assessment Studies of RELAP5 Performed in Support of AP600 Thermal-Hydraulic Analysis," *Proceedings of the Fifth International Topical Meeting on Reactor Thermal-Hydraulics (NURETH-5)*, Salt Lake City, Utah, September 1992.
	Westinghouse Electric Co., *AP600 Standard Safety Analysis Report*, DE-AC03-90SF18495, June 1992.
	S. M. Modro, et al., *Evaluation of Scaled Integral Test Facility Concepts for the AP600*, EGG-NE-10239, EG&G Idaho, Inc., May 1992.
	T. D. Ratcliff, *Visualization and Control of Vortical Flow in the Lower Plenum of Westinghouse AP600 Reactor*, M.S. Thesis: University of Tennessee, May 1992.
	R. J. Beelman and S. M. Sloan, "Modeling AP600 with RELAP5", *1991 ANS International Topical Meeting on the Safety of Thermal Reactors*, Portland, Oregon, July 1991.
	M. M. Corletti and L. E. Hochreiter, *AP600 Passive Residual Heat Removal Heat Exchanger Test*, Westinghouse Electric Co. (Proprietary Class 2), WCAP-12666, February 1990.
	L. E. Conway, *Tests of Heat Transfer and Water Film Evaporation from a Simulated Containment to Demonstrate the AP600 Passive Containment Cooling System*, Westinghouse Electric Co. (Proprietary Class 2), WCAP-12667, January 1990.
	C. M. Vertes, "Passive Safeguards Design Optimization Studies for the Westinghouse AP600," *Fifth Proceedings of Nuclear Thermal-Hydraulics, 1989 ANS Winter Meeting*, November 1989.

Table G-4. (continued).

Code	Reference
E1 Cont.	W. A. Stewart, et al., *Tests of Heat Transfer and Water Film Evaporation on a Heated Plate Simulating Cooling of the AP600 Reactor Containment*, Westinghouse Electric Co. (Proprietary Class 2), WCAP-12665, September 1988.
	L. E. Conway, "The Westinghouse AP600 Passive Safety Systems-Key to a Safer, Simplified PWR," *Proceedings of the International Topical Meeting on the Safety of Next Generation Power Reactors*, Seattle, Washington, 1988.
	R. P. Vijuk and S. N. Tower, *Reactor Coolant System Design of the Advanced Westinghouse 600 MWe PWR*, IECED, 1987.
	S. M. Sloan and K. R. Jones, *CMT Condensation Sensitivity Studies*, Letter Report PDB-19-93, EG&G Idaho, Inc., December 31, 1993.
	C. B. Davis, *Upper Plenum Entrainment Studies*, Letter Report PDB-20-94, EG&G Idaho, Inc., June 23, 1994.
	C. B. Davis, *Development of a Simplified AP600 RELAP5 Model for PIRT Validation*, Letter Report GEW-29-94, EG&G Idaho, Inc., August 3, 1994.
	J. E. Fisher, *AP600 Vessel Nodalization Sensitivity Study*, Letter Report PDB-21-94, EG&G Idaho, Inc., July 13, 1994.
	C. B. Davis and M. B. Rubin, *MSLB in AP600 with Maximum Cooldown*, Letter Report PDB-33-94, Lockheed Idaho Technologies, Inc., November 22, 1994.
E2	R. A. Shaw, T. Yonomoto, and Y. Kukita, *Quick Look Report for ROSA/AP600 Experiment AP-CL-03*, Japan Atomic Energy Research Institute, Memo 06-249, October 1994.
	Westinghouse Electric Company, *Quick Look Report for SPES-2 Matrix Test S00401*, PXS-T2R-020 (Proprietary), Preliminary, July 1994.
	Westinghouse Electric Company, *Quick Look Report for OSU Matrix Test SB1*, LTCT-T2R-021 (Proprietary), Preliminary, Revision 0, August 1994.
	Westinghouse Electric Company, *Quick Look Report for OSU Matrix Test SB3*, LTCT-T2R-023 (Proprietary), Preliminary, Revision 0, August 1994.
	Westinghouse Electric Company, *Quick Look Report for OSU Matrix Test SB4*, LTCT-T2R-024 (Proprietary), Preliminary, Revision 0, August 1994.
	Westinghouse Electric Company, *Quick Look Report for OSU Matrix Test SB5*, LTCT-T2R-025 (Proprietary), Preliminary, Revision 0, August 1994.
	Westinghouse Electric Company, *Quick Look Report for OSU Matrix Test SB7*, LTCT-T2R-027 (Proprietary), Preliminary, Revision 0, August 1994.

Table G-4. (continued).

Code	Reference
E3	C. D. Fletcher, et al., *Adequacy Evaluation of RELAP5/MOD3 for Simulating AP600 Small Break Loss-of-Coolant Accidents*, INEL-96/0380 (Proprietary), October 1996.
	C. B. Davis, et al., *Evaluation and Assessment of RELAP5/MOD3 Version 3.2.1.2 for Simulating the Long-Term Phase of Small Break Loss-of-Coolant Accidents in the AP600*, INEL-96/0395, October 1996.
	M. G. Ortiz, et al., *Application of the Global Scaling Analysis Tools to the AP600 Integration Study*, INEL-96/0117, November 1996.
	S. Banerjee, et al., *Topdown Scaling Analysis Methodology for the AP600 Integral Tests*, INEL-96/0400, November 1996.

Table G-5. Sublevel phenomena descriptions for the PIRTs.

ALWR PIRT development is hierarchial; the criteria for judging the relative importance of phenomena is developed from a hierarchial treatment of the safety criteria to which the plants must conform. The level of phenomena shown in the PIRT tables is one that is most appropriate for determining the required code capability and uncertainty. However, when assessing code capabilities, it will be necessary in some cases to evaluate lower level phenomena. For example, flashing may be the phenomenon of primary interest, but sublevel phenomena, such as interphase heat and mass transfer, may be of great importance. The obvious sublevel phenomena are described below for each of the primary phenomena used in the PIRTs. It is likely that at the time the code is assessed additional sublevel phenomena will be identified. The "code" column shows the indicator used in the master PIRTs to reference the information given in this table.

Code	Primary Phenomena	Sublevel Phenomena
S1	Break mass flow and energy release	Critical and friction flow, flashing, two-phase pressure drop
S2	Stored energy release and ambient heat loss	Conduction and convection heat transfer
S3	Core mass flow	Friction flow
S4	Core power and decay heat	Reactor kinetics (power) or power history (decay heat), gap conductance, conduction and wall-fluid heat transfer, boron transport
S5	Flashing	Interphase heat/mass transfer, wall-fluid heat transfer, liquid thermal distribution, pressure
S6	Not used	
S7	Steam generator secondary level	Interphase drag, pressure, flashing, level swell, wall-to-fluid heat transfer
S8	Phase separation	Flow regime, interphase drag, entrainment
S9	Loop asymmetry effects	Fluid mixing, interphase drag
S10	Differential density	Conduction and convection heat transfer, equipment elevations, thermal stratification, liquid thermal distribution, wall-fluid heat transfer, pressure, void distribution
S11	Flow resistance	Wall friction and form loss (area change, orifice, bend) effects
S12	Noncondensible effects	Wall and interphase heat transfer, flow regime, gas expansion characteristics
S13	Level	Interphase drag, flashing, level swell, liquid thermal distribution, gas expansion relationship
S14	Pump coastdown performance	Inertia, shaft friction, flow momentum
S15	Pump flow resistance	Locked rotor resistance
S16	Tube voiding	Flashing, wall-to-fluid heat transfer, interphase heat and mass transfer, flow regime, interphase drag
S17	Steam generator secondary pressure	Wall-to-fluid heat transfer
S18	Condensation	Interphase and/or/wall heat transfer, noncondensible gas effects
S19	Thermal stratification	Liquid to wall and vapor to wall heat transfer, fluid mixing

Table G-5. (continued).

Code	Primary Phenomena	Sublevel Phenomena
S20	Accumulator flow	Friction and orifice flow resistance, gas expansion relationship
S21	ADS mass flow and energy release	Critical and friction flow, flashing, two-phase pressure drop, phase separation in tees, void transport
S22	Not used	
S23	Entrainment/De-entrainment	Interphase drag, flow regime, void distribution, CCFL
S24	IRWST pool flow	Thermal stratification, fluid mixing, interphase condensation, wall-to-fluid heat transfer, natural convection
S25	IRWST pool level	Boiling heat transfer, interphase condensation, evaporation, draining
S26	IRWST pool to tank structure heat transfer	Conduction, convection, ambient heat loss
S27	CCFL	Interphase drag, geometry dependence
S28	Heat transfer between the PRHR and IRWST	Wall-to-fluid heat transfer, conduction, and void distribution
S29	Subsonic break flow and energy release	Friction flow, flashing, two-phase pressure drop
S30	Convective heat transfer	Wall-to-fluid heat transfer, natural circulation
S31	Two-phase mixture level	Level swell, interphase drag, void distribution
S32	Counter current flow	Interphase drag, flow regime
S33	Fluid stratification	Fluid mixing, temperature distribution, flow regime, interphase condensation
S34	Sump fluid temperature	Containment pressure, ambient heat loss
S35	Nonuniform steam/air distributions	Gas species density, fluid mixing, natural convection, wall condensation, noncondensible effects
S36	Natural convection	Wall condensation, fluid mixing, noncondensible effects, gas species density
S37	Condensate transport	Flow of film on wall, droplet formation, interphase drag, conduction and convection heat transfer, CCFL
S38	Liquid distribution and liquid holdup	Flow of film on wall, droplet formation, interphase drag, conduction and convection heat transfer, CCFL, pooling
S39	PCCS evaporation	Interphase heat and mass transfer, natural convection, conduction, flow of film on wall, flow regime, droplet formation, ambient humidity and temperature
S40	PCCS water flow	Line and orifice flow resistance, film and droplet formation, interphase drag, surface tension
S41	Chimney effects	Wind direction and velocity, natural convection
S42	PCCS wetting	Surface tension, surface characteristics
S43	Atmospheric temperature	Worst-case environment
S44	Not used	
S45	Radiation heat transfer	Gas properties, emissivities, view factors

Table G-5. (continued).

Code	Primary Phenomena	Sublevel Phenomena
S46	Humidity	Worst-case environment
S47	Not used	
S48	Not used	
S49	Heater power	Control as function of pressure, level
S50	SG SRV mass flow	Critical flow, flashing, two-phase pressure drop, valve actions
S51	SG SRV energy release	Critical flow, flashing, two-phase pressure drop, valve actions
S52	Subcooling margin	Primary pressure, fluid temperature distribution
S53	Heat transfer between the primary and secondary	Wall-to-fluid heat transfer, conduction, and void distribution
S54	Voiding	Flashing, draining, wall-to-fluid heat transfer, flow regime, interphase drag
S55	Core channeling	Fluid mixing, fluid thermal distribution
S56	Boron reactivity feedback	Fluid mixing, core channeling, boron transport, diffusion
S57	Critical heat flux	Pressure, wall-to-fluid heat transfer, void distribution, core power, decay heat
S58	Moderator temperature feedback	Fluid mixing, core channeling, wall-to fluid heat transfer
S59	Thermal driving head	Differential density, void distribution, natural circulation, wall-to-fluid heat transfer
S60	Vapor space behavior	Interphase heat and mass transfer, flow regime, interphase area, gas expansion/compression characteristics, wall-to-fluid heat transfer
S61	Preferential loop cooldown and asymmetric behavior	Wall-to-fluid heat transfer, fluid mixing, loop asymmetry, flow split, core channeling, reactor kinetics feedback
S62	Tube dryout	Void distribution, level depletion, critical heat flux, wall heat transfer, flow regime
S63	Liquid carryover	Entrainment, deentrainment, centrifugal separation, flow regime, void distribution, interphase drag
S64	Downcomer/lower plenum flow distribution	Flow split, fluid mixing, fluid temperature distribution
S65	Upper head/upper plenum flow split	Fluid mixing, entrainment, deentrainment, flow regime, CCFL, interphase drag
S66	Choking in complex geometries	Geometry dependence, critical and friction flow, flashing, single- and two-phase pressure drop
S67	Passive heat sink	Natural convection heat transfer, wall condensation
S68	Steam-noncondensible mixing	Diffusion, natural convection, buoyancy
S69	Air flow	Buoyancy, flow resistance, wall heat transfer
S70	Exterior-to-ambient heat transfer	See S39 through S48, and S69
S71	Noncondensible segregation	Diffusion, buoyancy, natural convection, condensation heat and mass transfer
S72	Interior-to-wall heat transfer	See S18, S35 through S38, S45, S68, and S71

Table G-5. (continued).

Code	Primary Phenomena	Sublevel Phenomena
S73	Mixing	Thermal stratification, buoyancy, turbulence
S74	Upper head-to-downcomer bypass flow	Flow resistance, condensation, steam flow, local depressurization
S75	Sparger pipe level	Condensation, flashing, local depressurization, vacuum
S76	Containment pressure	Condensation, flashing, wall heat transfer, pool formation, natural circulation
S77	Condensation in ADS stages 1, 2, and 3, and in spargers in IRWST	Wall condensation, interphase condensation, vacuum
S78	Boiling	Wall heat transfer, interphase heat and mass transfer, pressure, subcooling
S79	CMT-to-IRWST differential head	Density, density distribution, thermal stratification, static head, differential pressure
S80	Two-phase level in upper plenum	Level swell and depletion, entrainment/de-entrainment, flashing, phase separation, hot leg horizontal stratification
S81	Liquid distribution	Flow split, gravity drain, thermal stratification, flow resistance
S82	Liquid subcooling	Pressure, liquid temperature, thermal stratification, saturation temperature

Appendix H - Top-Down Scaling Analysis Assessment of Important Parameters affecting PIRT Findings

This appendix discusses the results of the Top-Down Scaling Analysis for the AP600 Integral Tests (Reference H-1), and the significance of the results with regard to the interim findings of the Phenomena Identification and Ranking Table (PIRT). The main objective of the top-down scaling effort was to develop an analysis methodology to interpret the data from various scaled facilities and relate this data to the full size plant. The results from the scaling analysis will then be used to determine the sufficiency and relevance of the data for code assessment. Since the scaling analysis is intended to determine whether the experimental data envelopes the important phenomena in each phase of a particular AP600 transient, some insights can be gained by comparing important system parameters or behavior from the top-down scaling with important phenomena derived from the PIRT process. These comparisons, however, are by necessity limited to first order effects influencing system behavior and component interactions on a global basis since the derivation of the nondimensional groups used in the top-down scaling was based on averaged conservation equations for participating system components in each phase of the transients analyzed. Therefore, local phenomena identified in the PIRT, such as condensation in the CMT or thermal stratification in the IRWST cannot be directly compared with system level results from the top-down scaling analysis. These local phenomena, however, may be important because of their potential influence on the important system level responses, and therefore, should be addressed in the bottom-up scaling approach which is being conducted in parallel with this top-down scaling effort.

Scaling Methodology

The traditional approach to scaling is to establish similitude between experimental facilities of different size through development of a separate set of non-dimensional scaling groups for each facility or system. The principal of similitude requires that the scaling groups for the different scale systems be the same in order to ensure critical system phenomena are preserved. While this dimensional analysis approach works well for relatively simple systems, as the number of variables increases or as the system of interest becomes more complex, this process becomes increasingly difficult. The difficulty stems from the resulting large numbers of nondimensional groups and the potential for conflicting requirements among groups. Experimental effort required to determine the functional dependence of system response on all the groups is time consuming, expensive, and can become impractical. Therefore, in very complex scaled facilities like the three AP600 experimental facilities, it is desirable todevelop a methodology that reduces the complexity and eliminates conflicting requirements among scaling groups while preserving first order system effects.

Reference H-1 provides a detailed description of the top-down scaling methodology used in this study. The methodology used averaged conservation equations and other simplifications to reduce the dimensionality of the problem down to the system component level. This approach tended to remove fine-scale phenomena while preserving the desired first order features of the system response. The scaling methodology, described in detail and demonstrated in Reference H-1, consisted of the following steps:

1. Defining the phenomenologically distinct phases of the transient; clearly identifying initiating and end events. Although the PIRT was used as a guide, it was necessary to divide the transient into finer periods for which dominant processes were easily identified.

2. Identification and definition of subsystems and components and the interactions of importance. During a transient, AP600 exhibits many time varying system phenomena, and not all components participate all the time. Focusing on the participating components make it possible to simplify the system and better define the interactions between components.

3. Definition of the topology. A lumped parameter approach was used and found very valuable in the definition of system variables, system interactions, and in establishing the framework from which to derive dynamic system equations.

4. Development of governing equations for the topology constructed in Step 3 along with necessary closure equations. Having identified the components, phenomena, and potential interactions, system equations consisting of a closed and complete set of governing equations were defined. As a result of this exercise, several local or "bottom-up" relationships required for closure were identified and noted for further study. Among these, the most notable ones are an entrainment model for ADS-4 and flow through ADS-4 valves.

5. Nondimensionalization of the equation set developed in Step 4. This is a mechanical but vital step that leads to the definition of the nondimensional groups (IIs) that govern the similarity of the system solutions.

6. Definition and selection of reference parameters for the Order of Magnitude Analysis. A most important and sensitive step in which the reference variables are chosen according to the objectives of the analysis. Our focus was on the response of the reactor vessel inventory and on the interactions between all relevant components.

7. Order of Magnitude analysis to identify dominant nondimensional groups and equations. The result of this step is a reduced set of nondimensional groups and equations that allow for the selection of important variables, parameters, and relationships to evaluate and compare the data and the plant.

8. Evaluation of results with experimental data. This step represents the validation of our choices for reference parameters, equations, and interactions. It is where distortions caused by non-anticipated phenomena are identified, and where distortions from known geometry and operational parameters are evaluated.

Applicability of Scaling Results to PIRT

The above methodology was applied to three distinct phases of the AP600 SBLOCA transient (Reference H-1). These phases were the subcooled blowdown phase, the ADS-4 blowdown phase, and the beginning of IRWST injection. However, the discussions in this appendix focus on the latter two phases of the SBLOCA (the ADS-4 blowdown and the beginning of IRWST injection) since the dominant processes and interactions during these phases are expected to have the greatest influence on vessel liquid inventory, which is the parameter of primary interest in both the PIRT and scaling study. Detailed descriptions of the transient and the associated phases are contained in Section 3.1 of this PIRT report, and in Section 5.0 of the Scaling Report. Although the scaling results obtained to date are relatively limited and the transient phases used in the scaling analysis do not correspond directly to the transient phases used in the PIRT, the scaling results confirm the PIRT results in those areas where comparisons can be made. In addition, a review of the top-down scaling analyses underway for the remaining transients evaluated in the PIRT (Reference H-2) has not indicated results that would change the interim PIRT findings.

Although the purpose of the top-down scaling was to determine the applicability and sufficiency of experimental data for code assessment, and not to validate or confirm PIRT results, some observations on the relative importance of phenomena derived from the scaling analysis and important phenomena derived from the PIRT can be made. To make comparisons between the PIRT and top-down scaling results, system parameters and variables that influence vessel inventory were identified. This was accomplished through the order of magnitude analysis in step 7 of the scaling analysis, which identified the dominant nondimensional groups and equations that allow for the selection of important parameters and variables affecting vessel inventory.

This approach resulted in the following dominant nondimensional groups for the ADS-4 blowdown and IRWST Injection Phases.

Based on the results obtained to date, these dominant groups are several orders of magnitude larger than other non-dimensional groups derived for these two phases, and no other important phenomena have been identified that would change these groupings.

Four "important" phenomena resulting from the above dominant non-dimensional groups were identified which can be related to the PIRT findings. These phenomena are 1) the CMT level and flow resistance, 2) the IRWST level and flow resistance, 3) flow through the ADS-4 valves, and 4) entrainment from the upper plenum to the hot legs and from the hot legs to the ADS-4 /line. In addition to the above phenomena, an implication of the scaling analysis is that the pressurizer has a first order effect on when the ADS-4 blowdown ends because the liquid in the pressurizer represents a manometric head on top of the hot leg pressure and system pressure "seen" by the IRWST. While these phenomena relate specifically to the ADS-4 blowdown and the beginning of IRWST injection for an SBLOCA, as discussed later, these same component-related phenomena would be expected to be important during the same phases of other transients when the system components are operating in a similar mode with similar boundary conditions. Each of the above scaling related phenomena is discussed in more detail in the following subsections.

CMT Level and Flow Resistance. The PIRT identified CMT level as one of the parameters of primary importance during ADS blowdown because it is one of the determining factors in the timing of ADS staging and the RCS depressurization rate. Similarly, the scaling analysis identified CMT level as an important parameter during the ADS-4 blowdown phase based on the dominant II groupings. Since CMT liquid level also influences vessel mass inventory during the ADS stages 1, 2, and 3, CMT liquid level during these stages should also be a dominant parameter in the scaling analysis for these phases. The top-down scaling also includes CMT flow resistance as an important parameter during the ADS-4 stage. Although flow resistance is given a medium priority in the PIRT, it is the combination of CMT elevation head and CMT flow resistance that determines the driving potential between the CMT and vessel.

The importance of CMT liquid levels during the ADS-4 blowdown stage was demonstrated in Reference 1 with examples from OSU and SPES experiments that had incorrect initial CMT levels at the start of the ADS-4 blowdown. The signal that opened ADS-4 based on CMT level, was too early in the OSU experiment, and too late in the SPES experiment. This resulted in too much CMT inventory available to the vessel during its draining phase in the case of OSU and too little inventory available to SPES. These results translated into a higher than expected inventory for OSU (higher level in the vessel) and lower for SPES. While these anomalies were a result of experiment conduct, and not scaling distortions, they do point out the importance of CMT level in determining the phase duration and vessel minimum inventory.

Other than the combination of CMT liquid level and flow resistance, no other phenomena relating to the CMT were identified by the scaling analysis that would change the PIRT results.

IRWST Level and Flow Resistance. IRWST level and flow resistance were identified in the PIRT and top-down scaling analysis as important phenomena during the IRWST injection phase of a SBLOCA. The combination of these parameters will affect the IRWST injection rate and the resulting vessel mass inventory. The interim PIRT also identified IRWST pool thermal stratification as important during the IRWST injection phase. Thermal stratification, however, is not identified in the scaling analysis since it is a local IRWST phenomena that is not addressed in the scaling analysis approach, which uses average property lumped parameters to characterize system level responses. In addition, discussions in the PIRT identify the potential for unsteady or oscillating IRWST flows. This type of phenomena would also not be recognized in the system scaling analysis since these are considered secondary affects. However, there is the potential that this unsteady behavior can influence liquid entrainment and carryover in the vessel. If

this behavior causes an increase in average entrained liquid flow out the ADS-4 valves, for example, then the affect of the unsteady IRWST injection would influence ADS-4 flow, which is identified as an important phenomenon in the scaling analysis (discussed next). Therefore, although local IRWST phenomena cannot be confirmed in the global top-down scaling approach, the importance of IRWST level and flow resistance are captured by the dominant non-dimensional scaling groups. No other phenomena relating to IRWST inventory or transient behavior have been identified that would influence the interim PIRT results.

Flow through ADS-4 Valves. Flow through the ADS-4 valves is identified as an important phenomena during both the ADS blowdown and initial IRWST phases in both the interim PIRT and the top-down scaling analysis. The PIRT identifies mass flow and energy release as important ADS phenomena because of their influence on primary system pressure, and the timing and rate of IRWST injection. The top-down scaling also captures mass flow and energy release in the dominant nondimensional groupings that include thermodynamic fluid conditions and flow quality. In addition, the Reference 1 scaling report noted that local parameter or variable relationships influencing entrainment and the quality of the fluid leaving the system through the ADS valves should be investigated from a "bottom-up" point of view to adequately address the ADS valve mass and energy release characteristics. The scaling report also notes that, while the pressurizer is not a significant contributor of mass to the vessel during the ADS-4 blowdown, it is a component that imposes head on the hot legs and thus influences the duration of the ADS-4 blowdown. These insights from the scaling analysis confirm the importance of the ADS-4 mass flow and energy release phenomena identified in the PIRT, but also suggest that potential local relationships and component interactions should be investigated further from a bottom-up scaling point of view, and may influence the PIRT rankings in the future.

Entrainment. Entrainment from the upper plenum to the hot legs and from the hot legs to the ADS-4 line was identified in the scaling report as a phenomenon that should be given special attention because of its potential for influencing vessel inventory. The potential for entrainment affecting ADS-4 mass flow and energy release was discussed in the previous section. Entrainment can also influence mass distribution within the primary system and between the primary system and the containment. Redistribution of mass between hot and cool regions of the primary system due to entrainment can influence depressurization characteristics and phase durations. Similarly, entrainment can influence flow quality out the ADS-4 valves, resulting in the redistribution of mass between the primary system and the containment. Since the PIRT identified reactor coolant system mass and energy balances as dominant processes during all phases of a SBLOCA, and containment mass and energy balances were identified as important during the IRWST phase, the potential impact of entrainment on these processes could be important. However, the local processes and phenomena influencing entrainment behavior cannot be characterized using the top-down scaling methodology described herein. Therefore, entrainment is identified as a phenomenon requiring more evaluation.

Conclusions

With regard to phenomena listed in the PIRT document, the most relevant phenomena from the top-down scaling point of view were 1) the CMT level and flow resistance, 2) the IRWST level and flow resistance, 3) flow through ADS-4 valves, and 4) entrainment from the upper plenum to the hot legs and from the hot legs to the ADS-4 line. The dominant nondimensional groupings from the scaling analysis confirmed the importance of these parameters with regard to their influence on vessel liquid inventory and the duration of the transient phases. Beyond the observation that some local variable influences, like liquid entrainment, may require more detailed "bottom-up" analysis, no new phenomena or behavior were identified that would change the interim PIRT findings. Although the results discussed here are limited to the scaling analysis for the SBLOCA ADS-4 blowdown and initial IRWST phases, continuing analyses of other transients listed in the PIRT (Reference 2) have not identified any significant discrepancies or omissions in the interim PIRT findings.

In terms of information from the scaling analysis that could be useful as feedback to the PIRT, it was concluded that system parameters and variables which determine the vessel inventory should be given special attention. The order of magnitude analysis (step 7 of the scaling analysis) which focused on the response of the reactor vessel inventory and on the interactions between all relevant components provided a basis for this feedback. Results from the order of magnitude analysis indicated that line resistance values are important factors in the values of the dominant nondimensional scaling groups and the overall response of the system, and are therefore very important. Also, initial tank levels are also very important in determining the duration of a phase and the primary safety criterion of the PIRT, the vessel minimum inventory. Although unsteady behavior and oscillations in variables or parameters like pressurizer level and IRWST injection appeared to be of secondary importance from a top-down scaling standpoint, more detailed bottom-up analysis of this behavior may be warranted since the top-down scaling effort was not intended to capture these behaviors. In addition, several other relations between variables were identified as needing further study from a local or bottom-up point of view. The most important of these were entrainment and the quality of the fluid leaving the system through the ADS-4 valves.

REFERENCES

H-1. Banerjee, S., Ortiz, M. G., Larson, T. K. and Cozzuol, J. M., *Top-Down Scaling Analysis Methodology for AP600 Integral Tests*, INEL-96/0400, November 1996.

H-2. Ortiz, M. G., Lenglade, C. E., Sloan, S. M., Teerlink, L., *Application of the Global Scaling Analysis Tools to the AP600 Integration Study*, INEL-96/0117, November 1996.

Appendix I - Application of the Analytical Hierarchy Process to the AP600 SBLOCA Short-Term PIRT

I-1. INTRODUCTION

The AP600 is a new design for which there is no existing plant. Early in the PIRT development,[a] there existed minimal experimental and analytical data with which to judge relative phenomena importance. Accordingly, in the PIRT development through Revision 1 of this report, it was judged that there was an insufficient technical basis to warrant the use of a detailed numerical ranking scheme. Rather, the ranking was based on low, medium and high importance categories with respect to a phenomenon's influence on the parameter of importance.[b] However, by December 1995, sufficient data from the AP600 devoted experiments and analytical studies had been obtained to make numerical phenomena ranking attractive. Moving to a numerical ranking scheme allows for more precise evaluations of relative importance. In addition, use of a numerical ranking process, such as the Analytical Hierachy Process (AHP), forces a structured, logical and consistent ranking of the data base, taken as a whole. Therefore, even though further new experimental and analytical evidence was to be available after December 1995, it was judged results from the application of the AHP to the initial phases[c] of the SBLOCA would be most useful in helping confirm more realistic ranking of the phenomena. Such application would also give insights regarding the feasibility of combining the transient initial phases into a single treatment (i.e., a short-term SBLOCA PIRT). It is the purpose of this appendix to document the AHP effort.

The remainder of this appendix documents the application of the AHP to the AP600 SBLOCA short-term PIRT development. Section 2 describes the specific approach to developing AHP based insights regarding the relative importance of phenomena to the plant response during the initial phases of the transient. Section 3 provides the significant results from the AHP exercise. Section 4 summarizes the significant conclusions derived from the AHP results. Pertinent references noted in the first four sections are listed in Section 5.

I-2. APPROACH

I-2.1 Background

Humans have a high proficiency to determine the relative importance of items, one-to-another, when the number of items does not exceed four. As the number of items in a group increases beyond four, the ranking capability decreases at an increasing rate. Accordingly, methodologies have been developed to organize large ranking problems into subsets that capitalize on innate human talents. One such methodology is the AHP which has been used to help justify the AP600 SBLOCA short-term PIRT described elsewhere in this report.

As decisions become more and more complex, decision makers are faced with the challenge of sorting through many variables to arrive at a sound decision. The AHP is a tool developed by T. L. Saaty,[I-1] that allows a systematic, logical approach to reduce complex issues into manageable pieces. The decision maker can then sort through the variables and determine to what degree a particular variable will

---

[a] Preliminary PIRTs, and Revsion 0 and Revision 1 of this report.

[b] Minimum vessel inventory as described elsewhere in this report.

[c] High pressure, ADS blowdown, and initial IRWST injection.

influence the final decision. The power of the AHP is centered in its reduction of complex problems to one of many pair-wise decisions. Only two items need be compared against one another; a much simpler task than comparing an item to all others simultaneously. By arranging the items that influence a decision in the form of a matrix and comparing appropriate pairs in this matrix to each other, each item is automatically compared with every other item via the matrix algebra used in the process. Thereby, the relative importance, one-to-another, of all the items on the final decision is determined.

As the name suggests, the AHP contains hierarchies or levels. The structuring of a complex problem into hierarchies is the second strength of the methodology in that it also supports partitioning a complex problem into subsets more amenable to ranking determinations. Each level contains items that will be ranked one-to-another on the basis of their influence on an item in the next higher level. By starting at the lowest level, the most fundamental level, the decision maker can rank items with respect to a more general item contained in the next higher level. As the decision maker proceeds through the levels, the items become more general until the most general item, the goal, is reached. Thus, the decision maker proceeds as if building a pyramid. At the bottom he makes many specific decisions. As the process proceeds toward the top fewer and fewer decisions are made and they become increasingly more general. Finally the AHP manipulates the pair-wise decisions made at each level to determine how important each are with respect to the most general item, the goal.

I-2.2 Approach

The general approach is shown conceptually in Figure I-1. Based on the evidence indicated in the figure, independent pair-wise ranking was performed by three of the PIRT Subgroup Thermal Hydraulic (T/H) expert consultants for:

- The relative importance of the phases that constitute the short-term PIRT, and
- The relative importance of the phenomena within each phase.

The INEEL staff then used AHP software[I-2] to generate:

- The relative importance of the phases taken as a whole,
- The relative importance of the phenomena within each phase, and
- The relative importance of the phenomena for the combined phase short-term PIRT,

for each of the three pair-wise ranking input sets provided by Brent Boyack (BB), Peter Griffith (PG) and Gearld Lellouche (GL).

Because the Revision 1 PIRT was considered to contain all plausible phenomena, it formed the basis for the components and phenomena treated in the AHP application. A pair-wise ranking scale of 1 to 5 was used by the PIRT Subgroup, where in judging the relative importance of two items, a and b:

1 = Items a and b are of equal importance
3 = Item a is somewhat more important than item b
5 = Item a is significantly more important than item b
1/3 = Item b is somewhat more important than item a
1/5 = Item b is significantly more important than item a.

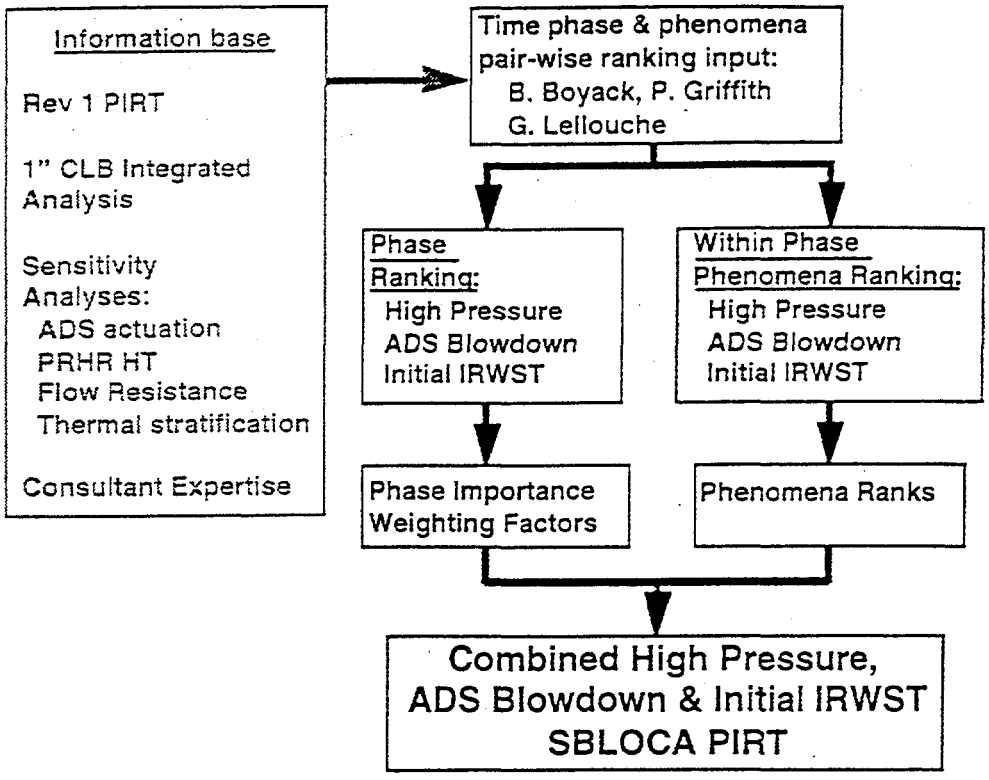

Figure I-1. Conceptual application of AHP to AP600 SBLOCA short-term PIRT.

Ranks of 2 and 4, and 1/2 and 1/4 were available to further refine the above ranks if desired.[d]

The number of pair-wise ranks, and each specific rationale for those ranks, constitute a very large body of information that is not believed to be warranted for recording here. This information has been archived by the INEEL staff. However, the general rationale for the ranking is given in the next section.

I-2.3 General Ranking Rationale

Information from several sources feed the phenomena ranking process. In general order of decreasing importance these are: 1) test data, 2) scaling analyses, 3) code calculations, and 4) experience. To the extent supported by this data base at any one point in time, the initial ranking rationale was centered in implicit judgments of the combined importance of subsystems (components) and the specific phenomena within each component. In addition, because of the minimal amount of AP600 specific data early in the program, an absence of significant information resulted in escalation of the ranks of those specific phenomena to high; a conservative, but not necessarily realistic safety perspective. The expectation was that as more AP600 specific evidence became available with time, updates of the PIRTs would undergo a general tendency to decrease the ranks. This has proven to be true; however, it is generally believed the PIRTs continued to be conservative rather than best estimate.

---

[d] The input ranking scale is arbitrary; however, the AHP matrix algebra produces "absolute" ranks in a 0 to 1 scale as is common to this class of mathematical solutions. In addition, the software is designed to produce "normalized" output ranks on a scale of 1 to 9, where it is normally interpreted that ranks of 1 to 3 denote low importance, 4 to 6 moderate importance, and 7 to 9 high importance.

Another element in the ranking rationale was consideration whether a component was active or inactive in any particular time period. If inactive, no further effort was made to rank the processes/phenomena in that component; they are "insignificant". For example, during the blowdown phase the PSIS is inactive, therefore, there is no need to consider further the importance of the system, its component or its phenomena.

Although the early PIRTs were component/within component phenomena centered, it was increasingly recognized that in the AP600 design there were significant interactions between subsystems. The most important of these are: 1) depressurization, 2) inventory depletion, 3) inventory replacement, and 4) core cooling. Depressurization is a key process because it is impossible to transition to long-term core cooling until the PCS pressure is reduced sufficiently to permit accumulator injection and gravity-induced injection from the IRWST and sump. Inventory depletion is a key process because the removal of too much inventory can degrade core cooling and potentially result in core damage. Inventory replacement is a key process because inventory depletion is an inherent feature of the transition to long-term cooling. Cooling the core is the process most directly related to public safety and protecting the investment in the plant. Core cooling considers both coolant flow and core power, which is the traditional power-to-cooling relationship.

In summary, the ranking rationale remains strongly focused toward the component/within component phenomena orientation. However, the system level interactions (see above) have been increasingly introduced into the ranking process, albeit in a more implicit than explicit manner.[e] For example, see the system level related dominant processes in Figures 7 - 8 in the main body of this report.

I-3. AHP RESULTS

I-3.1 Phase Importance

The initial SBLOCA phases considered in the AHP application were:

- High pressure - Break initiation to ADS-1 actuation
- ADS blowdown - ADS-1 actuation to initiation of IRWST injection
- Initial IRWST injection - Initial dynamic phase of IRWST injection

The results from the AHP application are summarized in Table I-1.

[e] Explicit consideration of system level interactions is considered to be one of the significant lessons learned. That is, in reactor designs that are strongly dependent on weak gravity induced flows, system level interactions should be explicitly introduced into the ranking process at the second hierarchical level (i.e., above the component/within component phenomena level[s]).

Table I-1. Ranking of time phase importance.[f]

	Absolute Rank			Normalized Rank			INEEL Composite Rank	
Phase	BB	PG	GL	BB	PG	GL	Absolute	Norm
High pressure	0.0897	0.1460	0.0982	1	1	1	0.1113	1
ADS blowdown	0.6070	0.4738	0.5679	9	9	9	0.5496	9
Initial IRWST Injection	0.3033	0.3802	0.3339	4	7	5	0.3391	5

It may be noted that from the 1-9 normalized rank perspective there was no essential difference among the three sets of ranks for the high pressure and ADS blowdown phases. There may be some difference for the initial IRWST injection phase in that strictly speaking the phase was ranked moderate and high by the different Subgroup members. In any case, there was a common view that the ADS phase was most important, the initial IRWST phase of second importance and the high pressure phase least important.[g] The INEL composite rank shown in the table was somewhat arbitrarily formulated by averaging the three individual ranks for each phase, and is provided just for information.[h]

I-3.2 Within Phase Phenomena Importance

"Within phase" is used to denote the relative phenomena importance within each of the three time phases noted in the previous section. That is, these ranks have not been weighted by the relative importance of the three time phases. The results of applying the AHP software to each of the three individual sets of pair-wise ranking are summarized in Tables I-2 through I-4 for the three time phases of interest. The AHP numerical ranks have been converted to their corresponding alpha ranks (see footnote d) to allow for direct comparison with the published Revision 1 PIRT. In addition, the column "AHP suggested Phase 1 ranks" lists the highest of the three individual ranks for each phenomenon. Shaded cells indicate phenomena that were considered insignificant by the individual performing the ranking.

---

[f] The only value in recording the absolute ranks to four significant figures is to illustrate the numerical consistency maintained by the AHP software.

[g] This perspective of phase importance is also similar to that documented in a separate scaling analysis report.

[h] The individual consultant phase rank sets are maintained for the subsequent ranking reported in this appendix.

Table I-2. AHP within phase phenomena importance for high pressure phase.

Component	Phenomena	Rev 1 PIRT	AHP ranks			AHP suggested Phase 1 ranks
			Bovack	Griffith	Lellouche	
Accumulators	Flow	H	L	L	L	L
	Noncondensible effects	L	L	L	L	L
Break	Energy release	M	M	L	H	H
	Mass flow	H	H	H	H	H
Cold legs	Condensation	H	L	L	L	L
	Flashing	L	L	L	M	M
	Loop asymmetry effects	M	L	L	L	L
	PBL-to-cold legs tee phase separation	H	L	L	M	M
	Stored energy release	L	L	L	L	L
	Thermal stratification	H	L	L	L	L
Core	Flashing	L	L	L	M	M
	Flow resistance	L	M	L	L	M
	Mass flow, including bypass	L	M	L	L	M
	Stored energy release	L	M	L	L	M
CMT	CMT-to-loop differential density	H	M	L	M	M
	Condensation	L	M	L	L	M
	Flashing	H	H	L	M	H
	Flow resistance	M	M	L	L	M
	Level	H	H	L	L	H
	Thermal stratification and mixing	H	M	L	L	M
Downcomer/ lower plenum	Condensation	M	L	L	L	L
	Flow distribution	M	L	L	L	L
	Level	L	M	L	L	M
	Loop asymmetry effects	M	L	L	L	L
	Stored energy release	L	L	L	L	L
Fuel rods	Core power/decay heat	H	H	L	M	H
	Stored energy release	L	M	L	M	M
Hot legs	Flashing	L	M	L	M	M
	Horizontal fluid stratification	M	M	L	M	M
	Loop asymmetry effects	L	L	L	L	L
	Phase separation in tees	L	M	L	M	M
	Stored energy release	L	L	L	L	L
	Voiding	M	M	L	M	M
IRWST	Flow and temperature distribution in PRHR bundle region	M	L	L	M	M
	Interphasic condensation	L	L	L	L	L
	Pool flow	L	L	L	L	L
	Pool level	M	L	L	L	L
	Pool thermal stratification	M	L	L	L	L
Pressurizer	Flashing	M	L	L	M	M
	Level (inventory)	M	L	L	M	M
PRHR	Condensation	M	L	L	L	L
	Differential density	M	M	L	M	M
	Flow resistence	M	M	L	M	M
	Heat transfer between PRHR and IRWST	H	M	L	M	M
	Noncondensible effects	M	L	L	L	L
	Voiding	M	M	L	M	M
Pumps	Coastdown performance	L	L	L		L
	Flow resistance	L	L	L		L
	Mixing	M	L	L		L
Steam generators	Primary to secondary heat transfer	M	L	L	M	M
	Secondary level	L	L	L		L
	Secondary pressure	M	L	L		L
	Tube voiding	M	L	L	M	M
Upper head/ upper plenum	Flashing	L	L	L	L	L
	Loop asymmetry effects	L	L	L		L
	Stored energy release	L	L	L	L	L
	Upper head/downcomer bypass flow	L	L	L		L
	Voiding	L	L	L	M	M

Table I-3. AHP within phase phenomena importance for ADS blowdown.

Component	Phenomena	Rev 1 PIRT	AHP ranks			AHP suggested Phase 2 ranks
			Boyack	Griffith	Lellouche	
Accumulators	Flow	H	H	H	H	H
	Noncondensible effects	M	M	L	M	M
ADS	Energy release	H	M	M	H	H
	Mass flow	H	H	H	H	H
	Choking in complex geometry	M	H	L	M	H
	Flow resistance	M	M	L	L	M
	Noncondensible effects	M	M	L	L	M
Break	Energy release	M	M	M	M	M
	Flow resistance	L	M	L	L	M
	Mass flow	M	M	M	M	M
	Noncondensible effects	L	L	L	L	L
Cold legs	Condensation	L	L	L	L	L
	Flashing	L	L	L	M	M
	Noncondensible effects	M	L	L	L	L
	PBL-to-cold legs tee phase separation	M	L	L	L	L
	Stored energy release	L	L	L	L	L
	Thermal stratification	L	L	L	L	L
Core	Flashing	H	M	L	M	M
	Flow resistance	H	M	L	L	M
	Stored energy release	L	M	L	L	M
	Subcooling margin	H	M	L	L	M
	Two-phase mixture level	H	H	L	H	H
CMT	Flashing	M	L	L	M	M
	Flow resistance	M	L	L	L	L
	Level	H	M	L	L	M
	Thermal stratification and mixing	M	L	L	L	L
Downcomer/ lower plenum	Condensation	M	L	L	L	L
	Flashing	L	L	L	M	M
	Noncondensible effects	L	L	L	L	L
	Stored energy release	L	L	L	L	L
Fuel rods	CHF/dryout	M	M	L	M	M
	Core power/decay heat	H	H	L	L	H
	Stored energy release	L	M	L	L	M
Hot legs	CCFL	M	L	L	L	L
	Condensation	M	L	L	L	L
	Countercurrent flow	M	L	L	L	L
	Entrainment	M	L	L	L	L
	Flashing	M	L	L	M	M
	Horizontal fluid stratification	M	L	L	L	L
	Noncondensible effects	L	L	L	L	L
	Phase separation in tees	H	L	L	L	L
	Stored energy release	L	L	L	L	L
IRWST	Interphasic condensation	M	L	L	L	L
	Pool flow	M	L	L		L
	Pool level	L	L	L		L
	Pool to tank structure heat transfer	L	L	L		L
	Pool thermal stratification	M	L	L	L	L
	Sparger pipe level	H	L	L	M	M

Table I-3. (continued).

Component	Phenomena	Rev 1 PIRT	AHP ranks			AHP suggested Phase 2 ranks
			Bovack	Griffith	Lellouche	
Pressurizer	CCFL	M	L	L	L	L
	Entrainment/de-entrainment	M	M	L	L	M
	Level (inventory)	H	L	L	L	L
	Level swell	M	M	L	M	M
	Noncondensible effects	L	L	L	L	L
	Stored energy release	L	L	L		L
PRHR	Differential density	L	L	L		L
	Flow resistence	L	L	L		L
	Flashing	L	L	L		L
	Heat transfer between PRHR and IRWST	L	L	L		L
	Noncondensible effects	L	L	L		L
	Phase separation in tees	L	L	L		L
Steam generators	Primary to secondary heat transfer	L	L	L		L
Upper head/ upper plenum	Condensation	M	L	L	L	L
	Entrainment/de-entrainment	M	L	M	L	M
	Flashing	M	L	L	L	L
	Stored energy release	L	L	L	L	L
	Upper head/downcomer bypass flow	L	L	L	L	L
	Voiding	M	L	L	M	M
Containment (interior)	Pressure	M	M	L		M

Table I-4. AHP within phase phenomena importance for initial IRWST injection.

Component	Phenomena	Rev 1 PIRT	AHP ranks			AHP suggested Phase 3 ranks
			Bovack	Griffith	Lellouche	
ADS	Energy release	H	M	M	H	H
	Mass flow	H	M	M	H	H
	Flow resistance	H	L	H	L	H
	Noncondensible effects	L	L	L		L
	Condensation in stages 1, 2, and 3 ADS and spargers (in IRWST)	L	L	L		L
Break	Energy release	M	L	L	M	M
	Mass flow	M	L	L	M	M
	Noncondensible effects	L	L	L		L
Cold legs	Condensation	L	L	L	L	L
	Noncondensible effects	L	L	L		L
	PBL-to-cold legs tee phase separation	L	L	L	L	L
Core	Boiling	M	H	L	H	H
	Flashing	M	M	L		M
	Flow resistance	M	M	L	L	M
	Mass flow, including bypass	M	H	L	L	H
	Subcooling margin	M	M	L		M
	Two-phase mixture level	H	H	H	H	H
CMT	CMT-to-IRWST differential head	H	L	L	H	H
	Condensation	H	L	L		L
	Flow resistance	M	L	L	L	L
	Noncondensible effects	H	L	L		L
Downcomer/ lower plenum	Condensation	M	M	L		M
	Level	H	H	L		H
Fuel rods	CHF/dryout	L	M	L	M	M
	Core power/decay heat	H	H	L	H	H
Hot legs	Countercurrent flow	M	L	L		L
	Horizontal fluid stratification	M	L	L		L
	Phase separation in tees	H	L	L	L	L
IRWST	Flow resistance (Injection rate - Lellouche)	H	M	H	H	H
	Pool flow	H	H	L		H
	Pool to tank structure heat transfer	L	M	L		M
	Pool thermal stratification	H	M	L	M	M
	Sparger pipe level	L	M	L		M
Pressurizer	Level (inventory)	M	L	L	M	M
Steam generators	Primary to secondary heat transfer	L	L	L		L
Sump	Level	H	H	L	M	H
Upper head/ upper plenum	Condensation	L	L	L		L
	Noncondensible effects	L	L	L		L
	Two-phase level in upper plenum	H	L	L		L
Containment (interior)	Liquid distribution	L	H	L		H
	Liquid subcooling	L	M	L		M
	Pressure	M	M	M	L	M

I-3.3 Phase Weighted Phenomena Importance

"Phase weighted" is used to denote the AHP analysis in which the phase importance given in Section 3.1 is applied to the within phase phenomena importance presented in Section 3.2. The product of this two level hierarchy is the ranking for the three combined phases, or the short-term AHP PIRT. The significant results are summarized in Table I-5. The descriptions of the column AHP PIRT information are:

- Individual AHP phase weighted ranks - The ranks generated by the AHP software based on application of the phase weighting described in Section 3.1 to the within phase phenomena ranks described in Section 3.2 for each of the three individual sets of ranking,
- Revision 1 combined PIRT - The highest phenomenon rank during the three phases of interest that were reported in the Revision 1 issue of this report,
- Highest AHP phase weighted ranks - The highest phenomenon rank shown in any one of the three individual AHP phase weighted ranks, and
- Highest AHP within phase ranks - The highest phenomenon rank shown for any of the three within phase individual ranks for any of the three phases (Tables I-2 - I-4).

I-4. SUMMARY AND CONCLUSIONS

I-4.1 Summary

Considerable new, but not necessarily complete, experimental, analytical and scaling AP600 specific evidence evolved through December 1995. This evidence was considered sufficient to warrant numerical ranking of the high pressure, ADS blowdown and initial IRWST injection phases of the SBLOCA. Accordingly, three members of the PIRT Subgroup of T/H Expert Consultants were requested to provide individual pair-wise ranking of the relative importance of the phases of interest and the phenomena that occur within each phase. Using this information the INEEL staff applied AHP software to determine:

- The relative importance of the phases taken as a whole (Table I-1),
- The relative importance of the phenomena within each phase (Tables I-2 - I-4), and
- The relative importance of the phase weighted phenomena for the combined phase short-term AHP PIRT (Table I-5).

This data was further sorted to provide:

- The highest AHP phase weighted ranks of the three sets of individual ranking (Table I-5), and
- The highest AHP within phase ranks of the three sets of individual ranking for all three phases of interest (Table I-5).

I-4.2 Significant Conclusions

The significant conclusions drawn from the information in Tables I-1 - I-5, in their perceived order of importance, are:

- **The new evidence combined with the strengths of AHP analysis has confirmed prior SBLOCA PIRTs contain a high degree of conservatism.** This was to be expected based on the practice of assigning high importance to insufficiently understood phenomena until such time as evidence existed to down-rank. The AHP analysis provides a more rigorous and consistent basis to evaluate the degree of conservatism as a whole.

Table I-5. AHP phase weighted ranks for the combined SBLOCA high pressure, ADS blowdown and initial IRWST injection phases.

Component	Phenomena	Individual AHP phase weighted ranks			Rev 1 Combined PIRT	Highest AHP phase weighted ranks	Highest AHP within phase ranks
		Boyack	Griffith	Lellouche			
Accumulators	Flow	M	M	M	H	M	H
	Noncondensible effects	M	L	L	M	M	M
ADS	Energy release	M	M	H	H	H	H
	Mass flow	M	H	H	H	H	H
	Choking in complex geometry	M	L	M	M	M	H
	Flow resistance	M	M	L	H	M	H
	Noncondensible effects	M	L	L	M	M	M
	Condensation in stages 1, 2, and 3 ADS and spargers (in IRWST)	L	L		L	L	L
Break	Energy release	M	M	M	M	M	H
	Flow resistance	M	L	L	L	M	M
	Mass flow	M	M	M	H	M	H
	Noncondensible effects	L	L	L	L	L	L
Cold legs	Condensation	L	L	L	H	L	L
	Flashing	L	L	M	L	M	M
	Loop asymmetry effects	L	L	L	M	L	L
	Noncondensible effects	L	L	L	M	L	L
	PBL-to-cold legs tee phase separation	L	L	M	H	M	M
	Stored energy release	L	L	L	L	L	L
	Thermal stratification	L	L	L	H	L	L
Core	Boiling	M	L	M	M	M	H
	Flashing	M	L	M	H	M	M
	Flow resistance	M	L	L	H	M	M
	Loop asymmetry effects	L	L	L	L	L	L
	Mass flow, including bypass	M	L	L	M	M	H
	Stored energy release	M	L	L	L	M	M
	Subcooling margin	M	L	L	H	M	M
	Two-phase mixture level	H	M	H	H	H	H

Table I-5. (continued).

Component	Phenomena	Individual AHP phase weighted ranks			Rev 1 Combined PIRT	Highest AHP phase weighted ranks	Highest AHP within phase ranks
		Boyack	Griffith	Lellouche			
CMT	CMT-to-loop differential density	L	L	L	H	L	M
	CMT-to-IRWST differential head	L	L	M	H	M	H
	Condensation	L	L	L	H	L	M
	Flashing	M	L	M	H	M	H
	Flow resistance	M	L	L	M	M	M
	Level	M	L	L	H	M	H
	Noncondensible effects	L	L		H	L	L
	Thermal stratification and mixing	L	L	L	H	L	M
Downcomer/ lower plenum	Condensation	M	L	L	M	M	M
	Flashing	L	L	L	L	L	M
	Flow distribution	L	L	L	M	L	L
	Level	M	L	L	H	M	H
	Loop asymmetry effects	L	L	L	M	L	L
	Noncondensible effects	L	L	L	L	L	L
	Stored energy release	L	L	L	L	L	L
Fuel rods	CHF/dryout	M	L	M	M	M	M
	Core power/decay heat	H	L	M	H	H	H
	Stored energy release	M	L	L	L	M	H
Hot legs	CCFL	L	L	L	M	L	L
	Condensation	L	L	L	M	L	L
	Countercurrent flow	L	L	L	M	L	L
	Entrainment	L	L	L	M	L	L
	Flashing	L	L	M	M	M	M
	Horizontal fluid stratification	L	L	L	M	L	M
	Loop asymmetry effects	L	L	L	L	L	L
	Noncondensible effects	L	L	L	L	L	L
	Phase separation in tees	L	L	M	H	M	M
	Stored energy release	L	L	L	L	L	L
	Voiding	L	L	L	M	L	M

Table I-5. (continued).

Component	Phenomena	Individual AHP phase weighted ranks			Rev 1 Combined PIRT	Highest AHP phase weighted ranks	Highest AHP within phase ranks
		Boyack	Griffith	Lellouche			
IRWST	Flow and temperature distribution in PRHR bundle region	L	L	L	M	L	M
	Flow resistance	L	M		H	M	H
	Interphasic condensation	L	L	L	M	L	L
	Pool flow	M	L	L	H	M	H
	Pool level	L	L	L	M	L	L
	Pool to tank structure heat transfer	L	L		L	L	M
	Pool thermal stratification	M	L	M	H	M	M
	Sparger pipe level	L	L	L	H	L	M
Pressurizer	CCFL	L	L	L	M	L	L
	Entrainment/de-entrainment	M	L	L	M	M	M
	Flashing	L	L	L	M	L	M
	Level (inventory)	L	M	M	H	M	M
	Level swell	M	L	M	M	M	M
	Noncondensible effects	L	L	L	L	L	L
	Stored energy release	L	L		L	L	L
PRHR	Condensation	L	L	L	M	L	L
	Differential density	L	L	L	M	L	M
	Flow resistence	L	L	L	M	L	M
	Flashing	L	L		L	L	L
	Heat transfer between PRHR and IRWST	L	L	L	H	L	M
	Noncondensible effects	L	L	L	M	L	L
	Phase separation in tees	L	L		L	L	L
	Voiding	L	L	L	M	L	M
Pumps	Coastdown performance	L	L		L	L	L
	Flow resistance	L	L		L	L	L
	Mixing	L	L		M	L	L
Steam generators	Primary to secondary heat transfer	L	L	L	M	L	M
	Secondary level	L	L		L	L	L
	Secondary pressure	L	L		M	L	L
	Tube voiding	L	L	L	M	L	M

Table I-5. (continued).

Component	Phenomena	Individual AHP phase weighted ranks			Rev 1 Combined PIRT	Highest AHP phase weighted ranks	Highest AHP within phase ranks
		Boyack	Griffith	Lellouche			
Sump	Level	M	L	M	H	M	H
Upper head/ upper plenum	Condensation	L	L	L	M	L	L
	Entrainment/de-entrainment	L	M	L	M	M	M
	Flashing	L	L	L	M	L	L
	Loop asymmetry effects	L	L		L	L	L
	Noncondensible effects	L	L		L	L	L
	Stored energy release	L	L	L	L	L	L
	Two-phase level in upper plenum	L	L		H	L	L
	Upper head/downcomer bypass flow	L	L	L	L	L	L
	Voiding	L	L	M	M	M	M
Containment (interior)	Liquid distribution	M	L		L	M	H
	Liquid subcooling	L	L		L	L	M
	Pressure	M	M	L	M	M	M

- **The introduction of the relative importance of time in the transient provides a new perspective relative to making the PIRTs more realistic.** In principle it is logical to assign less importance to a high ranked phenomenon in a time period that is less important, than to a high ranked phenomenon in a time period where the ongoing processes dominate the ultimate outcome of the plant response (for example the ADS blowdown phase). This also allows further simplification of the PIRTs in that phases may be combined into larger blocks of time. There is a potential down side to this approach, however. From the perspective that a phenomenon's behavior in a subsequent time period is at least somewhat dependent on behavior in previous time periods, phase weighted ranking could, in principle, tend to under-rank some phenomena. The risk of such under-ranking is considered to be essentially nonexistent when several independent AHP analyses are performed and the most conservative view taken of the several results. This has been done in the analysis reported here (Table I-5, next to last column). The risk is further reduced by considering other evidence from such sources as parameter specific sensitivity studies, scaling analysis, etc. as is done elsewhere in this report. The three independent views of the relative importance of the three time phases of interest here have been generally supported by other evidence from scaling analysis. The scaling analysis also well supports the plausible phenomena used in the AHP study.
- **The AHP analysis that ignored the importance of time (or alternately assigned the same importance to all time phases), the within phase AHP ranking, provides a most conservative perspective of phenomena importance.** This is particularly true where the most conservative ranks from three independent within phase ranks are considered (Table I-5, last column). However, this perspective lends itself to helping identify the most cost effective areas where phase weighted ranking should be further confirmed with other evidence.
- **Review of the AHP analysis ranking rationale, and other evidence, helped identify an important potential improvement in the PIRT process**. That is, system level interactions (i.e., between subsystem/components) should be explicitly considered in reactor designs that are strongly dependent on weak gravity induced flows. The PIRT process can be improved by the introduction of system level interactions at the second hierarchical level (i.e., above the component/within component phenomena level[s]).

I-5. REFERENCES

I-1. T. L. Saaty, *Decision Making for Leaders*, Lifetime Learning Publications (1982).

I-2. L. S. Ghan, J. C. Watkins, *AHP Version 5.1 Users Manual*, EGG-ERTP-10585, October 1992.

NRC FORM 335 (2-89) NRCM 1102, 3201, 3202

U.S. NUCLEAR REGULATORY COMMISSION

BIBLIOGRAPHIC DATA SHEET

(See instructions on the reverse)

1. REPORT NUMBER (Assigned by NRC, Add Vol., Supp., Rev., and Addendum Numbers, if any.)
NUREG/CR-6541
INEL-94/0061, Rev. 2

2. TITLE AND SUBTITLE
Phenomena Identification and Ranking Tables for Westinghouse AP600 Small Break Loss-of-Coolant Accident, Main Steam Line Break, and Steam Generator Tube Rupture Scenarios

3. DATE REPORT PUBLISHED
MONTH: June
YEAR: 1997

4. FIN OR GRANT NUMBER
J6008

5. AUTHOR(S)
G. E. Wilson, C. D. Fletcher, C. B. Davis, J. D. Burtt, T. J. Boucher

6. TYPE OF REPORT
Technical

7. PERIOD COVERED *(Inclusive Dates)*

8. PERFORMING ORGANIZATION - NAME AND ADDRESS *(If NRC, provide Division, Office or Region, U.S. Nuclear Regulatory Commission, and mailing address; if contractor, provide name and mailing address.)*
Idaho National Engineering and Environmental Laboratory
Lockheed Idaho Technologies Company
P. O. Box 1625
Idaho Falls, ID 83415-3890

9. SPONSORING ORGANIZATION - NAME AND ADDRESS *(If NRC, type "Same as above"; if contractor, provide NRC Division, Office or Region, U.S. Nuclear Regulatory Commission, and mailing address.)*
Division of Systems Technology
Office of Nuclear Regulatory Research
U. S. Nuclear Regulatory Commission
Washington, D. C. 20555-0001

10. SUPPLEMENTARY NOTES
T. Lee, NRC Project Manager

11. ABSTRACT *(200 words or less)*

This report documents the results of Phenomena Identification and Ranking Table (PIRT) efforts for the Westinghouse AP600 reactor. The purpose of this PIRT is to identify important phenomena so that they may be addressed in both the experimental programs and the RELAP5/MOD3 systems analysis computer code. The responses of AP600 during small break loss-of-coolant accident, main steam line break, and steam generator tube rupture accident scenarios were evaluated by a committee of thermal-hydraulic experts. Committee membership included Idaho National Engineering and Environmental Laboratory staff and recognized thermal-hydraulic experts from outside of the laboratory. Each of the accident scenarios was subdivided into separate, sequential periods or phases. Within each phase, the plant behavior is controlled by, at most, a few thermal-hydraulic processes. The committee identified the phenomena influencing those processes, and ranked the influences as being of high, medium, low, or insignificant importance. The primary product of this effort is a series of tables, one for each phase of each accident scenario, describing the thermal-hydraulic phenomena judged by the committee to be important, and the relative ranking of that importance. The rationales for the phenomena selected and their rankings are provided.

12. KEY WORDS/DESCRIPTORS *(List words or phrases that will assist researchers in locating the report.)*
PIRT
AP600
phenomena identification and ranking tables
small break loss-of-coolant accident
steam generator tube rupture

13. AVAILABILITY STATEMENT
unlimited

14. SECURITY CLASSIFICATION
(This Page) unclassified
(This Report) unclassified

15. NUMBER OF PAGES

16. PRICE

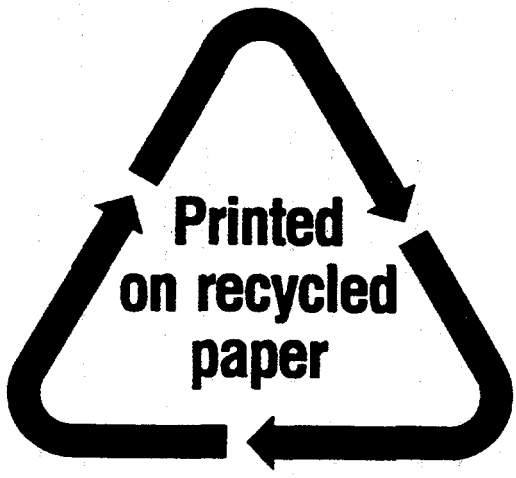

Federal Recycling Program